Muscle pathology in a mouse model of Amyotrophic lateral sclerosis

A Thesis submitted to University College London for the degree of Doctor of Philosophy in the Faculty of Science

By

Emem Edet-Amana BSc (Hons)

Sobell Department of Motor Neuroscience and Movement disorders

Institute of Neurology

University College London

March 2011

ACKNOWLEDGEMENTS

I thank my supervisors Prof. Linda Greensmith, who gave me this invaluable opportunity and Dr. Peter Kirkwood and Dr. Bernadett Kalmar for the continued support, time, teaching and guidance through my studentship. Many thanks to all members of the Graham Watts lab, with a special thanks to Dr. Bilal Malik for all the out of hours of guidance and support throughout the 2nd and 3rd year of my studentship.

I would also like to give a special thanks to all my family... Mum, the power of the nag is one of nature's most amazing, renewable energy sources. I will never underestimate the terrible power it holds. Also, special thanks to Alice Sverdlik, to whom fell the thankless task of exorcising the grammatical sins that once inhabited these pages. Demon hunters and exorcists quake in your wake.

ABSTRACT

Recent evidence has shown that non-neuronal cells within the CNS play a role in motoneuron degeneration in ALS. However, while it is accepted that various muscles are differentially affected within the disease, it is still unclear whether muscle has a causal role in ALS. In this Thesis, using a mouse model of ALS (mutant SOD1 transgenic mice), I examined muscle and NMJ pathology in two different muscle types, at various stages of disease progression.

Using morphological and functional markers of innervation, I found that mSOD1-mediated pathology was present in fast-twitch muscles of mSOD1 mice prior to motoneuron degeneration. This occurred at a time when slow-twitch muscles remain innervated. This difference in the vulnerability of fast-twitch and slow-twitch muscles to disease was reflected in a differential heat shock response (HSR), with the slow-twitch soleus muscle displaying higher heat shock protein (hsp) levels over a longer duration of disease than the fast-twitch TA muscle.

Equally, examination of the NOS response revealed a significant difference in nNOS expression between the fast-twitch TA and slow-twitch soleus muscles. Furthermore, fast-twitch muscles from mSOD1 mice also demonstrated greater vulnerability to cell stress such as glucose deprivation and caffeine stress *in vitro*.

This Thesis also examined the effect of treatment with Arimoclomol, a pharmacological co-inducer of the HSR, on muscle and NMJ pathology. I found that treatment with was sufficient to decrease muscle pathology, augment the HSR and reduce mSOD1-meditated changes in nNOS expression. These findings support previous suggestions that targeting the periphery, in conjunction with the CNS, is an effective therapeutic strategy against ALS. Furthermore, that Arimoclomol's previously reported beneficial effects are due, at least in part, to its effect in the periphery.

Abbreviations

ALS	Amyotrophic lateral sclerosis
ACh	Acetylcholine
CNS	Central Nervous System
DAKO	Dakocytomation
DHPR	Dihydropyridine Receptor
DGC	Dystrophin associated glycoprotein complex
DMD	Duchenne muscular dystrophy
DPX	Di-n-butylPhthalate in Xylene
EDL	Extensor digitorum Longus
ERK	extracellular-signal-regulated kinase
fALS	Familial ALS
FOXO	Fork head box transcription factor family
GRP4	Glucose related protein-4
hsp	Heat shock protein
HSR	Heat shock response
IBM	Inclusion body myostisis
IHC	Immunohistochemistry
JNK	c-Jun N-terminal kinase
MAFbx	Muscle atrophy F box
MG	Medial Gastronemius

MGF	Mechano-growth factor
mIGF-1	Muscle expressed insulin-like growth factor
MOM	Mouse on mouse kit
mSOD1	SOD1G93A
mSOD1mus	Muscle restricted mSOD1 transgenic mice
mATPase	Myosin Adenosine Triphosphate
MuF1	Muscle RING finger 1
MyHCI	Myosin heavy chain I
MyHCIIa	Myosin heavy chain IIa
MyHCIIb	Myosin heavy chain IIb
NMJ	Neuromuscular junction
PMSF	Phenylmethylsulfonylfluride
PNS	Peripheral Nervous System
sALS	Sporadic ALS
SDH	Succinate Dehydrogenase
TA	Tibialis Anterior
tSCh	Terminal Schwann cells
WB	Western blot
WT	Wild-type non-transgenic
wtSOD1	human wild-type SOD1 transgenic
XOR	Xanathine oxidoreductase
SR	Sarcoplsmic reticulum

NMDA	N-methyl-D-aspartate
HOP	Hsc70-Hsp90-organizing protein
NMDA	N-methyl-D-aspartate
AMPA	Amino-3-hydroxy-5-methly-4-isoxazoleproprionicacid receptors
GluR2	
TDP-43	TAR DNA-binding protein-43
FUS	RNA-binding protein that was *FU*sed in *S*arcoma
OPTN	Optineurin

CONTENTS

LIST OF FIGURES

List of Tables

Chapter 1 : General Introduction

1.1 Introduction

Amyotrophic lateral sclerosis (ALS) was first described by the French physician Jean-Martin Charcot, and is characterised by a progressive degeneration of motoneurons in the spinal cord and brainstem. For a long time, the disease was regarded as one that exclusively affects motoneurons, and consequently most research focused on motoneuron pathology. However, over the last decade, it has been demonstrated that non-neuronal cells such as astroglia and microglia, within the CNS, play an important role in the onset and progression of ALS (Clement et al., 2003, Boillee et al., 2006). However, very little is known about the role that other non-neuronal cells play in the disease or how they might contribute to disease progression. In particular, the role of the muscle in the periphery has not been extensively investigated. Thus, in this Thesis, I examine pathological events occurring in muscle and whether treatment with Arimoclomol, a pharmacological co-inducer of the heat shock response, previously shown to be beneficial in ALS models, acts in the periphery as well as the CNS.

The neuromuscular junction (NMJ) is the point of interface between muscle and nerve. During the course of embryonic and early post embryonic development of the NMJ, the muscle and the motoneuron go through a phase of co-ordinated developmental steps to ensure the best arrangement for muscle innervation. There is a wealth of evidence that demonstrates the inter-dependent relationship of motoneurons and skeletal muscles throughout the formation and maturation of the NMJ (Vrbova and Gordon, 1994). Therefore, it is possible that not only can pathology within motoneurons affect muscle function, but also that events occurring within muscles may contribute to motoneuron function, stability and ultimately survival.

1.2 Formation of the NMJ

Prior to the stage when motor nerve terminals and muscle fibres first contact each other, each cell type is independent on the other for its development. However, from the point at which these two cells first make contact, they become critically

dependent upon each other for their continued development. As the motor nerve terminal reaches its target, the motoneuron growth cone makes contact and early synaptic transmission is initiated between axon terminals and muscle fibres**,** which have acetylcholine receptors (AChR) on their surface. Initially, transmission is spontaneous and evoked as well as very inefficient. Synaptic efficiency is improved by the differentiation of both presynaptic and postsynaptic sites. Presynaptic and postsynaptic differentiation is essential for improved synaptic efficiency.

Following contact between the motor nerve terminal and muscle fibre, muscle derived factors such as fibroblast growth factor 2 and laminin β^2 stimulate synaptic vesicle clustering within the axon terminal (Dai and Peng, 1995, Porter et al., 1995). Subsequently, the axon terminal develops active zones: densely packed areas with synaptic vesicles within the nerve terminal (Ko, 1985, Buchanan et al., 1989)

During postsynaptic differentiation, AChR, which up to this point are expressed in a quasi-random distribution across the sarcolemma, begin to cluster at the point of nerve contact. This process is modulated by the motoneuron via factors such as agrin, acetylcholine and neuregulin (Jo et al., 1995). Agrin released from the motor nerve results in the production of muscle-specific tyrosine kinase at the synaptic site as well as the recruitment rapsyn, which promotes AChR clustering and stabilisation (Anderson et al., 1977, Gautam et al., 1995). As AChRs cluster at the synapse, the density of extrasynaptic AChR declines, resulting in a distribution of AChRs that resembles the distribution seen in mature adult muscle.

During this period of development a number of myogenic regulatory factors such as MyoD, Myf-5, myogenin and Myf-6, and the paired box transcriptional factors, muscle cells are expressing Pax3 and Pax7. These factors regulate muscle-related gene expression and ensure the formation of the myogenic lineage (Duprey and Lesens, 1994). Further somite differentiation is due to positive signalling from Wnts

and Sonic hedgehog (Shh), as well as negative signalling from bone morphogenic factor 4 (Kobayashi et al.).

During early development, individual nerve terminals establish contact with more than one muscle fibre. This phenomenon is termed polyneuronal innervation (PNI) (Korneliussen and Jansen, 1976, Dangain and Vrbova, 1983). Thus, despite the differentiation of both the presynaptic and postsynaptic membranes, synaptic transmission efficiency is still poor as PNI, characterised by large motor units that overlap, predominates (O'Brien et al., 1982) and results in unrefined movements. As the neuromuscular system matures and PNI is reduced, movement becomes more refined. Synaptic elimination enables the reorganisation of synaptic contacts and ensures that only one highly efficient motor axon innervates a muscle fibre (Buffelli et al., 2003, Kasthuri and Lichtman, 2003). This process, which is driven by neuromuscular activity, is directed by Cholineacetyltransferase (ChAT) activity at the presynaptic site. At a given endplate, the more active nerve terminal, as determined by ChAT levels, will compete with weaker terminals. In all cases, the more active terminal will win. This results in the retraction and elimination of the weaker terminal (Buffelli et al., 2003, Kasthuri and Lichtman, 2003, Deschenes et al., 2005). The elimination of superfluous nerve terminals does not result in motoneuron death, but rather a reduction in the size of the peripheral field of motoneurons. By the end of this process, the synapse now resembles a mature NMJ, where each muscle fibre has one endplate that is innervated by a single axon (Buffelli et al., 2003).

The NMJ is plastic and can be altered by a number of factors. It can undergo pathological changes as a result of neuropathy or myopathy (Dastur and Razzak, 1973, Frey et al., 2000). For example, following denervation of muscle fibres, Neuronal nitric oxide synthase (nNOS) expression, which is normally found in presynaptic nerve terminals and the adjacent postsynaptic muscle membrane, is down regulated (Ribera et al., 1998). This precipitates the down-regulation of postsynaptic proteins such as rapsyn and agrin (Blottner and Luck, 2001). NNOS is

concurrently up-regulated in surrounding terminal Schwann cells (tSChs), where it is thought to promote sprouting (Percival et al., 2008). The role of nNOS (a protein usually found bound to a protein called syntrophin at the sarcolemma) in denervation will be discussed in greater detail in Chapter Six.

Denervation also results in tSCh activation. Once activated, tSChs from intact NMJs extend their processes and migrate to the site of injury guiding reinnervated axons (Auld & Robitalle, 2003). This results in the reinnervation of denervated endplates by different nerve terminals and the loss of the mosaic-like pattern of fibre typing seen in healthy muscle. Thus, as shown by Vrbova & Gordon (1994), muscle fibres re-innervated by a specific motoneuron will acquire the phenotype specified by that motoneuron: for example, fast firing, phasic motoneurons innervate fast fatigable muscle fibres.

1.3 Enzymatic markers of neuromuscular transmission: AChE and ChAT

ChAT and AChE are two critical enzymes involved in neuromuscular transmission. They are responsible for the metabolism and catabolism, respectively, of acetylcholine (ACh), the primary neurotransmitter at the NMJ. The expression and activity of these enzymes can be used as markers of NMJ activity (Ellman et al., 1961, Diamond et al., 1974).

ChAT is an enzyme that catalyses the synthesis of acetylcholine. It acts by catalysing the condensation reaction between Acetyl coenzyme A and Choline. The newly formed ACh is then stored in vesicles at the active zone in the presynaptic nerve terminal and is subsequently released into the synaptic cleft upon the arrival of an action potential in the presynaptic terminal.

Once the NMJ is established, the level of ACh, released by the axon terminal, increases dramatically (Witzemann, 2006). Acetyl Cholinesterase (AChE), one of the key enzymes involved in the breakdown of ACh, is expressed at the new NMJ

shortly after synaptic transmission is established. This enzyme catalyses the hydrolysis of acetylcholine into acetyl coenzyme A (AcCoA) and Choline (Wilson and Deschenes, 2005). It is found both at the presynaptic junction and postsynaptic junction of the NMJ, and in the basal lamina in very high concentrations (Wooten and Cheng, 1980, Fernandez et al., 1986). The expression of AChE is tightly regulated in the muscle by neuromuscular activity (Rotundo, 2003). AChE expression is therefore restricted to the NMJ junction where synaptic neuromuscular activity is localised.

1.4 Muscle Fibre Types

Muscle heterogeneity is a well-documented phenomenon in all mammals. This heterogeneity exists not only between muscles but also within muscles (Kernell, 1998). The three main muscle fibre groups (see Table 1.1) are typically characterised by the type of myosin heavy chain that the fibres express. These groups are Myosin heavy chain I (MyHCI), Myosin heavy chain IIa (MyHCIIa) and Myosin heavy chain IIb (MyHCIIb) (Vrbova and Gordon, 1994).

Table 1.1: Muscle fibre characteristics

	Type of fibre		
Characteristic	Slow oxidative (I)	Fast oxidative (IIa)	Fast glycolytic (IIb)
Myosin ATPase activity	LOW	HIGH	HIGH
Speed of contraction	SLOW	FAST	FAST
Fatigue resistance	HIGH	Intermediate	LOW
Oxidative capacity	HIGH	HIGH	LOW
Anaerobic enzyme content	LOW	Intermediate	HIGH
Mitochondria	MANY	MANY	FEW
Capillaries	MANY	MANY	FEW
Myoglobin content	HIGH	HIGH	LOW
Colour of fibre	RED	RED	WHITE
Glycogen content	LOW	Intermediate	HIGH
Fibre diameter	SMALL	Intermediate	LARGE
Intracellular lipid levels	HIGH	HIGH	LOW
nNOS expression	LOW	LOW	HIGH

These differences in muscle fibre type allow for the execution of a number of tasks, which are carried out by these various muscle groups (Vrbova and Gordon, 1994). These tasks range from postural actions like maintaining a standing position, to high-powered actions such as braking from a sprint, or finer movements such as writing (Vrbova and Gordon, 1994). The muscle types that give rise to these movements vary in a number of key features including their metabolism, blood supply, protein expression, as well as their activity (Aitman et al., 1979, Moruzzi and Bergamini, 1983, Reichmann and Nix, 1985, Wineinger et al., 1991, Muthny et al., 2008). This results in muscles having contractile profiles appropriate for their function. For instance, a high proportion of tonic motoneurons innervate a slow-twitch postural muscle like the soleus muscle in the leg. It has a phenotype suited to slow and regular contraction (Vrbova and Gordon, 1994). It also has a very high resistance to fatigue, which is necessary to maintain posture. In contrast, fast-twitch muscles, like the Extensor Digitorum Longus (EDL) and the Tibialis Anterior (TA) muscles, are innervated by a larger proportion of phasic motoneurons and have much faster and variable rates of contraction (Vrbova and Gordon, 1994). They are consequently far more fatigable - thus suited to rapid**,** powerful movement that occurs in short bursts.

1.5 Plasticity of the NMJ - the effects of denervation

During embryonic development, the motoneuron is critically dependant on nerve-muscle interaction for survival (Chu-Wang and Oppenheim, 1978, Oppenheim, 1987, Martinou et al., 1992, Hughes et al., 1993, Li et al., 1994, Ikeda et al., 1996). However, during post-natal development, the dependence of motoneuron on interaction with the target muscle diminishes, in rodents during early postnatal development (Lowrie et al., 1987, Harding et al., 1996). It is thought that this dependence is due, at least in part, to the release of neurotrophins from muscles (Oppenheim et al., 1991).

Following axotomy, the distal portion of the motor nerve terminal can remain functional for up to 8 hours (Kernell, 2006). After this period, the extent of ACh

release and other functional markers declines and within 24 hours the motor nerve terminal and distal axon have fragmented and disintegrated (Rotundo, 2003). During the period of denervation the muscle fibre can undergo denervation-induced atrophy. In cases of chronic denervation, this can result in up to an 80% loss in muscle mass (Kernell, 2006).

Following partial denervation, the proximal end of the motor nerve terminal can form a growth cone and grow toward the denervated empty endplates (Vrbova and Fisher, 1989, Keilhoff et al., 2002). This regenerative response is called sprouting (Brown et al., 1980, Fisher et al., 1989, Vrbova and Fisher, 1989, Rosenheimer, 1990). The phenomenon of sprouting is a natural compensatory mechanism that can result in the expansion of the motor unit, up to 8-fold their original size, and results in the maintenance of muscle innervation and therefore muscle force (Tam et al., 2002, Tam and Gordon, 2003, Steele and Yi, 2006). The process of sprouting can result in some endplates receiving innervation by more than one nerve terminal, resulting in PNI (Herrera and Werle, 1990). This situation resembles that observed during early development. There are different types of sprouting, which can be categorised morphologically into three groups as described by Brown et al. (1981):

- Ultra-terminal sprouts – where the sprout grows out of the endplate. After denervation of the endplate, the tSChs form a bridge between the innervated and denervated endplate, allowing the motoneuron terminal to arborise and grow along this tSCh sheath into the neighbouring denervated endplate (Astrow et al., 1998).
- Pre-terminal sprouts – where the motor nerve terminal bifurcates before entering the endplate.
- Nodal sprouts – where the axon sprouts at the Nodes of Ranvier, away from the terminal.

Pre-terminal and ultra-terminal sprouting are most prevalent following partial denervation (Koirala et al., 2000).

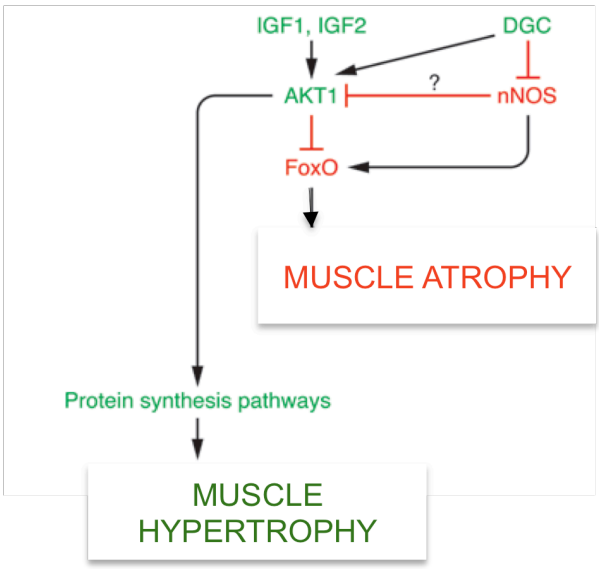

Figure 1.1: A proposed pathway for denervation induced muscle atrophy

The above schematic shows the Akt/FOXO pathway, which can initiate muscle atrophy (red) or muscle hypertrophy (green). Following denervation and muscle inactivity, nNOS dissociates from the dystrophin glycan complex (DGC) and initiates FOXO activity, which mediates the transcription of E3 ligases, resulting in muscle atrophy. (adapted from Glass et al. 2007).

A number of studies have revealed that the prevalence of sprouting within different muscles following denervation varies. For example, Rosenheimer et al. (1990) found that there is a differential sprouting response between fast-twitch and slow-twitch muscles following denervation in rodents. Their findings revealed that pre-terminal and ultra-terminal sprouting became more prevalent in the EDL muscle, in aged rodents and following denervation, compared to young rodents. In contrast, denervation did not result in any changes with age in its sprouting profile of the slow-twitch muscle soleus muscle. These results suggest that fast-twitch muscles, such as the EDL muscle are intrinsically more vulnerable to denervation with age.

Muscle atrophy is a natural consequence of denervation, disuse, injury and aging (Bodine et al., 2001). At present the aetiology behind muscle atrophy remains unclear. However, one pathway known to mediate muscle atrophy is the nNOS/Akt pathway (Rommel et al., 2001). Upon denervation, nNOS is reported to upregulate the forkhead box (FOXO) transcription factor, resulting in the upregulation of a family of E3 ligases (Stitt et al., 2004). This in turn increases the ubiquitination and degradation of proteins via the proteosome (Glass et al., 2007; see Figure 1.1).

1.6 NMJ in pathological conditions

The NMJ can undergo pathological changes as a result of neuropathy or myopathy (Dastur and Razzak, 1973, Frey et al., 2000). NMJ insult typically results in denervation and the retraction of nerve terminals. Shortly after nNOS expression, which is normally localised to presynaptic nerve terminals and the adjacent postsynaptic muscle membrane, is down-regulated (Ribera et al., 1998). This precipitates the down-regulation of postsynaptic proteins such as rapsyn and agrin (Blottner and Luck, 2001) and upregulation of nNOS in surrounding tSChs, where it is thought to promote reactivity (Percival et al., 2008).

Once activated, tSChs from intact NMJs extend their processes and migrate to the site of injury, guiding reinnervated axons (Auld & Robitalle, 2003). This results in

the random reinnervation of denervated endplates by nerve terminals and the loss of the mosaic-like pattern of muscle fibre types typically seen in healthy muscle so that grouping of muscle fibres with a similar fibre types is observed (Atkin et al., 2005). Endplates reinnervated by a motoneuron with a different firing frequency will undergo re-specification and become a member of that motor unit (Vrbova and Gordon, 1994).

1.7 Amyotrophic lateral Sclerosis

Amyotrophic lateral sclerosis (ALS) is the most common form of adult motoneuron disease, affecting approximately 1-2 per 100,000 of the population (Bruijn et al., 2004). ALS is a progressive neurodegenerative disease, with symptomatic onset characteristically occurring after midlife (Bruijn et al., 2004). Life expectancy is approximately 2-5 years from the onset of disease symptoms (Cleveland and Rothstein, 2001). The disease is characterised by the degeneration of large alpha motoneurons in the motor cortex and spinal cord (Bruijn et al., 2004). Degeneration of these motoneurons is reflected by a progressive decline in muscle function with accompanying muscle atrophy. Spasticity, hyperreflexia and extensor plantar reflexes are the clinical manifestations of upper motoneuron degeneration (Bento-Abreu et al., 2008). Symptoms include muscle paresis, weight loss, muscle paresis and eventual paralysis. Ultimately, death occurs usually as the result of failure of respiratory muscles, often exacerbated by swallowing problems.

ALS can also be considered as a neuromuscular disorder (NMD), and indeed some of the pathological characteristics of ALS muscle are shared with other non-neurodegenerative NMDs such as Duchenne Muscular Dystrophy (DMD) and Inclusion Body Myositis (IBM). As illustrated in Table 1.2, these neuromuscular disorders have some shared pathology such as denervation, muscle atrophy, mitochondrial dysfunction and the preferential vulnerability of fast-twitch muscles to disease (Lott and Landesman, 1984).

Table 1.2: Myopathies that share symptoms/pathology with ALS

Disease	Shared pathology and symptoms	Reference
Duchenne muscular disease	Reduced nNOS expression and NO activity, denervation & progressive muscle atrophy, Ca^{2+} signalling dysfunction, oxidative stress & increased fast-twitch fibre vulnerability.	(Dastur and Razzak, 1973, Gissel, 2005, Whitehead et al., 2006, Adams et al., 2008)
Inclusion body myositis	Muscle atrophy, weakness & oxidative stress & increased fast-twitch fibre vulnerability.	(Amato and Barohn, 2009, Askanas et al., 2009, Parker et al., 2009)

Despite intensive research, particularly over the last 20 years, there has been little success in the treatment of ALS. At present, the only drug that is available is Riluzole, which only extends lifespan by approximately 2-4 months (Bensimon et al., 1994, Miller, 2003, Traynor et al., 2006).

1.7.1 The genetics of ALS pathology

The majority of cases (90%) have no clear genetic cause and are therefore usually defined as sporadic ALS (sALS). While approximately 10% of ALS cases have a clear genetic determinant and are thus termed familial ALS (fALS). Several genes have now been identified to cause fALS. The genes known to cause classical ALS as well as juvenile onset ALS and those responsible for ALS with an autosomal recessive genetic component are detailed in Table 1.3 and Table 1.4, respectively. The associated proteins and their function are summarised in Table 1.3 and 1.4, respectively. Despite the recent identification of new gene mutations that cause ALS, including TAR DNA-binding protein-43 (TDP-43) (Kuzuhara, 2008), RNA-binding protein that was *FU*sed in *S*arcoma (FUS) (Lagier-Tourenne and Cleveland, 2009) and optineurin (OPTN) (Maruyama et al., 2010). These mutations each account for only 1-4% and 4-5% of fALS cases for TDP-43 and FUS, respectively. Due to its recent identification the percentage of fALS cases due to OPTN remains unclear.

The large majority of fALS cases are due to mutations in the Copper/Zinc Superoxide dismutase (SOD1) gene. This mutation was first identified in 1993 by Rosen et al., still accounts for 15-20% of fALS cases (Shaw et al., 2001, Bento-Abreu et al., 2008).

1.8 Mutant Copper/Zinc Superoxide Dismutase

In 1993, a mutation in the SOD1 gene, on chromosome 21q22.1, was first identified as causative for ALS (Rosen et al., 1993). Today, more than 150 different mutations have been identified in the SOD1 gene (Turner and Talbot, 2008).

The SOD1 enzyme is a ubiquitously expressed, predominantly cytoplasmic enzyme, which acts as a cellular antioxidant by catalysing the conversion of superoxide radicals into hydrogen peroxide and water.

Table 1.3 Classical ALS

Gene	Loci	Protein	Function	Reference
ALS1 (SOD1)	21q22.1	SOD1	Detoxifies O_2- to H_2O_2 & prevents oxidative damage	Siddique et al., 1991
ALS3	18q21	-	-	Hand et al., 1993
ALS6	16p11	FUS	Nuclear protein that is involved in DNA & RNA metabolism	Ruddy et al., 2003
ALS7	20p13	-	-	Sapp et al., 2003
ALS9	14q11	Angiogenin	Mediates vasculature & is induced by hypoxia	Wu et al., 2007
ALS10	1p36	TDP-43	Involved in RNA biogenesis, apoptosis & cell division	(Ferrari et al., 2011)

Table 1.4 ALS

Gene	Loci	Protein	Function	Reference
ALS2	2q33	Alsin	Involved in vesicle transport & intracellular trafficking	Kunita et al., 2004
ALS4	9q34	Senataxin	DNA helicase involved in DNA repair and RNA production.	Chance et al., 1998
ALS5	15q21	Spatacsin	Possibly membrane associated	Hentati et al., 1998
ALS8	20q13.33	Vesicle associated membrane protein B	Associated with ER & Golgi membranes	Sapp et al., 2003
ALS 12	10p15	OPTN	Interacts with Huntingtin & regulates TNF-α induced activation of NF-κB	(Maruyama et al., 2010)
ALS with frontotemporal dementia 1	9q21-q22	-	-	Hosler et al., 2000
ALS with frontotemporal dementia 2	9p21.3-p13.2	-	-	Hosler et al., 2000

The functional enzyme exists as a homodimer that requires copper and zinc binding for catalytic activity and stabilisation, respectively (Shaw et al., 2001), reducing the concentration of free superoxide radicals in the cell by catalysing the conversion of superoxide to oxygen and hydrogen peroxide. This is illustrated below:

$$Cu^{2+}\text{–SOD1} + O_2 \rightarrow Cu^{2+}\text{–SOD1} + O_2$$

$$Cu^{2+}\text{–SOD1} + O_2 - 2H+ \rightarrow Cu^{2+}\text{–SOD1} + H_2O_2$$

Initially, mutations in the SOD1 enzyme were suggested to reduce the dismutase activity and enhance oxidative stress; however, genetic ablation of endogenous SOD1 did not induce motoneuron disease in knockout mice (Reaume et al., 1996). Furthermore, mutant SOD1 (mSOD1) was found to have similar catalytic activity to wild type (WT) (Bruijn et al., 2004).

In 1994, the first genetic mouse model of ALS was generated (Gurney et al, 1994). These mice express the human SOD1 gene containing a Glycine to Alanine base pair mutation at the 93rd codon (Gurney et al., 1994). Following the initial generation of the G93A mutant mice, a number of additional transgenic mice expressing a variety of SOD1 mutations have been generated, and been found to exhibit a phenotype that closely resembles human ALS (Gurney et al., 1994, Bruijn and Cleveland, 1996). Despite intensive investigation, the precise mechanism by which mutations in this ubiquitously expressed gene results in motoneuron degeneration remains unclear. The mechanism is known to involve a toxic gain of function, as knockout SOD1 mice do not develop motoneuron pathology (Bruijn et al., 2004). This toxic gain of function is independent of SOD1 activity levels (Borchelt et al., 1994, Dal Canto and Gurney, 1994, Ripps et al., 1995, Wong et al., 1995, Bruijn and Cleveland, 1996).

The generation of transgenic mice expressing mutations in the human SOD1 enzyme has provided an excellent research tool to investigate the pathogenesis of ALS. It has also enabled the preclinical testing of potential therapeutic agents. Indeed, mSOD1 mice demonstrate many of the pathological features seen in humans, including neurofilament inclusions, ubiquitin positive aggregates and selective motoneuron loss (Gurney, 1994, Ripps et al., 1995, Wong et al., 1995,

Bruijn and Cleveland, 1996). mSOD1 transgenic mice expressing the G93A mutation are the most widely used animal model of ALS and have therefore been well characterised. There are two variants of this model: the most commonly used high copy number variant, which express mSOD1 approximately 25 times higher than the normal level and the low copy number transgenic mouse, which express mSOD1 approximately 8 times higher than normal levels (Henriques et al.). In this study, the high copy number mice have been used in all experiments and are referred to simply as mSOD1 mice.

mSOD1 mice develop muscle fasciculation, weight loss, hindlimb paresis and eventual hindlimb paralysis and display selective motoneuron death (Ilieva et al., 2009). The mSOD1 mice on the BL6/SJL background typically exhibit signs of hindlimb weakness at 75 days**,** progressing to severe muscle paralysis and atrophy by 120 days and endstage at around 125-130 days of age (Gurney et al., 1994, Kieran et al., 2004). They undergo progressive motoneuron death from approximately 70-80 days until endstage (Gurney et al., 1994). By this stage over 70% of motoneurons have died (Kieran et al., 2004, Sharp et al., 2006). Using mSOD1 mice**,** it has been possible to identify a number of important cellular pathways that are affected in ALS.

1.9 ALS Pathogenesis in the CNS

A number of pathological mechanisms are known to contribute to the selective degeneration of motoneurons in ALS (Ilieva et al., 2009) and are summarised in Fig.1.2. Since a large number of pathological mechanisms involved in the aetiology of the disease, a full discussion of each mechanism is beyond the scope of this Thesis. Therefore, some of the mechanisms shall only be discussed briefly, whilst those that have greater relevance to the experiments undertaken within this Thesis shall be expanded upon in relevant Chapters.

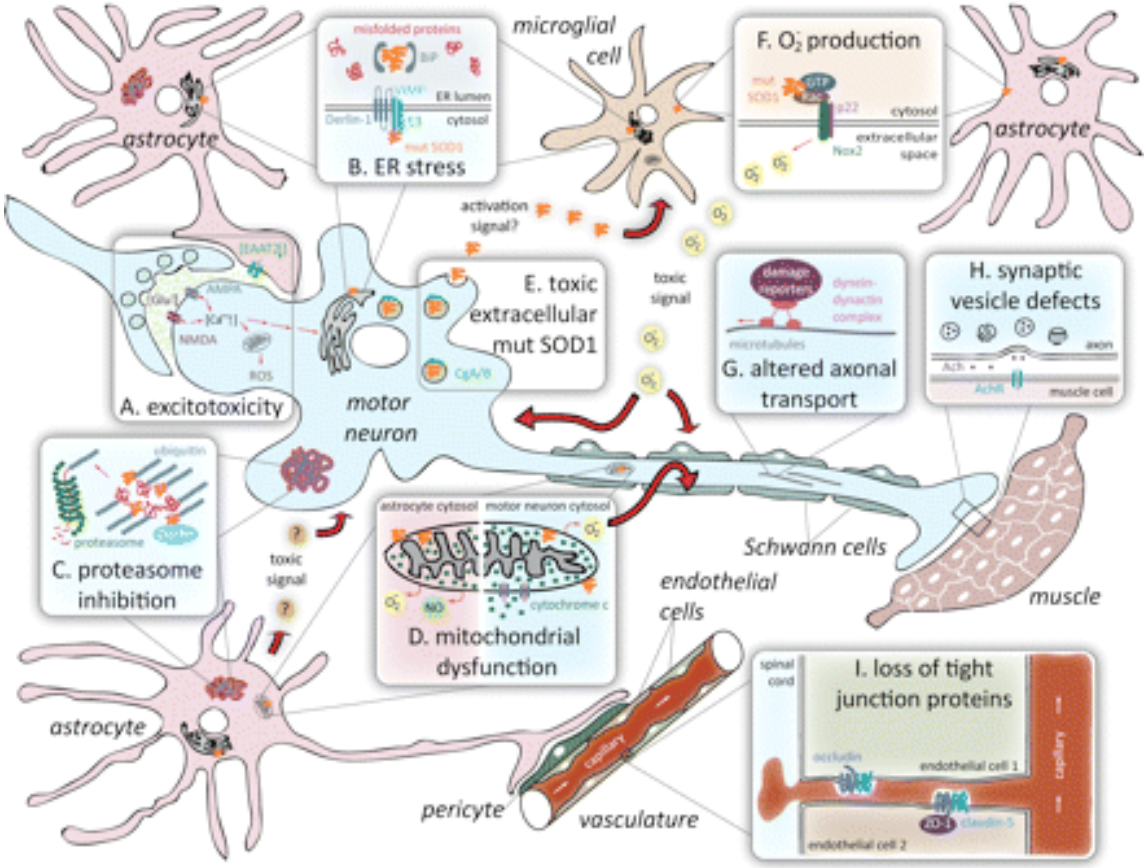

Figure 1.2 Proposed pathological mechanisms in ALS (insert the altered text)

(A) Excitotoxicity is the hyperactivation of motoneurons resulting from the slow removal of glutamate from synapses. (B) ER stress is induced by the abnormal interaction of mSOD1 with ER proteins. (C) Proteasome dysfunction results in ubiquitinated misfolded protein aggregates. (D) Mitochondrial dysfunction provokes the release of cytochrome-C in motoneurons. (E) Oxidative stress caused by microglia and astrocytes damages neighbouring motoneurons. (F) Axonal transport dysfunction resulting in decreased retrograde transport of proteins. Image from (Ilieva et al., 2009).

1.9.1 Motoneuron Pathology

At an ultrastructural level, degenerating motoneurons in ALS patients display accumulations of intermediate filaments and ubiqutinylated intracellular aggregates in perikarya and proximal axons, abnormalities in mitochondrial structure and mitochondrial degeneration, as well as fragmentation of the Golgi apparatus (Gomes et al., 2008). Many of these features are also characteristic of other neurodegenerative conditions (Kanazawa, 2001). A number of pathological pathways are activated in ALS pathogenesis, including glutamate excitotoxicity, oxidative damage, mitochondrial dysfunction, protein aggregation, axonal transport deficits and neuroinflammation (Bento-Abreu et al., 2008).

1.9.2 Glutamate excitotoxicity

In non-pathological conditions, glutamate acts as an excitatory neurotransmitter in the CNS and is released from neurons, activating glutamate receptors on postsynaptic neurons. These glutamate receptors can be classified as ionotrophic, or metabotrophic receptors. Ionotrophic receptors largely fall into three categories: N-methyl-D-aspartate (NMDA) of amino-3-hydroxy-5-methly-4-isoxazoleproprionic acid receptors (AMPA) and kainaite receptors (Van Den Bosch and Robberecht, 2008). In non-pathological conditions, NMDA receptors are permeable to Na^+, Ca^{2+} and K^+, AMPA receptors are only permeable to Na^+ and K^+, unless they are missing a functional GluR2 unit making them more permeable to Ca^{2+} - a feature commonly found in AMPA receptors on motoneurons (Van Den Bosch and Robberecht, 2008).

In ALS patients and mSOD1 mice, NMDA and AMPA receptors become excessively activated causing the excessive firing of motor neurons. The receptors also became more permeable to Ca^{2+}, resulting in Na+ and Ca^{2+} influx, resulting in ER stress as well as disrupted Ca^{2+} signalling (Takuma et al., 1999, Bruijn et al., 2004).

1.9.3 Oxidative Stress

In non-pathological conditions, anti-oxidative enzymes like SOD1 and SOD2 are present to reduce the levels of H_2O_2 and super oxide. Following the discovery of mSOD1 and the generation of mSOD1 mice, the role of oxidative stress in the disease was investigated. Studies examining ALS patients and mSOD1 mice for markers of oxidative stress revealed elevated protein nitrosylation, lipid peroxidation and protein carboxylation in the spinal cord and CNS (Ferrante et al., 1997).

1.9.4 Mitochondrial dysfunction

Mitochondrial dysfunction is also present in motoneuron in ALS. The main function of mitochondria is to generate energy, in the form of ATP. In ALS, mitochondria, which are sensitive to damage from free radicals, are thought to become compromised by increased generation of reactive oxygen species (ROS) and reactive nitrogen species (RNS) (Heath and Shaw, 2002), which in turn results in alterations in the mitochondrial membrane potential and exacerbates excitotoxicity (Heath and Shaw, 2002). In addition, in mSOD1 mice, mSOD1 has been found to accumulate in the intermembrane space of mitochondria, resulting in mitochondrial vacuolisation (Jaarsma et al., 2000). However, mitochondrial vacuolisation is not observed in ALS patients (Sasaki and Iwata, 1998). Mitochondrial dysfunction causes metabolic dysfunction within the motoneuron (Browne et al., 1998) as well as potentially precipitating the release of cytochrome-C into the cytosol, initiating apoptosis (Higgins et al., 2003).

1.9.5 Protein aggregation

Protein aggregation is a well-characterised pathomechanism in several neurodegenerative disorders, including ALS. In ALS, intracellular aggregates are present in motoneurons from the spinal cord of ALS patients as well as mSOD1 mice (Leigh et al., 1991, Bruijn and Cleveland, 1996, Cleveland et al., 1996, Watanabe et al., 2001, Jonsson et al., 2004). However, as in other neurodegenerative disorders, their precise role in the disease is unclear. One

school of thought is that aggregates exert a protective effect, sequestering aberrant proteins away from cell organelles (Imai et al., 2003, Arrasate et al., 2004). However, the predominant view is that these aggregates arise from misfolded proteins that accumulate as a result of inadequate refolding by molecular chaperones, which are often sequestered (Garofalo et al., 1991, Bruijn and Cleveland, 1996, Jaarsma et al., 2000, Watanabe et al., 2001). Intracellular aggregations of misfolded proteins found in motoneurons and glial cells are thought to exert toxicity by the disruption of axonal transport, as well as increasing the likelihood of aberrant protein interactions and the sequestration of key organelles and essential proteins (Bruijn and Cleveland, 1996, Watanabe et al., 2001, Cheroni et al., 2005). Ultimately, these aggregates are thought to overburden the proteasome within motoneurons (Johnston et al., 2000, Bruijn et al., 2004), further increasing their prevalence.

1.9.6 The role of exosomes in ALS

Exosomes are small membranous vesicles secreted by a number of cell types and can be isolated from conditioned cell media. Exosome biogenesis involves the inward budding of multivesicular bodies to form intraluminal vesicles. Intraluminal vesicles of multivesicular bodies are either sorted for degradation into lysosomes, or secreted as exosomes (Trajkovic et al., 2008). The mechanisms underlying the sorting of the membrane into the different populations of intraluminal vesicles are unknown. However, this occurs via one of two known pathways: either via a pathway that requires endosomal sorting complexes endosomal required for transport (ESCRT) or sphingolipid ceramides (Cutler et al., 2002).

The release of the vesicles into the extracellular environment as exosomes, enables cell-cell signalling, as well as the transferral of pathogens as seen in Creutzfeldt-Jakob disease (Vella et al., 2008). Interestingly, exosome mediated pathology has also been proposed as a mechanism for neuron death in

neurodegenerative disease. Indeed, in Alzheimer's disease, recent studies have found that APP fragments are associated with exosomes (Vella et al., 2008).

A role for the exosome mediated pathogenesis has also been found in ALS. In 2002 Cutler et al. reported increased levels of sphingomyelin, ceramides (found in purified exosomes), and cholesterol esters in the spinal cords of ALS patients and in mSOD1 mice, which preceded symptomatic onset. They also showed that the pharmacological inhibition of sphingolipid synthesis prevented the accumulation of ceramides, sphingomyelin, and cholesterol esters and protected motoneurons from exosome mediate oxidative stress and cell death (Cutler et al., 2002). Furthermore, ESCRT dysfunction, which is present in ALS (Gomes et al., 2007), has been shown to facilitate the accumulation of cytoplasmic protein aggregates containing ubiquitin, and TDP-43 (Rusten & Simonsen, 2008).

1.9.7 The role of non-neuronal cells in ALS pathogenesis

The French physiologist Claude Bernard first established the idea that cells function autonomously (Reynolds, 2007). From that time until 2003, researchers assumed that damage within a specific cell population was sufficient to cause disease (Ilieva et al., 2009). Thus, for a number of years research into ALS pathogenesis focused primarily on motoneurons. However, Clement et al. (2003) with mouse chimeras elegantly demonstrated that the transplantation of neighbouring WT glia into the spinal cord of mSOD1 mice was sufficient to reduce motoneuron death and prolong survival. The converse was shown to cause the development of ubiquitinated inclusions and also diminished motoneuron viability. This study sparked extensive research into the role of glia in ALS. However, while non-neuronal cells have been shown to influence disease progression, the exclusive expression of mSOD1 in motoneurons, muscle or glia, is not sufficient to induce the progressive loss of motoneurons that typifies ALS (Gong et al., 2000, Pramatarova et al., 2001, Wong and Martin). Indeed, whether astroglia were a primary target of ALS was examined by Gong et al. (2000). The selective transgenic expression of mSOD1 in the astrocytes of mice resulted in significant

glial pathology, but was insufficient to alter motoneuron morphology or survival. Likewise, Pramatarova et al. (2001) showed that selective expression in neurons did not result in any motor deficits (Pramatarova et al., 2001). However, it is now widely agreed that astrocytes and microglia determine disease duration with increased mSOD1 expression in microglia and astrocytes accelerating disease progression (Bento-Abreu et al., 2008). While the increased expression of mSOD1 in Schwann cells slows disease progression (Ilieva et al., 2009).

1.10 Muscle pathology in ALS

In ALS, muscle fasciculations and muscle weakness and paralysis are the main manifestation of the disease. Indeed, the first signs of disease appear in muscle, with denervation of the NMJ occurring prior to motoneuron death (Frey et al., 2000, Fischer et al., 2004, Pun et al., 2006, Steele and Yi, 2006).

1.10.1 Selective vulnerability of fast-twitch muscle fibres in ALS

However, studies on the muscles of ALS patients and mSOD1 mice have revealed that the extent and rate of denervation between different muscle types varies. Examination of muscle in mSOD1 mice has shown that some muscles are affected earlier and to a greater extent than other muscles (Frey et al., 2000; Fisher et al., 2004; Hegedus et al., 2007). Thus, there appears to be a preferential vulnerability of muscles that are largely composed of fast-twitch muscle fibres, and muscles with a high proportion of slow-twitch fibres are affected later in the disease and usually to a lesser extent. Thus, in mSOD1 mice, fast-twitch muscles such as the tibialis anterior (TA), medial gastrocnemius (MG) and extensor digitorum longus (EDL) deteriorate faster and more dramatically than slow-twitch muscles such as the soleus muscle (Frey et al., 2000).

While it is now well established that some muscles have a greater susceptibility disease than other groups, the underlying cause of this preferential vulnerability of

specific muscle fibres, or more specifically, the motoneurons that innervate them, remains unknown.

The observation that fast-twitch muscles fibres are more vulnerable to disease is also observed in other neuromuscular diseases. This phenomenon is also seen in both IBM and Charcot Marie Tooth disease, which represent neuromuscular diseases with heterogeneous aetiology (Michael et al., 2006). This preferential vulnerability of fast-twitch muscle fibres to disease suggests that there may be a common feature within fast-twitch muscles that facilitates pathological changes. Conversely, there may be a feature in slow-twitch muscles that leaves them better equipped to resist pathological insult. There is evidence that suggests that the former possibility is more likely. For example, it has been shown that fast-twitch muscles are more susceptible to oxidative stress, as they are generally only equipped to handle short-lived rises in ROS, a key mediator of oxidative stress (Ferreira and Reid, 2008). Fast muscles also have a less robust heat shock response and have a lower concentration of anti-oxidative proteins (Daugaurd et al., 2001; Tarricone et al., 2008; Kieran et al., 2004), which may alter their response to systemic stress.

Until recently, it was thought that changes in muscle phenotype are dependent on innervation characteristics and are not determined by the muscle (Kernell, 2006). However, studies by Santos et al (2003) and Frey et al (2000a) suggest that motor units of fast-fatigable nature are more likely to undergo denervation (Santos & Caroni, 2003). Additionally, it has been suggested that they may also have a decreased capacity for sprouting, both in ALS and non-ALS mice (Santos and Caroni, 2003). Equally, the fast-twitch glycolytic fibres are some of the first to atrophy with old age (Lexell, 1995).

In ALS, the reason for the differential vulnerability of fast-twitch and slow-twitch muscle fibres to disease is still unclear. Although the differential vulnerability of these muscle fibres may in fact lie within the specific motoneurons that innervate

them, it is also possible that fast-twitch muscles are intrinsically more vulnerable to stress, since evidence shows that they are more vulnerable to a variety of pathological stresses such as ischemia and reperfusion injury (David et al., 2007). A small number of studies have examined muscle pathology in an aneural setting and some have examined the propagation of muscle phenotype *in vitro* (Bryla and Karasinski, 2001). However, to date there is little evidence examining the differential vulnerability of fast and slow-twitch mSOD1 muscles in an aneural environment.

One of the consequences of the selective loss of fast-twitch muscle fibres in ALS is the transformation in the phenotype of fast-twitch muscles such as TA and EDL, into muscles with a slow-twitch phenotype composed of highly oxidative muscle fibres (Sharp et al., 2005). This phenotypic transformation is reflected in a change in the contractile characteristics of the muscle: muscles that normally contract and relax rapidly change into muscles with prolonged contraction and relaxation times (Kieran et al., 2004). It is likely that this transformation in fast-twitch muscle phenotype is the result of the selective loss of fast phasic motoneurons and the consequent compensatory sprouting of less vulnerable, surviving motoneurons that normally innervate slow-twitch muscle (Amphlett et al., 1975), with a tonic pattern of activity that drives the expression of a slow muscle phenotype (Sharp et al., 2005).

It is known that the phenotype of a muscle fibre is largely determined by the activity pattern of the innervating motoneuron (Tyc and Vrbova, 1995, Slawinska et al., 1996). Thus, a similar 'fast-to-slow' twitch transformation is seen experimentally when a fast-twitch muscle is cross-innervated by a nerve from a slow-twitch muscle (Ip et al., 1988). However, although a 'fast-to-slow' muscle transformation also occurs following adult nerve injury (Lowrie and Vrbova, 1984), in this case the transformation of the muscle is not the result of the selective death of fast motoneurons and subsequent sprouting of slow motoneurons, but is rather due to a change in the activity pattern of the reinnervating motoneurons. Following nerve

injury, normally fast motoneurons become hyperactive and exhibit an increase in the level of tonic activity, which results in a change in the muscle fibre phenotype (Navarrete &Vrbova, 1984).

1.10.2 Mitochondrial dysfunction in ALS muscle

It is well established that alterations in mitochondrial function are not restricted to motoneurons in mutant SOD1 mice, but also exist in mSOD1 muscle (Dupuis et al., 2003). In mSOD1 muscle mitochondria display altered ATP production as well as calcium signalling (Dupuis et al., 2003), which is likely to result in the generation of ROS. Furthermore, levels of mitochondrial uncoupling proteins are elevated even before disease onset. This is not observed in motoneurons, despite the fact that mitochondrial dysfunction is considered to be a contributing factor to disease aetiology in the CNS (Bruijn and Cudkowicz, 2006). Dupuis et al (2009) also found reduced ATP levels in myogenic but not neural tissue. Furthermore, these changes were independent of denervation, but appear to reflect mSOD1-mediated pathophysiological changes that are exclusive to the muscle and may be evidence of an underlying systemic metabolic dysfunction (Fergani et al., 2007).

A large number of cellular stresses are due to elevated oxidative species and aberrant protein-protein interactions affecting diverse cellular systems, such as energy metabolism and muscle regeneration (Dupuis et al., 2009, Dupuis and Loeffler, 2009). Mitochondrial dysfunction in ALS muscle is discussed in greater detail in Chapter 6.

1.10.3 Oxidative stress in ALS muscle

Oxidative stress arises from an imbalance between the rate of production of reactive oxygen species (ROS) and the rate of the elimination of ROS. Markers of oxidative damage include increased levels of ROS, decreased glutathione levels, lipid peroxidation and DNA damage (Barber et al., 2006). ALS patients display evidence of oxidative stress with increased protein carboxyl levels and 3-

nitrityrosine in the CNS (Abe et al., 1997a, Abe et al., 1997b). This is also present in spinal cord of mSOD1 mice before disease onset (Bruijn et al., 2004).

Elevated ROS levels in skeletal muscle occur frequently, even under normal physiological conditions such as strenuous exercise (Ferreira and Reid, 2008). This can result in contractile damage and raised ROS levels. Consequently, skeletal muscle has adaptive mechanisms that enable the fast induction of anti-oxidative pathways within the muscle fibre, such as the upregulation of anti-oxidative enzymes, such as superoxide dismutase and catalase as well as increased expression of cytoprotective heat shock proteins (hsps) (McArdle et al., 2001). Despite these protective mechanisms, in mSOD1 mice there is evidence of oxidative damage in muscle, with lipid peroxidation, increased COX-1 activity and levels of protein carbonyls (Soraru et al., 2007, Dobrowolny et al., 2008, Wong and Martin, 2010). Muscle from ALS patients has been shown to display higher levels of lipid peroxidation (Siciliano et al., 2002), as well as increased generation of mitochondrial uncoupling proteins (Dupuis et al., 2009). It has been proposed that continued oxidative stress within mSOD1 muscle contributes to mitochondrial dysfunction in mSOD1 muscle and subsequently disrupted metabolic function within the muscle (Dupuis et al., 2003).

Some muscles are better adapted to deal with oxidative stress than others. These muscles often have a high oxidative capacity, typically rich in slow-twitch muscle fibres. Currently, there is limited knowledge of how oxidative stress that arises from physiological activity affects mSOD1 muscle pathology. This will be discussed in greater depth in Chapter Six.

1.10.4 Neuronal NOS expression in muscle

Neuronal NOS (nNOS) has been implicated in muscle atrophy and reinnervation. nNOS has been shown to be differentially regulated in the CNS of mSOD1 mice (Lee et al., 2009). However, it is most abundantly expressed in skeletal muscle.

Notably, nNOS is preferentially expressed in fast-twitch muscle in mice (Soraru et al., 2007). There is some evidence that indicates that nNOS and possibly inducible nitric oxide synthase (iNOS) may play a role in muscle pathology in ALS and mSOD1 mice (Soraru et al., 2007).

In the PNS, nNOS acts predominantly as a signalling protein, where it has been implicated in the activation of Forkhead box (FOXO) transcription factors (Suzuki et al., 2007b). The FOXO family of transcription factors are involved in a number of cellular events including the induction of muscle atrophy (Suzuki et al., 2007b). nNOS expression has also been implicated in nerve terminal sprouting. Indeed, using nNOS-deficient mice, Marques et al. (2006) have shown that nNOS plays a pivotal role in the regenerative effort at the NMJ following denervation. Following denervation, nNOS-/- mice were capable of displaying pre-terminal sprouting but not ultra-terminal sprouting. NNOS has also been implicated in tSCh activation (Marques et al., 2006), and reactive tSChs are integral to ultra-terminal sprouting. Thus, it is possible that nNOS may be involved in the differential regulation of muscles response to denervation and muscle atrophy. Changes in nNOS levels in muscles of mSOD1 mice are expanded upon in the Thesis in Chapter 5.

1.11 The role of the Heat Shock Response in ALS

The term ‘Heat shock response’ (HSR) was first established by Ritossa in 1962, after observing induction of a family of proteins in the salivary glands of Drosophila melanogaster larvae, following incubation at 30-32°C (Soti and Csermely, 2006). It is an evolutionarily conserved, ubiquitously expressed, cell defence mechanism that results in the induction and upregulation of cytoprotective proteins, following exposure to a variety of cell stresses. These proteins are called hsps and are responsible for the refolding of misfolded proteins and targeting irreparably damaged proteins to the proteosome for degradation (Bruijn et al., 2004). hsps therefore work to maintain normal protein-protein interactions in the cell under normal conditions and conditions of stress (Brown, 2007) and are essential for the

homeostasis of the protein pathway. However, they also have strong anti-apoptotic capabilities (Tonkiss and Calderwood, 2005, Voellmy and Boellmann, 2007).

There are six families of heat shock proteins, defined according to their molecular weight. The main families of hsps are: the small hsp25; hsp40; hsp60; hsp70; hsp90; hsp110 and hsp170. The largest families of Hsps are the Hsp70 and Hsp90 families (Brown, 2007). These have inducible isoforms that can be upregulated upon a variety of cellular insults (Wood et al., 2003). This phenomenon is associated with increased cellular tolerance to oxidative stress, glutamatergic excitotoxicity and trauma (Bento-Abreu et al., 2008). Ultimately, the induction of the HSR acts to increase cell survival.

Two key features of all neurodegenerative disorders are protein aggregation and aberrant protein interactions, which suggests that elements of the heat shock response may be involved in the aetiology of the disease (Wood et al., 2003). The expression of most hsps is controlled by the transcription factor, Heat shock factor-1 (HSF-1), which trimerises upon activation, translocating to the heat shock element (HSE) in the nucleus to initiate the transcription of hsp genes (Henderson et al., 1996)

The HSR has been implicated in the pathogenesis of ALS, since motoneurons have a surprisingly reduced ability to upregulate hsp expression upon exposure to cellular stress (Batulan et al., 2003). Thus, it has been proposed that this inability to induce a robust HSR may contribute, at least in part, to the selective vulnerability of motoneurons in ALS. Furthermore, it appears that motoneurons may be dependent on hsps expressed and secreted by their neighbouring non-neuronal cells (Tonkiss and Calderwood, 2005, Brown, 2007).

1.11.1 Hsp90

Hsp90, a 90kDa protein chaperone, is one of the most abundant proteins in mammalian cells. It is integral to cell proliferation and differentiation, signal transduction, protein folding and degradation as well as cell survival and adaptation (Sreedhar et al., 2004). Hsp90 has a number of isoforms: hsp90β: the constitutively expressed form, hsp90α: the inducible form, hsp90N: a glucose related protein-4(GRP94) found in the endoplasmic reticulum and hsp75/TRAP, which is found in mitochondria. During muscle development, hsp90 plays a fundamental role where it is essential for myofibrillogenesis (Willis et al., 2009).

Hsp90 is normally found within the sarcoplasm of muscle, where it exists as a homodimer or is associated with its client proteins, such as HSF1 (Ali et al., 1998). Hsp90 has over one hundred clients, the majority of which are involved in signal transduction (Richter and Buchner, 2001). Hsp90's actions fall largely into two categories. When bound with its chaperones p50 & p23, hsp90 targets misfolded proteins, stabilising them and protecting them from degradation by the proteosome (Taiyab et al., 2009); alternatively, hsp90 can also facilitate protein degradation, via the proteosome, when bound to hsp70, Hsc70-Hsp90-organizing protein (HOP) and other chaperones (Adachi et al., 2007). Following cell stress, hsp90 targets misfolded proteins within the cytosol and results in the release of HSF1, which trimerises and induces the HSR (Ali et al., 1998, Bornfeldt, 2000).

1.11.2 Hsp70

Four major forms of hsp70 have been found in muscle:

- The heat shock cognate, which weighs 73kDa (HSC70) and is a constitutively expressed form of hsp70.
- The glucose related protein, which weighs 75kDa (GRP75) and is found in mitochondria.

- The inducible hsp70 (hsp72), which weighs 73kDa and is induced following the trimerisation of HSF1.
- The glucose related protein, which weighs 78kDa (GRP78) and is found in the sarcoplasmic reticulum.

The actions of hsp72 include the stabilization of partially folded proteins via interactions with HOP and hsp90, the re-folding of denatured proteins and the targeting of misfolded proteins to the proteosome (Asea, 2007). This is carried out via Carboxyl-terminus of hsp70 Interacting Protein (CHIP) interactions (Kampinga et al., 2003). Hsp72 also has strong anti-apoptotic properties, blocking the recruitment of procaspase-9 following cytochrome-C release, thereby reducing the likelihood of cell apoptosis (Gabai et al., 2002). Hsp72 is also known to increase NMJ activity (Karunanithi et al., 2002).

1.11.3 Hsp60

Hsp60 is a mitochondrial and cytosolic protein that is found in all cells and in large quantities in skeletal muscle (Oishi et al., 2002). Hsp60 expression in muscle is known to vary with mitochondrial content (Lin et al., 2001). It is therefore expressed at greater levels in slow-twitch muscles such as the soleus muscle (Carrier et al., 2000, Liu and Steinacker, 2001, Oishi et al., 2002). Following exercise stress, hsp60 levels increase are five times greater in the slow-twitch soleus muscle than in the fast-twitch EDL muscle in mice (McArdle et al., 2001). Hsp60 synthesis is induced in skeletal muscle following a number of stresses within the muscle, including: exercise, ischemia reperfusion injury and mitochondrial uncoupling (McArdle et al., 2001).

1.11.4 Hsp25

Hsp25 is the murine orthologue of human hsp27. In the unstressed cell, it exists in large 400-800kDa oligomers (Adhikari et al., 2004). In this form, it facilitates the correct folding of proteins and carries out other essential chaperone duties

(Abruzzo et al., 2010). In muscle, hsp25 is primarily involved in the maintenance of cytoskeletal integrity of the muscle fibre, both during development as well as throughout adulthood (Ding and Candido, 2000). Hsp25 has been shown to stabilise microfilaments within the muscle fibre, via its associations with Z-disks within fibres (Huey et al., 2004). Following cell stress, hsp25 is a key component of the HSR and has strong anti-apoptotic actions. Hsp25 is also involved in minimising oxidative stress within the muscle fibre (Lee et al., 2008).

Following the induction of the HSR, hsp25 is quickly phosphorylated at a number of sites. This leaves it unable to bind to itself or form large oligomeric structures (Bryantsev et al., 2002). As a monomer, it is able to translocate to the nucleus as well as F-actin filaments within the cell (Ho et al., 2006). In muscle, this transformation is so complete that hsp25 is found almost exclusively as a monomer following the activation of the HSR (Ding and Candido, 2000, Adhikari et al., 2004). During this period, hsp25 is redistributed from the cytosol to actin filaments. As a monomer, hsp25 binds preferentially to misfolded proteins in the muscle fibre and is known to bind with mSOD1 in motoneurons where it traps aggregate prone folding intermediates and prevents further aggregation (Okado-Matsumoto and Fridovich, 2002) and targets the misfolded proteins to the proteosome. In motoneurons, hsp25 accumulates in the nucleus during the HSR, and directs the degradation of misfolded proteins within the nucleus (Lee et al., 2008).

1.11.4.1 Heat shock protein expression in the muscle

Hsps are differentially expressed in fast and slow-twitch muscles. Interestingly, the difference in regenerative capacity between fast and slow-twitch muscles is reflected in the hsp profile of these muscles (Oishi et al., 2005). Slow-twitch muscles have a high constitutive expression of many of the most prominent hsps, including the Hsp70 family (Oishi et al., 2002).

Following cell stress, the soleus muscle has also been shown to induce hsp72 for long periods (Locke et al., 1991, Oishi et al., 2002), while fast-twitch muscle displays a rapid but short-lived HSR, with hsp72 peaking after 1-2hrs then steadily declining (Kayani et al., 2008a, Kayani et al., 2008b). Therefore, it is possible that the differential vulnerability of fast and slow-twitch muscles to denervation (Lowrie and Vrbova, 1984) and degeneration (Frey et al., 2000, Fischer et al., 2004) in ALS is related to, or at least influenced by a difference in the hsp profile of these two muscle fibre types. This possibility is investigated in this Thesis in Chapter 4.

1.12 Therapeutic strategies for ALS

At present, Riluzole, a glutamate inhibitor, is the only licensed drug for treating ALS patients. However, Riluzole's success is limited (Bensimon et al., 1994). In mSOD1 mice, presymptomatic treatment with Riluzole can delay disease onset and extends survival (Yanagisawa and Shindo, 1996, Ludolph et al., 2010). Thus, a considerable research effort was focused on identifying novel therapeutic targets for ALS. Some of these therapeutic strategies are summarised in Table 1.5. The multi-factorial nature of the ALS suggests that a therapeutic strategy that can act on a variety of pathological mechanisms within the disease may be more successful (see Table 1.6). Indeed, research has shown that treatment combining Riluzole with Minocycline (a microglial inhibitor) plus nimodopine (a blocker of voltage-gated calcium channels) exerts significantly greater beneficial effects in mSOD1 mice on disease progression and lifespan than is achieved individually with these agents (Kriz et al., 2003).

Table 1.5: ALS therapies

Therapy	Mechanism	Increase in lifespan	Reference
AR-R 17,477	nNOS inhibition	13%	(Facchinetti et al., 1999)
Riluzole	Anti-glutamate	10.5%	(Traynor et al., 2006)
Arimoclomol	HSP co-induction	22%	(Kieran et al., 2004)
Celecoxib	COX2 inhibition	25%	(Drachman et al., 2002)
NDGA	Inhibition of TNFα release	32%	(West et al., 2004)
WHI-PI3I	Tyrosine kinase inhibition	49%	(Trieu et al., 2000)
ZVAD-fmk	Caspase inhibition	22%	(Li et al., 2000)
High energy diet	Metabolic dysfunction	20%	(Dupuis et al., 2004)

Table 1.6: Combined therapies for ALS

Combined therapies	ALS model	Lifespan (%)	References
Riluzole & Minocycline & nimodopine	$SOD1^{G37R}$	12%	(Kriz et al.,2003)
Creatine & Celecoxib/ refoecoxib	$SOD1^{G93A}$	29%	(Klivenyi et al., 2004)
Creatine & Minocycline	$SOD1^{G93A}$	28%	(Zhang et al., 2003)
Exercise & insulin growth factor (IGF-I)	$SOD1^{G93A}$	31%	(Kaspar et al., 2005)

1.12.1 Manipulation of the HSR as a disease modifying therapy for ALS

The HSR has been targeted as a therapeutic approach in several neurodegenerative disorders, including ALS (Kurthy et al., 2002, Rakonczay et al., 2002, Kalmar et al., 2003, Phukan, 2010). This pathway has been manipulated in NMD models both genetically with varying success; for example, Manipulation of the HSR in the nervous system has been shown to be neuroprotective (Kalmar and Greensmith, 2009). Adachi et al. 2003 shows that the overexpression of hsp70 in a model of SBMA ameliorated disease. However, the overexpression of hsp70 in mSOD1 mice by crossing transgenic hsp70 mice with transgenic mSOD1 mice did not result in a significant improvement in disease progression (Liu et al., 2005) as hsp70 became sequestered in aggregates and was therefore unable to undertake its cytoprotective function. Likewise, disease progression in hsp27/mSOD1 transgenic mice remained unchanged (Krishnan et al., 2006, Krishnan et al., 2008).

1.12.1.1 Pharmacological manipulation of the HSR in ALS: a therapeutic strategy

Pharmacological manipulation of the HSR has had some significant success in improving disease progression in animal models of ALS. Treatment with exogenous hsp70 has been shown to increase motoneuron survival, motor function innervation and lifespan in mSOD1 mice (Gifondorwa et al., 2007). Equally, pharmacological manipulation of the HSR response has increased lifespan in mSOD1 mice (Kieran et al., 2004, Kiaei et al., 2005).

There are a small number of therapeutic compounds that induce the HSR in cells. Of these compounds, two drugs that can induce the HSR in mammals have been shown to manipulate the HSR in ALS (Traynor et al., 2006). These are Celastrol and Arimoclomol. However, they have slightly different modes of action. Celastrol is an anti-inflammatory triterpene that induces the HSR Allison et al., 2001). Arimoclomol is a hydroxylamine derivative that co-induces the HSR and has powerful cytoprotective capabilities (Kurthy et al., 2002)

HSR inducers, such as Celastrol, are able to initiate the HSR in a cell without prior stress, while co-inducers like Arimoclomol are only able to enhance an already-initiated HSR. Co-inducers are likely to be a safer way of manipulating the HSR, as they only augment a response that is already occurring, while HSR inducers, as the name suggests, can induce the HSR, even in unstressed cells, causing potentially pathological events and may even act as cell stressors. A table detailing known inducers and co-inducers of the HSR can be found in Table 1.7.

In vivo, both Celastrol and Arimoclomol have been reported to be cytoprotective within the CNS of mSOD1 mice (Kieran et al., 2004, Kiaei et al., 2005). Treatment of mSOD1 mice with Arimoclomol improves motoneuron survival, motor function and increased the lifespan of mSOD1 mice by 22% (Kieran et al., 2004). Treatment

with Arimoclomol has also been shown to decrease the prevalence of ubiquitin-positive aggregations within the motoneuron (Kalmar et al. 2008).

Table 1.7: Pharmacological agents that induce/co-induce the HSR

Compound	Inducer/ co-inducer	Reference
Sodium salicylate	Inducer	(Jurivich et al., 1992)
Indomethacin	Inducer	(Locke et al., 2002)
Geldanamycin	Inducer	(Winklhofer et al., 2001)
Arachidonic acid	Inducer	(Zeke et al., 2005)
Geranylgeranylacetone	Inducer	(Endo et al., 2007)
Carbenoxolone	Inducer	(Kawashima et al., 2009)
Polaprezinc	Inducer	(Ueda et al., 2009)
Paeoniflorin	Inducer	(Yan et al., 2004)
Glycyrrhizin	Co-inducer	(Yoh et al., 2002)
Celastrol	Inducer	(Brown, 2007)
Arimoclomol	Co-inducer	(Kieran et al., 2004)
Curcumin	Co-inducer	(Chang, 2001)

1.12.2 Muscle as a therapeutic target in ALS

The earliest signs of pathology in ALS manifest in the periphery, at the NMJ (Fischer et al., 2004). A number of therapies has therefore been designed to target the muscle in ALS (Turner and Talbot, 2008) or as a target to administer potential therapies and this has had some success. Treatment with various trophic factors administered to the muscle has been shown to alleviate symptoms of the disease in mSOD1 mice (Ates et al., 2007). Recent studies have shown that trophic factors

such as muscle Glial cell derived neurotrophic factor (mGDNF) and insulin-like growth factor (IGF-I) /Mechano-growth factor (MGF) promote motoneuron survival and function in mSOD1 mice (Yamamoto et al., 2001, Kaspar et al., 2003, Dobrowolny et al., 2005, Li et al., 2007, Riddoch-Contreras et al., 2009). Furthermore, Li et al. (2007) have uncovered evidence that only GDNF derived from muscle has neuroprotective qualities. Mice that were given intramuscular grafts of genetically modified myoblasts that overproduced GDNF displayed reduced denervation and had an increased lifespan (Mohajeri et al., 1999). Yamamto et al. (2001) demonstrated that these trophic factors enter the motoneuron via retrograde transport. Despite the obvious benefits that GDNF and IGF have on elements of muscle function in mSOD1 they are unable to significantly increase the lifespan of the mice (Suzuki et al., 2007a).

1.13 Aims of Thesis

The overall aim of the Thesis is to investigate the role of muscle in disease progression in the SOD1 mouse model of ALS. This will be achieved by characterising the stress induced changes that occur in mSOD1 skeletal muscle during disease progression. In addition, since our group has previously established that upregulation of the HSR in the CNS by treatment with Arimoclomol has been beneficial in mSOD1 mice, I will examine whether some of these positive effects are due, at least in part, to an enhanced HSR in skeletal muscle. Furthermore, in view of the established differential vulnerability of fast and slow-twitch muscle to ALS pathology, I will also examine whether there is an intrinsic difference in the stress response of fast and slow-twitch muscles and investigate the effects of treatment with Arimoclomol on this response.

Therefore in this thesis I will address the following questions:

- What are the pathological effects of mSOD1 expression in muscles of mSOD1 mice? Do these effects differ between fast and slow-twitch muscles?

- Does pharmacological upregulation of the stress response have an effect on muscle pathology in the mSOD1 mouse model of ALS?
- Is there an intrinsic difference in the vulnerability of fast and slow-twitch muscle fibres to cellular stress, which may increase their susceptibility to ALS pathology?

Chapter 2 : Methods

2.1 Introduction

A variety of methods were utilised to investigate muscle and NMJ pathology, and these methods are outlined in this Chapter. Details of the specific methods employed in each individual results Chapter are also indicated at the start of each Chapter. At the beginning of each results Chapter, the specific methods employed will also be indicated.

2.1.1 Breeding and maintenance of transgenic mouse colonies

All experimental mice used in this study were maintained and bred in the Biological Services Unit at the Institute of Neurology, University College London. Every effort was made to ensure that reduction, refinement and replacement was considered during the design of these experiments, in order to minimise the number of mice used and maximize [maximise] their welfare. All experiments were carried out under license from the Home Office, in accordance with the Animals (Scientific procedures) Act 1986 and following approval from the Institute of Neurology Ethical Review Committee.

Transgenic mice carrying a human SOD1 gene with a G93A mutation (TgN [SOD1-G93A] 1Gur) were originally purchased from Jackson Laboratories (Bar Harbour, ME). In addition, mice overexpressing wild type human SOD1 (wtSOD1) were also obtained as a control for the overexpression of the SOD1 protein. These two colonies were maintained by breeding male heterozygous carriers with female B6SJLF1 hybrids. The SOD1G93A (mSOD1) mice were originally generated and characterised by Gurney et al., (1994) and contain 25 copies of the mSOD1 transgene. This line is commonly referred to as the high copy number line of mutant SOD1 mice. The wtSOD1 mice also contain 25 copies of the WT transgene and therefore a good control.

All mice were housed in conventional cages, with woodchip bedding and cardboard tubes for environmental enrichment. The temperature was maintained at 19-23°C,

humidity at ~40-70%, with 12-15 air changes per hour. The mice were kept in a 12 hours light/dark cycle, with access to food and water *ad libitum*. The mice were fed a pellet diet from hoppers placed in food racks, and water was provided in bottles via an overhead rack. The mice were monitored and weighed regularly. In this colony of mice, maximum body weight was usually attained at approximately 70 days of age. Upon the onset of symptoms, the affected mSOD1 mice and their littermates were weighed weekly and the cage identified as housing an affected mouse. This ensured appropriate monitoring of each mouse. As hindlimb muscle paralysis progressed, the affected mice were provided with food pellets that had been soaked in water. This ensured efficient nourishment and hydration.

2.1.2 Characterisation of SOD1G93A mice

High copy number mSOD1 and wtSOD1 mice were used throughout all experiments described in this Thesis. Disease progression in our colony of mSOD1 mice is well-established and the different stage are classified as:

- Presymptomatic stage – less than 70 days, represented in this study at 45 days
- Symptomatic onset – taken as the time that the onset of hindlimb weakness is first observed. This occurs around 75 days.
- An early symptomatic stage – when mice show clear signs of hindlimb weakness, which occurs at 90-100 days.
- Late symptomatic stage – when hindlimb paralysis is significant and the mice have difficulties moving around the cage, at approximately 120 days.
- Endstage – defined as when the mice have lost 15% of their body weight, or when they are no longer able to right themselves within 30 seconds after being placed on their sides. This usually occurs at approximately 125 days in male mice and 132 in female mice (Kieran et al., 2004).

The Table below summarises these different disease stages and how they relate to the presentation of symptoms and pathology within the mSOD1 mice.

Table 2.1: The presentation of symptoms and pathology in mSOD1 mice during disease progression

Disease stage	Symptoms	Pathology	Age	Reference
Presymptomatic stage	None	Axonal transport dysfunction, mitochondrial dysfunction	45 ±5 days	(Ilieva et al., 2009)
Disease onset	Muscle fasciculation, Muscle weakness,	Motoneuron death, reactive tSCh, NMJ denervation	75 ±5 days	(Fischer et al., 2004)
Early symptomatic stage	Weight loss, further weakness	Decreased muscle fatigability and force	100 ±5 days	Kieran et al., 2004, Atkin et al., 2005
Late symptomatic stage	Hindlimb paralysis	Severe muscle atrophy, muscle fibre type alterations, extensive denervation and motoneuron death	120 ±5 days	(Atkin et al., 2005)
Endstage	15% loss in body weight	80% motoneuron death and muscle atrophy	125/132 days	(Frey et al., 2000, Fischer et al., 2004)

2.1.3 Genotyping of mSOD1 mice by polymerase chain reaction

The mice carrying a human SOD1 transgene were identified by polymerase chain reaction (PCR) amplification of the transgene from genomic DNA. Tail snips (<0.5cm) were taken days after birth or ear notches were collected just before weaning. This procedure was carried out using local anaesthesia. The tissue sample was then digested using rapid digestion buffer.

For PCR, 2.5μl of each DNA sample was added to a reaction tube that contained 17.65μl sterile water, 2.5μl PCR buffer, 0.75μl MgCl2 (50mM), 0.5μl dNTP solution, 0.25μl of both forward and reverse primers for the endogenous SOD1 enzyme and human mutant SOD1 enzyme, and 0.1μl Taq polymerase to make the final volume of 25μl. In order to differentiate the human transgene from murine SOD1, primers with the following sequences were used:

5' CAT CAG CCC TAA ATC TGA 3'

5' CGC GAC TAA CAA TCA AAG 3'.

The samples were then temperature cycled, as summarised in Table 2.2.

Table 2.2: Summary of the cycles involved in PCR analysis of mSOD1 samples

No. of cycles	Temperature	Duration of cycle
1	95°C	3 minutes
36	95°C	30 seconds
36	60°C	30 seconds
36	72°C	45 seconds
1	72°C	2 minutes

The PCR products were subsequently visualised by gel electrophoresis by running 10μl of each PCR product on a 2% gel agarose gel at 60mV for 40 minutes.

2.2 In vivo experiments

2.2.1 Treatment with Arimoclomol

In some experiments, the effect of intraperitoneal (i.p.) treatment with Arimoclomol was examined in mSOD1 mice. The mice were randomly assigned to one of two treatment groups: (A) Arimoclomol (10mg/kg; i.p.) or (B) Saline (10ml/kg; i.p.). Both mSOD1 and WT mice were treated daily from 35 days until the tissue was harvested and stored as detailed below.

2.2.2 Muscle dissection

Experimental mice were terminally anaesthetised using 4% choral hydrate, (1ml/100g body weight i.p.). Under anaesthesia, unless stated otherwise, the right soleus and TA muscles of each mouse were removed and cooled in isopentane, then frozen and then stored at -80˚C for immunohistochemical analysis. The left soleus and TA muscles were removed, snap frozen in liquid nitrogen and stored so that they could be used for western blot analysis. In some experiments, the soleus and EDL muscles were removed for the analysis of muscle innervation. For these experiments, muscles were dissected fresh and fixed as described in Chapter 3.

2.2.3 Immunohistochemistry

Cross sections of muscle were serially cut on a cryostat at 12µm. These sections were collected onto polyornithine coated glass slides and were fixed with a chilled Methanol/Acetone (1:1) fixative solution for 1 minute. The sections were then rinsed with a PBS (pH 7.4) solution and incubated with a blocking solution of 5% milk fat and 3% normal serum for one hour at room temperature. The blocking solution was then removed and the sections rinsed in PBS (3x 5 minutes). The sections were incubated in primary antibody in PBS, overnight at 4°C. Following incubation, the sections were washed in PBS (3x 5 minutes) and were incubated with secondary antibody diluted in PBS, at the appropriate concentration, for 2 hours at room temperature. Following this, the sections were rinsed again as before and incubated with the necessary fluorophore diluted in PBS for one hour at room temperature. The sections were then rinsed in PBS (3x 5 minutes) and

coverslipped using dakocytomation (DAKO) mounting medium. Detailed information regarding all primary and secondary antibodies used in this Thesis and their concentrations can be found in Tables 2.3 and 2.4, respectively.

2.2.4 Mouse-on-mouse Immunohistochemistry

When using antibodies raised in mice, on tissue sections from mice, a mouse-on-mouse (MOM) kit was used to reduce cross reactivity (MOM kit, Vector labs, cat #BMK-2202). The first step involved blocking endogenous peroxidase activity by incubating sections in 0.3% H_2O_2 for 30 minutes. Sections were incubated for 1 hour in mouse IgG blocking reagent at room temperature.

Table 2.3: Primary antibodies used

Name of antibody	IHC	WB	Code	Company
Anti- hsp90	1:100	1:1000	SC: 7947	Santa Cruz
Anti-hsp72	1:250	1:2000	SPA- 810	Stressgen
Anti-hsp60	1:100	1:1000	Santa Cruz: N-20	Santa Ruz
Anti-hsp25	1:200	1:2000	SPA-801	Stressgen
Anti-nNOS	1:100	1:1000	SC- 648	Santa Cruz
Anti CD11b	1:100	-	ab53187	Abcam
Anti- Myosin heavy chain I & II	1:10	-	NCL-MHCs and NCL-MHCf	Novocastra
Anti-iNOS	1:500	1:2000	ab3523	Abcam

Table 2.4: Secondary antibodies used

Name of antibody	IHC	WB	Code	Company
Goat anti-rabbit IgG antibody Alexa Fluor 488 conjugated	1:200	-	A11034	Invitrogen
Goat anti-rabbit IgG antibody Alexa Fluor 569 conjugated	1:200	-	A21069	Invitrogen
Rabbit anti –goat IgG antibody FITC conjugated	1:200	-	Ab5750	Abcam
Swine anti-goat IgG HRP	-	1:2000	ACI0404	Invitrogen
Goat anti-rabbit IgG HRP	-	1:2000	65-6120	Invitrogen
Goat anti-mouse IgG HRP	-	1:2000	62-6520	Invitrogen

After incubation, sections were rinsed twice in PBS for two minutes each. Sections were then incubated in MOM diluents for 5 minutes before incubation in primary antibody–at the appropriate concentration, for 30 minutes–at room temperature. This was followed by two 2-minute rinses in PBS, and MOM biotinylated IgG reagent was then applied for 10 minutes before incubation with Alexa 488 for 1 hour. The sections were then rinsed three times in PBS for 5 minutes and mounted with DAKO fluorescent mounting medium.

2.2.5 Silver cholinesterase staining of nerve terminals and endplates

Freshly removed EDL and soleus muscles were fixed in a slightly stretched position using buffered 4% formaldehyde fixative (40% Formaldehyde, 10% $CaCl_2$, 5%$MgCl_2$, 1% $CdCl_2.2^{1/2}H_20$) in Veronal Acetate buffer for 6 hours. Muscles were then incubated in 10% sucrose overnight at 4°C. Longitudinal sections (40µm thick) were then cut on a freezing microtome and held as free floating sections in distilled water on ice for 10 minutes. The muscle sections were then incubated on ice for 20 minutes in an acetylcholine iodide solution (0.04% acetylcholine iodide, 56% 0.1M sodium hydrogen maleate, 4% 100mM tri-sodium citrate, 8.7% 30mM copper sulphate, 8.7% distilled water, 8.7% 5mM potassium ferricyanide, and 13% sucrose). Following a brief wash in distilled water for 30 seconds, muscle sections were immersed in potassium ferricyanide solution (0.25% potassium ferricyanide)

for 9 minutes. The sections were then processed for silver in order to visualise axon terminals, and were then incubated in a silver solution (0.1% $CaCO_3$, 0.06% $CuSO_4.5H_2O$, 10%$AgNO_3$) for 45 minutes at 37°C. The sections were then rinsed, immersed in reducer solution (1%$C_6H_4(OH)_2$, 10%Na_2SO_3) and monitored under a dissection microscope, in order to determine nerve terminal staining. The muscle sections were then washed in water, mounted on gelatinised slides and coverslipped Di-n-butylPhthalate in Xylene (DPX) mounting solution. The extent and pattern in innervation was examined and recorded under a light microscope.

2.2.6 Succinate dehydrogenase staining

Some transverse muscle sections were also stained for succinate dehydrogenase (SDH) activity: an indicator of the oxidative capacity of muscle fibres.

A working solution was prepared, which consisted of 0.1M phosphate buffer, pH7.6, 1M sodium succinate, 15mM nitroblue tetrozolium, 0.1M potassium cyanide and 10mM phenazine methosulphate, according to the protocol described by Nachlas et al. (1957). The working solution was prepared and filtered; the photosensitive solution was subsequently stored in a brown glass bottle, away from light. Before sections were treated with the solution, both sections and an appropriate volume of working solution were heated to 37°C in an incubator for 20 minutes. Muscle sections were then incubated in this solution at 37°C for 5 minutes. Following incubation, sections were then rinsed on 0.9% NaCl for 1 minute followed by dehydration in graded alcohols (70%, 90% and then two rinses in 100%). Sections were then cleared with histoclear for two minutes each. Coverslips were then mounted onto the slides with DPX mounting solution.

2.2.7 Muscle homogenisation

The snap frozen, dissected hindlimb muscles were thawed and homogenised in lysis buffer in a 1:3 ratio (5mM Tris, 2% SDS, 2mM EDTA, 2mM EGTA, 2mM phenylmethylsulfonylfluride (PMSF), 10μM leupeptin pH6.8). In each experimental

group, the homogenate consisted of a minimum of three muscles were pooled in order to provide a single sample for specific muscles (TA, EDL and soleus). Debris was removed by low speed centrifugation at 1000xg for 10 minutes and the supernatant collected. Protein levels were then established and normalised using a protein assay (Bio-Rad, cat# 500-01116) and protein content was determined using a BSA standard curve, which was read at absorbance 750nm. Samples were diluted with a 1:1 ratio with SDS-PAGE sample buffer (0.5M Tris-HCL, pH 6.8, glycerol, 10% (wt/vol) SDS, β-Mercaptoethanol and 1.0% bromophenol blue) and then heated to 95°C for 5 minutes before SDS-PAGE.

2.2.8 Protein Assay

Protein levels were determined using a BioRad assay and BSA standards (0.1, 0.25, 0.5, 0.75, 1, 1.5mg/ml). Following the calculation of protein content, protein levels were normalised for western blotting. Western blot samples were aliquoted and stored in -80ºC until needed.

2.2.9 Western blotting

Hsp, nNOS and iNOS levels were examined in a fast and slow-twitch muscle in mSOD1 mice using western blotting. For each Western blot described in this Thesis, muscles from at least three different mice were pooled, providing one sample for each experimental group. This sample was run in duplicate in each blot and each western blot was repeated at least twice. Equal amounts of protein were loaded and electrophoresed using an acrylimide SDS gel and separated at 160mV for 60 minutes (Laemelli, 1970). The protein was then electrophoretically transferred to Hybond tm ECL TM nitrocellulose membrane in a buffer consisting of 25mM Tris, 192mM glycine and 20% (v/v) methanol. For immunodection, non-specific binding sites were blocked with 5% non-fat dried milk and 0.1% Tween X-100 in PBS for 1 hour at room temperature. The blots were then incubated in primary antibody in 2.5% non-fat dried milk and 0.1% Tween X-100 overnight at 4°C. After three washes in PBS containing 0.1% Tween, for 20 minutes each, the membranes were incubated in secondary antibody at a dilution of 1:2000 in PBS,

containing 0.1% Tween, for 2 hours. The membranes were then rinsed three times, for 20 minutes each, in PBS with 0.1% Tween and subsequently treated with a chemilumescent detection reagent (ECL TM, Amersham Pharmacia Biotech, cat: # RPN2106).

The blots were then visualised using Kodak films and subsequently fixed. For each blot a loading control was also run. Western blot line densities of β-actin were established using ImageQuant software. The line densities of all bands were normalised against line densities of β-actin bands. Line density values were then represented as a percentage of the corresponding WT line densities for ease of comparison.

2.2.10 Choline Acetyltransferase Assay

ChAT activity was assessed using a sensitive radiochemical bioassay in which [1-14C] acetyl-CoA and choline were used as substrates and the radioactivity of the reaction product was measured (Ellman et al., 1961). The TA, EDL and soleus muscles were dissected from WT and mSOD1 mice and stored in liquid nitrogen. They were then thawed and immediately processed for the assessment of ChAT activity.

For each experimental group, muscles from at least three mice were analysed. Muscle homogenates (5%w/v) were prepared in 10mM eythlenediamine tetra acetate, pH7.4, containing 0.5% Triton X-100, to ensure the total release of enzyme activity. The muscle homogenate was incubated with an incubation medium containing (final concentration): 0.4mM [1-14C] acetyl-CoA (50.0mCi/mM Amersham), 300mM NaCl, 50mM sodium phosphate buffer (pH7.4) and 0.1mM eserine. The reaction was initiated by mixing each homogenate with 25µl of the incubation medium, and before transferring this solution to a 37°C water bath for one hour. The reaction was terminated by adding 4.5mls of 10mM sodium phosphate buffer (pH7.4, 4°C). All samples were assayed in duplicate, including

blanks. The solution was poured into a scintillation vial along with 2ml of acetonitrile 0.5% tetraphenylboron (Kaligonost) and 10ml of toluene scintillation mixture (0.5% 2,5diphenyloxazole and 0.02 1,4-bis[phenyl-2-oxazoly]-benzene;2,2-p-phenylene-bis[phenyloxazole]). The vial was shaken gently for 1 minute in order to extract the acetylcholine into the toluene phase, leaving the acetyl-CoA in the aqueous phase. The two layers were allowed to separate for 10 minutes before measurement in a Beckman liquid scintillation spectrometer. Enzymatic activity was calculated as counts per minute (CPM) of C-14. The assay was repeated at least twice to ensure that a similar and reproducible pattern of ChAT activity was obtained from each experimental condition.

2.2.11 Acetyl Cholinesterase Assay

Acetyl cholineEsterase (AChE) activity in TA, EDL and soleus muscles was quantified using a colorimetric assay based on methods described in Ellman et al (1961) and Nostrandt (1993) with slight modifications. A 1% solution in homogenised medium (pH7.4, 0.4 10mM EDTA, 0.5% Triton X-100) was made. The homogenised tissue was incubated for 35 minutes at room temperature with 2.5mM DNTB and 5mM acetylthiocholine iodide substrate. At the end of the reaction, optical density was measured at 412nm using a spectrophotometer (FLOUstar Omega, BMG Labtech). Optical densities were compared to a standard curve that was generated using the assay reaction buffer and L-Glutothione as a positive control dilution series. The colorimetric changes were measured and analysed using Omega software (BMG Labtech). Each sample was run in triplicate. For each sample, the results were correlated with readings obtained from a negative control sample containing the AChE inhibitor erserine. This enables the exclusion of any contribution that other esterases might make to the experimental results. Results were then calculated as the nmol of ACh converted per min per mg tissue (nmol ACh/min/mg tissue).

2.2.12 Imaging

Unless otherwise stated, in this study all sections were examined under fluorescent microscope (Leica) and images were acquired using Leica Imaging software. On some occasions, images obtained using confocal microscopy were acquired using a Zeiss 510 Laser Scanning confocal microscope (Oberkocken, Germany).

2.3 In vitro experiments

2.3.1 Preparation of culture plates

Glass coverslips were sterilised in the Class II microbiological safety unit, by passing through the flame of a Bunsen burner and then placed into a well of a culture plate. A solution of gelatin (2mg/ml in sterile PBS) was prepared and 500µl was added to each well. The plates were left overnight in an incubator. The following day, the gelatin was removed and the plates were left to dry for 1 hour in a fume hood.

2.3.2 Primary mixed muscle cultures

Primary hindlimb muscle cultures were prepared, according to a protocol described by Bryla et al. (2001). Following the determination of genotype, P0-P3 pups were decapitated, the hindlimb was skinned, and the feet removed. The hindlimb muscles were dissected from the bone and minced with sterile forceps. The minced muscles were maintained in Hank's balanced salt solution (HBSS) with penicillin-streptomycin (5000 units/ml: HBSS - Invitrogen, Paisley, UK) supplemented with 1ml penicillin- streptomycin per 50ml HBSS, until genotyping was complete. A collegenase solution of penicillin-streptomycin enriched HBSS with 0.01% collegenase IV, and muscle media was prepared (79% Dulbecco's Modified Essential Medium (DMEM; Invitrogen, Paisley, UK: supplemented with 1% penicillin-streptomycin: 20% foetal calf serum). The minced muscle was pooled according to genotype, and then each muscle from genotype was cultured separately.

The pooled muscle tissue was transferred into a 0.01% collegenase IV solution (PBS: 5% penicillin streptomycin). The solution was incubated in a waterbath at 37°C for 15 minutes, removed and triturated with a pipette 20 times and then replaced into a waterbath. This process was repeated once. The solution was incubated for another 15 minutes and triturated 10 times. It was removed from the waterbath and placed in a sterile hood and the solution was passed through a 100μm mesh (Marathon, London, UK) into a 50ml falcon tube. The solution was then diluted with in muscle media to 1:2 ratio and then centrifuged at 20°C for 5 minutes at 200xg. The supernatant was discarded and the pellet resuspended in 1ml of DMEM supplemented with 10% FCS, 1% penicillin streptomycin. Following this, the cell density was determined using a haemocytometer. The cells were seeded at $5x10^5$cells/cm^2 for immunoflourescence and $1x10^6$cells/cm^2 for cell viability experiments. The cells were seeded onto the gelatin coated 9mm permanox chamber coverslips for imaging or 96-well-plates for assays.

The cells were maintained in muscle media in a sterile 37°C, 5%CO_2 humidified incubator for 7 days, in order to allow for maturation of myotubes. The percentage of muscle cells within the muscle cultures was determined by immunostaining the cultures for desmin and myosin, a marker for muscle cells, as well as DAPI, a nuclear marker (0.01% Molecular probes, Paisley, UK). The percentage of DAPI stained desmin/myosin positive cells was calculated. Cultures with less than 40% myogenicity were discarded.

2.3.3 Primary fast and slow-twitch muscle cultures from neonatal mice

In some experiments, primary muscle cultures were established from WT, mSOD1 and wtSOD1 transgenic neonate mice using a modified protocol initially described by Bryla et al. (2001) and seeded at 1,000,000 cells/cm^2. Neonates were genotyped one day before muscle dissection. The soleus and TA muscles for from each genotype were pooled appropriately, so that 6-8 TA and 6-8 soleus muscles of each genotype were used for every culture. The soleus muscle was taken as a

predominantly slow-twitch muscle culture, and the TA muscle as a fast-twitch muscle culture.

2.3.4 Neuronal cell lines

SH-SY5Y *(ECACC*; Catalogue number 94030304) cell lines originally derived from female, human neuroblastoma cells were grown in Neural Basal media that contained Dulbecco's modified Eagle's medium (DMEM-F12) containing 15% FCS, 2mM L-glutamine, 10 IU/ml penicillin, 100µg/ml streptomycin and 1% final volume non-essential amino acids. Cells were maintained at 37°C in a saturated humidity atmosphere of 95% air and 5% CO_2. Cells were then seeded onto uncoated 96-well-plates at a cell density of 2000 cells/cm^2 .

2.3.5 Glucose deprivation (metabolic) stress

All experimental procedures were performed on fully differentiated cells at 8-10 days *in vitro* (DIV). In glucose deprivation experiments, the cells were incubated in glucose-free DMEM supplemented with 2% FCS and 1% penicillin-streptomycin for 24 hours. The cultures were then processed for the assessment of cell viability using an LDH assay as detailed in Section 2.3.10. Control cultures were incubated with a high glucose DMEM (4.5g/l) supplemented with 2% FCS, 1% penicillin-streptomycin media for 24 hours.

2.3.6 Contractile/oxidative stress (caffeine) stress

At 8 DIV, spontaneous contraction of myotubes is present, signalling the maturity of the contractile machinery in muscle cultures. This time point was therefore chosen to assess the effects of caffeine-induced stress. Application of caffeine, a Ryanodine receptor (RyR) agonist, initiates Ca^{2+} release from the sarcoplasmic reticulum (SR), resulting in the activation of the ECC machinery. Over time, this results in increased sarcoplasmic Ca^{2+} resulting in the production oxidative stress and contractile damage. At 8 DIV, muscle cultures were incubated with 150µl muscle media enriched with 2% FCS, 1% penicillin streptomycin 1mM, 5mM or

10mM caffeine for 24 hours. Following this, the supernatant was collected for an LDH cell viability assay and the pellet used for a protein assay.

2.3.7 Glucose deprivation plus caffeine stress

All experimental procedures were performed on fully differentiated cells at 8-10 days in vitro (DIV). Muscle cultures were incubated with 150µl glucose-free muscle media enriched with 2%FCS, 1% penicillin streptomycin, 1mM, 5mM or 10mM caffeine for 24 hours. Following this, the supernatant was collected for an LDH assay and the pellet used for a protein assay.

2.3.8 Preparation of Muscle-conditioned media

Muscle-conditioned medium was prepared according to a modified protocol by Taylor et al. (2007). Mixed muscles were cultured as described above and were maintained and fed every 3–4 days. At 8 DIV, cultures were incubated in basal media (DMEM containing 2% FCS and 1% penicillin-streptomycin) for 48 hours. The media was collected from cultures and centrifuged at 400x*g* to remove free cells and membrane debris. The supernatant was then centrifuged at 20,800x*g* for 1 hour. The pellet was resuspended in serum free muscle media. The protein content was then assessed and normalised using a protein assay, (section 2.2.8). The solution was then filter-sterilised and frozen at -80°C until use.

2.3.9 Treatment of neuronal cells with Muscle-conditioned media

SH-SY5Y cells seeded in a 96-well-plate were treated with MCM and left for 72 hours. In some wells, the cells were treated with 2% Triton X-100 in DMEM, in order to determine the maximum LDH release. After 72 hours, a cell viability assay was carried out by means of an LDH assay. LDH levels in unexposed DMEM were taken to be the baseline and the maximal LDH release was taken from SH-SY5Y cell incubated with 2% Triton X-100. All subsequent values were then represented as a percentage of that maximum, which was given the value of 100%.

2.3.10 Cell viability assay

Muscle cultures were assayed for LDH release as a measure of cytotoxicity following treatment with the biologically relevant stressors.

Two control groups were set up. Unexposed media was assayed in order to determine the baseline amount of LDH in the media. Untreated wells incubated with 2% Triton X-100 were also used to determine the maximal LDH release, the LDH levels of media from muscle cultures exposed to a metabolic stress, contractile and oxidative stress, combined metabolic and oxidative stress or SH-SY5Y cells exposed to MCM were then examined using the LDH assay kit, which contained solution 1 (assay buffer preparation) and solution 2 (LDH diaphorase).

The 96-well-plates were centrifuged at 250xg for 5 minutes and the supernatant from each well was removed, leaving a pellet. The supernatant was placed into the corresponding wells in an empty 96-well plate. The pellet, which contained cells, was kept for protein analysis. Each experiment was repeated in six wells per plate and each experiment was undertaken at least four times.

The assay required the addition of 100µl of Diaphorase (a catalyst) and 9.6ml INT (the dye solution). These were mixed and 100µl added to each well. The 96-well plate was incubated at room temperature in the dark for 15 minutes. Absorbance was measured at 490nm on a spectrophotometer. Absorbance values for each well was expressed as a percentage of the maximum LDH release determined by the addition of 2% Triton X-100, and then normalised against protein values obtained from a protein assay on the pellet. These values were then averaged to give a value for each condition.

2.3.11 Statistical analysis

The results were analysed and the significance was set. All quantitative data is presented as the mean ± standard error of the mean. In Chapters, 3, 4 and 5, data was statistically assessed using the one-way ANOVA test on data from a multivariate group. This was then followed by analysis using the student's t-test for comparisons between two groups. The level of significance was set as $p<0.05$, unless otherwise stated.

Chapter 3 : Pathological changes in muscle during disease progression in mSOD1 mice and the effect of treatment with Arimoclomol

3.1 Introduction

The earliest clinical manifestation of disease in ALS patients and mSOD1 mice is muscle weakness and atrophy, resulting from the denervation of muscle (Frey et al., 2000, Fischer et al., 2004). This has motivated a number of therapeutic strategies focusing on limiting denervation and protecting muscle function. Furthermore, as recent findings report the differential vulnerability of fast and slow-twitch skeletal muscle fibres to disease in ALS (Frey et al., 2000), two different muscle types, the fast-twitch EDL muscle and the slow-twitch soleus muscle, were studied. In this Chapter, the pathological changes that occur in fast and slow-twitch muscles were characterised and compared.

3.1.1 Denervation in ALS occurs before motoneuron death

Recent studies have suggested that mSOD1-mediated pathological events in the PNS may not be simply secondary to motoneuron death (Pinelli et al., 1991, Frey et al., 2000, Fischer et al., 2004, Hegedus et al., 2007). In fact, it was demonstrated by Fischer et al. (2004) that in mSOD1 mice, at 47 days, well before motoneuron death, 40% of endplates are already denervated. Results indicated that denervation precedes both motoneuron death and glial activation, two major components of the disease aetiology. This evidence has led to the controversial hypothesis that ALS may in fact be a ‘distal axonopathy’, with pathology originating from the distal axon and working back to the soma (Fischer et al., 2004). Furthermore, pathological changes at the NMJ in ALS recreate many of the events observed during NMJ development, when muscle provides trophic support to vulnerable motoneurons (Oppenheim and Haverkamp, 1988). This supports the possibility that mSOD1 muscle may influence motoneuron viability and susceptibility to stress, injury or disease.

3.1.2 Differential vulnerability in mSOD1 muscle

The onset of muscle atrophy and paralysis is not homogenous across muscle types, with fast-twitch muscles displaying preferential vulnerability to mSOD1

pathology (Frey et al., 2000). A few studies have suggested factors that may contribute to the preferential denervation, atrophy and paralysis of fast-twitch muscles in the disease. For instance, it was suggested that the differential plasticity of synapses present in fast and slow-twitch muscle contributes to the early and more aggressive denervation in mSOD1 mice (Santos and Caroni, 2003). Furthermore, a study by Frey et al., (2000) established that these endplates are not just simply more susceptible to mSOD1 pathology. They demonstrated that the application of Botulinum toxin-A to the mSOD1 muscle resulted in the early and preferential loss of innervation in fast-twitch muscle fibres in the gastrocnemius muscle, while slow synapses, in the medial region of the gastrocnemius muscle remained innervated. Their study revealed that this difference in vulnerability was the result of the increased ability of NMJs on slow fibres to sprout, following partial denervation of the muscle. However, as fast-twitch muscle remains vulnerable to pathology in a number of neuromuscular diseases and myopathies, it is likely that a number of factors contribute to the consistent preferential vulnerability of fast-twitch muscle to disease.

3.1.3 Synaptic transmission in ALS

Pathogenesis in ALS is characterised by the selective loss of motoneurons (Bruijn et al., 2004). At a late stage of disease, when motoneuron death is substantial there is a significant reduction in the synaptic transmission enzymes ChAT and AChE in the CNS and muscles of ALS patients and mSOD1 mice (Fernandez et al., 1986, Pinelli et al., 1991, Gurney, 1994, Yoshihara et al., 1998). Studies examining the expression of enzymes involved in synaptic transmission within the CNS indicate the involvement of AChE and ChAT during disease progression (Oda et al., 1995, Niebroj-Dobosz and Janik, 1999). However, it is not clear when synaptic enzyme activity is altered in the periphery and muscle, or how enzyme activity changes over the course of the disease.

3.1.4 Therapeutic targeting of muscle function in mSOD1 mice

A number of therapies has been shown to improve mSOD1 motoneuron survival *in vitro* and *in vivo*; however, those that solely target the CNS have rarely translated into improved muscle function (Suzuki et al., 2007). However, skeletal muscle may also be a good therapeutic target as well as a delivery route for potential neuroprotective treatment. Indeed, targeting of the muscle has proven more effective in improving muscle function, even when first used as a conduit to deliver neuroprotective agents to motoneurons. For example, with retrograde viral delivery of insulin-growth factor 1 (IGF-1), results in muscle hypertrophy, increased motoneuron survival and the preservation of muscle function in mSOD1 mice (Kaspar et al., 2003). Similarly, treatment with the IGF-1 splice variant, Mechano-growth factor (MGF), which is expressed locally within the muscle, has been shown to induce muscle hypertrophy, as well as increase motoneuron survival (Riddoch-Contreras et al., 2009). As such, it is possible that a therapy that targets events in the CNS as well as the periphery may be the most effective approach to modify disease progress in ALS.

3.1.5 Upregulation of the Heat shock response as a therapeutic strategy for ALS

In 2004, Kieran et al. demonstrated that the systemic delivery of Arimoclomol, a co-inducer of the HSR, was sufficient to increase lifespan in mSOD1 mice by over 20%, improve muscle function and increase motoneuron survival. Kalmar et al. (2008) showed that Arimoclomol reduced protein aggregation in motoneurons. Both papers successfully demonstrated Arimoclomol's central effects, but it is not clear from these studies whether the improvement in muscle function was due wholly to Arimoclomol's actions in the CNS or whether some of its effects may be solely within skeletal muscles of mSOD1 mice.

3.1.6 Aim

The aim of this Chapter is to characterise the time course of muscle pathology in fast and slow-twitch muscle of mSOD1 mice, studying muscle innervation and changes in enzymatic markers of neuromuscular activity. In addition, this Chapter will investigate whether treatment with Arimoclomol can delay the early pathological changes occurring at the NMJ and in the muscle of mSOD1 mice.

3.2 Methods

3.2.1 Animals

The mice were housed and fed *ad libitum* as detailed in Chapter Two, Section 2.1.1. mSOD1 transgenic mice were identified from an ear notch, using human SOD1 PCR as detailed in Chapter 2, Section 2.1.3. In these experiments, male and female, age-matched mSOD1 mice and their WT littermates were examined at different stages of disease. These stages were detailed in Table 3.1. In some experiments, mice were treated as detailed in Chapter Two, Section 2.2.1.

3.2.2 Muscle dissection

The animals were terminally anaesthetised using 4% choral hydrate, 1ml/100g body weight administered intraperitoneally. Under anaesthesia, the soleus and EDL muscles from one side of one set of mice were taken and processed for analysis of muscle innervation (see Chapter 2, Section 2.5). The soleus, TA and EDL from the other side were removed for biochemical analysis of cholinergic enzymes (Chapter 2, Section 2.10 & 2.11).

The TA, EDL and soleus muscle from a different set of mice were dissected, snap frozen in melting isopentane and stored at -80°C until processed for histochemical analysis.

3.2.3 Morphological assessment of Muscle Innervation

The silver cholinesterase stain is a combined stain, used for the simultaneous visualisation of both the motor nerve terminal and Acetyl Cholinesterase at the endplate. The stain employs potassium ferricyanide for the staining of cholinesterase, which labels the endplate, while silver impregnation allows for the detection of the nerve terminals (Namba et al., 1967). The detailed staining procedure is described in Chapter 2, Section 2.5. The stained muscle sections were analysed using a light microscope. For each muscle a minimum of 100

endplates from at least three animals per experimental group were examined and the following features assessed:

- The level of innervation of each muscle.
- The extent of polyneuronal innervation (PNI).
- The extent of nerve terminal sprouting in the muscles.
- Endplate size.

An endplate was classified as denervated if the whole endplate surface was void of nerve terminal contact. Nerve terminal sprouts were identified the total number established for each muscle and the number of sprouts expressed as a ratio to the number of endplates examined. The extent of PNI was determined by counting the number of endplates that were innervated by more than one nerve terminal. This data was expressed as a percentage of the total number of endplates investigated for each muscle.

3.2.4 Endplate size

Endplate size in each muscle was examined at 45 days and 120 days of age, in sections of EDL and soleus muscle that had been stained with Silver Cholinesterase staining. The sections were examined under a light microscope and an image of each endplate taken at x20 magnification using a Leica camera. The circumference of each endplate was measured. A minimum of 150 endplates was assessed in each muscle examined, and a minimum of three muscles was examined for each experimental group (for details see Chapter 2, Section 2.5)

3.2.5 Assessment of Cholinergic enzyme activity

The activity levels of ChAT and AChE, two key enzymes involved in neuromuscular transmission, were examined as a measure of neuromuscular activity. This was carried out as detailed in Chapter 2, Section 2.10 & 2.11 (Ellman et al., 1961).

3.2.6 Succinate Dehydrogenase Stain

A SDH stain was used in order to examine the oxidative profile of the muscles examined at 45 and 120 days of age. Muscle sections, cut on a cryostat transversely at 12μm were stained according to the protocol described by Nachlas et al. (1957).

3.2.7 Statistics

All data is presented as the mean ± standard error of the mean. Data were statistically assessed using the one-way ANOVA test on data from a multivariate group. This was then followed by the student's t-test for comparisons between two groups. The level of significance was set as $p<0.05$, unless otherwise stated.

3.3 Results

3.3.1 Denervation in fast and slow-twitch muscles of mSOD1 mice

The changes in muscle innervation in the EDL and soleus muscles of mSOD1 mice was determined by the assessment of the following features:

- The number of denervated endplates.
- The number of polyneuronally innervated endplates.
- The extent of nerve terminal sprouting.

3.3.1.1 Denervation in EDL muscle of mSOD1 mice

In the first instance, the extent of muscle denervation in WT mice was compared to that in mice that overexpressed wtSOD1. The results showed that in WT mice, at all ages studied, the number of muscle fibres that were denervated was minimal and an average of 3.2% (±0.3 SEM; n=5) of endplates were denervated. In the WT EDL muscle, this was not significantly different from level of denervation in the EDL muscles of wtSOD1 mice, where 4.4% (±0.4 SEM; n=3; p=0.06) of endplates were denervated (Appendix 1). As wtSOD1 EDL muscle showed no signs of denervation in this study the changes in muscle innervation in mSOD1 mice were compared to muscles from WT mice only.

During disease progression in mSOD1 mice, there was a steady increase in the proportion of denervated endplates. As shown in Fig.3.1, at 45 days of age, before the onset of symptoms, there was a small but significant percentage of denervated endplates, 8.0% (±0.4 SEM; n=5; $p<0.05$), compared to WT mice. By 75 days, 24.2% (±1.0 SEM; n=4; $p<0.05$) of the endplates examined were denervated. Denervation in EDL muscle continued to increase as disease progressed, so that by 90 days, 31.3% (±3.2 SEM; n=4; $p<0.01$) of the endplates were denervated and by 120 days, 55.4% (±2.0 SEM; n=4; $p<0.01$) of the endplates in the EDL muscle were denervated. Treatment with Arimoclomol significantly reduced the extent of denervation from 75 days onwards (see Fig.3.1). At 45 days, 7.8% (±0.3 SEM; n=3; p=0.741) of the endplates were denervated in Arimoclomol treated mSOD1 mice

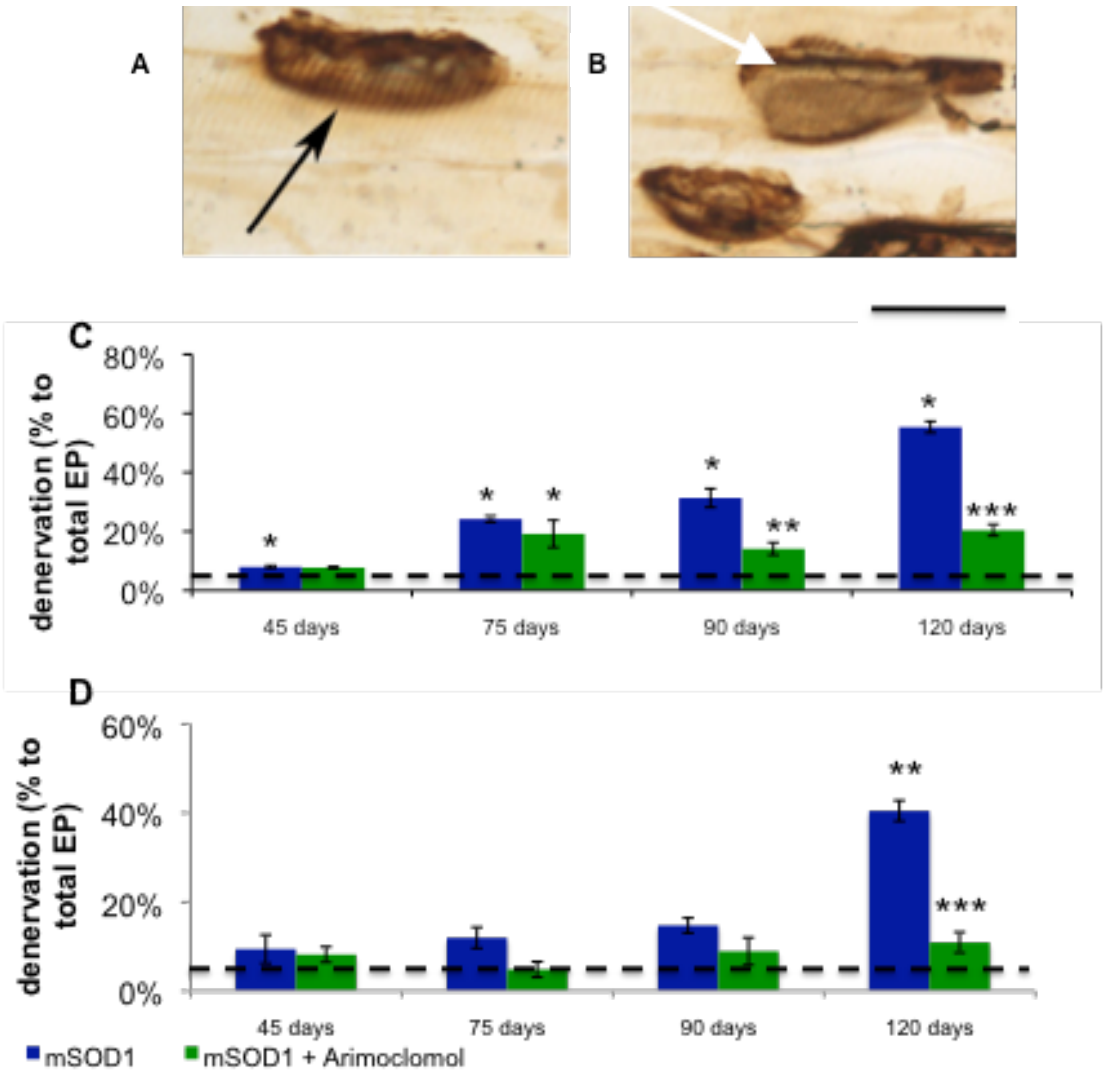

Figure 3.1: Denervation in the EDL & soleus muscles of WT, mSOD1 and Arimoclomol treated mSOD1 mice

The extent of denervation of EDL muscles in WT, mSOD1 and Arimoclomol treated mSOD1 mice was observed at 45, 75, 90 and 120 days of age stained by silver cholinesterase. The black arrow shows an example of a normally innervated endplate (A) and the white arrows shows a denervated endplate (B) in the photomicrographs. The extent of denervation in the EDL and soleus muscle at each stage of disease progression is summarised in the bar charts (C & D), respectively.

n=4; *=p<0.05;**=p<0.01 ***=p<0.001; error bars=SEM; Scale bar=25μm

At 75 days, EDL from Arimoclomol treated mSOD1 mice was significantly less denervated than EDL from untreated mSOD1 mice, with 19.2% (±4.6 SEM; n=3; $p<0.05$). This preservation of innervation in Arimoclomol treated mSOD1 EDL muscle was maintained as disease progressed, so that at 90 days only 14.1% (±2.1 SEM; n=3; p=0.009) of the endplates were denervated in Arimoclomol treated EDL compared to untreated muscles. Even at 120 days only 20.5% (±2.0 SEM; n=3; p=0.001) of endplates were denervated compared to 55% in untreated mSOD1 mice.

3.3.1.2 Denervation in the soleus muscle of mSOD1 mice

The extent of denervation in the soleus muscles was also examined (see Fig.3.1). In the soleus muscle of WT mice, from 45 to 120 days: an average of only 4.9% (±1.4 SEM; n=5) endplates. This was similar to that seen in wtSOD1 soleus muscle where 4.9% (±0.3 SEM; n=3; p=1.00) were denervated. Thus, the soleus muscle from WT mice was used as control.

In mSOD1 soleus muscle, 9.4% (±3.2 SEM; n=4; p=0.245) of the endplates were denervated at 45 days, which was not significantly different from the normal levels of denervation observed in WT soleus muscle. Surprisingly, the extent of denervation increased only slightly with disease in mSOD1 mice and even at 75 days, only 12.0% (±2.4 SEM; n=4; p=0.003) of the endplates were denervated and at 90 days only 14.7% (±1.7 SEM; n=4; p=0.004) of endplates were denervated. However, by 120 days, denervation was more extensive with 40.5% (±2.3 SEM; n=4; p=0.003) denervated endplates (see Fig.3.1). However, even at 120 days of age, the extent of denervation in soleus muscle of mSOD1 mice was not as great as that observed in EDL muscle, where 55.5% of endplates were denervated at 120 days of age.

Treatment with Arimoclomol had very little effect on denervation in the mSOD1

soleus muscle during the early stages of disease. However, at 120 days, although there was a significant level of denervation in untreated mSOD1 soleus, treatment with Arimoclomol only displayed 10.9% (±2.3 SEM; n=3; p=0.0003) denervation.

3.3.2 Sprouting in mSOD1 mice

Nerve terminal sprouting is a characteristic response of denervation and muscle paralysis and can be used as a marker of regeneration (Brown et al., 1981). Thus, sprouting was assessed in the EDL and soleus muscles of WT, mSOD1 and Arimoclomol treated mSOD1 mice at various disease stages.

3.3.2.1 Sprouting in mSOD1 EDL muscle

In WT EDL, only 1.1% (±0.5 SEM; n=3) of the endplates examined were innervated by sprouts, at all ages, therefore, the data from all ages studied was pooled in order to obtain a mean value (see Fig.3.2). The level of sprouting in the EDL muscle of mSOD1 mice differed considerably from WT mice. Even as early as 45 days of age, EDL muscles in mSOD1 mice displayed a significant level of sprouting at the NMJ, with 6.4% (±2.0 SEM; n=3) of endplates innervated by sprouts, compared to WT EDL muscle (p=0.0239). As disease progressed, the level of sprouting increased, so that by 75 days, 24.3% (±5.6 SEM; n=4; p=0.0022) of endplates were contacted by sprouts. The extent of sprouting then began to decline and at 90 days 18.0% (±1.1 SEM; n=4; p=0.0001) of endplates were innervated by sprouts. At 120 days sprouting declined to only 7.3% (±1.4 SEM; n=4; p=0.0025). As can be seen in Fig.3.2, treatment with Arimoclomol increased sprouting at all ages studied. At 45 days, 9.2% (±3.5 SEM; n=3; p=0.4905) endplates were innervated by sprouts in Arimoclomol treated mSOD1 EDL muscle. By 75 days, sprouting had reached 30.7% (±6.0 SEM; n=3; p=0.4761) and by 90 days, 25.3% (±3.1 SEM; n=3; p=0.0535). By 120 days, sprouting was significantly higher in Arimoclomol treated EDL muscle compared to untreated mSOD1 EDL muscle, with 25.4% (±1.4 SEM; n=3; p=0.003).

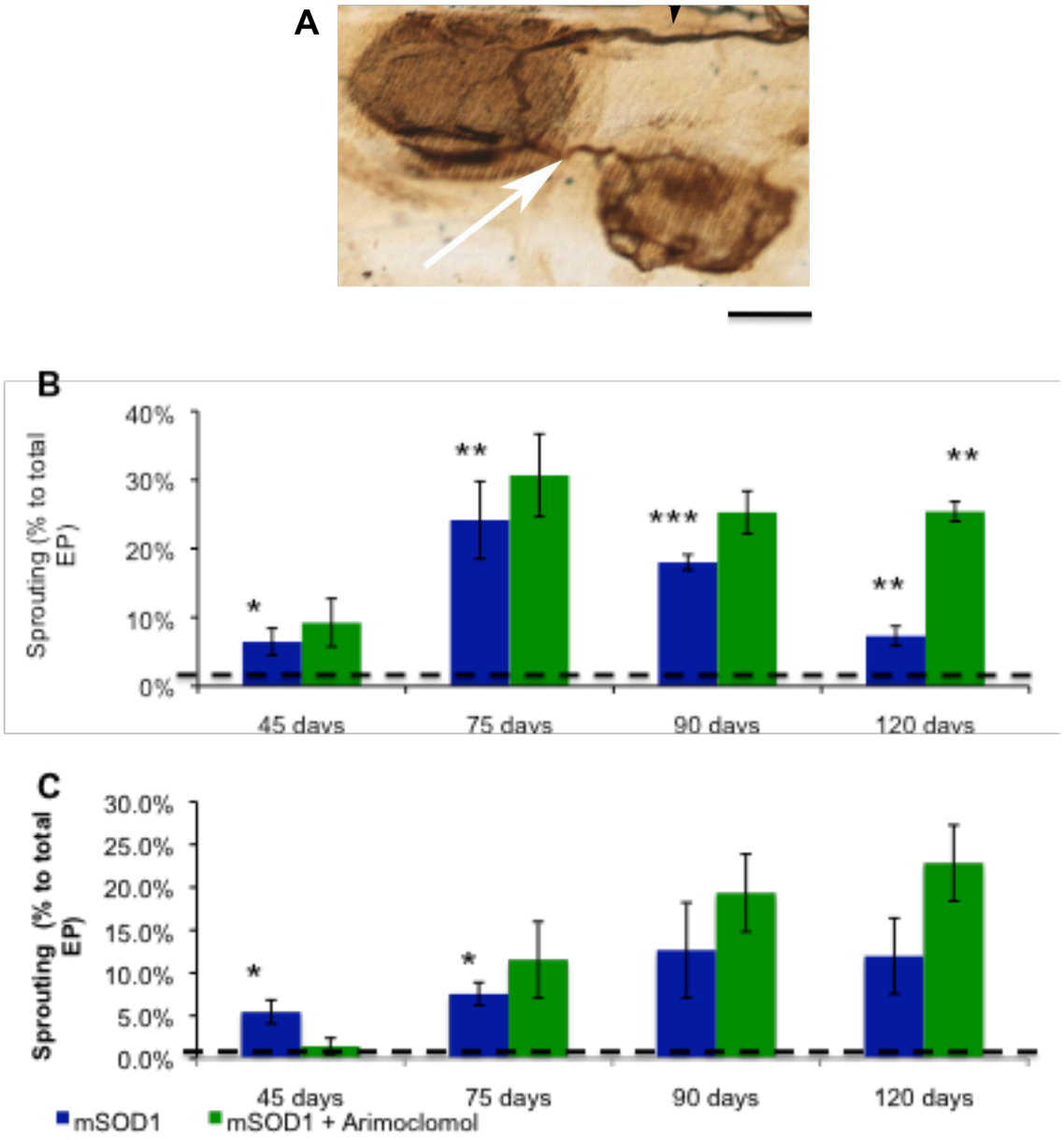

Figure 3.2: Nerve terminal sprouting in the EDL and soleus muscle of WT, mSOD1 and Arimoclomol treated mSOD1 mice

The extent of nerve terminal sprouting in the EDL and soleus muscles of WT, mSOD1 and Arimoclomol treated mSOD1 mice were established at 45, 75, 90 and 120 days of age. (A) An example of an EDL muscle stained with silver-cholinesterase**,** in which a nerve terminal sprout can be seen (arrow). The extent of sprouting in EDL and soleus muscles at all ages is summarised in the bar charts (B & C), respectively.

n=4; *=p≤0.05; **=p≤0.01; ***=p≤0.001; error bars= SEM; Scale bar=50μm

3.3.2.2 Sprouting in the soleus muscle mSOD1 mice

As seen in Fig.3.2, sprouting in the soleus muscle of WT mice did not change with age, and at all ages studied an average of 2.2% (±1.1 SEM; n=4) of endplates were innervated by sprouts. In the soleus muscle of mSOD1 mice, a significant increase in the extent of sprouting was only observed from 75 days onwards. At 75 days, sprouting was 7.5% (±1.3 SEM; n=4; p=0.032). By 90 days, it had increased to 12.7% (±5.6 SEM; n=4; p=0.115). This level of sprouting was maintained, so that by 120 days of age 12.0% (±4.4 SEM; n=3; p=0.054) of endplates were innervated by a sprout, compared to WT.

Treatment with Arimoclomol resulted in a marked increase in sprouting in soleus muscle, compared to untreated soleus muscle of mSOD1 mice (see Fig.3.2). At 75 days, 11.5% (±4.4 SEM; n=3; p=0.362) of endplates investigated. At 90 days, this increase in sprouting was maintained, so that 19.3% (±4.5 SEM; n=3; p=0.4228) of endplates were innervated by sprouts, compared to untreated mSOD1 soleus muscle. By 120 days, 22.8% (±4.4 SEM; n=3; p=0.0142) of endplates were innervated by sprouts, compared untreated soleus muscle from mSOD1 mice.

3.3.3 Polyneuronal innervation in mSOD1 mice

Following denervation and the ensuing sprouting, some endplates can become polyneuronally innervated. Therefore, the extent of PNI in the EDL and the soleus muscles of WT, mSOD1 and Arimoclomol treated mSOD1 mice at different stages of disease were examined.

3.3.3.1 Polyneuronal innervation in the EDL muscle of mSOD1 mice

In WT EDL muscle at all stages examined, the level of polyneuronal innervation (PNI) was very low, and an average of 1.0% (±0.4 SEM; n=4) of endplates (Fig.3.3) was innervated by more than one nerve terminal. In the EDL muscles of mSOD1 mice, as can be seen in Fig.3.3, PNI was minimal during all stages of disease.

Thus, at 45, 75, 90 and 120 days of age, the level of PNI in mSOD1 EDL muscles was 4.4% (±1.8 SEM; n=6; p=0.71), 3.9% (±0.7 SEM; n=5), 6.6% (±3.2 SEM; n=3) and 2.5% (±1.1 SEM; n=4; p=0.768), respectively. Statistical comparison with WT levels revealed that this slight increase in PNI in mSOD1 EDL muscles is not significant at any of the ages studied, except for 75 days of age, where the very low standard error in the data indicates that PNI at this age was statistically greater than in WT EDL (p=0.71; p=0.01; p=0.64 and p=0.77) for 45, 75, 90 and 120 days of age, respectively. However, despite this apparent increase in PNI at 75 days of age, it is clear that there is a very minimal increase the number of endplates contacted by more than one nerve terminal in EDL muscles of mSOD1 mice.

Treatment with Arimoclomol increased PNI in the EDL muscles of mSOD1 mice at all ages studied, but this did not reach significance until 120 days of age. Thus, at 45 days PNI was 5.1% (±1.9 SEM; n=3; p=0.84); at 75 days it was 7.2% (±1.5 SEM; n=3; p=0.75), and at 90 days it was, 6.0% (± 0.8 SEM; n=4; p=0.95) compared to untreated mSOD1 EDL muscle. By 120 days, PNI had dramatically increased so that 14.9% (±1.1 SEM; n=3; p=0.0006) of the endplates in the EDL were polyneuronally innervated, compared to untreated mSOD1 EDL muscle.

3.3.3.2 Polyneuronal innervation in the soleus of mSOD1 mice

At all stages studied, the level of PNI in WT soleus muscle did not vary, and so all data from all ages studied was pooled. A total of 1.8% (±1.1 SEM; n=3) of the endplates were polyneuronally innervated. In mSOD1 mice, the extent of PNI at the NMJ of soleus muscle did not alter significantly over the course of the disease and was between 4.0-6.0% at all ages studied. As seen in Fig.3.3, following treatment with Arimoclomol, there was a slight increase in PNI after 75 days, but this only reached significance at 120 days, when 14.7% (±3.5 SEM; n=3; p=0.034) of all endplates were polyneuronally innervated compared to untreated mSOD1 soleus muscle at the same stage of disease.

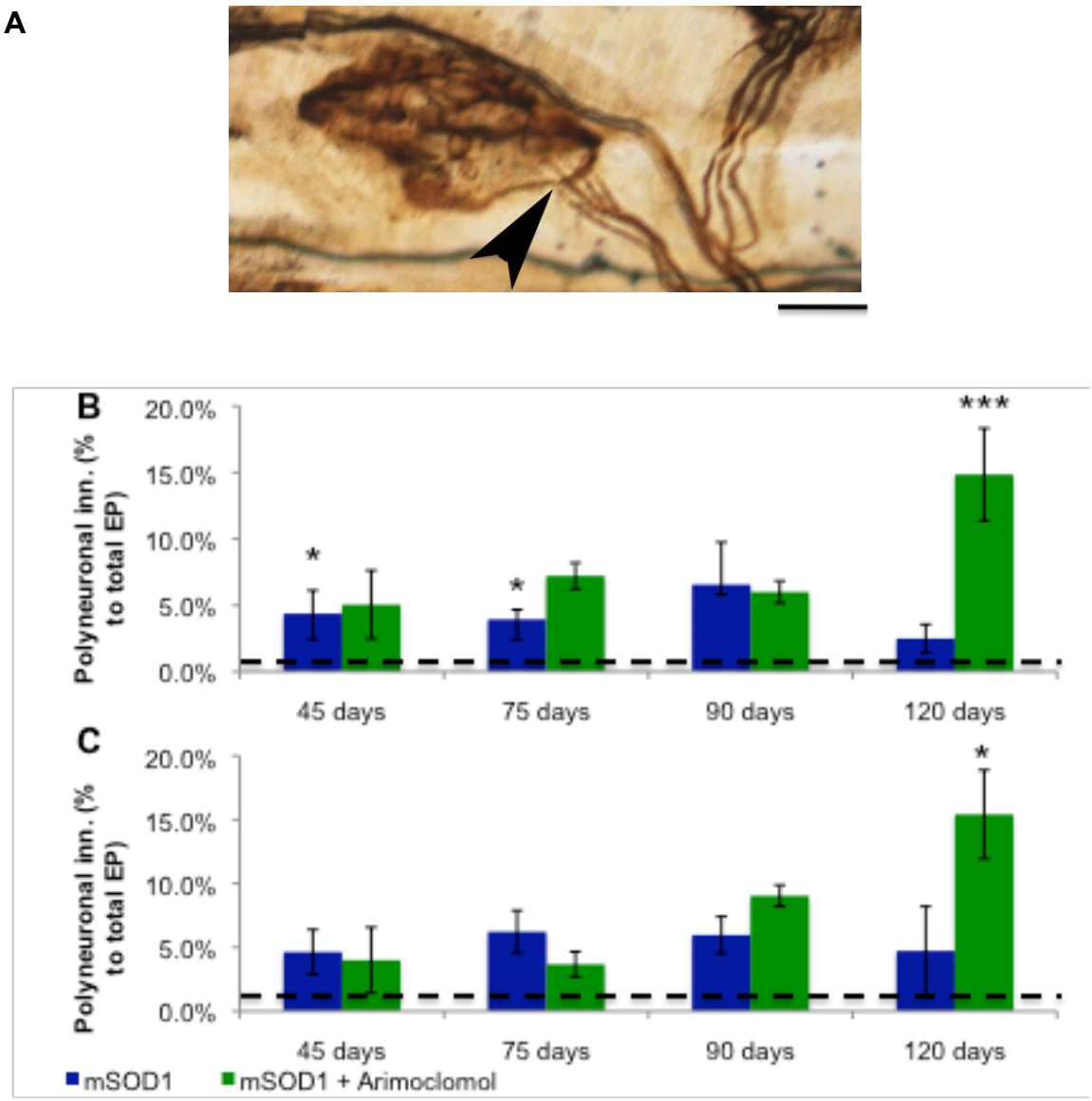

Figure 3.3: Polyneuronal innervation in the muscle of WT, mSOD1 and Arimoclomol treated mice

The number of endplates contacted by more than one nerve terminal was established and expressed as a percentage of the total number of endplates examined. An example of an EDL muscle stained with a silver cholinesterase stain is shown in (A), in which a PNI endplate can be seen (arrowhead). The mean number of PNI endplates in the EDL and soleus muscles at each stage of disease is summarised in the bar charts (B &C), respectively.

n=4; *=p<0.05; ***=p<0.001; error bars = SEM; Scale bar=25μm

3.3.4 Endplate size in mSOD1 mouse muscle

Alterations in endplate size are a known to occur in circumstances of NMJ pathology. As mSOD1 mice exhibit significant NMJ pathology, it is possible that endplate size is altered. Thus, the size of endplates in the EDL and soleus muscles was assessed in WT, mSOD1 and Arimoclomol treated mSOD1 mice at a presymptomatic stage (45 days of age), when denervation is low and then at late symptomatic stage (120 days of age), when denervation is high.

3.3.4.1 Changes in endplate size in mSOD1 EDL muscle

As can be seen in Fig.3.4, in WT mice, endplate size in the EDL muscle did not change significantly with age, so the data from all age groups was combined. The mean endplate size in WT mice was 787.54μm^2 (±30.29 SEM; n=3). In mSOD1 mice, the mean endplate size at 45 days, when fewer than 10% of endplates were denervated in the EDL muscle, was 613.27μm^2 (±20.12 SEM; n=3). This was already 20% smaller than the mean endplate size in WT EDL muscle (p=0.0087). However, there was no further decrease in the mean endplate size in the EDL muscle of mSOD1 mice, so that at 120 days, the mean endplate size was 628μm^2 (±19.98 SEM; n=3; p=0.0117), compared to WT endplates. Treatment with Arimoclomol prevented this decrease in endplate size in mSOD1 EDL muscle. Thus, at 120 days, in mSOD1 EDL muscles, the average endplate size was 725.05μm^2 (±34.85 SEM; n=4; p=0.049), which was significantly larger than endplate size in untreated mSOD1 EDL muscle.

3.3.4.2 Changes in endplate size in mSOD1 soleus muscle

The average size of endplates in the soleus muscle was also examined. As the size of endplates in the soleus muscle of WT mice did not change significantly with age, so data from 45 days and 120 days of age was pooled together, averaged, and found to be 598.03μm^2 (±50.17 SEM; n=3). This was ~20% smaller than the mean endplate size in the EDL muscle of WT mice (p=0.0319).

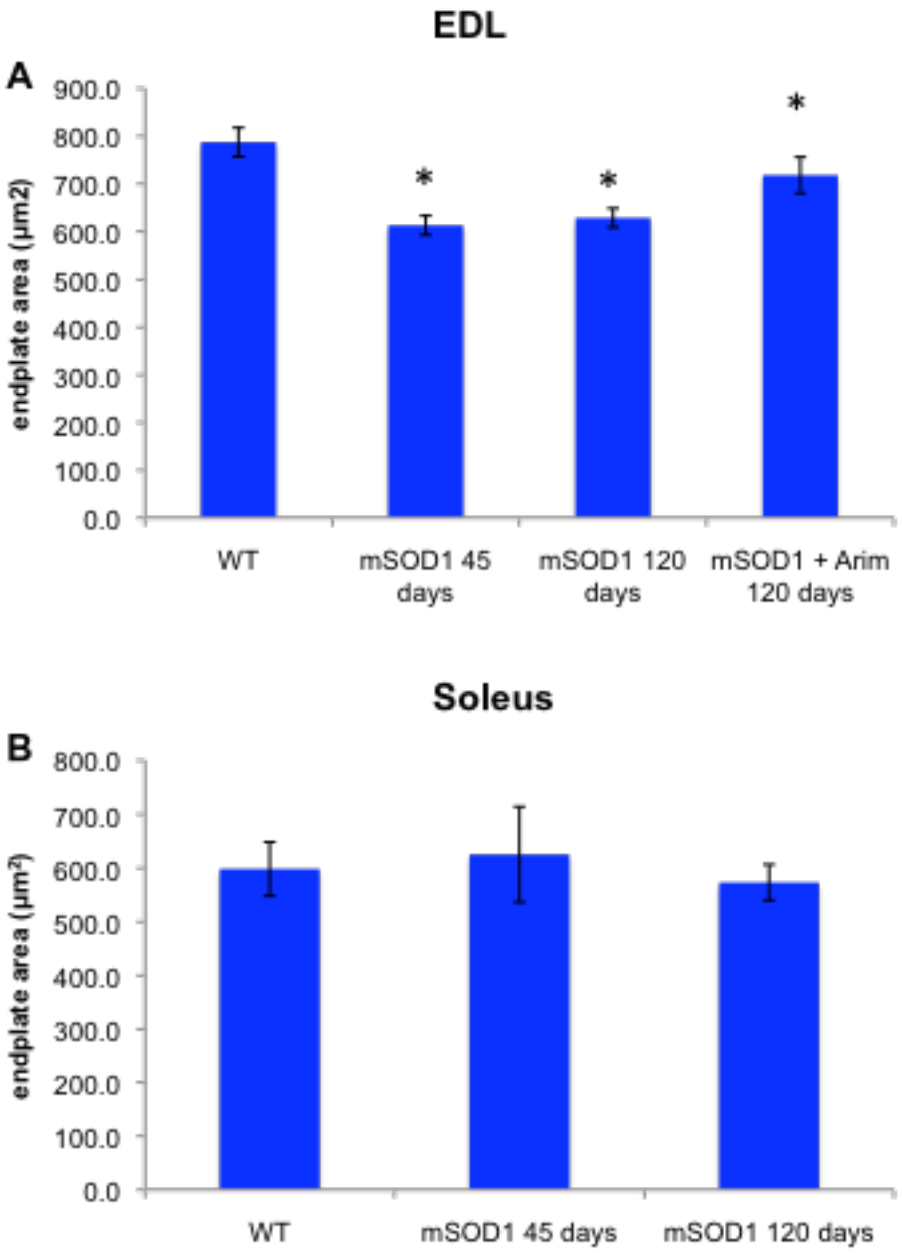

Figure 3.4: The mean endplate size in the EDL and soleus muscles of WT, mSOD1 and Arimoclomol treated mSOD1 mice

The mean endplate size in the (A) EDL and (B) soleus muscles of WT, mSOD1 mice at 45 and 120 days of age is summarised in the bar chart. In the EDL muscle, the effect of treatment with Arimoclomol was also examined (A).

n=4; *=$p<0.05$; error bars = SEM

The average endplate size in mSOD1 soleus muscle was measured (see Fig.3.4) and surprisingly, the mean size of endplates in mSOD1 soleus did not change significantly over the course of the disease. At 45 days the mean endplate size was 625μm^2 (±89.07 SEM; n=3; p=0.805) and at 120 days of age, it was 572.89μm^2 (±33.30SEM; n=3; p=0.698), which is not significantly different. As there was no change in endplate size in the soleus muscle during disease, the effect of treatment with Arimoclomol was not examined.

3.3.5 Changes in the oxidative capacity of hindlimb muscles of mSOD1 mice

A change in the oxidative capacity of fast-twitch muscle fibres is a characteristic of muscle pathology in mSOD1 mice (Atkin et al., 2005). In view of the improvement in muscle innervation in Arimoclomol treated mSOD1 mice, the effect of Arimoclomol on the oxidative capacity of the TA, EDL and soleus muscles were examined. Muscles were stained for SDH in order to distinguish between darkly stained, highly oxidative fibres, intermediately stained, moderately oxidative fibres and lightly stained, highly glycolytic muscle fibres. The number of darkly stained muscle fibres, intermediately stained muscle fibres and pale fibres was counted in the TA, EDL and soleus muscles of WT, mSOD1 and Arimoclomol treated mSOD1 mice at 45 and 120 days of age. Examples of SDH stained muscle can be seen in Fig.3.5.

3.3.5.1 The effect of Arimoclomol on the oxidative capacity of mSOD1 TA muscle

The pattern of SDH staining in WT TA muscle was assessed at 45 and 120 days and was found to be similar at each age. Therefore, data from WT muscle at these ages was pooled and averaged. Thus, 29.46% (±0.85 SEM; n=3) of fibres were stained darkly for SDH. 33.58% (±4.02 SEM; n=3) of WT TA muscle fibres had an intermediate level of staining, and 37% (±4.87 SEM; n=3) of fibres stained faintly for SDH (see Fig.3.6).

As can be seen in Fig.3.6, in the TA muscle of 45-day-old mSOD1 mice, 27.45% (±3.53 SEM; n=3; p=0.6093) of fibres were darkly stained, 46.47% (±3.55 SEM; n=3; p=0.0760) of the fibres were intermediately stained and only 26.08% (±1.20 SEM; n=3; p=0.0959) of the fibres stained lightly for the SDH stain. By 120 days of age, the oxidative profile of the mSOD1 TA was significantly different from that seen in WT TA muscle. 75.28% (±4.25 SEM; n=3; p=0.001) of fibres were darkly stained compared to WT. This represented an increase of 170%, compared to 45-day-old mSOD1 mice (p=0.001). The percentage of intermediately stained fibres was significantly lower in 120-day-old mSOD1 TA muscle, with only 23.57% (±3.63 SEM; n=3; p=0.009) of fibres stained compared to WT. There were also significantly fewer lightly stained muscle fibres, with only 1.15% (±0.62 SEM; n=3; p=0.0001), compared to WT.

As can be seen in Fig.3.6, treatment with Arimoclomol prevented this change in the pattern of SDH staining, in the TA muscle of mSOD1 mice. In 120-day-old Arimoclomol treated mSOD1 TA muscle, significantly fewer fibres were darkly stained, with 56.45% (±3.38 SEM; n=3; p=0.026) of muscle fibres staining darkly for SDH, compared to untreated mSOD1 TA muscle. Significantly more fibres were moderately stained, so that 40.95% (±3.36 SEM; n=3; p=0.035) of fibres were stained, compared to 23.57% in untreated mSOD1 TA muscle. Only 2.60% (±0.02 SEM; n=3; p=0.038) of muscle fibres were lightly stained, which was significantly more than in untreated mSOD1 TA muscle, but still significantly less than in WT TA muscle.

3.3.5.2 The effect of Arimoclomol on the oxidative capacity of mSOD1 EDL muscle

The oxidative profile of the EDL muscle in WT, untreated and Arimoclomol treated mSOD1 mice was also examined. As there was no change in the pattern of SDH staining in WT EDL muscle with age, the data from the two ages was pooled and averaged. Thus, in WT EDL muscle, 23.72% (±2.60 SEM; n=3) of the muscle fibres

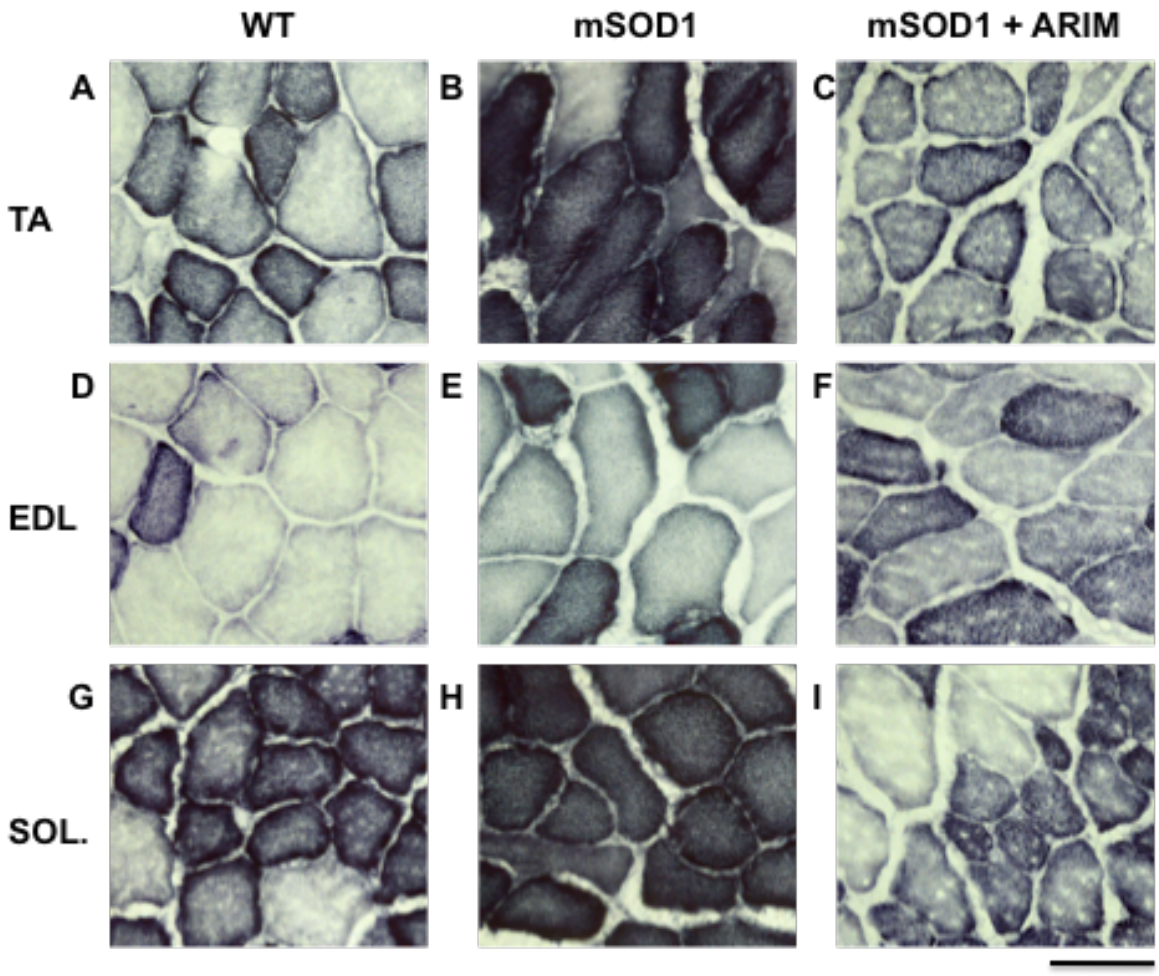

Figure 3.5: The pattern of SDH staining in hindlimb muscles of WT, untreated and Arimoclomol treated mSOD1 mice

Sections of TA, EDL and soleus muscles of WT mice as well as 120-day-old mSOD1 and Arimoclomol treated mSOD1 mice. Typical examples of each muscle from WT, mSOD1 and Arimoclomol treated mSOD1 are shown. An example of the TA (A-C), the EDL (D-F) and the soleus muscle (G-I) from each experimental group is shown in high power images are shown.

Scale bar = 50μm; n=4

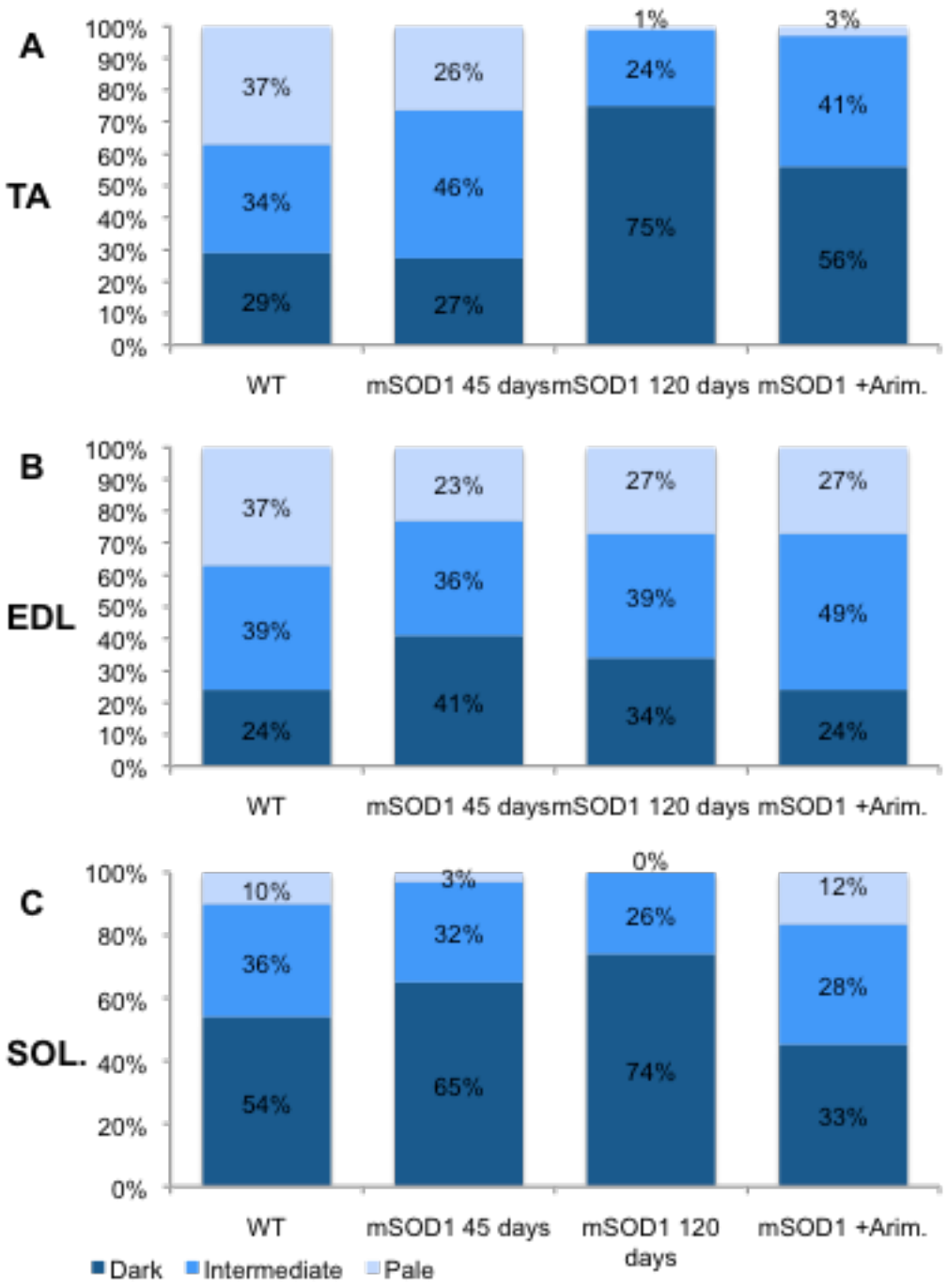

Figure 3.6: The pattern of SDH staining in the hindlimb muscle of WT, untreated and Arimoclomol treated mSOD1 mice

The staining intensity of muscle stained for SDH was quantified in the TA, EDL and soleus muscles of WT mice and untreated mSOD1 mice at 45 and 120 days of age, as well as Arimoclomol treated mice at 120 days of age is shown. The bar charts (A-C) summarise the proportion of these fibres in the TA, EDL and soleus muscles respectively. n=4

were darkly stained. The proportion of muscle fibres that were intermediately stained was 39.38% (±7.36 SEM; n=3), and the percentage of lightly stained muscle fibres was 36.90% (±9.96 SEM; n=3).

As can be seen in Fig.3.6, in mSOD1 EDL muscle, at 45 days of age, there was a significant increase in darkly stained fibres with 41.42% (±2.53 SEM; n=3; p=0.0082), of fibres staining intensely for SDH. The level of intermediately stained fibres was similar to WT with 31.58% (±7.81 SEM; n=3; p=0.5076) of fibres intermediately stained. However, the proportion of pale muscle fibres at 45 days of age was a significantly fewer fibres stained lightly for SDH, with only 22.91% (±3.50SEM; n=3; p=0.02557), compared to WT EDL muscle. These changes in the oxidative profile of the EDL muscle of mSOD1 mice did not change further as disease progresses, so that at 120 days of age, 37.87% (±4.22 SEM; n=3; p=0.046), 32.97% (±6.94 SEM; n=3; p=0.56) and 29.19% (±2.86 SEM; n=3; p=0.49) of fibres stained darkly, intermediately and faintly for SDH, respectively (see Fig. 3.6).

Treatment with Arimoclomol prevented the change in SDH staining pattern in the EDL muscles of mSOD1 mice, so that at 120 days of age, only 23.79% (±9.13 SEM; n=3; p=0.034) of the fibres examined were dark, compared to ~38% in untreated mSOD1 EDL muscle. However, treatment with Arimoclomol did not alter the proportion of intermediately stained fibres, thus, 42.79% (±8.76 SEM; n=3; p=0.4292) of fibres were intermediately stained compared to untreated mSOD1 EDL muscle. Arimoclomol also had a limited effect on the proportion of the palest muscle fibres, 33.07% (±6.08 SEM; n=3; p=0.992) of the fibres were pale.

3.3.5.3 The effect of Arimoclomol on the oxidative capacity of soleus muscle

The oxidative capacity of muscle fibres in the soleus muscle was also assessed. As pattern of staining in the soleus from WT mice did not alter with age, data from

all ages was pooled and averaged. As shown in Fig.3.6, 53.77% (±4.99 SEM; n=3) of muscle fibres were darkly stained; 35.87% (±4.81 SEM; n=3) of fibres were intermediately stained and a small population of fibres, 10.35% (±6.56 SEM; n=3) were lightly stained.

In the soleus muscle of mSOD1 mice, at 45 days of age, the pattern of SDH staining was similar to WT. Thus, 65.38% (±5.38 SEM; n=3; p=0.189) of muscle fibres were darkly stained; 31.58% (±5.48 SEM; n=3; p=0.588) were intermediately stained and only 3.71% (±2.03 SEM; n=3; p=0.388) of muscle fibres were lightly stained. By 120 days, 73.81% (±4.91 SEM; n=3; p=0.046) of all muscle fibres were darkly stained, which was significant more than WT. The proportion of intermediately stained, moderately oxidative muscle fibres had decreased to 26.19% (±4.93 SEM; n=3; p=0.233), and there were no pale fibres (0.00% (±0.00SEM; n=3; p=0.19)).

As can be seen in Fig.3.6, treatment with Arimoclomol prevented this change in the oxidative capacity of the soleus muscle in mSOD1 mice. In soleus muscles of 120-day-old Arimoclomol treated mSOD1 mice, only 55.92% (±13.63 SEM; n=3; p=0.285) of fibres were darkly stained, compared to untreated mSOD1 soleus muscle. There was a modest increase in the number of intermediately stained fibres, so that 35.43% (±10.03 SEM; n=3; p=0.455) of fibres were intermediately stained compared to untreated mSOD1 soleus muscle. Treatment also significantly increased the proportion of lightly stained fibres, which was 8.65% (±3.06 SEM; n=3; p=0.048) of the soleus, compared to untreated mSOD1 mice.

3.3.6 Biochemical assessment of neuromuscular activity in the muscles of mSOD1 mice

As a measure of neuromuscular transmission, the activity of the cholinergic enzymes ChAT and AChE were determined in the TA, EDL and soleus muscles of WT, mSOD1 and Arimoclomol treated mSOD1 mice.

3.3.6.1 The effect of Arimoclomol on ChAT activity in the TA muscle

ChAT activity in the TA muscles from WT mice did not change over time and so data from all ages was pooled. In WT TA muscle, the mean ChAT activity was 13098.53cpm (±643.32 SEM; n=10).

As can be seen in Fig.3.7a, at 45 days, ChAT activity in the TA muscle of mSOD1 mice was 10745.67cpm (±384.85 SEM; n=6; p=0.019), compared to WT TA muscle. By 75 days, activity had declined further to 9105.67cpm (±419.11 SEM; n=6; p<0.001), and by 90 days, ChAT activity in the TA muscle had fallen even further to 7495.00cpm (±102.00SEM; n=4; p<0.001). This was more than 50% less than in WT TA muscle (p<0.001). After 90 days ChAT activity remained stable so that at 120 days ChAT activity was 9455.25cpm (±273.76 SEM; n=3; p=0.012). Treatment with Arimoclomol increased ChAT activity at all ages studied. However, this did not reach significance until 120 days, when it was 10609.00cpm (±195.02 SEM; n=6; p=0.011), compared to untreated mSOD1 mice.

3.3.6.2 ChAT activity in the EDL muscle of mSOD1 mice and the effect of Arimoclomol

ChAT activity in the EDL muscle of WT mice was examined and found to be stable with age, so data from all ages was grouped together and the mean ChAT activity in WT EDL was 16248.08cpm (±712.68 SEM; n=12).

As seen in Fig.3.7b, at 45 days of age, in mSOD1 mice, there was no difference in the level of ChAT activity compared to WT EDL muscle. At 75 days, the level of ChAT activity had decreased and was 12845.67cpm (±838.78 SEM; n=3; p=0.042) at 90 days, declined further to 9120.67cpm (±1754.91 SEM; n=4; p<0.001), compared to WT. At 120 days, ChAT activity stabilised and was 10607.38cpm (±455.36 SEM; n=8; p<0.001) compared to WT.

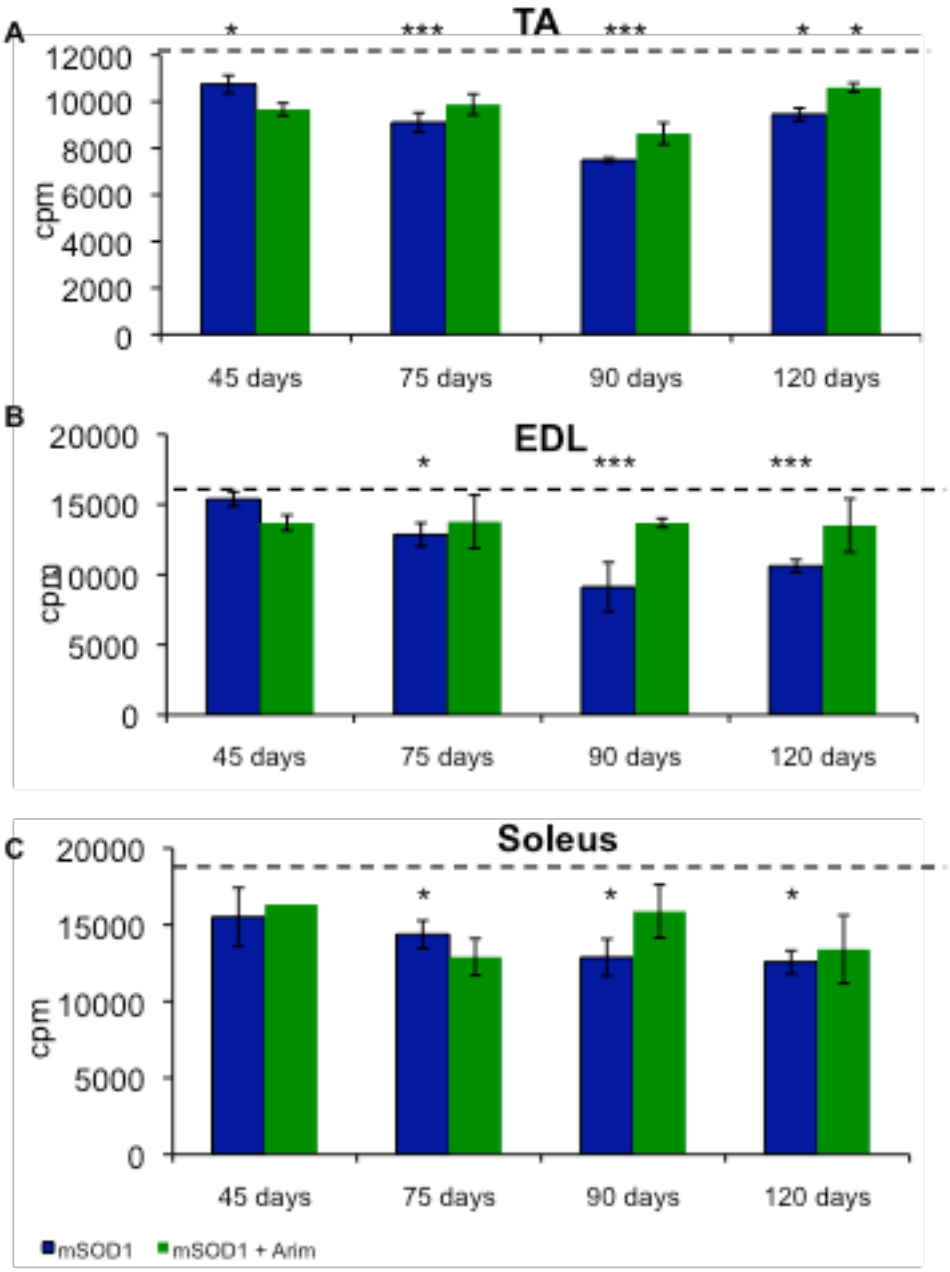

Figure 3.7: ChAT activity in the muscle of WT, mSOD1 and Arimoclomol treated mSOD1 mice

ChAT activity was assessed in hindlimb muscles of WT, mSOD1 and Arimoclomol treated mSOD1 muscles at 45, 75, 90 and 120 days. The mean ChAT activity in the (A) TA, (B), EDL and (C) soleus muscles is summarised in the bar charts. The dotted line represents the mean ChAT activity in corresponding muscles of WT mice.

n=4; *=p<0.05; error bars = SEM

The results in Fig.3.7b shows that treatment with Arimoclomol slightly increased ChAT activity in the EDL muscles of mSOD1 mice, although, this did not reach significance. Thus, ChAT activity in Arimoclomol treated mSOD1 EDL muscle was 13778.33cpm (±1888.79 SEM; n=3; p=0.675) and at 90 days, ChAT activity was 13686.3cpm (±321.51 SEM; n=4; p=0.0627), and at 120 days, ChAT activity was 13509.20cpm (±1905.41 SEM; n=5; p=0.093).

3.3.6.3 The effect of Arimoclomol on ChAT activity in the soleus muscle of mSOD1 mice

The examination of ChAT levels in the soleus muscles of WT mice revealed that ChAT activity did not change with age, so data from all ages was pooled, averaged and found to be 19793.59cpm (±1051.63 SEM; n=14). As can be seen in Fig.3.7c, in mSOD1 mice, ChAT activity declined moderately with disease progression. While ChAT activity at 45 days of age was similar to WT. However, by 75 days, the level of ChAT activity was 14372.75cpm (±907.70SEM; n=4; p=0.0175), compared to WT. By 90 days, ChAT activity in mSOD1 soleus had fallen further to 12863.50cpm (±1214.46 SEM; n=4; p=0.0125) compared to WT. At 120 days, ChAT activity in the mSOD1 soleus was 12562.50cpm (±758.10 SEM; n=3; p=0.008) compared to WT. However, treatment with Arimoclomol had little effect on ChAT activity in the soleus muscle of mSOD1 soleus muscle at any age examined (see Fig. 3.7c).

3.3.7 AChE activity in the hindlimb muscles of mSOD1 mice

The level of AChE activity in the TA, EDL and soleus muscles of mSOD1 mice and the effect of treatment with Arimoclomol was examined.

3.3.7.1 The effect of Arimoclomol on AChE activity in the TA muscle

The level of AChE in the TA muscle from WT mice was examined and did not change over time. Therefore, data from WT mice was pooled and the mean AChE

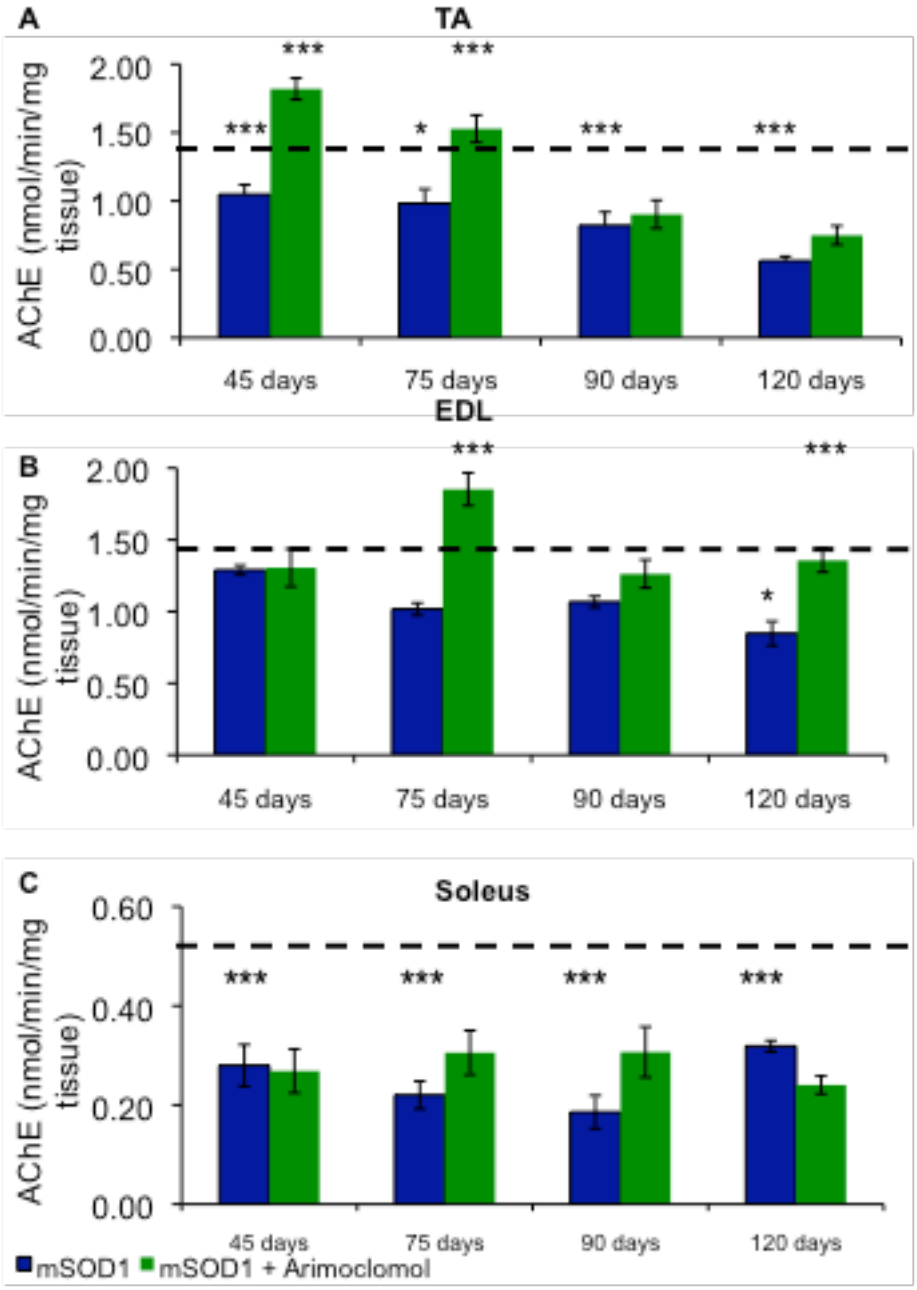

Figure 3.8: AChE activity in the muscle of WT, mSOD1 and Arimoclomol treated mSOD1 mice

AChE activity was assessed in hindlimb muscles of WT, mSOD1 and Arimoclomol treated mSOD1 muscles at 45, 75, 90 and 120 days. The mean AChE activity in the (A) TA, (B) EDL and (C) soleus are summarised in the bar charts. The dotted line represents AChE activity in WT mice for the corresponding muscle.

*=$p<0.05$; n=12; error bars = SEM

activity was taken as 1.36 nmol/min/mg (±0.06 SEM; n=12) of tissue.

As can be seen in Fig.3.8a, the level of AChE activity was significantly decreased in mSOD1 TA muscle compared to WT TA, at all ages studied. Even at 45 days, there was significantly less AChE activity in the mSOD1 TA muscle and AChE activity was 1.05nmol/min/mg (±0.07 SEM; n=12; $p<0.001$). AChE activity continued to decrease with disease, and by75 days AChE activity had fallen to 0.98nmol/min/mg (±0.11 SEM; n=12; $p=0.002$). By 90 days, AChE levels in the mSOD1 TA muscle had declined further, to only 0.82nmol/min/mg (±0.10SEM; n=8; $p<0.001$). AChE levels decreased even further so that by 120 days, levels were only 0.56nmol/min/mg (±0.03 SEM; n=9; $p<0.001$).

Treatment with Arimoclomol resulted in an increase in AChE activity in the TA muscle, particularly during the earlier stages of disease. At 45 days, AChE activity was 1.82nmol/min/mg (±0.08 SEM; n=12; $p<0.001$) compared to untreated mSOD1 littermates. By 75 days, AChE activity was 1.53nmol/min/mg (±0.10SEM; n=12; $p<0.001$), compared to untreated mSOD1 TA and by 90 days, the level of activity in the Arimoclomol treated TA had declined to 0.90nmol/min/mg (±0.10SEM; n=7; $p=0.001$). By 120 days, it was only 0.75nmol/min/mg (±0.07 SEM; n=9; $p=0.24$), compared to untreated mSOD1 TA muscle.

3.3.7.2 AChE activity in the EDL muscle of mSOD1 mice and the effect of treatment with Arimoclomol

In WT EDL muscle, the level of AChE activity did not alter with the age of the mice, so data from all ages was pooled, averaged and AChE activity was taken as 1.32 nmol/min/mg (±0.10SEM; n=20).

As can be seen in Fig.3.8b, AChE activity in the EDL muscle of mSOD1 mice was relatively stable over the course of disease, and no significant change was

observed until 120 days, when, AChE activity was 0.85nmol/min/mg (±0.08 SEM; n=10), compared to WT EDL muscle (p=0.005).

Treatment with Arimoclomol increased AChE activity in mSOD1 EDL muscle, so that at 120 days activity was 1.36nmol/min/mg (±0.08 SEM; n=7; p<0.001), compared to untreated mSOD1 EDL muscle.

3.3.7.3 The effect of Arimoclomol on AChE activity in the soleus muscle

AChE activity in the soleus muscle was also assessed in WT mice. This did not change over time, so data from all ages was pooled and the mean was taken as 0.50nmol/min/mg (±0.06 SEM; n=20; p<0.001).

AChE activity in the soleus of mSOD1 mice was then examined. As seen in Fig.3.9c, AChE activity was 0.28nmol/min/mg (±0.04 SEM; n=7; p=0.047) in mSOD1 soleus at 45 days, compared to WT. As disease progressed, AChE activity declined further, so that at 75 days activity was 0.22nmol/min/mg (±0.03 SEM; n=7; p=0.013). At 90 days of age, AChE activity was 0.19nmol/min/mg (0.03 SEM; n=7; p=0.0003). By 120 days, AChE activity had slightly increased to 0.32nmol/min/mg (±0.01 SEM; n=7; p=0.092).

Treatment with Arimoclomol did not significantly alter AChE activity in soleus muscles over the course of the disease until 120 days. Surprisingly, in Arimoclomol treated soleus muscle, AChE activity fell to 0.24nmol/min/mg (±0.02 SEM; n=7; p=0.004) compared to untreated mSOD1 soleus muscle.

3.4 Discussion

In this Chapter, the disease progression in hindlimb muscles was investigated in mSOD1 mice. The pattern of innervation in WT, and mSOD1 at 45, 75, 90 and 120 days of age was assessed as well as endplate size, and ChAT and AChE activity. In addition, the oxidative capacity of these muscles was also assessed. Since our lab has previously shown the beneficial effects of Arimoclomol in this ALS model. The effect of Arimoclomol on these disease characteristics was also investigated.

The results presented in this Chapter revealed significant, early denervation in the hindlimb muscles of mSOD1 mice, which was apparent from as early as 45 days in the EDL muscle and 120 days of age in the soleus muscle. In the EDL muscle, compensatory mechanisms such as sprouting and polyneuronal innervation occurred at symptomatic onset, but were of a short duration. mSOD1 pathology also resulted in the presymptomatic reduction in endplate size in the more vulnerable EDL muscle. In the more resistant soleus muscle sprouting and PNI were minimal and endplate size was not altered by disease. mSOD1 mice also demonstrated moderately decreased ChAT activity and dramatically decreased AChE activity in both fast and slow-twitch muscles.

3.4.1 Differential pathology in fast and slow-twitch muscles in mSOD1 mice

This study showed that there is a greater loss of innervation in the fast-twitch EDL muscle compared to the slow-twitch soleus muscle in mSOD1 mice at each disease time point examined. Similar findings have also been observed in nerve injury models (Albuquerque and McIsaac, 1970), suggesting an intrinsic vulnerability of fast-twitch muscles to denervation. Indeed, following partial denervation caused by nerve crush, fast-twitch muscles such as the EDL have been shown to undergo more extensive denervation than slow-twitch muscles like the soleus muscle (Raffaello et al., 2006). Frey et al., (2000a) who also demonstrated differential denervation in fast and slow-twitch muscles in mSOD1 mice.

In response to denervation, it is well established that motor axons attempt to compensate for the loss of innervation by sprouting to occupy the denervated fibres. The extent of such compensatory mechanisms can be quantified by counting the extent of sprouting and PNI. In this study these compensatory mechanisms were found to also vary between fast and slow-twitch muscles of mSOD1 mice. While sprouting and PNI in both muscles were low, an early and strong regenerative response was present in the EDL muscle at disease onset, but this quickly declined. Interestingly, PNI is a common consequence of reinnervation was minimal in both muscles examined.

Denervation in the EDL muscle was accompanied by a reduction in the average size of endplates. Moreover, this decrease was present before disease onset. However, the mean endplate size did not decline further, despite the progressive decline in innervation. Interestingly, while denervation was also present in mSOD1 soleus muscle, this was not accompanied by a reduction in endplate size. It is of interest to note that while models of nerve injury, demonstrate a reduction in the mean size of endplates as a consequence of denervation (Suzuki et al., 2009), Murray et al., (2008) found no such correlation between endplate occupancy and endplate size. Likewise, my results indicate that changes in mean endplate size in mSOD1 mice does not correlate with innervation and thus, may be dependant on additional unknown factors in the disease.

A change in the oxidative profile of a muscle is a common consequence of denervation (Somasekhar et al., 1996) or age (Nishizaka et al., 2010). Following long-term denervation and with age, the oxidative profile of a muscle declines significantly (Adami et al., 1985; Nishizaka et al., 2010). While partial denervation, followed by reinnervation, results in the lost of the mosaic-like pattern of SDH staining, with fibres that stained a similar intensity for SDH grouped together.

Unlike, aged muscles, or muscle that had undergone long-term denervation, all of the muscles examined in mSOD1 mice exhibited an increase in SDH staining; indicative of their oxidative capacity during disease progression, with the preferential loss of pale glycolytic fibres. This change was greatest in the fast-twitch TA and EDL muscles. Increases in oxidative capacity in the muscles are usually indicative of an increased oxidative metabolism (Jeppesen et al., 2003) and increased mitochondrial activity. As both oxidative stress and mitochondrial damage have been implicated in ALS pathogenesis, it is possible that changes in muscle metabolism may also play a part in muscle pathology in mSOD1 mice.

3.4.2 The ratio between ACh production and breakdown differs between fast and slow-twitch muscle

Previous authors have reported that ChAT activity is significantly greater in the slow more resilient soleus muscle compared to the vulnerable fast-twitch muscles such as the TA and EDL muscles of rodents (Diamond et al., 1974, Wooten and Cheng, 1980). Furthermore, the while the amount if ChAT increases with age in the soleus, this is not the case with fast muscles such as the EDL. Rather, aged EDL muscle has been shown to display increased AChE levels (Washio et al., 1987). It is thought that such differences between the age-related changes in ChAT and AChE contribute to the degree to which muscle activity is maintained with age.

With this in mind, it is interesting to note that in the present study when the ratio ChAT to AChE (two enzymes with opposing effects) is compared an interesting pattern emerges. Thus, as is shown in Fig.3.9, the ratio of ChAT: AChE for the soleus muscle is very high: 45449.75 (±564.63 SEM: n=14) to 1, compared to only 12991.68 (±877.46 SEM; n=12; $p<0.001$): to 1, in the EDL and 9990.39 (±564.63 SEM; n=10; $p<0.001$) to 1, in the TA muscle Thus, the ChAT: AChE ratio was significantly lower in more vulnerable TA muscle than the EDL muscle ($p=0.012$). Since synaptic strength, as determined by ChAT activity (Buffelli et al., 2003), is known to influence NMJ morphology and efficacy, particularly during development,

it is possible that it has lasting implications for innervation in the muscles of mSOD1 mice. These findings indicate a potential role for synaptic strength in NMJ vulnerability in ALS. Whereby the strongest nerve terminals with high levels of ChAT activity are less vulnerable to mSOD1 pathology.

3.4.3 Arimoclomol reduces mSOD1-mediated muscle pathology

Treatment with Arimoclomol significantly reduced the level of denervation in the muscles of mSOD1 mice, at 45 days of age, and maintained the level of innervation until 120 days-of-age. It also increased the level of sprouting and PNI in EDL and soleus muscles after disease onset. These effects were greatest in the more vulnerable fast-twitch EDL muscle. Arimoclomol also increased endplate size and prevented the change in the oxidative profile of the fast-twitch TA and EDL muscles in mSOD1 mice and Arimoclomol also moderately increased ChAT and AChE activity in the more vulnerable fast-twitch muscles.

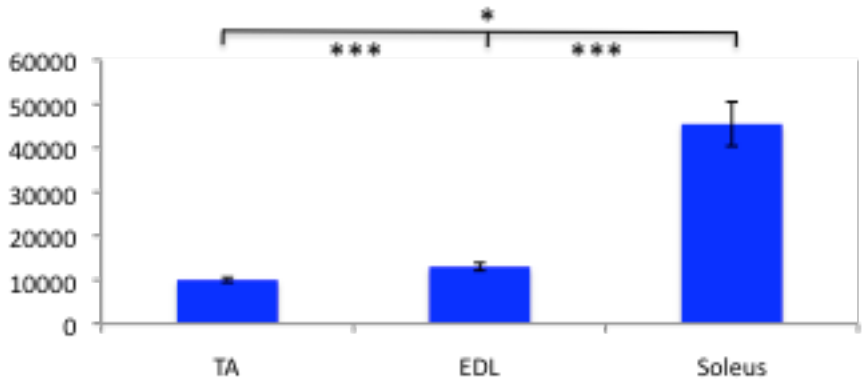

Figure 3.9: The ratio of ChAT:AChE in the TA, EDL and soleus muscle of WT mice

The above bar chart shows the Amount of ChAT per unit of AChE in the TA, EDL and soleus muscle of WT mice.

These findings suggest that treatment with Arimoclomol may effect synaptic plasticity, a mediating factor for NMJ vulnerability (Santos and Caroni, 2003), preferentially rescuing the more vulnerable NMJs. As Arimoclomol is a co-inducer of the HSR and hsps are the primary modulators of the HSR. It is likely that at least one mechanism by which Arimoclomol exerts these effects is mSOD1 muscle is via the HSR within muscle. In addition to its established ability to increase this cytoprotective mechanism within the CNS (Kieran et al 2004), this suggests that the endogenous effect HSR is normally insufficient to deal with mSOD1-induced toxicity within muscle.

3.4.4 Conclusions

In conclusion, the results presented in this Chapter demonstrate that denervation occurs first in fast-twitch muscles, and before motoneuron death. Furthermore, treatment with Arimoclomol delays the rate of denervation and promotes compensatory mechanisms such as sprouting, resulting in an increase in PNI at the NMJ of mSOD1 muscles. This study also highlights the differential decrease in functional markers of cholinergic transmission and endplate size, which treatment with Arimoclomol also increases. These results therefore indicate that Arimoclomol acts both centrally on motoneurons (Kieran et al, 2004; Kalmar et al., 2008) but also has a significant beneficial effect on muscle pathology. This is likely to be due to an additional peripheral effect and not just a consequence of increased motoneuron survival, as Arimoclomols beneficial effect was present at 45 days in the fast EDL muscle, and resulted in a reduction in denervation, when motoneuron loss has yet to begin.

Chapter 4 : The effect of Arimoclomol on the HSR in the muscle of mSOD1 mice

4.1 Introduction

The precise role of muscle in ALS and mSOD1-mediated pathology remains controversial. While there is evidence demonstrating significant and differential pathology in ALS muscle, its role as a primary target in the disease is still debated. Results presented in Chapter three, confirmed previously reported evidence supporting a differential NMJ and muscle pathology in mSOD1 mice. These results also revealed that treatment with Arimoclomol reduces pathology at the NMJ and within the muscle. As Arimoclomol's action is reported to be mediated by hsps, it was concluded that manipulation of the HSR might be beneficial to mSOD1 muscle.

Hsps are known to promote motoneuron survival and muscle function in a number of neurodegenerative diseases (Adachi et al., 2003, Kieran et al., 2004, Howarth et al., 2007). They are also known to play a role in combating muscle stress (Broome et al., 2006). However, very little is known about hsp expression in the periphery in ALS. Therefore, this Chapter examines whether mSOD1 muscle has an intrinsic HSR and whether treatment with Arimoclomol alters this HSR. Furthermore, owing to the previously established preferential vulnerability of fast-twitch muscle to disease, the HSR in a fast and slow-twitch muscle is examined over the course of the disease.

4.1.1 The HSR in skeletal muscle

The HSR is a well-conserved, rapid and robust defence mechanism against a variety of damaging events in a cell. This 'defence' is orchestrated by a family of proteins called heat shock proteins (hsps). While every cell is capable of upregulating hsps and thus mounting a HSR, evidence indicates that different cell types and tissues vary in hsp expression (Oishi et al., 2002). In addition, hsp expression in the same tissues or cell type can vary with gender and age. Within skeletal muscle, hsp expression varies with muscle-type (Oishi et al., 2002, Voss et al., 2003, Kayani et al., 2008). For example, hsp72 is expressed more readily in the slow-twitch soleus muscle than fast-twitch muscles like the TA and EDL; while,

hsp60 and hsp25 are expressed at greater levels in fast-twitch muscles such as the Plantaris, TA and EDL (Oishi et al., 2002, Huey et al., 2007). This is most apparent following stress, when hsp60 is upregulated faster in the fast-twitch Plantaris muscle and hsp25 is more readily phosphorylated in fast-twitch muscles such as the Plantaris and EDL muscle (Huey et al., 2004).

4.1.2 The role of hsp90 in muscle: implications for neuromuscular disease

Hsp90 has been shown to promote AChR aggregation (Luo et al., 2008) and is implicated in the formation of muscle, notably myofibril organization (Du et al., 2007). During myofibril organisation hsp90α, an hsp90 isoform is strongly expressed for a short duration prior to MyoD expression in slow-twitch muscle progenitor cells. As hsp90α levels decline in slow-twitch muscle progenitor cells, levels increase in fast-twitch muscle progenitor cells (Sass et al., 1999).

Hsp90 is implicated in muscle pathology in both myopathies and neuromuscular diseases. In inclusion body myostitis (IBM), hsp90's role is unclear. Muscle biopsies from IBM patients show increased hsp90 expression in regenerating fibres, suggesting a cytoprotective role (De Paepe et al., 2009). However, there is also evidence demonstrating high hsp90 levels in iNOS positive macrophages found which necrotic muscle fibres in IBM models. This co-expression of iNOS and hsp90 implies a possible role for hsp90 in inflammation. In Spinal bulbar muscular atrophy (SBMA), a neuromuscular disease, hsp90 has been found in intranuclear aggregates of skeletal muscle, and this may indicate a role for muscle-derived hsp90 within the disease (Thomas et al., 2006). Such findings precipitated research examining the manipulation of hsp90 as a therapeutic target.

There are a number of neuromuscular degenerative diseases in which the targeting of hsp90 has resulted in a reduction of motoneuron death and muscle atrophy for example, in SBMA (Sobue, 2003). Most of these hsp90 therapies inhibit hsp90 function, which leads to the prolonged activation of HSF-1 and the

consequent upregulation of hsps (Tokui et al., 2009). These events ultimately increase protein refolding and degradation, significantly reducing the level of denatured proteins present in the cell (Bruijn et al., 2004).

4.1.3 The role of hsp72 in muscle: implications for neuromuscular disease

Hsp72 has been shown to be upregulated in skeletal muscle following heat shock, ischemia-reperfusion injury, following exercise and muscle overload (Yamashita et al., 1997, Oishi et al., 2005). Furthermore, hsp72 has been shown to protect muscle following damage, via interactions with myofibrils (Paulsen et al., 2007) and is also thought to regulate Ca^{2+} handling capacity in skeletal muscle via the sarcoplasmic reticulum (SR) of skeletal muscle (Tupling et al., 2008).

Hsp72 is also known to play a role in muscle pathology in some myopathies and neuromuscular diseases and is reported to have strong cytoprotective capabilities in the muscle. Indeed, hsp72 has been found in inclusions within the muscle from IBM patients (Fratta et al., 2005). It also has increased expression in the muscle of DMD patients (Bornman et al., 1995), where it enhances muscle cell survival (Bouchentouf et al., 2004). However, hsp72's role in muscle in neuromuscular disease is limited.

As Duchenne muscular dystrophy (DMD), IBM, and mSOD1 muscle share a number of pathologies, such as oxidative and SR stress (Baker and Austin, 1989, Nogalska et al., 2007, Nguyen et al., 2009), they may also share a role for hsp72 in the protection of muscle from pathology.

4.1.4 The role of hsp60 in muscle: implications for neuromuscular disease

The majority of hsp60 resides in the mitochondrial matrix, facilitating the import of nascent proteins into the mitochondria (Carrier et al., 2000). Another of its reported actions roles is the rescue of proteins that have undergone spontaneous

denaturation within mitochondria (McArdle et al., 2001). This role is particularly important in muscles, which have a high protein turnover and contain the high concentrations of mitochondria necessary to respond rapidly to changes in energy demand (Locke, 1997).

Interestingly, hsp60 has been implicated in neurodegenerative disease, with hsp60 mutations resulting in spastic paraplegia (Hansen et al., 2002, Magen et al., 2008). Although very little is known about the role of hsp60 in skeletal muscle pathology, hsp60 has been shown to increase the presence of cytoprotective proteins like IGF-1 stimulated receptor (Shan et al., 2003). Furthermore, as the administration of IGF-1 has been shown to increase muscle function and motoneuron survival in mSOD1 mice (Dobrowolny et al., 2005), increased hsp60 expression may also be beneficial to mSOD1 muscle. Furthermore, as skeletal muscle is a tissue rich in mitochondria and since mitochondrial damage is present in mSOD1 muscle, it is likely that a robust hsp60 response is required to maintain normal mitochondrial function.

4.1.5 The role of hsp25 in muscle: implications for neuromuscular disease

Hsp25 expression is essential for the development of contractile machinery within the cell during embryogenesis (Gernold et al., 1993). Under conditions of oxidative stress, it is more prone to phosphorylation in fast-twitch muscles compared to slow-twitch muscles (Huey et al., 2007). This differential response to stress in fast and slow-twitch muscles may indicate a lower threshold for a stress response in fast-twitch muscles.

Interestingly, in disease, it is well acknowledged that mutations in hsp27 (the hsp25 human homologue) result in Charcot Marie tooth disease, a neuromuscular disease (Brown et al., 2007). It is also known that hsp25 levels are increased in muscles that are more resistant to DMD pathology (Lewis and Ohlendieck, 2010). These muscles tend to be predominantly slow-twitch muscles (Carnwath and

Shotton, 1987). These findings suggest that hsp25 in mSOD1 muscle may help protect muscle from mSOD1-mediated pathology.

4.1.6 Hsps promote muscle innervation

Results from Chapter 3revealed that sprouting at mSOD1 NMJs is limited and that the extent of nerve terminal sprouting was increased by treatment with Arimoclomol. As Arimoclomol's primary action is the upregulation of hsps and in view of its established neuroprotective effect in the CNS, it is possible that its neuroprotective actions facilitate the maintenance of innervation and sprouting in the PNS via increased hsp expression.

It is known that hsp90 expression can promote neurite outgrowth *in vitro*, during development of the NMJ. Indeed, Ishimoto et al. (1998) discovered that hsp90 from chick muscle increased neurite outgrowth in spinal neurons *in vitro*. Hsp25 has also been implicated in the muscle's response to denervation (Huey et al., 2004) and it too is reported to increase neurite outgrowth during development, with the overexpression of hsp25 increasing neurite length and branching in dorsal root ganglion neurons (Read and Gorman, 2009).

As events at the NMJ have been shown to recapitulate some of the events that occur during development and evidence is available for the role of hsp90 and hsp25 in promoting neurite growth, it is possible that both hsp90 and hsp25 promote the sprouting of mature, injured motor axons. If so, they may be beneficial to the reinnervation of denervated endplates in the muscle of mSOD1 mice.

4.1.7 Manipulation of the HSR in mSOD1 mice

Every cell has an intrinsic HSR. However, during continued cell stress this HSR can become overwhelmed, and may benefit from augmentation. Upregulation of the HSR in mSOD1 mice has proven an effective therapeutic strategy. Both pharmacological and genetic approaches have been used to upregulate the HSR

in mSOD1 models (Bruijn et al., 2004). Genetic approaches have revealed limited beneficial effects, with the overexpression of hsp70 and hsp40 conferring little benefit *in vivo* (Liu et al., 2005). The delivery of exogenous hsp70 increased motoneuron survival (Gifondorwa et al., 2007). However, only pharmacological manipulation has yielded significant and consistent results. Indeed, the use of pharmacological agents to augment the HSR in mSOD1 mice has been shown to increase motoneuron survival, muscle function and lifespan (Gifondorwa et al. 2007, Kalmar et al., 2008, Kieran et al., 2004, Kiaei et al., 2005).

4.1.8 Induction and the Co-induction of the HSR in disease

A small number of pharmacological agents can induce the HSR. Celastrol, a quinone methide triterpene derivative, is such a drug. It also possesses some anti-inflammatory properties, as well as inhibiting NO production in the CNS. Celastrol's neuroprotective abilities have been demonstrated in various models of ALS (Kiaei et al., 2005), Parkinson's disease (Cleren et al., 2005), and Huntington's disease (Wang et al., 2005). However, its applicability as a therapy for neurodegenerative disease has been questioned, as it induces of the HSR. Kalmar et al. (2009) recently demonstrated that treatment with Celastrol induces the HSR in normally unstressed cells, an effect that is toxic in motoneurons (Kalmar et al., 2009).

An alternative approach is to co-induce the HSR. This results in the upregulation of hsps in a targeted fashion, so that only stressed cells are affected. Arimoclomol is such a drug. It only augments the HSR in cells that have already activated the HSR. It is neuroprotective in models of ALS, diabetes, and nerve trauma (Kalmar et al., 2002, Kurthy et al., 2002, Kieran et al., 2004, Kalmar and Greensmith, 2009) and currently, it is in Phase II clinical trials for ALS patients in the USA. In both *in vitro* and *in vivo* models of ALS, Arimoclomol has been shown to co-induce a number of hsps including, hsp60, hsp70 and hsp90 in both motoneurons and astroglia (Kieran and Greensmith, 2004, Kalmar et al., 2008). *In vivo*, the systemic delivery of Arimoclomol to mSOD1 mice increases motoneuron survival, muscle function and lifespan (Kieran et al., 2004). Currently, it is known to have strong

cytoprotective actions in the CNS, but its actions in the PNS have yet to be examined. However, given the effect of Arimoclomol observed in Chapter three, it is possible that some of Arimoclomol's beneficial effects arise from its ability to manipulate the HSR in the periphery.

4.1.9 Aim

In view of the results from Chapter three, in this Chapter, the HSR response in skeletal muscle in mSOD1 mice is examined, over the course of disease. Specifically, the expression of stress response proteins in the fast-twitch TA muscle and slow-twitch soleus muscle of WT, wtSOD1 and mSOD1 mice is investigated and the effect of treatment with Arimoclomol on the HSR examined in these muscles.

4.2 Methods

4.2.1 Animals

Animals were housed, genotyped and maintained until various stages of disease, as detailed in Chapter 2,Section 2.1.1, 2.1.2 and 2.1.3.

4.2.2 Muscle Dissection and homogenisation

Muscles were dissected as detailed in Chapter 2,Section 2.2.2. Snap frozen muscles were homogenised and then processed (Chapter 2,Section 2.2.8).

4.2.3 Western blotting

Following muscle homogenisation, a western blot was performed as described in Chapter 2,Section 2.2.9. Hsp line densities were normalised against β-actin line densities, and then all values were expressed as a percentage of WT, which was given the value 100%. Statistical analysis was carried out between wtSOD1 values and mSOD1 values, in order to assess whether the overexpression of SOD1 resulted in a change in hsp expression. Levels of protein expression did not vary with age in WT and wtSOD1 mice, so data from each respective group was pooled and subsequently referred to as WT and wtSOD1.

4.2.4 Immunohistochemistry and Microscopy

Muscle was taken from WT, wtSOD1 and mSOD1 mice as described in Chapter 2,Section 2.2.3. The muscles were then cryosectioned transversely at 12μm and stained with a variety of antibodies listed in Table 2.1 and Table 2.2. Unless otherwise stated, these sections were examined by light microscopy.

4.2.5 Statistical analysis

Statistical significance was assessed using a one-way ANOVA test. Post hoc, all pair-wise multiple comparisons were done using a student's T-test**,** unless

otherwise stated. Values are assessed as mean ± standard error of the mean (SEM). Significance was set at $p \leq 0.05$.

4.3 Results

As examination of the TA and EDL muscle yielded similar results in Chapter 3, only the TA muscle was examined as a sample of fast muscle, as it bulk facilitates ease of analysis from this chapter onwards.

In untreated and Arimoclomol treated mSOD1 mice, the expression of hsp90, hsp72, hsp60 and hsp25 was examined in WT, wtSOD1 and mSOD1 mice at various ages using western blotting and IHC. In order to allow for comparison between different western blots, all hsp line densities were normalised against the line densities for β-actin loading controls, and were then expressed as a percentage of the corresponding WT sample. The WT value was given the value 100%.

4.3.1 Hsp90 expression in mSOD1 TA muscle

Examination of hsp90 expression in the TA and soleus muscles of WT, wtSOD1 and mSOD1 mice revealed two hsp90 isoforms. These two bands were identified as the larger inducible alpha isoform and a smaller hsp90 beta isoform. This was present in all samples investigated (see Fig.4.1). When measuring the line densities of hsp90 western blots, the line densities of these two bands were combined. Examination of hsp90 expression in the fast-twitch TA and slow-twitch soleus muscle in WT mice revealed no difference between the two muscles under normal conditions (Fig.4.1).

In Fig.4.1, it can be seen that hsp90 expression in wtSOD1 TA muscle was 108.3% (±2.53 SEM; n=4) of WT TA. Examination of mSOD1 TA revealed that at 45 days of age, hsp90 expression was 136.7% (±7.72 SEM; n=4) of WT TA muscle, which was significantly greater than wtSOD1 ($p=0.043$). At 75 days of age, hsp90 expression remained stable and was 137.4% (±3.63 SEM; n=4) of WT TA levels. This was still significantly greater than wtSOD1 ($p=0.050$). By 100 days, hsp90 expression had fallen slightly, so that it was 117.3% (±7.52 SEM; n=4) of WT TA

levels, and was no longer significantly greater than wtSOD1 (p=0.795). By 120 days hsp90 expression had fallen even further so that is was 78.3% (±4.84 SEM; n=4) of WT TA muscle, significantly less than wtSOD1 (p=0.0495), and was only half of the amount of hsp90 found in 45-day-old mSOD1 TA muscle (p=0.0007).

The pattern of hsp90 expression in TA muscle was assessed using immunohistochemistry. Hsp90 immunoreactivity was very low in the TA muscle from wtSOD1 mice (Fig.4.1). In mSOD1 TA muscle, at 45 days, low levels of hsp90 were found in the sarcoplasm (Fig.4.1f, see, '*'). By 75 days of age, in the mSOD1 TA muscle, hsp90 expression had increased and was localised to the sarcoplasm and sarcolemma of the muscle fibres (Fig.4.1g, see '*'). At 100 days of age, hsp90 expression was greatly reduced in the TA muscle of mSOD1 mice. By 120 days, hsp90 immunoreactivity was not detected in muscle fibres but instead in the areas surrounding the muscle fibres, most likely connective tissue. Western blotting analysis revealed that treatment with Arimoclomol resulted in a clear increase in hsp90 levels that were 303.33% (±8.59 SEM; n=3) of WT. This was significantly more hsp90 than in untreated mSOD1 TA muscle (p=0.010). This upregulation was reflected in IHC, which showed increased sarcoplasmic hsp90 expression in Arimoclomol-treated muscle fibres compared to untreated mSOD1 TA muscle (Fig.4.1).

Since hsp90 has been shown to promote neurite outgrowth and AChR aggregation *in vitro*, hsp90 expression at the NMJ in the TA muscle of Arimoclomol-treated mSOD1 mice was examined and was found to accumulate in close proximity to the post-synaptic junction in Arimoclomol-treated mSOD1 TA muscle (Fig.4.2b, see '*'), but not untreated mSOD1 TA muscle.

Figure 4.1: Hsp90 expression in the TA muscle of WT, wtSOD1 and mSOD1 mice

(A) shows a representative western blot of TA and soleus muscle homogenate from WT mice. (B) shows a representative western blot of hsp90 levels in WT, wtSOD1 and untreated mSOD1 TA muscle at 45, 75, 90 and 120 days of age. (C) shows a representative western blot of TA muscle homogenate from WT, untreated mSOD1 and Arimoclomol-treated mice at 120 days of age. The bar chart (D) summarises the normalised line density measurements from blots like (B&C). This was carried out as described in Chapter 2,Section 2.2.8. The dashed line represents WT control values. (E) shows hsp90 expression in TA muscle of wtSOD1 mice. (F) demonstrates hsp90 expression in a mSOD1 TA muscle at 45 days. Some hsp90 is present at the sarcoplasm (*). (G) shows hsp90 expression in the mSOD1 TA muscle at 75 days, with strong expression in the connective tissue surrounding muscle fibres (*). (H&I) provide an example of hsp90 expression in TA muscle at 100 and 120-day-old in mSOD1 mice. (J) shows hsp90 expression in the TA muscle from Arimoclomol-treated mSOD1 mice.

Error bars = standard error of the mean; n=4; * = p≤0.05; ***=P≤0.001; Scale bar= 50μm; green (hsp90), blue (DAPI)

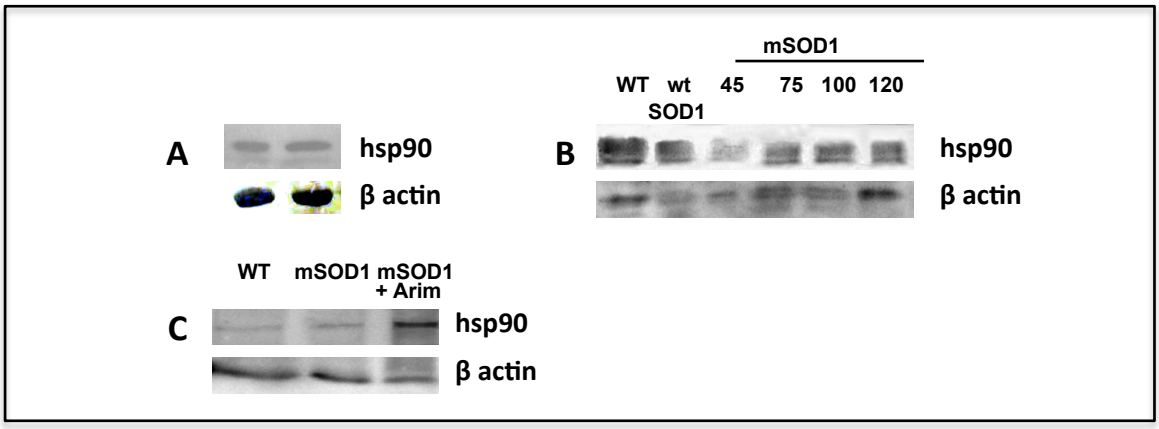
A
hsp90
β actin
B
mSOD1
WT
wt SOD1
45
75
100
120
hsp90
β actin
C
WT
mSOD1
mSOD1 + Arim
hsp90
β actin

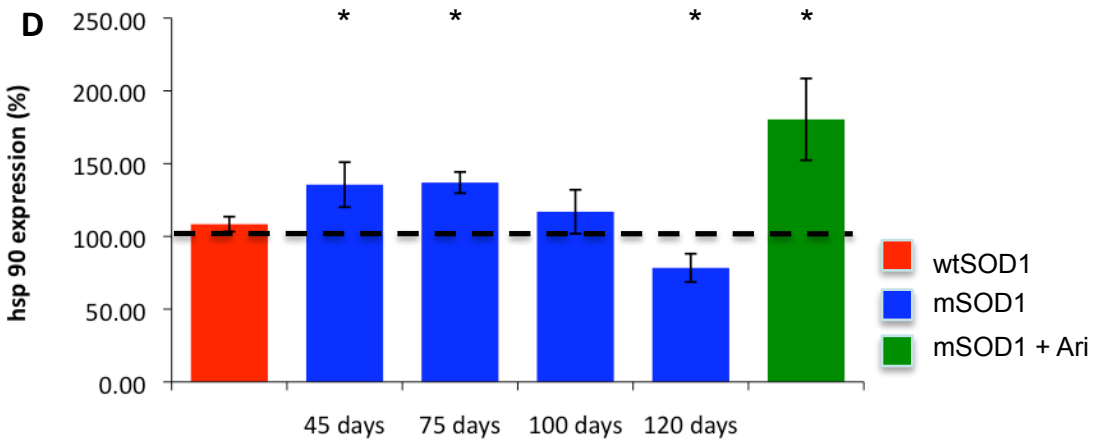
D
hsp 90 expression (%)
250.00
200.00
150.00
100.00
50.00
0.00
*
*
*
*
45 days
75 days
100 days
120 days
wtSOD1
mSOD1
mSOD1 + Ari

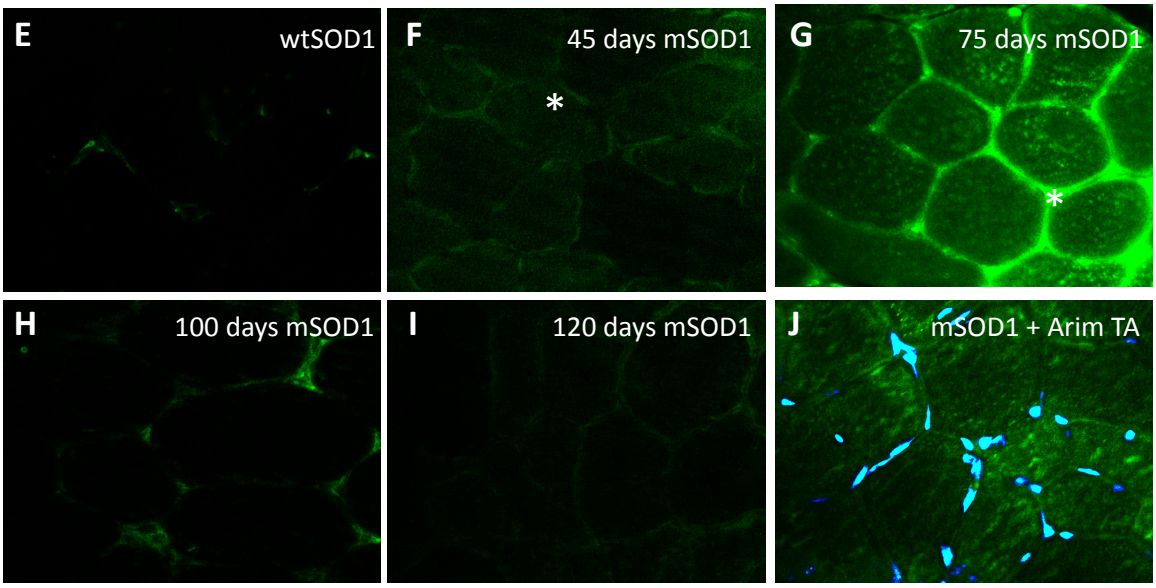
E
wtSOD1
F
45 days mSOD1
*
G
75 days mSOD1
*
H
100 days mSOD1
I
120 days mSOD1
J
mSOD1 + Arim TA

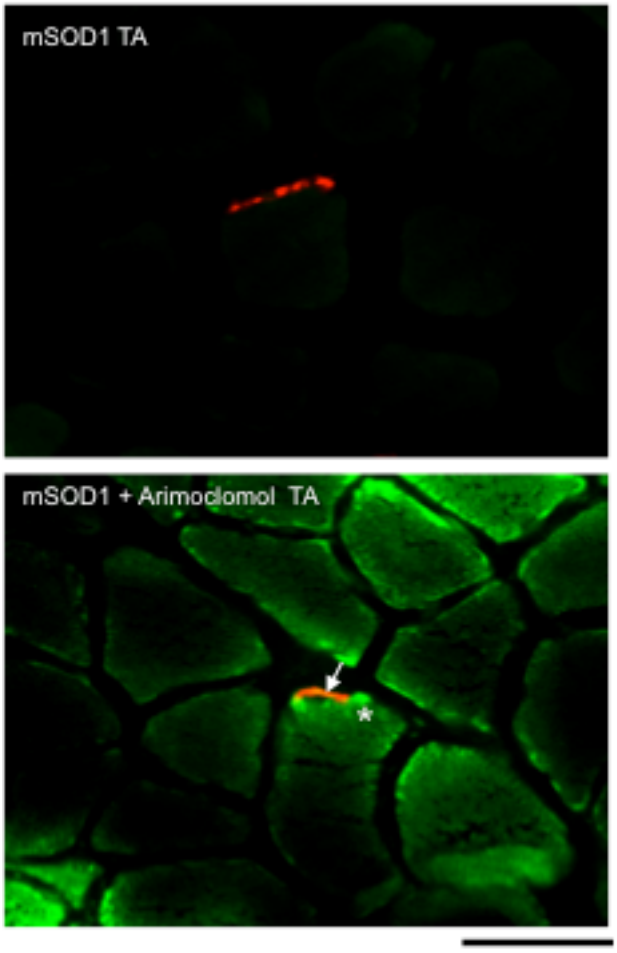

Figure 4.2: hsp90 expression at the NMJ of the TA muscle of untreated and Arimoclomol-treated mice

(A) shows a transverse section of TA muscle from untreated mSOD1 mice at 120-days of age stained for hsp90 (green) and AChR (red). (B) shows the colocalisation of hsp90 with the α-bungarotoxin (red; see arrow). Accumulations of hsp90 are present beneath the endplate (green; *) in the TA muscle of Arimoclomol-treated mSOD1 mice.

Scale bar = 50μm; n=4

4.3.2 Hsp90 expression in mSOD1 soleus muscle

Hsp90 expression in the slow-twitch soleus muscle was also examined using western blotting and IHC. As can be seen in Fig.4.3, hsp90 levels in wtSOD1 soleus muscle were 109.6% (±13.0 SEM; n=4) of WT (100%).

Figure 4.3: Hsp90 expression in the soleus muscles of WT, wtSOD1 and mSOD1 mice

(A) shows a representative western blot of hsp90 expression in soleus muscle from WT, wtSOD1 and untreated mSOD1 soleus muscle at 45, 75, 100 & 120 days of age. (B) shows a representative western blot of hsp90 expression in soleus muscle from WT, untreated mSOD1 and Arimoclomol-treated mSOD1 mice at 120 days of age. The bar chart (C) summarises the mean line densities of hsp90 expression. The dashed line at 100% represents hsp90 expression in WT soleus muscle. (D) shows an example of hsp90 expression in the soleus muscle of wtSOD1 mice. (E) displays an example of sarcoplasmic hsp90 expression (*) in the mSOD1 soleus muscle of 45-day-old mice. (F) shows an example of strong hsp90 expression (*) in 75-day-old mSOD1 mice. (G&H) display an example hsp90 expression in soleus muscle of 100-day-old and 120-day-old mSOD1 mice respectively. (I) demonstrates hsp90 staining in the soleus muscle from 120-day-old mice.

Error bars = standard error of the mean; n=4; * = p≤ 0.05; **=p≤0.01;

Scale bar= 50μm


A
WT
wt SOD1
mSOD1
45
75
100
120
hsp 90
β actin
B
WT
mSOD1
mSOD1 + Arim
hsp 90
β actin

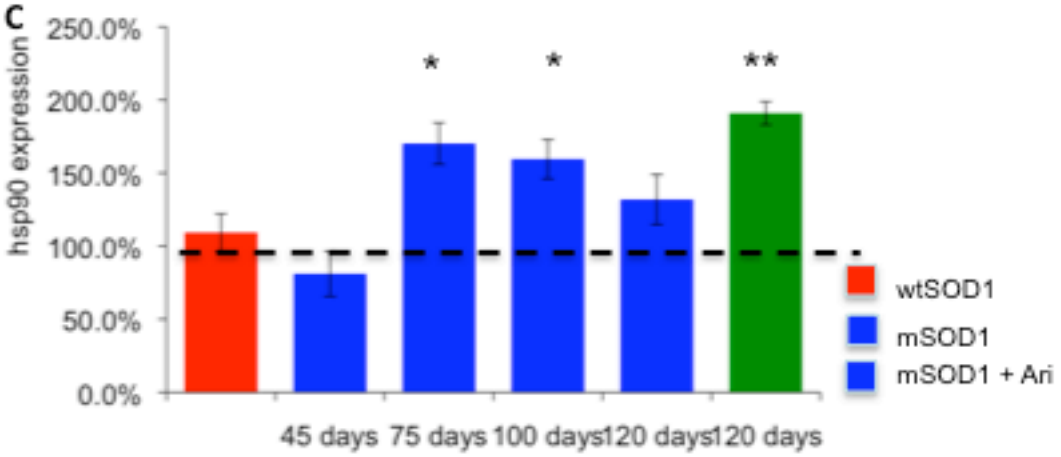
C
hsp90 expression
250.0%
200.0%
150.0%
100.0%
50.0%
0.0%
*
*
**
wtSOD1
mSOD1
mSOD1 + Ari
45 days
75 days
100 days
120 days
120 days

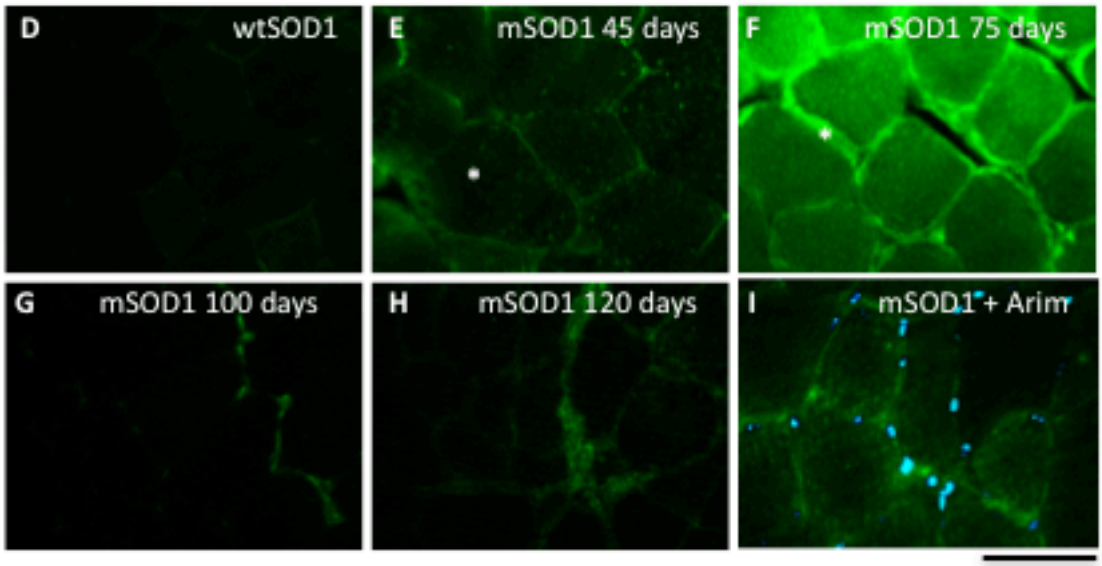
D
wtSOD1
E
mSOD1 45 days
F
mSOD1 75 days
G
mSOD1 100 days
H
mSOD1 120 days
I
mSOD1 + Arim

In mSOD1 mice, at 45 days of age, hsp90 expression was only 81.0% (±16.0 SEM; n=4) of WT soleus, which differed from wtSOD1 soleus (p=0.677; Fig.4.3). Hsp90 levels peaked at 75 days in mSOD1 mice, so that levels were 170.0% (±14.7 SEM; n=4) of WT mice and significantly higher than in wtSOD1 soleus muscle (p=0.047). From 75 days of age onwards, hsp90 levels began to decline, albeit marginally, so that by 100 days hsp90 levels were 159.76% (±13.54 SEM; n=4) of WT mice, which was still significantly more than wtSOD1 soleus muscle (p=0.037). By 120 days, hsp90 expression had further declined and was 132.2% (±17.6 SEM; n=4) of WT soleus, and was no longer differed significantly from wtSOD1 soleus muscle (p=0.836).

Immunohistochemistry revealed low hsp90 immunoreactivity in wtSOD1 mice (see Fig.4.3), with a clear upregulation in mSOD1 soleus muscle. At 45 days of age, hsp90 was localised to the sarcolemma of soleus muscles (see Fig.4.3e). By 75 days of age, hsp90 expression had increased, with intense staining found in the sarcoplasm throughout the muscle fibres and at the sarcolemma (Fig.4.3f, see '*'). By 100 days of age, hsp90 levels had declined (Fig.4.3g). At 120 days of age, hsp90 expression was restricted to the connective tissue of the soleus muscle, and hsp90 expression was particularly strong surrounding angular, atrophied muscle fibres (Fig.4.3h).

Treatment with Arimoclomol increased hsp90 levels in mSOD1 soleus muscle so that at 120 days of age they were 180.95% (±42.35 SEM; n=3) of WT. However, this did not reach significance when compared to untreated mSOD1 muscle (p=0.96). IHC indicated that treatment with Arimoclomol resulted in a modest increase in hsp90 expression in the soleus muscle of mSOD1 mice (Fig.4.3i).

4.3.3 Hsp72 expression in the TA muscle of mSOD1 mice

The expression of hsp72, a key protein involved in the refolding of misfolded proteins, was next examined in the TA and soleus muscle of WT, wtSOD1,

untreated and Arimoclomol-treated mSOD1 mice over the course of the disease. As can be seen in Fig.4.4, hsp72 expression in wtSOD1 TA muscle was similar to that in WT TA and was 107.39% (±2.04 SEM; n=4) of WT levels.

Hsp72 expression in untreated mSOD1 TA muscle was then examined, at 45, 75, 100 and 120 days of age. In mSOD1 TA muscle, at 45 days of age, hsp72 expression was similar to that observed in wtSOD1 TA muscle with hsp72 levels reaching 119.04% (±5.44 SEM; n=4) of WT TA muscle, which was significantly greater than wtSOD1 TA muscle ($p=0.046$). By 75 days of age, hsp72 levels in mSOD1 TA muscle had doubled to 224.15% (±9.06SEM; n=4) of WT, which was significantly above wtSOD1 TA muscle ($p<0.001$). As disease progressed, hsp72 levels declined. At 100 days, the amount of hsp72 was still marginally elevated, and in mSOD1 TA muscle hsp72 levels were 142.81% (±12.48SEM; n=4) of WT TA muscle, which was significantly more than wtSOD1 TA muscle ($p<0.01$). At 120 days, mSOD1 TA hsp72 levels were 115.5% (±11.17SEM; n=4) of WT, which was no longer significantly higher than hsp72 levels in TA muscle from wtSOD1 mice ($p=0.078$).

Immunohistochemical staining revealed that hsp72 expression was below detection levels in wtSOD1 TA muscle (Fig.4.4f). However, there was a clear increase in hsp72 expression in mSOD1 TA muscle compared to wtSOD1 TA at all ages examined. At 45 days, staining was mainly sarcoplasmic in muscle fibres, with some immunoreactivity present in surrounding connective tissue (Fig.4.4g,'*'). By 75 days, there was intense sarcoplasmic hsp72 staining in mSOD1 TA muscle fibres (Fig.4.4h,'*'). However, by 100 days, hsp72 expression had fallen a great deal in the TA muscle sarcoplasm (Fig.4.4i) and was greatly reduced by 120 days of age (Fig.4.4j).

Figure 4.4: Hsp72 expression in TA muscle of WT, wtSOD1 and mSOD1 mice

(A) shows a representative hsp72 western blot of TA and soleus muscle homogenate from WT mice. A representative blot displaying hsp72 levels in the TA muscle of WT, wtSOD1 and mSOD1 at various ages is seen in (B). (C) shows a representative blot of pre-absorbed soleus muscle homogenate from WT mice. This blot was stained for hsp72. A band at 70kDa was not present, indicating antibody specificity. (D) shows a representative blot for TA muscle homogenate from WT, untreated and Arimoclomol-treated mSOD1 mice. The bar chart (E) summarises the mean normalised line density from hsp72 blots (B&D). (F) shows an example of hsp72 immunoreactivity in wtSOD1 TA muscle. In 45-day-old mSOD1 mice (G), hsp72 is seen in mSOD1 TA muscle fibres as well as the connective tissue (*). In 75-day-old mSOD1 mice (H), very strong expression of hsp72 was found in the connective tissue surrounding the muscle fibres (*). (I) shows hsp72 expression in 100-day-old mSOD1 TA. In (J) preferential staining of some fibres in 120-day-old TA muscle from mSOD1 mice is visible (a, b). (K) shows an example of hsp72 expression in 120-day-old mSOD1 TA muscle following treatment with Arimoclomol. Nuclear staining is present (*), and there is a preferential upregulation of hsp72 expression in some muscle fibres compared to others (see a, b).

Error bars = standard error of the mean; n=4; *=p≤ 0.05; **=p≤ 0.01; Scale bar=50μm

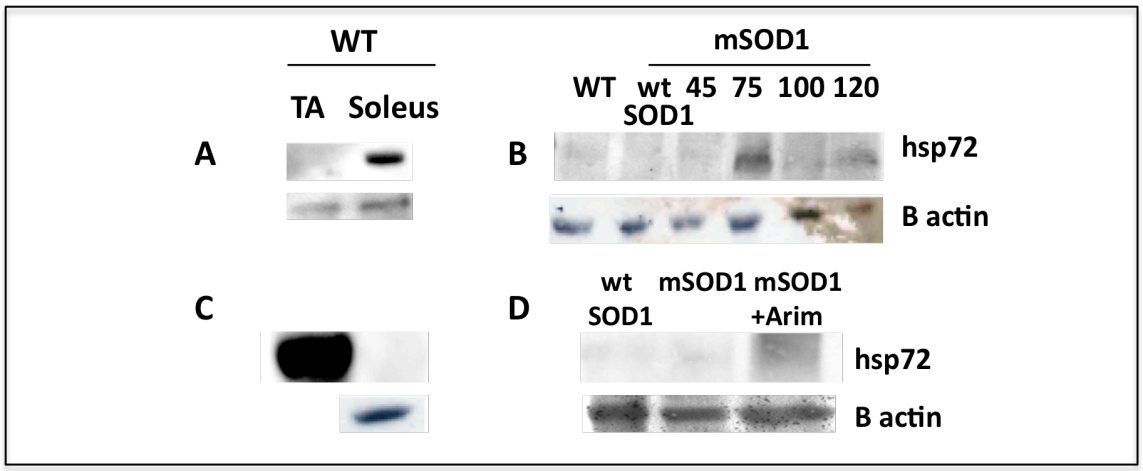
WT
mSOD1
TA Soleus
WT wt SOD1 45 75 100 120
A
B
hsp72
B actin
C
D
wt SOD1
mSOD1
mSOD1 +Arim
hsp72
B actin

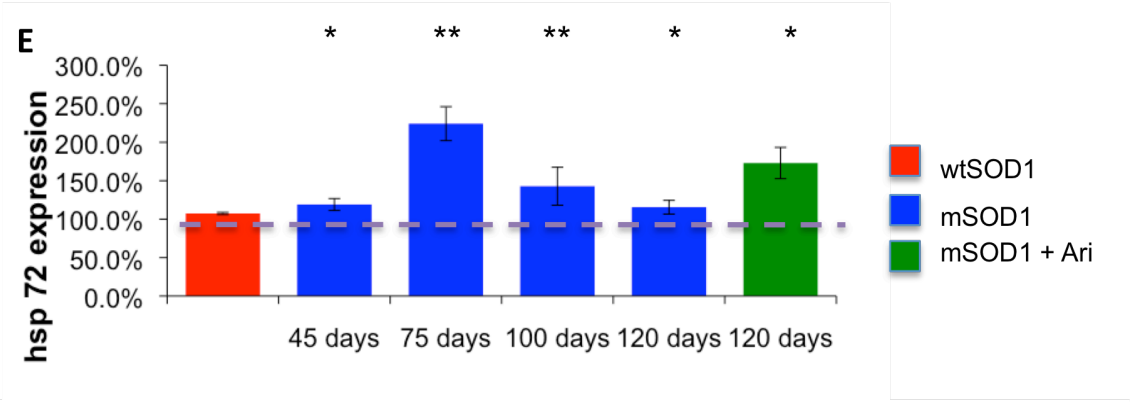
E
* ** ** * *
300.0%
250.0%
200.0%
150.0%
100.0%
50.0%
0.0%
hsp 72 expression
45 days 75 days 100 days 120 days 120 days
wtSOD1
mSOD1
mSOD1 + Ari

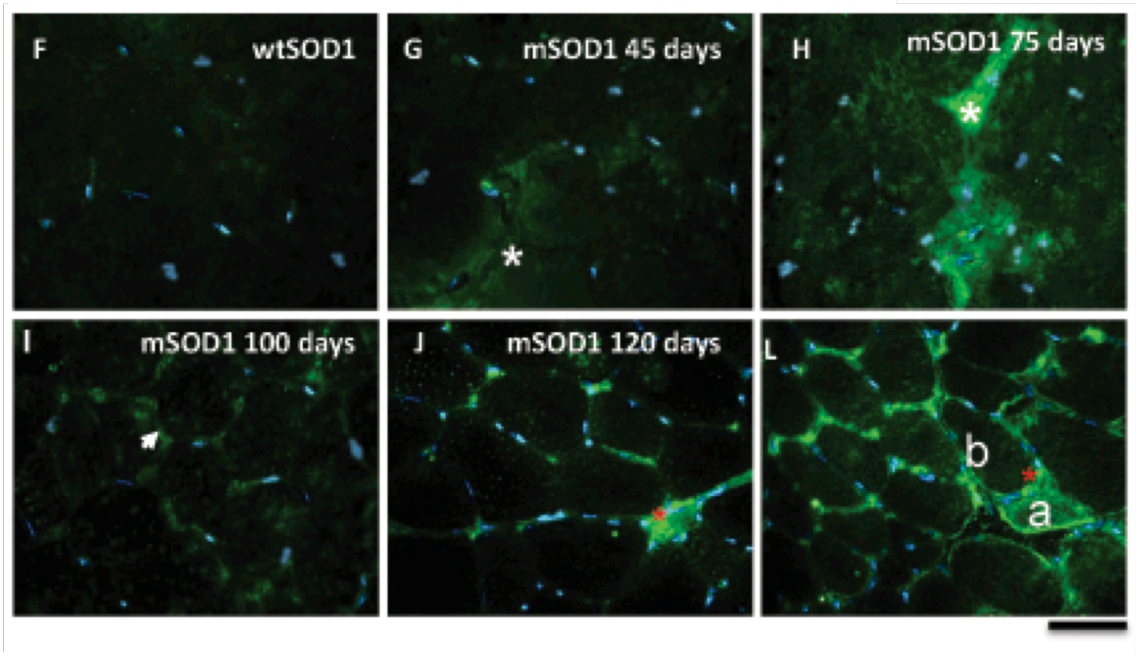
F wtSOD1
G mSOD1 45 days
H mSOD1 75 days
I mSOD1 100 days
J mSOD1 120 days
L
b
a

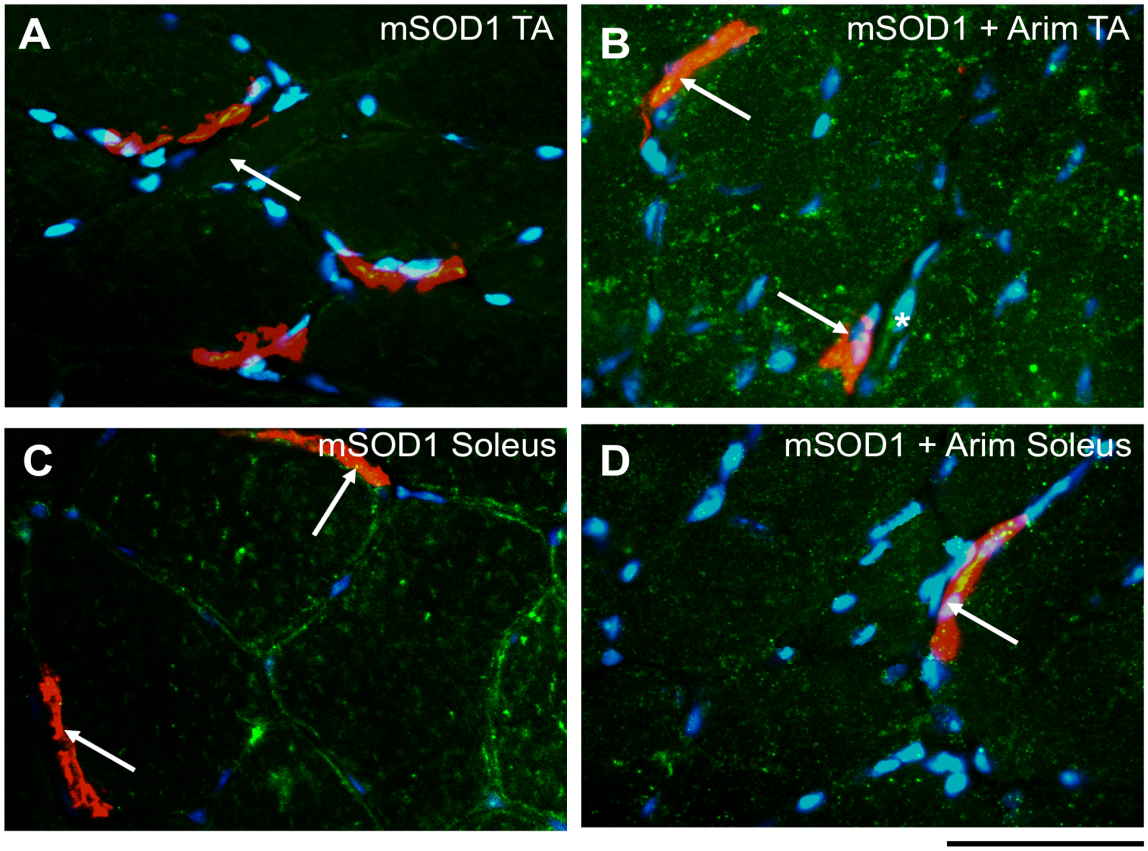

Figure 4.5: Hsp72 expression at the NMJ of TA and soleus muscles of untreated and Arimoclomol-treated mSOD1 mice.

Sections of TA and soleus muscle from untreated and Arimoclomol treated mSDO1 mice were stained with alpha bungarotoxin and immunostained for hsp72, (A) shows that hsp72 expression in the TA muscle of 120-day-old mSOD1 mice is present at the NMJ (see arrow). (B) shows an example of hsp72 expression in the TA muscle of mSOD1 mice treated with Arimoclomol. Hsp72 expression is present at the nucleus (*) and co-localises with some α-bungarotoxin but not all (see arrow). (C) shows hsp72 expression in the soleus muscle of 120-day-old mSOD1 mice, hsp72 is co-localised to some extent with α-bungarotoxin, but not all alpha bungarotoxin positive areas (see arrow). (D) shows an example of hsp72 in the soleus muscle of mSOD1 mice treated with Arimoclomol. There is clear co-localisation of hsp72 with α-bungarotoxin in the soleus (see arrow).

Scale bar =50μm; n=4

Treatment with Arimoclomol significantly increased hsp72 expression in TA muscles of mSOD1 mice compared to untreated mSOD1 mice. In Arimoclomol-treated TA muscle hsp72 levels were 173.02% (±20.33 SEM; n=3) of WT mice. This was significantly more than in untreated mSOD1 TA muscle (p=0.001). Examination of hsp72 expression using IHC revealed that treatment with Arimoclomol increased hsp72 expression within the sarcoplasm in some fibres, which also had centralised nuclei – a marker for muscle fibre regeneration (Fig.4.4i, see 'a'). However, some muscle fibres expressed very little hsp72 in the sarcoplasm (Fig.4.4i, see 'b'). Hsp72 expression was increased at nuclei within the muscle fibres (Fig.4.4i, see '*'). IHC also revealed that treatment with Arimoclomol resulted in a modest increase in hsp72 expression at the NMJ of TA muscle from mSOD1 mice (Fig.4.5b), compared to untreated TA muscle of mSOD1 mice.

4.3.4 Hsp72 expression in mSOD1 soleus muscle

Fig.4.6 shows that hsp72 expression in wtSOD1 soleus muscle was 86.8% (±9.0 SEM; n=4) of WT.

mSOD1 soleus muscle contained significantly more hsp72 than wtSOD1 soleus muscle, at all ages studied. At 45 days of age, hsp72 levels were already elevated to 144.6% (±10.4 SEM; n=4) of WT, which was not significantly elevated compared to wtSOD1 soleus muscle (p=0.229). Hsp72 levels continued to rise and by 75 days, hsp72 levels in mSOD1 soleus were 222.6% (±36.8 SEM; n=4) of WT soleus muscle, which was significantly more than wtSOD1 (p=0.007). Thus, hsp72 levels had approximately doubled between 45-75 days in mSOD1 soleus muscle. By 100 days of age, hsp72 increased further to 275.5% (±45.2 SEM; n=4) of WT soleus, which was also significant compared to wtSOD1 soleus muscle (p<0.001). By 120 days of age, hsp72 levels began to decline so that they were 161.5% (±7.7 SEM; n=4) of WT soleus, which was no longer differed significantly from wtSOD1 soleus muscle (p=0.160).

Sections of soleus muscle from wtSOD1 and mSOD1 mice were also immunostained for hsp72. No difference in the pattern of staining or intensity was observed at any age in wtSOD1 soleus muscle (Fig.4.6). By contrast, in mSOD1 soleus muscle, hsp72 immunoflourescence was more intense than that observed in wtSOD1 soleus muscle. At 45 days, hsp72 staining was restricted to the sarcoplasm of the muscle fibres (see Fig.4.6e). By 75 days (Fig.4.6f), some muscle fibres contained very large, dense accumulations of hsp72 (Fig.4.7g) within the sarcoplasm of the muscle fibres. As disease progressed, hsp72 immunoreactivity continued to increase in the connective tissue and by 120 days of age, hsp72 immunoflourescence had declined in the sarcoplasm of most muscle fibres and was greatest in the tissue surrounding the muscle fibres. Following treatment of mSOD1 mice with Arimoclomol, hsp72 levels in mSOD1 mice were 122.70% (±3.88 SEM; n=3) of WT. However, this was not significantly different to untreated mSOD1 soleus muscle ($p=0.619$).

IHC revealed that the amount of hsp72 was not significantly altered in Arimoclomol-treated mSOD1 soleus muscle. The pattern of staining within Arimoclomol-treated soleus muscle fibres was considerably different to that seen in untreated mSOD1 soleus muscle. Arimoclomol-treated mSOD1 soleus muscle displayed raised hsp72 levels in a sub-population of muscle fibres. Furthermore, hsp72 expression was also increased at the NMJ of some but not all endplates (Fig.4.5d, see arrow), as determined by double staining with the AChR marker, alpha bungarotoxin.

4.3.5 Hsp60 expression in mSOD1 TA muscle.

Next, hsp60 expression was examined and levels were found to be similar in TA and soleus muscles of WT mice. Fig.4.7 indicates that in wtSOD1 TA, hsp60 levels were not significantly different from those observed in WT TA muscle, with wtSOD1 TA muscle displaying hsp60 levels that were 103.7% (±8.2SEM; n=4) of WT.

Figure 4.6: Hsp72 expression in the soleus muscle of WT, wtSOD1 and mSOD1 mice

Image (A) shows a representative western blot of hsp72 in the soleus muscles of WT, wtSOD1 and mSOD1 mice at various ages. Image (B) shows a representative western blot of soleus muscle homogenate from WT, untreated mSOD1 and Arimoclomol-treated 120-day-old mSOD1 mice. The bar chart (C) summarises the normalised line density of hsp72 western blots. The dashed line represents the WT control line density (100%). Muscle sections were also stained for hsp72 immunohistochemistry. (D-F) show an example of hsp72 expression using immunofluoresent histochemistry on wtSOD1 and mSOD1 at 45,75,90 and 120 days of age, respectively. (H) shows hsp72 expression in the soleus muscle of mSOD1 mice following treatment with Arimoclomol. Hsp72 was preferentially expressed in nucleated muscle fibres ‘a’, indicating increased hsp72 expression in regenerating muscle fibres. While other fibres express very little ‘b’.

n=4; error bars= standard error of the mean; *=p≤ 0.05; **=p≤ 0.01; ***=p≤ 0.001; Scale bar = 50μm

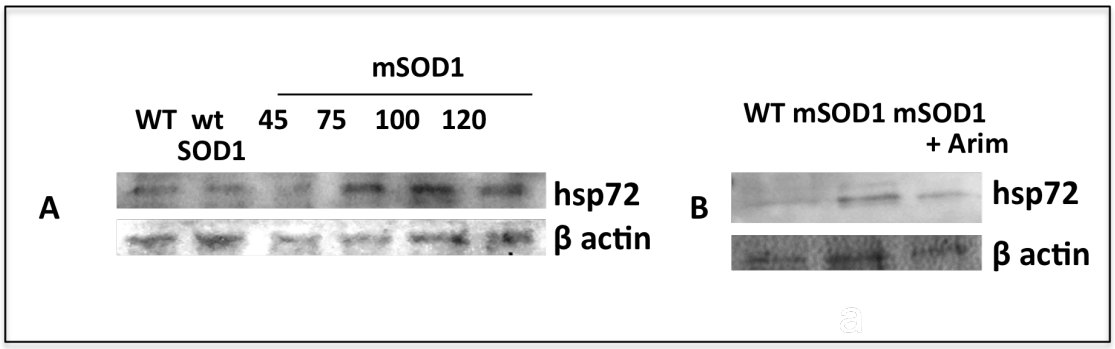

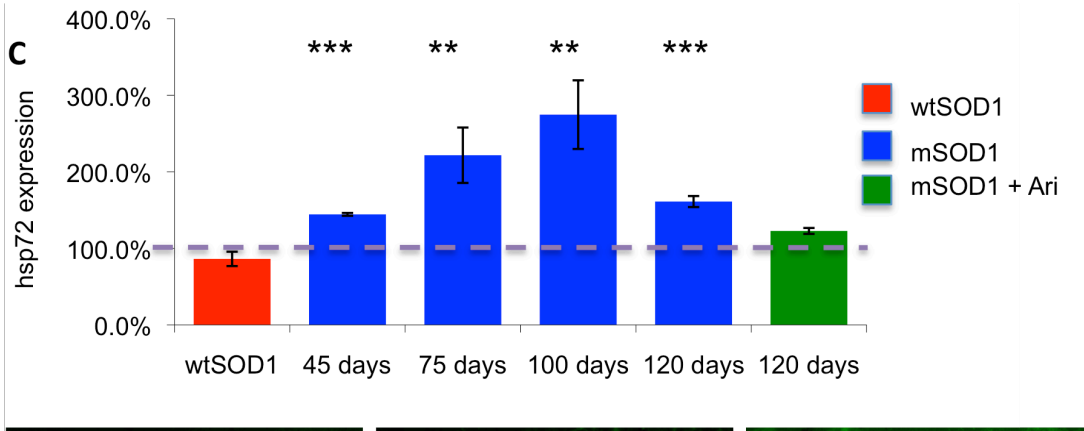

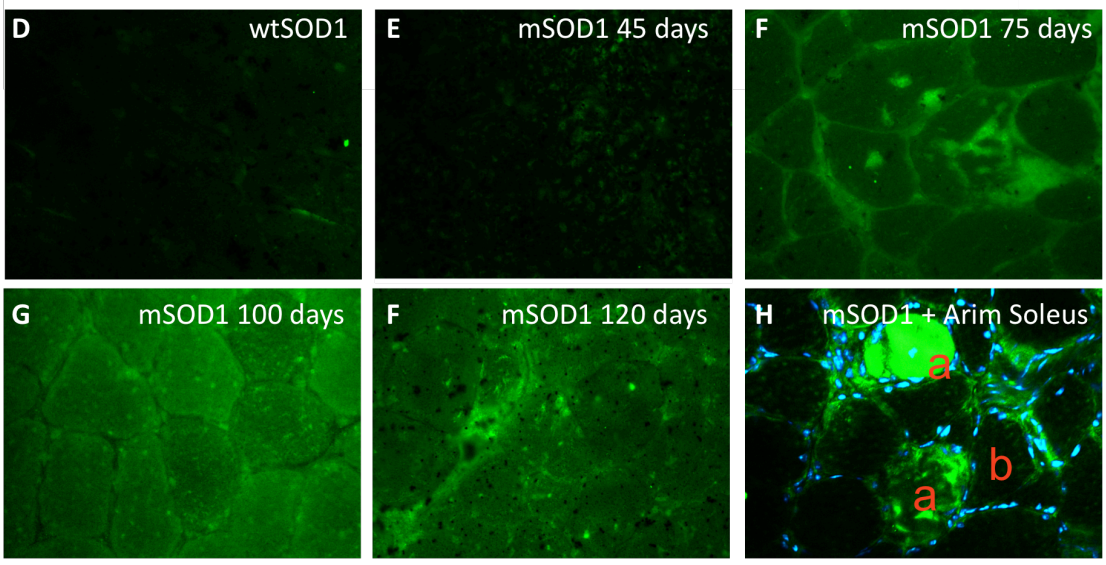

I mSOD1 Soleus J

In mSOD1 TA muscle, at 45 days of age, hsp60 levels were 137.8% ±8.7 SEM; n=4) of WT. This was not significantly more than wtSOD1 (p=0.376). At 75 days, hsp60 levels were 130.3% (±7.4 SEM; n=4) of WT TA muscle, which was still not significantly greater than wtSOD1 mice (p=0.133). At 100 days, hsp60 levels were 127.0% (±9.6 SEM; n=4) of WT TA muscle, which was similar to wtSOD1 (p=0.231). At 120 days, hsp60 levels were 116.2% (±8.0 SEM; n=4) of WT, which was not significantly greater than wtSOD1 mice (p=0.807). Hsp60 expression was also examined using IHC. As shown in Fig.4.7, there was very little hsp60 detected in wtSOD1 TA muscles. In mSOD1 TA muscle, immunoreactivity for hsp60 remained the same until 120 days. At 120 days, hsp60 immunoreactivity was higher at the periphery of muscle fibres (Fig.4.7j).

Treatment with Arimoclomol increased hsp60 levels significantly. Levels were 218.20% (±2.46SEM; n=3) of WT, which was significantly more than untreated mSOD1 TA muscle (p=0.002). IHC revealed that treatment with Arimoclomol increased hsp60 expression in the sarcoplasm of a sub-population of muscle fibres (Fig.4.7k, see 'a'), while other muscle fibres expressed far less hsp60 (Fig.4.7k, see 'b').

4.3.6 Hsp60 expression in mSOD1 soleus muscle

Hsp60 expression in the slow-twitch soleus muscle using western blotting and IHC was also examined. Overall, there was no significant change in hsp60 levels in the soleus muscle of mSOD1 at any age studied (n=4; p=0.353). As shown in Fig.4.8, IHC revealed that hsp60 expression in wtSOD1 soleus muscle was similar to mSOD1 soleus muscle. Additionally, hsp60 expression was similar in mSOD1 soleus muscle at all ages examined. Treatment with Arimoclomol did not increase hsp60 expression in mSOD1 soleus muscle and in Arimoclomol-treated soleus muscle; hsp60 levels were 95.61% (±12.49SEM; n=3; p=0.977) of WT (Fig.4.8). IHC revealed that hsp60 expression was slightly increased in the connective tissue of the soleus muscle from Arimoclomol-treated mSOD1 mice. (Fig.4.8, *).

Figure 4.7: Hsp60 expression in the TA muscle of WT, wtSOD1 and mSOD1 mice

(A) shows a representative hsp60 western blot of TA and soleus muscle from WT mice. (B) shows a hsp60 western blot of TA muscle from WT, wtSOD1 and mSOD1 mice at 45, 75, 100 and 120 days of age. (C) shows an example of a pre-absorbed hsp60 western blot. The band at 60kDa was not present, indicating antibody specificity. (D) shows an example of a hsp60 western blot of TA muscle from WT, untreated and Arimoclomol-treated 120-day-old mSOD1 mice. The bar chart (E) summarises normalised line density measurements from hsp60 western blots. Muscle sections were also processed for hsp60 using immunohistochemistry. (F) shows an example of hsp60 expression in TA muscle of wtSOD1 mice. (G) shows an example of hsp60 expression in the TA muscle of mSOD1 mice at 45 days of age. (H-J) shows hsp60 expression in the TA muscle of mSOD1 mice at 75, 100 and 120 days, respectively. (K) shows an example of hsp60 expression in 120-day-old following treatment with Arimoclomol, while ‘a’ highlights a muscle fibre with very little hsp60 immunoreactivity while ‘b’ conversely show a muscle fibre with high hsp60 immunoreactivity where immunoreactivity is localised to myofibrils within the muscle fibre.

Error bars = standard error of the mean; *=p≤ 0.05; **=p≤ 0.01; ***=p≤ 0.001; Scale bar=50μm; n=4

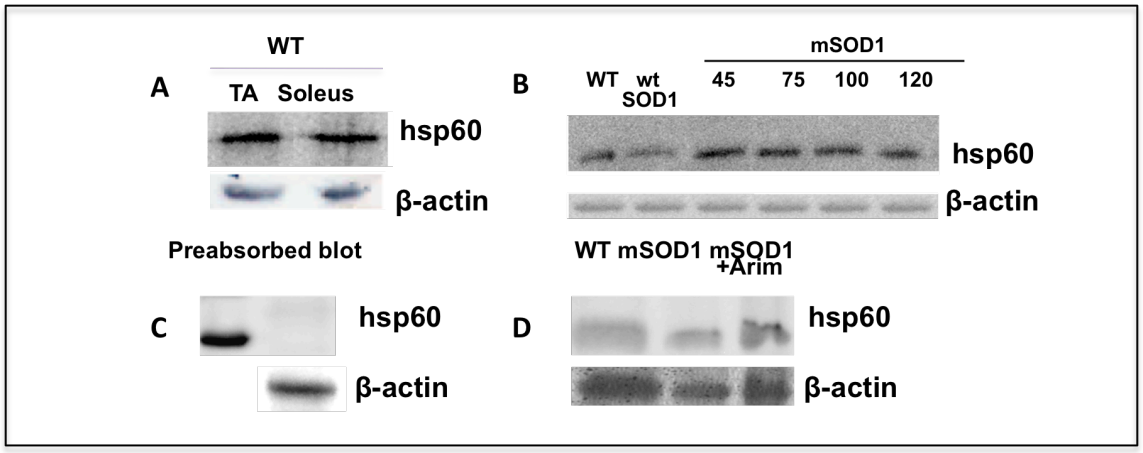
A
WT
TA Soleus
hsp60
β-actin
B
mSOD1
WT wt SOD1
45 75 100 120
hsp60
β-actin
Preabsorbed blot
C
hsp60
β-actin
WT mSOD1 mSOD1 +Arim
D
hsp60
β-actin

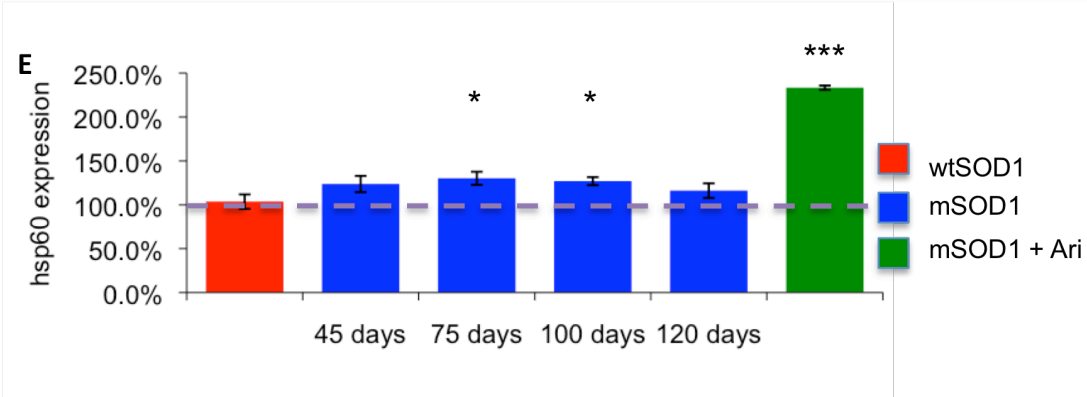
E
hsp60 expression
250.0%
200.0%
150.0%
100.0%
50.0%
0.0%
*
*
***
45 days
75 days
100 days
120 days
wtSOD1
mSOD1
mSOD1 + Ari

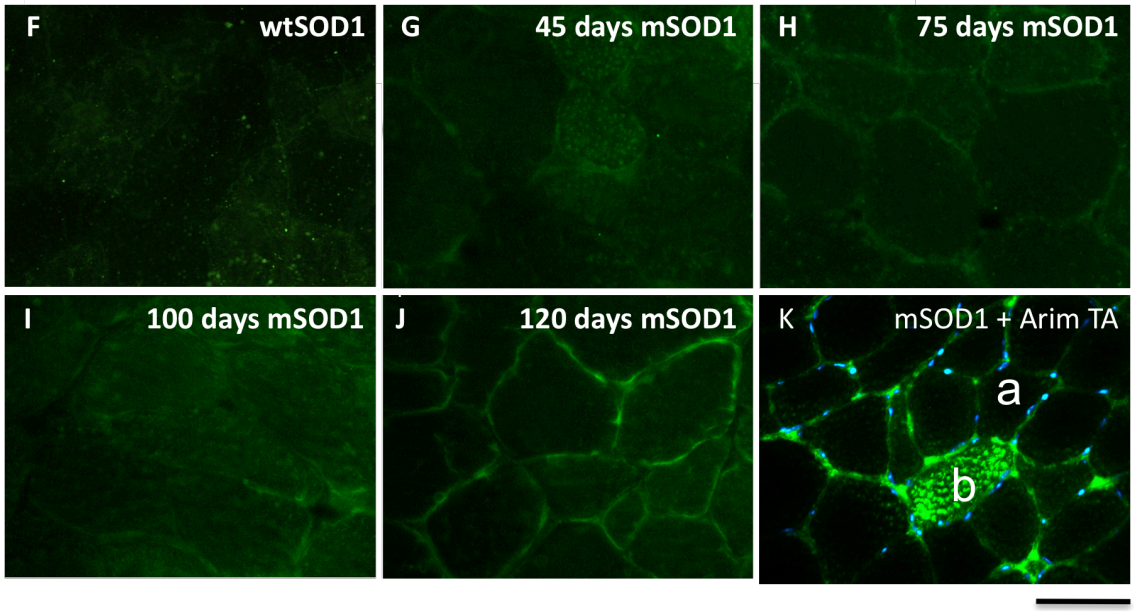
F wtSOD1
G 45 days mSOD1
H 75 days mSOD1
I 100 days mSOD1
J 120 days mSOD1
K mSOD1 + Arim TA
a
b

4.3.7 Hsp25 expression in the TA muscle of mSOD1 mice

Hsp25 is a key protein involved in counteracting the deleterious effects of oxidative stress within cells (Bryantsev et al., 2002). It is upregulated in skeletal muscle following oxidative stress and exercise (Koh, 2002). Hsp25 expression in TA and soleus muscles in WT, wtSOD1 and mSOD1 mice was examined at various stages of disease. Hsp25 levels were determined by western blotting as detailed in Chapter 2, Section 2.2.9 at the pattern of hsp25 expression examined with immunohistochemistry.

Examination of hsp25 expression in the fast-twitch TA and slow-twitch soleus muscle of WT mice was carried out in order to establish whether differential hsp25 expression took place in the absence of cell stress. Western blotting revealed similar levels of hsp25 expression in the TA and soleus muscles. Following this, hsp25 expression in wtSOD1 and mSOD1 mice was assessed. Fig.4.9 shows that hsp25 levels in wtSOD1 TA were 78.1% (±24.1 SEM; n=4) of WT. hsp25 expression in mSOD1 mice was then assessed. In presymptomatic mSOD1 TA muscle, and hsp25 levels were similar to wtSOD1 TA muscle, so that at 45 days of age, hsp25 levels in the TA muscle were 93.2% (±8.0 SEM; n=4) of WT, did not differ significantly from wtSOD1 ($p=0.983$).

However, by 75 days, hsp25 levels had more than doubled and were 223.7% (±SEM; n=4) of WT, which was significantly more than in wtSOD1 ($p<0.001$). By 100 days of age, levels had begun to decline and hsp25 levels were 139.3% (±13.1 SEM; n=4) of WT and no longer significantly greater than wtSOD1 ($p=0.124$). By 120 days of age, hsp25 levels had fallen to 127.7% (±26.7 SEM; n=4) of WT, which was not significantly more than wtSOD1 ($p=0.845$).

Figure 4.8: Hsp60 expression in mSOD1 soleus muscle

(A) shows a representative hsp60 western blot of TA muscle from WT, wtSOD1 and mSOD1 soleus muscle at various ages. (B) shows a representative hsp60 western blot of TA muscle from 120-day-old WT, untreated and Arimoclomol-treated mSOD1 mice. The bar chart (C) summarises the normalised line density measurements from hsp60 western blots. Muscle sections were also processed for hsp60 using immunohistochemistry. (D) shows the pattern of hsp60 expression in soleus muscle wtSOD1 mice. (E&F) illustrates the pattern of hsp60 expression in mSOD1 soleus muscle, at 45 and 75 days of age. (G&H) are examples of hsp60 expression in the soleus muscle at 100 and 120 days of age, respectively. (I) shows hsp60 expression in the soleus muscle of 120-day-old mSOD1 mice following treatment with Arimoclomol.

Error bars = Standard error of the mean; *=$p<0.05$; Scale bar=50μm; n=4

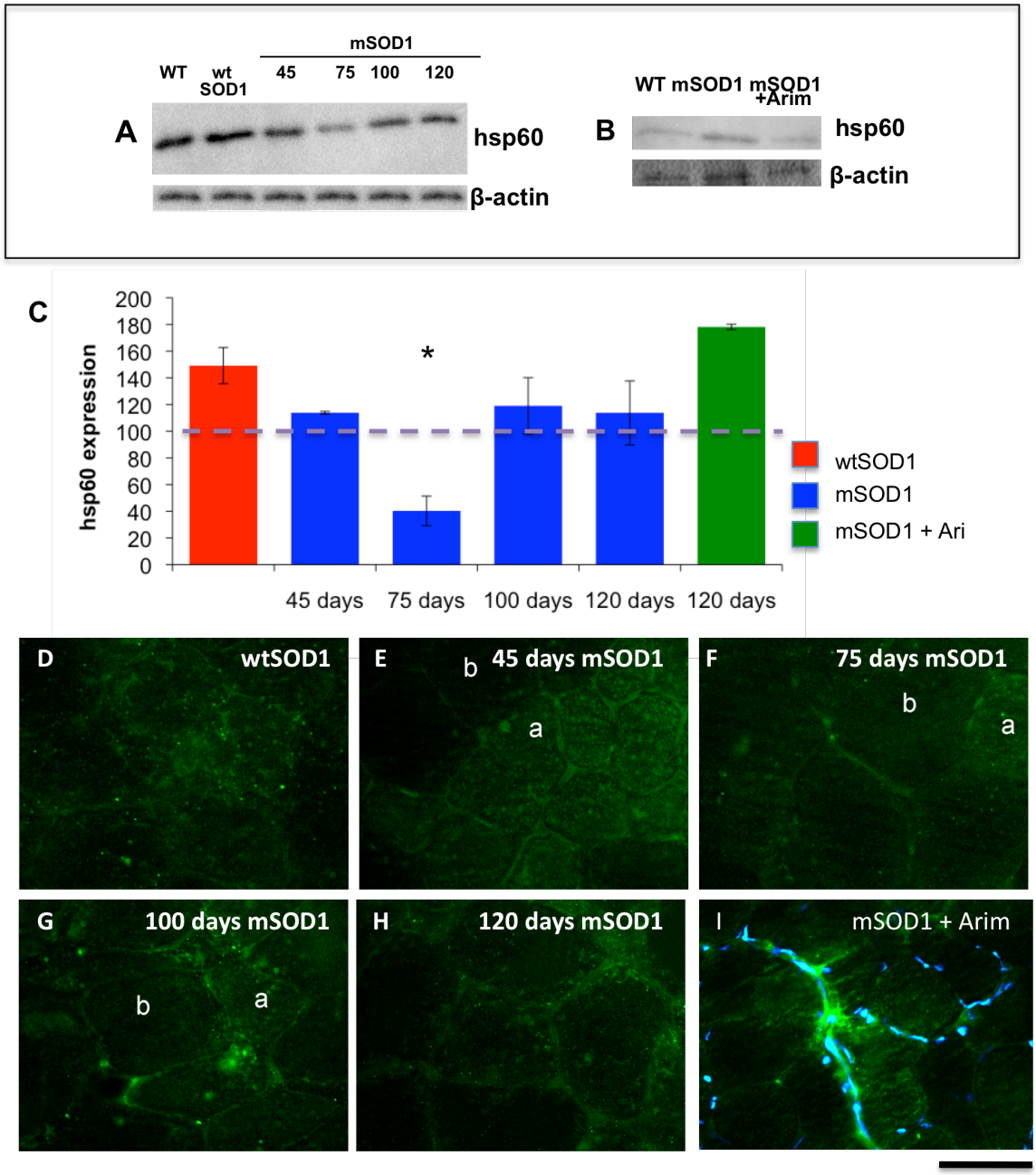
mSOD1
WT
wt SOD1
45
75
100
120
A
hsp60
β-actin
WT mSOD1 mSOD1 +Arim
B
hsp60
β-actin
C
hsp60 expression
200
180
160
140
120
100
80
60
40
20
0
*
45 days
75 days
100 days
120 days
120 days
wtSOD1
mSOD1
mSOD1 + Ari
D
wtSOD1
E
b
45 days mSOD1
a
F
75 days mSOD1
b
a
G
100 days mSOD1
b
a
H
120 days mSOD1
I
mSOD1 + Arim

The pattern of hsp25 expression in TA muscle was also examined using IHC (see Fig.4.9). In the TA muscle of wtSOD1 mice, hsp25 expression was negligible (Fig.4.9). Hsp25 expression was similar in mSOD1 TA muscle; in 45-day-old mSOD1 TA muscle, hsp25 expression was still low (Fig.4.9f). At 75, 100 and 120 days of age, hsp25 expression remained the same (Fig.4.9g-i), with no clear upregulation of any specific fibres at any stage of disease examined.

Treatment of mSOD1 mice with Arimoclomol increased hsp25 expression in TA muscle, so that levels were 250.05% (±9.0SEM; n=4) of WT, which was significantly more than untreated mSOD1 TA muscle ($p<0.0001$). However, this increase was not detected with IHC (Fig.4.10j), which showed no clear difference in the pattern or intensity of hsp25 expression in Arimoclomol treated TA muscle.

4.3.8 Hsp25 expression in mSOD1 soleus muscle

As can be seen in Fig.4.10, the level of hsp25 in wtSOD1 soleus muscle was 150.93% (±10.11 SEM; n=4) of WT. In mSOD1 soleus muscle, hsp25 levels changed significantly over the course of disease. At 45 days of age, hsp25 levels in mSOD1 soleus were 198.4% (±56.6 SEM; n=4) of WT, which was greater than wtSOD1, but did not reach significance ($p=0.378$). By 75 days of age, there was significantly more hsp25 in mSOD1 soleus ($p<0.001$): levels were 1324.28% (±197.65 SEM; n=4) of WT. From this stage onwards, hsp25 levels began to decline and by 100 days, levels were 853.58% (±95.81 SEM; n=4) of WT, which was still significantly more wtSOD1 ($p<0.001$). At 120 days, levels were 485.82% (±56.71 SEM; n=4) of WT, which was again significantly more than wtSOD1 ($p=0.001$).

Figure 4.9: Hsp25 expression in mSOD1 TA muscle

(A) shows a representative hsp25 western blot of TA and soleus muscle from WT mice. (B) shows a representative hsp25 western blot of TA muscle from WT, wtSOD1 and mSOD1 mice at 45, 75, 100 and 120 days of age. (C) shows a representative blot for hsp25 on TA muscle homogenate from WT, untreated and Arimoclomol-treated mSOD1 mice at 120 days of age. The bar chart (D) summarises the normalised line density measurements from hsp25 western blots. The dashed line at 100% represents WT control line density values. Muscle sections were also processed for hsp60 using immunohistochemistry. (E) shows hsp25 expression in the TA muscle of wtSOD1 mice. (F) shows TA muscle from 45-day-old mSOD1 mice. (G-I) shows hsp25 expression in TA muscle from 75-day-old, 100-day-old and 120-day-old mSOD1 mice. (J) shows an example of hsp25 expression in the TA muscle of 120-day-old mSOD1 mice following treatment with Arimoclomol.

Error bars = standard error of the mean; **= p≤ 0.01; ***=p≤ 0.001; Scale bar = 50μm; n= 4

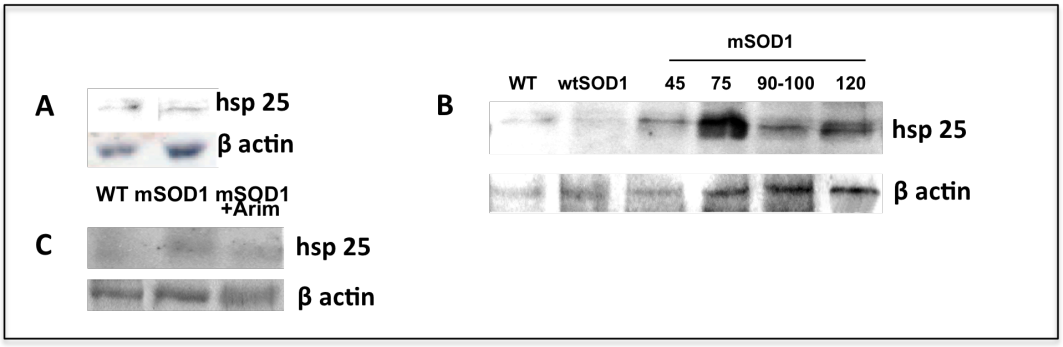
A
hsp 25
β actin
WT mSOD1 mSOD1 +Arim
C
hsp 25
β actin
B
mSOD1
WT wtSOD1 45 75 90-100 120
hsp 25
β actin

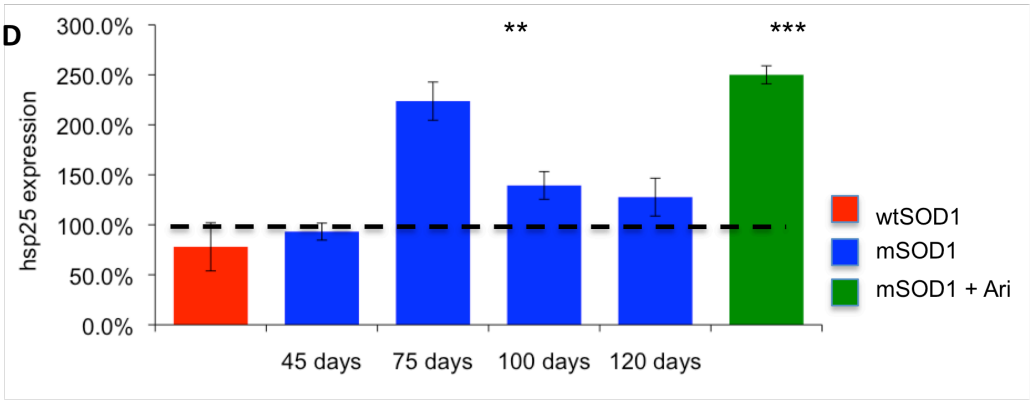
D
300.0%
250.0%
200.0%
150.0%
100.0%
50.0%
0.0%
hsp25 expression
**
***
45 days
75 days
100 days
120 days
wtSOD1
mSOD1
mSOD1 + Ari

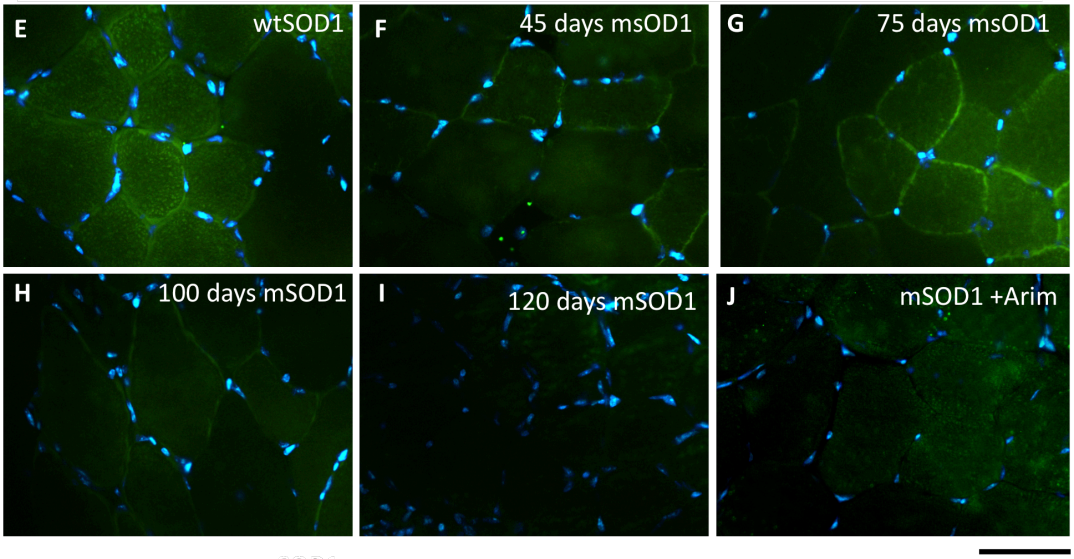
E wtSOD1
F 45 days msOD1
G 75 days msOD1
H 100 days mSOD1
I 120 days mSOD1
J mSOD1 +Arim

Immunohistochemical staining for hsp25 in soleus muscle sections revealed that hsp25 was present in the majority of wtSOD1 soleus muscle fibres (Fig.4.10d). At all ages studied, hsp25 immunoreactivity in mSOD1 soleus did not change significantly in the sarcoplasm of the mSOD1 soleus muscle. In mSOD1 soleus muscle, hsp25 was expressed in the majority of muscle fibres and did not change with age. From 45-120 days of age, there was also some sarcolemmal and sarcoplasmic hsp25 expression (Fig.4.10e-h).

Western blotting revealed that the treatment with Arimoclomol resulted in increased hsp25 levels, which were 1402.42% (±20.0SEM; n=4) of WT compared to untreated mSOD1 levels ($p=0.003$; Fig.4.10b). However, changes revealed by western blotting were not detected with IHC (Fig.4.10i).

Figure 4.10: Hsp25 expression in soleus muscle

(A) shows a representative hsp25 western blot of soleus muscle from WT, wtSOD1 and mSOD1 mice at 45, 75, 90 and 120 days of age. (B) shows a representative blot for hsp25 on soleus muscle homogenate from WT, untreated mSOD1 and Arimoclomol-treated mSOD1 mice at 120 days of age. The bar chart (C) summarises the normalised line density measurements from hsp25 western blots. The dashed line at 100% represents WT control line density. Muscle sections were also processed for hsp60 using immunohistochemistry. (D) represents hsp25 expression in the soleus of wtSOD1 mice. (E-H) represents hsp25 expression in the soleus muscle of mSOD1 mice at 45, 75, 90 and 120 days of age respectively. (I) shows hsp72 expression in the soleus muscle of 120-day-old mSOD1 mice following treatment with Arimoclomol.

Error bars = standard error of the mean; *** p≤0.001; **=p≤0.01; *=p≤0.05; Scale bar = 50μm; n= 4

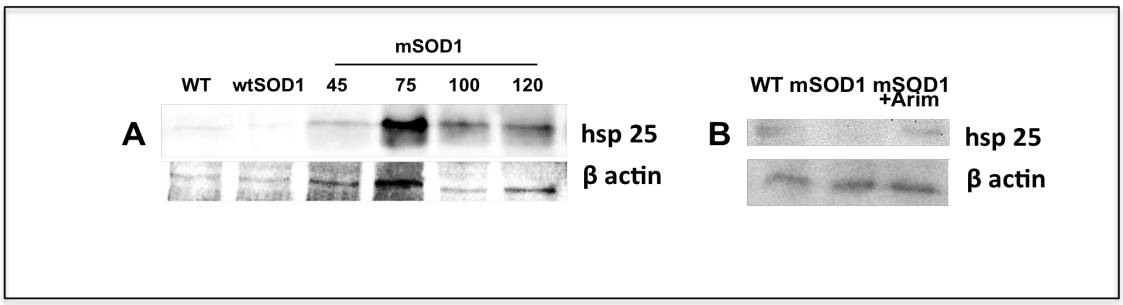
mSOD1
WT
wtSOD1
45
75
100
120
A
hsp 25
β actin
WT mSOD1 mSOD1 +Arim
B
hsp 25
β actin

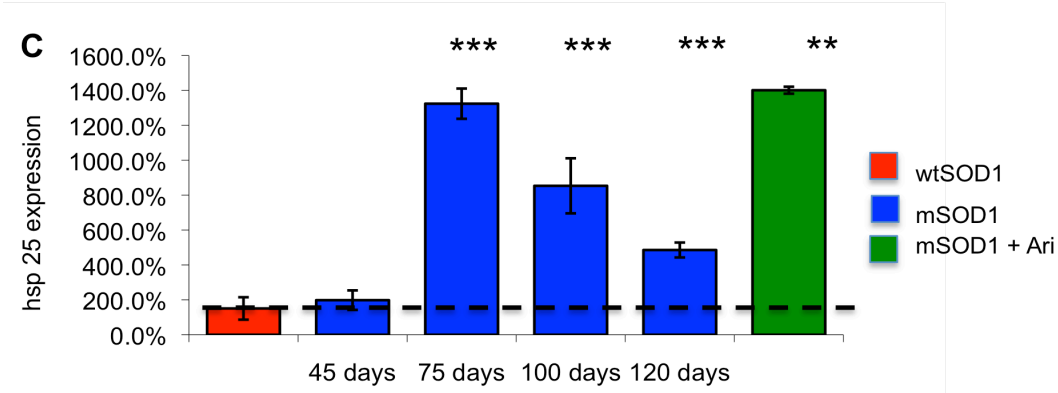
C
hsp 25 expression
1600.0%
1400.0%
1200.0%
1000.0%
800.0%
600.0%
400.0%
200.0%
0.0%
***
***
***
**
45 days
75 days
100 days
120 days
wtSOD1
mSOD1
mSOD1 + Ari

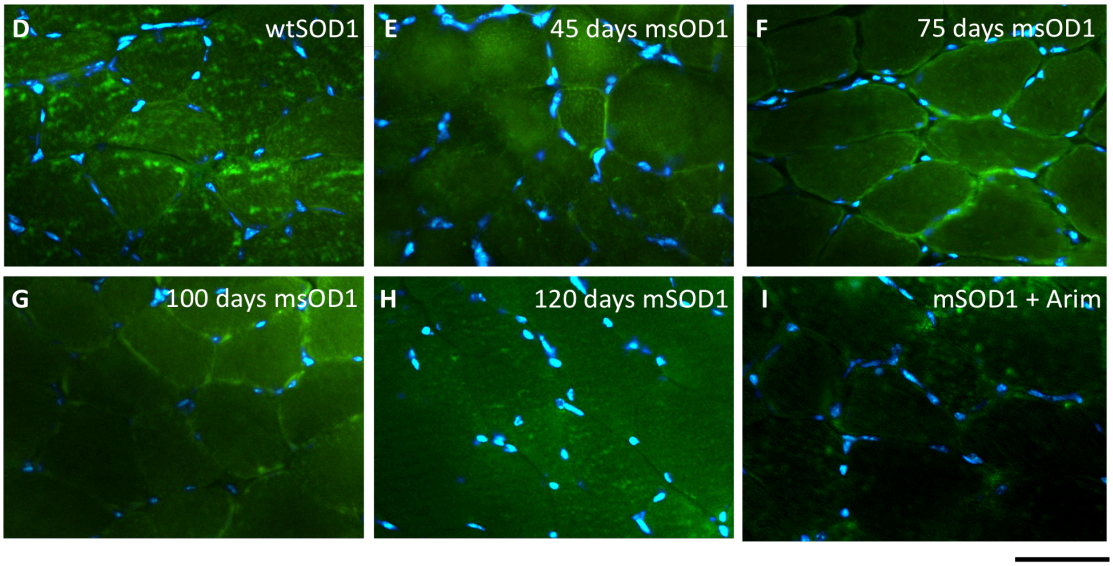
D
wtSOD1
E
45 days msOD1
F
75 days msOD1
G
100 days msOD1
H
120 days msOD1
I
mSOD1 + Arim

4.4 Discussion

In this Chapter, I undertook a systematic assessment of hsp levels in the fast-twitch TA and slow-twitch soleus muscle in mSOD1 mice over the course of the disease. The expression of hsp90, hsp72, hsp60 and hsp25 was examined in mSOD1 mice at a presymptomatic stage (45 days of age), symptomatic onset (75 days of age), and early stage of disease (100 days of age) and a late stage of disease (120 days of age). The role that these hsps play in muscle pathology in the disease was examined using western blotting and IHC, in order to ascertain how hsp levels are regulated throughout the disease. In addition, I investigated the effect of treatment with an inducer of the HSR, Arimoclomol, on the expression of these hsps in a fast-twitch and slow-twitch muscle in mSOD1 mice.

The results show that all hsps examined, except hsp60, were strongly upregulated in the hindlimb muscles of mSOD1, particularly between 45-75 days of age. After this point, hsp levels declined, which was accompanied by the worsening of symptoms. In addition, hsp90 and hsp25 levels were greater in the slow-twitch soleus, but upon the onset of disease, a similar 'fold' increase was seen in the fast-twitch TA and slow-twitch soleus muscle. Despite a similar fold increase in general, hsp90 and hsp25 was upregulated for a longer period in the soleus muscle than the more vulnerable TA muscle. Hsp72 levels were also greater in the slow-twitch soleus before disease onset.

Furthermore, this Chapter revealed that treatment with Arimoclomol increased significantly the expression of hsp90, hsp72, hsp60 and hsp25 in both TA and soleus muscles of mSOD1 mice.

4.4.1 Hsp expression in muscle may influence innervation in mSOD1 mice

A strong increase in hsp90, hsp72 and hsp25 expression was found between 45 and 75 days of age in both muscles; however, by 120 days (a late symptomatic stage) hsp levels in mSOD1 TA are similar to WT. Interestingly, the peak in hsp

levels coincided with the sprouting in both muscles. As hsp90 and hsp25 have also been shown to promote neurite outgrowth *in vitro* and are implicated in the denervation response, by suppressing muscle atrophy induced by atrogin-1 expression in muscle, it is possible that an increase in hsp expression in the muscle influences innervation at the NMJ (Ishimoto et al., 1998, Read and Gorman, 2009). Huey et al. (2005) and Abuzzo (2010) previously found a strong but short-lived increase in hsp25 following the denervation of muscle in rodents. These findings support the hypothesis that the upregulation hsp90 and hsp25 seen in mSOD1 muscle contributes to the simultaneous increase in sprouting (Chapter three). Interestingly, as hsp90 levels declined, sprouting also declined and the level of denervation increased. Therefore, it is possible that that hsp90 and hsp25 expression within muscle may augment the 'compensatory mechanisms' in muscle, helping to maintain innervation in the muscle of mSOD1 mice.

4.4.2 There is a differential HSR in fast and slow-twitch muscle

There was a clear hsp72 response in both the TA and soleus muscle. However, the magnitude of the upregulation of hsp72 expression differed between the two muscles considerably. In the mSOD1 TA muscle, hsp72 expression remained at WT and wtSOD1 levels until symptomatic onset, when there was a sharp approximately 2-fold increase in hsp72. However, this increase was short-lived and fell again to WT levels. In contrast to the TA muscle, a very strong, 3-fold increase in hsp72 expression occurred in the soleus muscle. This was initiated before symptomatic onset and in the mSOD1 soleus muscle, hsp72 levels continued to rise until 100 days (an early stage of the disease).

As both hsp72 and hsp25 have strong anti-oxidative actions and oxidative stress is a noted characteristic of mSOD1 pathology in muscle (Oishi et al., 2005, Gupte et al., 2009), the differential expression of hsp72 and hsp25 may also contribute to the established differential vulnerability between the two muscles to disease. Indeed, a less robust and weaker hsp72 response is likely to leave the TA muscle more vulnerable to oxidative stress, SR stress and subsequent mitochondrial

damage. Ultimately, this would render it more vulnerable to mSOD1-mediated pathology and less capable of dealing with neuromuscular pathology, such as denervation, and possibly reduced the effectiveness of compensatory mechanisms such as nerve terminal sprouting, which results in the reinnervation of denervated fibres.

4.4.3 Hsp levels are high at points of vascularisation

Furthermore, immnohistochemical analysis of hsp90 70, 60 and 25 expression revealed a general increase in the level of hsp expression outside of the muscle fibres at high points of vasculature. Thus, it is possible that hsps are not only released by the muscle but are also present within the blood. However, the examination of hsp content in the serum of mSOD1 mice, was outside of the parameters of this study.

4.4.4 Treatment with Arimoclomol increases hsp expression

Treatment with Arimoclomol resulted in a significant increase in the level of hsp90, hsp72, hsp60 and hsp25 in both the TA and the soleus muscles of mSOD1 mice. Kieran et al. (2004) and Kalmar et al. (2009) have previously shown the beneficial effects of increased hsp expression in the CNS of mSOD1 mice, induced by treatment with Arimoclomol. However, whether Arimoclomol also had a systemic effect in the periphery, which may contribute to its disease modifying effects in mSOD1 mice, has not yet been investigated. It is known that the upregulation of hsps can be beneficial to muscles under stress. For example, increased hsp60, a mitochondrial protein, can be beneficial to mitochondria, which are known to undergo significant pathology in the muscle of mSOD1 mice (Dupuis et al., 2004). In fact, its overexpression has been shown to confer strong cytoprotection to cardiac myocytes *in vitro*, reducing cell death following ischemia (Lin, Lin et al. 2001). Likewise, hsp72 and hsp25 are known to have strong cytoprotective actions in muscle. Their anti-oxidative capabilities act to counter contractile damage following exercise (Preville et al., 1998, Vasilaki et al., 2006). Thus, increased levels of hsp72 and hsp25 are likely to prove beneficial to ROS metabolism in

mSOD1 muscle, reducing oxidative stress. Furthermore, as excessive ROS has been shown to destabilise the NMJ, and promote denervation (Dupuis and Loeffler, 2009), Arimoclomol's action at the NMJ may indeed work to lower ROS, and increase sprouting (via hsp90 and hsp25 mediated pathways), ultimately increasing innervation via a number of hsp pathways within muscle.

This study also revealed that treatment with Arimoclomol increased the accumulation of hsp90 around the NMJ in the TA muscle, but not soleus muscle of mSOD1 mice. As hsp90 is known to regulate key proteins that mediate AChR aggregation (Luo et al., 2008) as well as neurite outgrowth (Ishimoto et al., 1998), it is likely to be cytoprotective to the preferentially vulnerable NMJs of the mSOD1 TA muscle.

4.4.5 Conclusion

In conclusion, the data presented in the Chapter show that there is a strong but short-lived HSR in both the fast-twitch TA and the slow-twitch soleus muscle of mSOD1 mice, which is initiated between 45 and 75 days of age. This upregulation in hsp expression coincides with the period during which mechanisms that attempt to compensate for the loss of innervation are most active. This is when sprouting becomes significant (Chapter 3). As disease progresses, hsp levels and the level of sprouting declined. Since hsp90 and hsp25 have been shown to promote neurite outgrowth, it is possible that they are involved in the sprouting response in the periphery in mSOD1 mice, following the denervation of endplates. Hsp levels were generally greater in the slow-twitch soleus muscle, and as hsps have strong cytoprotective actions, it is possible that this elevated level of hsps contributes to the comparative resilience of the soleus to disease. In addition, elevated hsp72 and hsp25 levels persisted in the more resilient soleus muscle. Hsp72 and hsp25 are potent anti-oxidative proteins, and they may therefore contribute to the differential vulnerability of fast and slow-twitch muscles to disease.

Although the level of Arimoclomol present in the TA and soleus muscles was not examined, I was able show that treatment with Arimoclomol elevated hsp90, hsp72, hsp60 and hsp25 expression in both TA and soleus muscle in mSOD1 mice. As hsp90 and hsp25 have been shown to increase neurite outgrowth, it is possible that they promote sprouting and thus the reinnervation of denervated endplates. Treatment also increased the expression of hsp72 and hsp90 at the NMJ, which is likely to be cytoprotective to both mSOD1 motoneurons and muscle. This was more apparent in the more vulnerable TA muscle. Together, these findings suggest that increased hsp expression is responsible, at least in part, for the beneficial effects of Arimoclomol in mSOD1 mice previously established in our group (Kieran et al., 2004).

Chapter 5 : The effect of treatment with Arimoclomol on Nitric oxide synthase expression in mSOD1 mice

5.1 Introduction

As neuromuscular disease and myopathies have a number of shared pathological characteristics, I was interested in examining the expression of proteins known to influence muscle in myopathies. One recurrent feature of muscle pathology across several pathological characters is the preferential vulnerability of fast-twitch muscles to pathology, which is also a feature of mSOD1 induced muscle pathology. For example, fast-twitch muscle is also preferentially vulnerable to disease in Duchene muscular dystrophy (DMD) (Grozdanovic and Baumgarten, 1999). One protein that has been implicated in such pathologies is neuronal nitric oxide synthase (nNOS), which has also been implicated in the muscle response to denervation (Ribera et al., 1998) and recently discovered to be implicated in ALS (Suzuki et al., 2010). Likewise, inducible nitric oxide synthase (iNOS) has a key role in the pathogenesis of inflammatory myopathy, Inclusion Body Myostitis (IBM) (Baron et al., 2000). Neuroinflammation is also significant in the CNS of ALS patients and mSOD1 mice (Chen et al., 2009). Thus, the expression of these two proteins was examined in fast and slow-twitch muscles of mSOD1 mice, in order to investigate whether nNOS and iNOS played may play a role in pathology in the muscles of mSOD1 mice.

5.1.1 Neuronal nitric oxide synthase

nNOS, a calcium-camodulin dependent enzyme, is expressed throughout the nervous system, however, it is most abundant in skeletal muscle, where it is found anchored to the sarcolemma via the dystrophin-glycoprotein complex (Stamler and Meissner, 2001) (See Fig.5.1). Furthermore, nNOS is expressed to a greater degree in fast-twitch muscle fibres (Stamler and Meissner, 2001). In addition, to its presence at the sarcolemma, accumulates at the NMJ, and within the presynaptic nerve terminal (Pereira et al., 2001), where it produces low levels of nitric oxide (NO) that act as a chemical messenger (Reid, 1998). NO produced by nNOS is involved in a number of pathways that are necessary for normal muscle function (Stamler and Meissner, 2001), such as the modulation of muscle contraction, NMJ stability, vasodilation and glucose uptake within skeletal muscle (Stamler and Meissner, 2001).

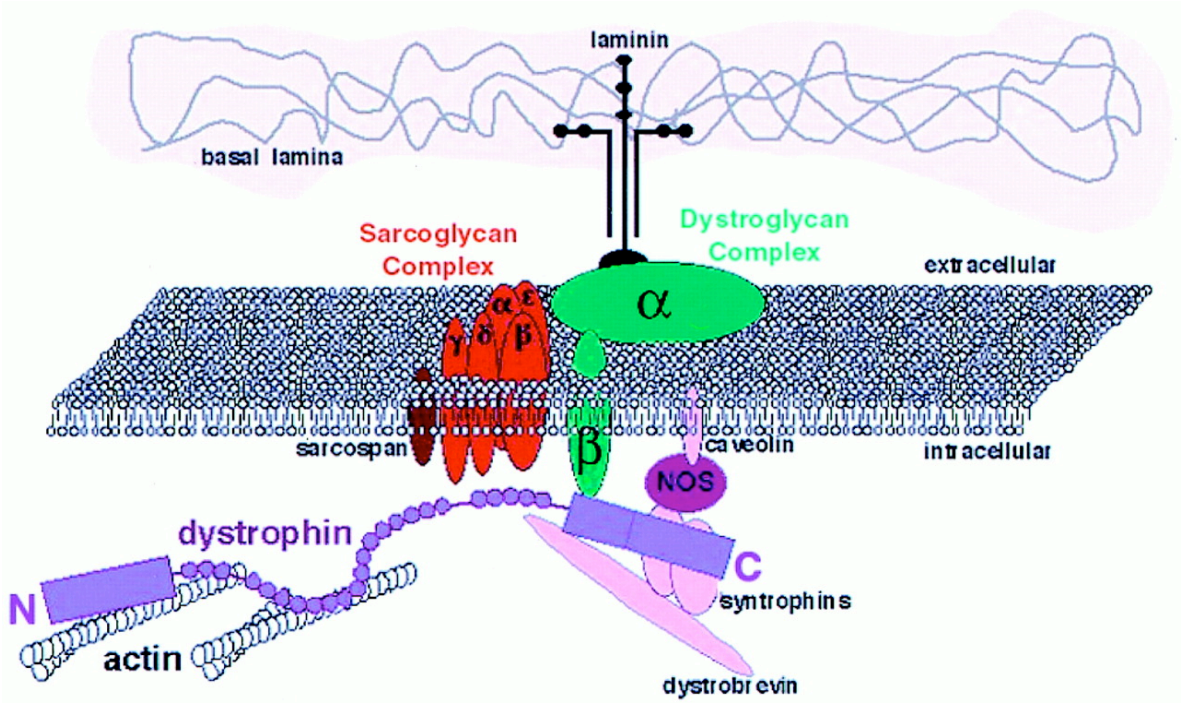

Figure 5.1: nNOS expression at the sarcolemma of skeletal muscle

This schematic representation illustrates the presence of nNOS in the DGC complex. It is anchored at the membrane by caveolin and is also associated with α-syntrophin, which is bound to dystrophin, which in turn is bound to actin (Sweeney and Barton, 2000).

nNOS is known to interact with hsp90 (Peng et al., 2009), which regulates its activity and turnover. Hsp90 is essential for the normal function of nNOS (Bender et al., 2004), stabilising it and promoting nNOS activity by preventing its binding to hsp70 and the subsequent degradation of nNOS (Peng et al., 2009). Increased hsp90/nNOS interactions are thought to increase vasodilation and alter cell metabolism (Pratt et al., 2008).

5.1.2 nNOS expression following denervation

nNOS expression alters significantly following denervation, with nNOS translocating from the sarcolemma to the sarcoplasm (see Fig.5.2). This results in the generation of reactive nitrogen species (RNS) and the upregulation of the transcription factor FOXO. FOXO plays an important role in the initiation of muscle atrophy (Senf et al., 2010), initiating the transcription of the ubiquitin ligase and atrogin-1 genes. This increases the ubiquitination of proteins and the ensuing increase in protein degradation by the proteosome, and thus muscle atrophy. Indeed, the importance of nNOS to denervation-induced muscle atrophy was successfully demonstrated by Suzuki et al. (2007) who used nNOS-deficient ($nNOS^{-/-}$) mice to show that in the absence of sarcoplasmic nNOS denervation does not result in the activation of the FOXO pathway, and thus $nNOS^{-/-}$ mice exhibit significantly less denervation-dependent muscle atrophy than WT mice (Suzuki et al., 2007).

Following muscle denervation, nNOS decreases within the presynaptic terminal (Suzuki et al., 2010). However, nNOS expression becomes apparent in terminal Schwann cells (tSChs), where it is thought to facilitate sprouting via tSCh projections (Keilhoff et al., 2002). In fact, Keilhoff et al. (2002) demonstrated using nerve injury in nNOS knockout mice that nNOS expression was necessary for normal Wallerian degeneration, the pruning of uncontrolled sprouts and even remyelination. They proposed suggested that nNOS was implicated in the remyelination of the proximal axon, the formation of new neuromuscular endplates,

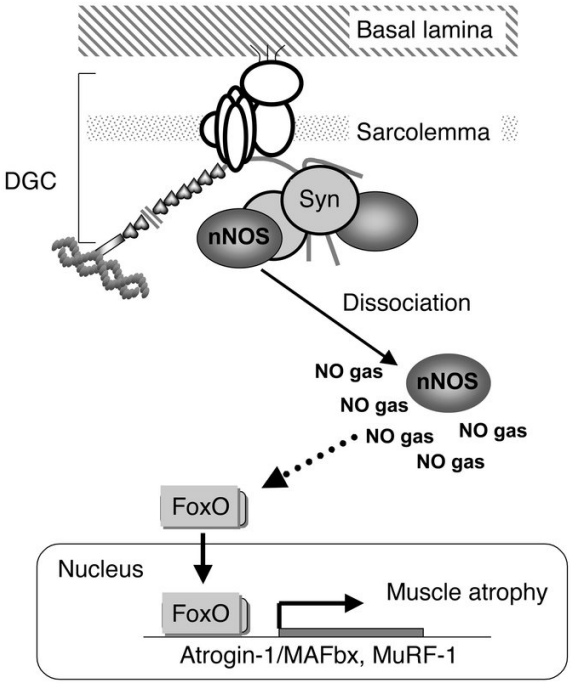

Figure 5.2: A model of the role of nNOS following denervation

Under normal conditions, nNOS is associated with the DGC at the sarcolemma. Following denervation nNOS dissociates from α1-syntrophin (Syn) and translocates to the sarcoplasm, where it continues to produce NO and regulates transcription factors such as FOXO. This results in increased muscle-specific ubiquitin ligase, MuRF-1 and atrogin-1, prompting muscle protein degradation via the proteosome (Diagram taken from Suzuki et al., 2007).

and the elongation of tSCh processes.

Marques et al. (2006) also found that in the absence of nNOS, tSCh processes do not occur. As this phenomenon promotes the reinnervation of denervated endplates, the manipulation of nNOS at the NMJ may be beneficial to mSOD1 mice (Marques et al., 2006). Although the precise role that tSChs play in the maintenance of NMJ integrity following insult is not fully understood, it has been consistently demonstrated that nNOS in tSChs plays a pivotal role in the reinnervation of denervated endplates in $nNOS^{-/-}$ mice (Ribera et al., 1998, Percival et al., 2008).

5.1.3 Neuronal nitric oxide synthase in neuromuscular disease

nNOS expression has been well-characterised in myopathies such as DMD (Pereira et al., 2001). In patients with DMD, nNOS is often absent from the sarcolemma and instead is distributed at reduced levels in the sarcoplasm. This pathology is more often observed in fast-twitch muscles (Webster et al., 1988, Grozdanovic and Baumgarten, 1999).

Although our understanding of nNOS in ALS is less extensive than DMD, nNOS expression is known to be altered in skeletal muscle of ALS patients and mouse models of the disease (Chao et al., 1996, Soraru et al., 2007). In addition to instigating denervation-induced muscle atrophy (Suzuki et al., 2007), it has been proposed that the loss of nNOS from the sarcolemma and its translocation to the sarcoplasm may effect the modulation of protein nitrosylation (Jaffrey et al., 2001), muscle contraction (Percival et al., 2010), as well as cell metabolism (Mulvey et al., 2005), NMJ stability (Auld and Robitaille, 2003) and vasodilation (Hare and Stamler, 1999). Therefore, it is possible that the disruption of nNOS expression in muscle in ALS may contribute to aspects of mSOD1-mediated pathology such as muscle atrophy, altered muscle contraction and cell metabolism and reinnervation. Furthermore, as fast and slow-twitch muscles are differentially effected by a

number of these pathological characteristics, it is possible that nNOS is also differentially expressed.

Manipulation of nNOS has been shown to benefit muscle in patients suffering from Becker's and Duchenne's muscular dystrophy, where the severity of the disease can be correlated to the presence of sarcoplasmic nNOS (Bredt, 1998). In a mouse model of DMD, the overexpression of nNOS in muscle has been shown to increase sarcolemmal nNOS and alleviate some defects at the NMJ and improve muscle function (Shiao et al., 2004). To date, a number of treatments inhibiting systemic NO production have been tried, but few have yielded significant results. The upregulation of nNOS in mSOD1 mice, particularly in the muscle, has not been extensively examined.

5.1.4 Inducible nitric oxide synthase in neuromuscular disease

While nNOS operates at a physiological level, NO synthesised by iNOS is commonly associated with pathological events within the cell, namely inflammation (Stamler and Meissner, 2001). In the muscle, iNOS is highly expressed in patients with chronic heart failure, autoimmune diseases and inflammatory myopathies such as IBM (Stamler and Meissner, 2001).

In addition, neuroinflammation is a pathological hallmark in the CNS of mSOD1 mice and contributes to motoneuron death (Hensley et al., 2006). Following symptomatic onset, iNOS is expressed at high levels in astrocytes and microglia within the spinal cord where it has been implicated in glial activation (Lee et al., 2009). However, the role of inflammation in the muscle in ALS remains unclear. In myopathies, muscle atrophy redundant can result from continued denervation, loss of activity, inflammation or metabolic dysregulation (Agusti et al., 2004, Atkin et al., 2005, Suzuki et al., 2007, Dupuis et al., 2009). All of these pathologies feature in ALS muscle to varying degrees and are present in the mSOD1 mouse model of ALS. More knowledge about iNOS's actions in the periphery, where symptomatic

onset first occurs, may provide further insight into the mechanisms underlying muscle atrophy, as well as suggesting effective therapeutic strategies to combat the disease.

Aim

In view of nNOS's role in DMD, denervation, and iNOS's role in IBM and neuroinflammation in the CNS in ALS, iNOS and nNOS expression in the fast-twitch TA and slow-twitch soleus muscle of mSOD1 mice will be examined over the course of disease. The effect of Arimoclomol, a known co-inducer of the HSR, on iNOS and nNOS expression in the TA and soleus muscles of mSOD1 mice will also be investigated.

5.2 Methods

5.2.1 Animals

Animals were housed, genotyped and maintained until various stages of disease, as detailed in Chapter 2, Section 2.1.1, 2.1.2 and 2.1.3.

5.2.2 Muscle Dissection and Muscle homogenisation

Muscles were dissected as detailed in Chapter 2, Section 2.2.2. Muscle homogenisation was carried out as detailed in Chapter 2, Section 2.2.8.

5.2.3 Western blotting

NNOS and iNOS western blots were undertaken as detailed in Chapter 2, Section 2.2.9. For each blot, a loading control was also run using β-actin and nNOS, and iNOS line densities from the experiments were normalised against line densities of β-actin bands using ImageQuant software (Amersham). For ease of presentation, data was then expressed as a percentage of the corresponding WT. Statistical analysis was carried out between the transgenic wtSOD1 and mSOD1 mice, in order to eliminate the effects of protein overexpression of SOD1 in the mSOD1 model when examining untreated samples. In experiments examining the effect of Arimoclomol, statistical analysis was carried out between untreated and Arimoclomol-treated hyphenate mSOD1 samples.

5.2.4 Immunohistochemistry and microscopy

Immunohistochemical stains for nNOS, AChR and hsp90 were carried out as described in Chapter 2, Section 2.2.3 using the antibodies detailed in Table 2.3 and 2.4.

5.2.5 Mouse-on-mouse Immunohistochemistry

For iNOS staining, a polyclonal mouse antibody was used. Consequently, immunohistochemical detection of iNOS in muscle sections required the use of a mouse-on-mouse (MOM) immunodetection kit (Vector Labs.). The protocol for MOM IHC can be found in Chapter 2, Section 2.2.4.

5.2.6 Statistical analysis

Statistical significance between the mean values was assessed using a one-way ANOVA test. Post hoc, all pairwise multiple comparisons were done using the T-test unless otherwise mentioned. Values are assessed as mean ± standard error of the mean (SEM). Significance was set at $p \leq 0.05$.

5.3 Results

nNOS expression was examined in TA and soleus muscles of WT, wtSOD1 and mSOD1 mice by Western blot and IHC. For Western blot data, the expression levels in the muscles of mSOD1 mice were expressed as a percentage of WT levels and then compared to those of wtSOD1 mice in order to take the effect of overexpression of the SOD1 protein into account.

5.3.1 nNOS expression in the TA muscle of mSOD1 mice

As shown in Fig.5.3, nNOS expression in wtSOD1 TA muscle was 148.1% (±7.2 SEM; n=4) of WT (100%). In mSOD1 TA muscle, nNOS levels changed significantly during disease progression. At 45 days of age, nNOS levels were 148.9% (±30.6 SEM; n=4) of WT. This was similar to that observed in wtSOD1 TA muscle ($p=0.981$). However, by 75 days, the level of nNOS present in mSOD1 TA muscle had increased dramatically, so that levels were 262.7% (±20.9 SEM; n=4) of WT, and this was significantly more than wtSOD1 TA muscle ($p<0.001$). As disease progressed**,** nNOS levels declined in mSOD1 TA muscle and by 100 days of age, nNOS levels were 114.7% (±9.1 SEM; n=4) of WT levels. However, this was not significantly less than wtSOD1 TA muscle ($p=0.076$). By 120 days of age, the level of nNOS had declined even further and was only 68.7% (±4.8 SEM; n=4) of WT; this level was significantly less than wtSOD1 TA muscle ($p=0.0008$).

Immunostaining for nNOS on TA muscle sections revealed that nNOS was expressed at the sarcolemma of wtSOD1 TA muscle (Fig.5.3). However, nNOS expression in mSOD1 TA muscle was considerably altered. Even at 45 days, immunoreactivity for nNOS was reduced at the sarcolemma (Fig.5.3c, see arrow). By 75 days of age, nNOS immunoreactivity had largely relocated to the sarcoplasm. By 120 days, nNOS immunoreactivity the majority muscle fibres is vastly reduced, with the little nNOS present limited to the sarcoplasm (Fig.5.3).

Figure 5.3: Neuronal nitric oxide synthase expression in mSOD1 TA muscle

Western blots for nNOS are shown (A-C) on TA muscle homogenate. (A) shows a pre-absorbed blot for nNOS run on a sample from wtSOD1 TA muscle. (B) shows a typical example of a nNOS western blot of TA muscle from WT, wtSOD1 and 45, 75, 100 & 120 day old mSOD1 mice. (C) shows a representative nNOS western blot of TA muscle from WT and 120-day-old untreated and Arimoclomol-treated mSOD1 mice. The bar chart (D) summarises the line densities. Examples of typical immunohistochemical staining for nNOS in wtSOD1 TA muscle are shown in (E). The pattern of nNOS expression in mSOD1 TA muscles is shown at (F) 45 days, (G) 75 days (H) 100 days (I) 120 days and (J) Arimoclomol-treated 120-day-old TA muscles from mSOD1 mice.

n=4; error bars= ± SEM; * = $p<0.05$; **= $p\leq0.01$; ***= $p\leq0.001$; Green= nNOS; scale bar =50μm

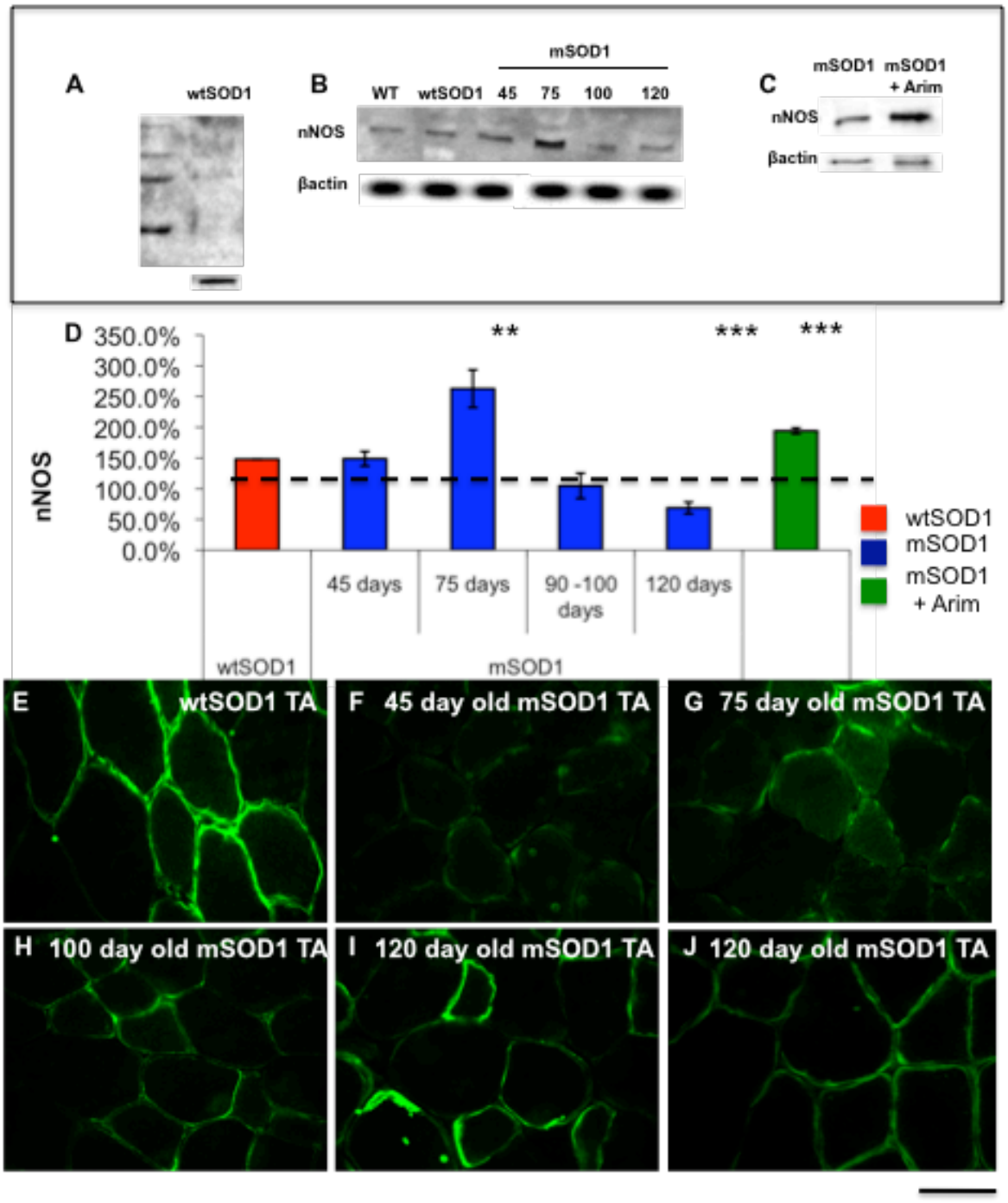
A
wtSOD1
B
mSOD1
WT
wtSOD1
45
75
100
120
nNOS
βactin
C
mSOD1
mSOD1 + Arim
nNOS
βactin
D
nNOS
350.0%
300.0%
250.0%
200.0%
150.0%
100.0%
50.0%
0.0%
**
***
***
45 days
75 days
90 -100 days
120 days
wtSOD1
mSOD1
wtSOD1
mSOD1
mSOD1 + Arim
E wtSOD1 TA
F 45 day old mSOD1 TA
G 75 day old mSOD1 TA
H 100 day old mSOD1 TA
I 120 day old mSOD1 TA
J 120 day old mSOD1 TA

Next, the effect of treatment with Arimoclomol was examined. The blots showed that nNOS in mSOD1 TA muscles was significantly greater in TA muscles from Arimoclomol-treated 120-day-old mSOD1 mice, so that they were 194.1% (±14.0 SEM; n=4) of WT. This was significantly more than seen in wtSOD1 (p=0.008).

nNOS expression at the NMJ of the TA muscle was also examined in longitudinal sections of muscle from 120-day-old WT and mSOD1 mice (Fig.5.4). The structure of the NMJ was represented clearly on these sections. In WT muscle, nNOS was closely associated with α-bungarotoxin. However, a large proportion of the NMJs on mSOD1 TA muscle displayed disrupted AChR clustering and nNOS expression was reduced or absent (Fig.5.4c,d, see arrow).

nNOS expression in mSOD1 TA at the NMJ was also examined using transverse sections of WT, wtSOD1 and untreated and Arimoclomol-treated 120-day-old mSOD1 TA muscle were co-stained with alpha bungarotoxin, DAPI and an antibody for nNOS. nNOS was closely associated with the NMJ and muscle. Transverse sections revealed that nNOS expression at the NMJ was greatly increased in wtSOD1 TA muscle fibres (Fig.5.4f, see arrow). In mSOD1 TA muscle there was a very different pattern of nNOS expression at the NMJ. In mSOD1 TA muscle, some NMJs did not colocalise with nNOS (Fig.5.4g, see white arrow). Treatment with Arimoclomol, however, increased nNOS expression at the NMJ of mSOD1 TA muscle (Fig.5.4h, see arrow).

Hsp90 is known to elevate nNOS expression in muscle fibres by binding with nNOS, thus preventing its degradation (Song et al, 2001; Brennan et al., 2008; Pratt et al., 2008). As the increased translocation nNOS is likely to exacerbate aberrant nNOS signalling, the pattern of hsp90 and nNOS staining was examined in mSOD1 muscle.

Figure 5.4: nNOS expression at the NMJ in TA muscle of mSOD1 mice

(A) shows an example of a longitudinal section of the WT TA muscle stained for nNOS (green) and (B) a merged representation of WT TA muscle stained for nNOS (green), α-bungarotoxin (red) and DAPI (blue). (C) a longitudinal section of mSOD1 TA muscle stained for nNOS (green) and (D) co-stained for nNOS (green), AChRs with α-bungarotoxin (red) and nuclei with DAPI (blue). (E-H) shows examples of nNOS expression in a transverse section of TA muscle stained for nNOS (green), α-bungarotoxin (red) and DAPI (blue), from WT (E), wtSOD1 (F), untreated mSOD1 (G) and Arimoclomol-treated (H) mSOD1 mice.

n=4; nNOS (green), α-bungarotoxin (red) and DAPI (blue); scale bar =50μm

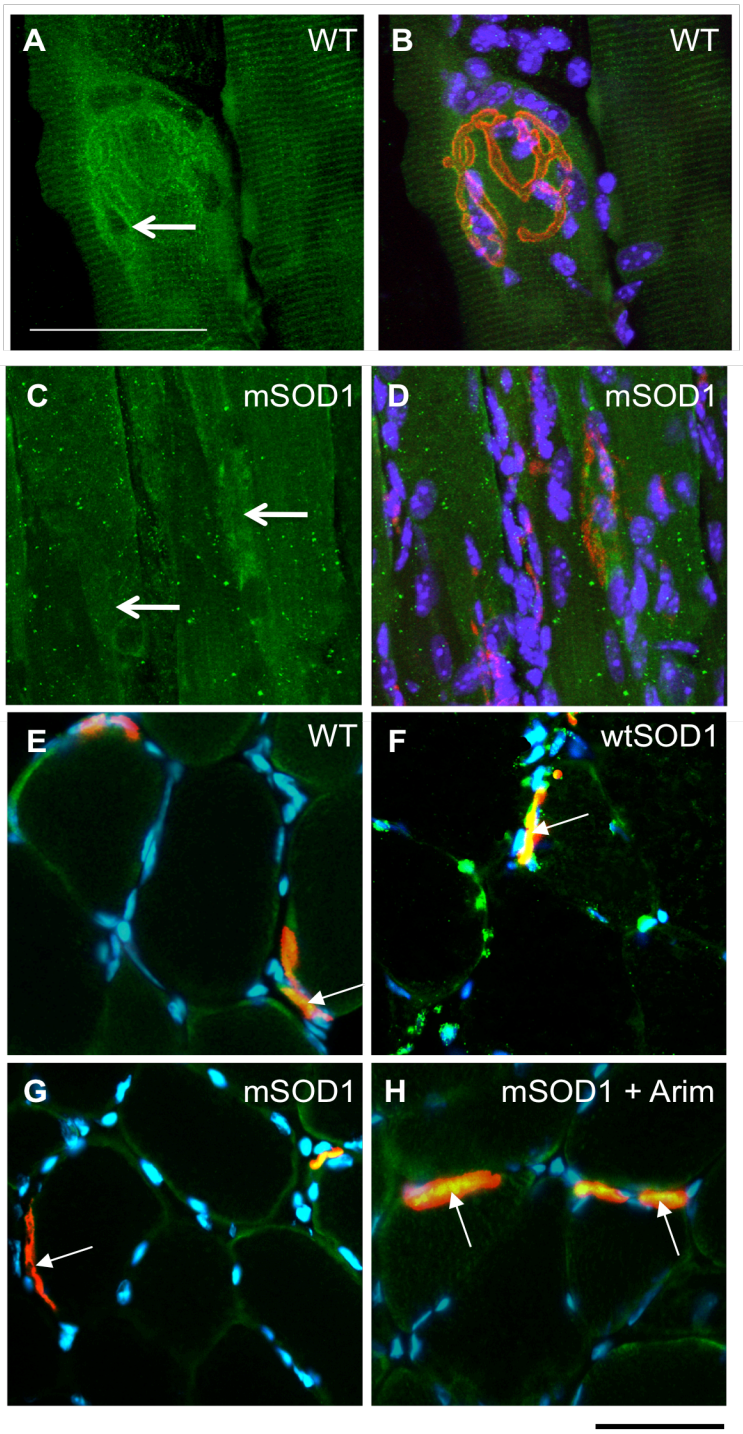
A
WT
B
WT
C
mSOD1
D
mSOD1
E
WT
F
wtSOD1
G
mSOD1
H
mSOD1 + Arim

The results showed that nNOS/hsp90 colocalisation differed between wtSOD1 and mSOD1 TA muscle (Fig.5.5). TA muscle from 100-day-old wtSOD1 and mSOD1 mice was stained with antibodies for nNOS, hsp90 and DAPI. The results revealed that there was very little colocalisation of nNOS with hsp90 in wtSOD1 TA muscle (Fig.5.5a), while there was a considerable level of colocalisation of nNOS and hsp90 expression at the sarcolemma and sarcoplasm of mSOD1 TA muscle (Fig.5.5c). Hsp90 colocalisation with sarcoplasmic nNOS was greatest [greater] in smaller, angulated muscle fibres (Fig.5.5b) than in the larger fibres (Fig.5.5c).

Having established that Arimoclomol is sufficient to increase nNOS levels, I examined whether treatment would alter nNOS/hsp90 interaction in the TA muscle of mSOD1 mice. As can be seen in Fig.5.5e, treatment with Arimoclomol greatly reduced nNOS/hsp90 colocalisation within the sarcoplasm, leaving some nNOS/hsp90 colocalisation at the sarcolemma of muscle fibres.

5.3.2 nNOS expression in the soleus muscle of mSOD1 mice

nNOS expression was also examined in the slow-twitch soleus muscle of WT, wtSOD1 and mSOD1 mice at 45, 70, 100 and 120 days of age. As can be seen in Fig.5.6, western blotting revealed that nNOS levels in wtSOD1 soleus were higher than in WT soleus muscle, and were found to be 190.7% (±4.2 SEM; n=4) of WT. Next, nNOS levels in the soleus muscle of mSOD1 mice were examined, and did not change significantly over the course of the disease. Thus, at 45 days, nNOS levels were 184.6% (±21.8 SEM; n=4) of WT, which was similar to wtSOD1 ($p=0.82$), and 214.3% (±88.0 SEM; n=4) of WT at 75 days, which was not significantly more than wtSOD1 ($p=0.30$). After this point nNOS levels began to decline, so that by 100 and 120 days of age, nNOS levels in mSOD1 soleus muscle were 124.4% (±40.9 SEM; n=4) and 95.2% (±62.8 SEM; n=4) of WT.

Figure 5.5: nNOS and hsp90 expression in TA and soleus muscle of mSOD1 mice

TA (A) and soleus (B) muscles of wtSOD1 mice at 100 days of age were stained for nNOS (red) and hsp90 (green). An example of hsp90 (green) and nNOS (red) co-staining in mSOD1 mice can be seen in the TA (C) and (D) soleus muscles. A representative stain of hsp90 and nNOS colocalisation in Arimoclomol-treated 120-day-old mSOD1 TA (E) and soleus (F) muscle can also be seen.

n=4; Green= hsp90; Red=nNOS; Blue= nuclei; scale bar =50μm

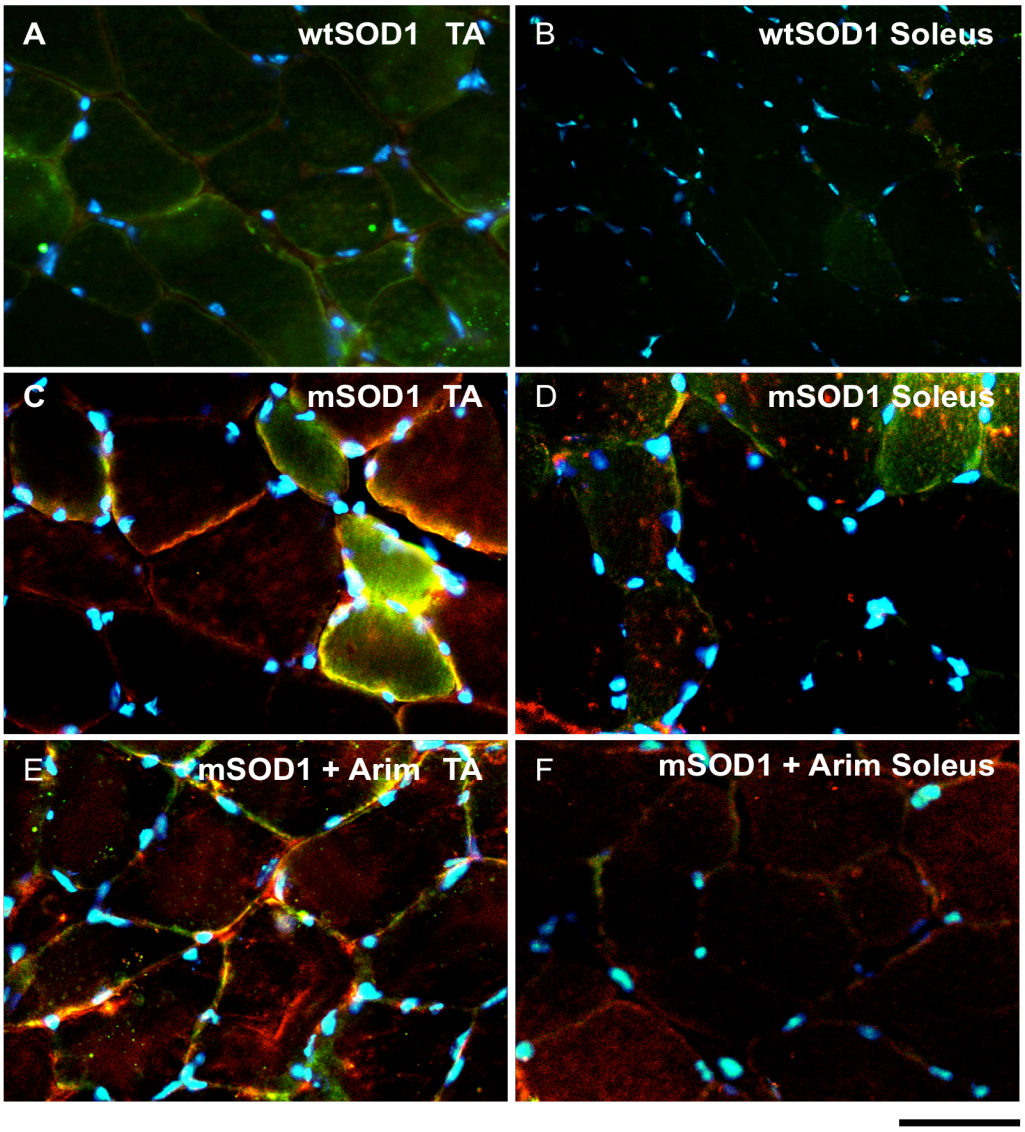
A
wtSOD1 TA
B
wtSOD1 Soleus
C
mSOD1 TA
D
mSOD1 Soleus
E
mSOD1 + Arim TA
F
mSOD1 + Arim Soleus

Figure 5.6: nNOS expression in the soleus muscle of mSOD1 mice

(A) shows a typical nNOS western blot of soleus muscle from WT, wtSOD1 mSOD1 mice at 45, 75, 100 and 120 days of age. (B) shows a typical nNOS western blot of soleus muscle from WT, untreated and Arimoclomol-treated mSOD1 mice at 120 days of age. The bar chart (C) summarises the line densities from (A&B). (D-I) shows an example of soleus muscles immunostained for nNOS. Examples of nNOS (green) staining in wtSOD1 mice are summarised in (D). An example of nNOS staining in the soleus muscle of mSOD1 mice at 45 days of age can be seen in (E). An example of nNOS expression in the soleus muscle of mSOD1 mice at 75 (F), 100 (G) and 120 (H) is also shown. (I) shows an example of nNOS (green) and DAPI (blue) expression in the soleus muscle of 120 day old Arimoclomol-treated mSOD1 mice.

n=4; error bars= ± SEM; * = $p<0.05$; scale bar =50μm

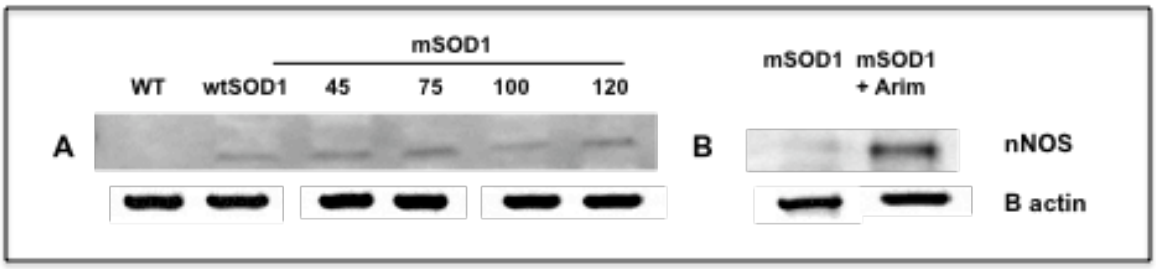
mSOD1
WT
wtSOD1
45
75
100
120
A
mSOD1
mSOD1
+ Arim
B
nNOS
B actin

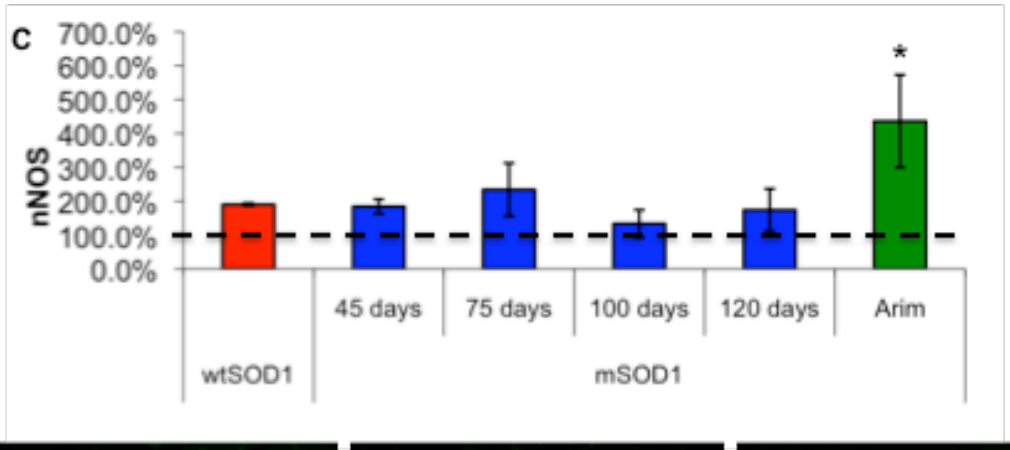
C
700.0%
600.0%
500.0%
400.0%
300.0%
200.0%
100.0%
0.0%
nNOS
*
45 days
75 days
100 days
120 days
Arim
wtSOD1
mSOD1

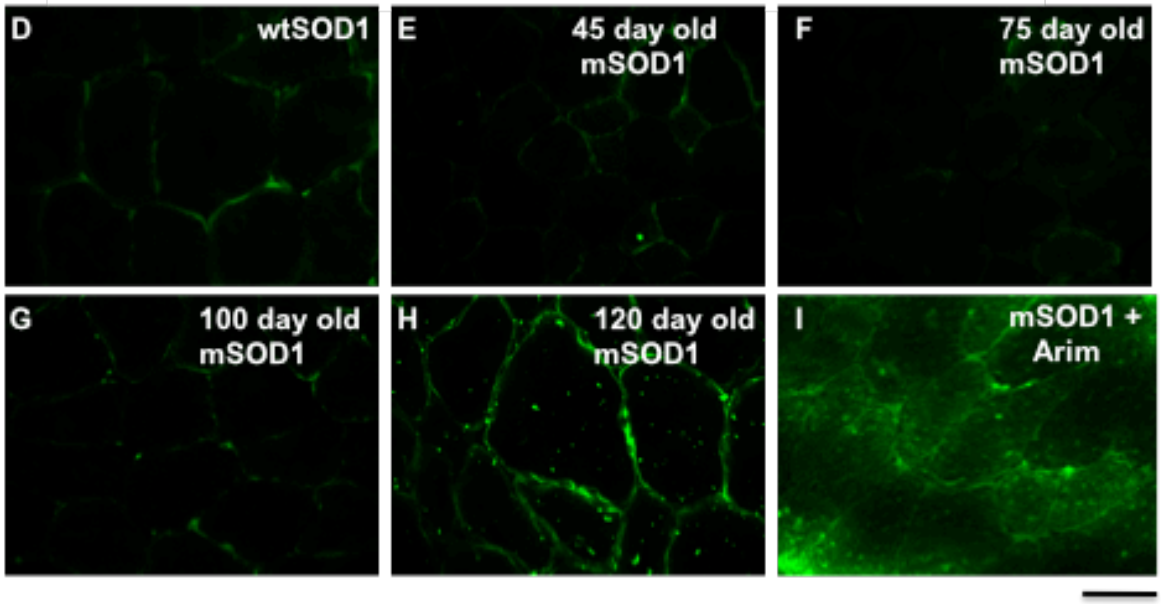
D
wtSOD1
E
45 day old
mSOD1
F
75 day old
mSOD1
G
100 day old
mSOD1
H
120 day old
mSOD1
I
mSOD1 +
Arim

Although these levels were reduced, they were not significantly less than wtSOD1: (p=0.40) and (p=0.87) respectively. Treatment with Arimoclomol increased nNOS expression, so that levels were 436.41% (±136.76 SEM; n=4) of WT. This is significantly more than untreated mSOD1 soleus muscle (p=0.0132).

The pattern of nNOS expression in WT, wtSOD1 and mSOD1 skeletal muscle was also examined using IHC. Immunostaining revealed that nNOS was present at the sarcolemma of muscle fibres of wtSOD1 soleus muscle (Fig.5.6) and nNOS immunoreactivity did not significantly differ in mSOD1 mice from that observed in wtSOD1 mice (Fig.5.6).

Examination of nNOS expression at the NMJ of soleus muscle from WT, wtSOD1 and mSOD1 mice showed that nNOS was present at the NMJ of WT soleus but was considerably increased at the NMJ of wtSOD1 soleus muscle. In 120-day-old mSOD1 soleus muscle, nNOS was also detected at the NMJs of WT soleus muscle, although this intensity was less (Fig.5.7). Staining of longitudinal mSOD1 muscle sections revealed that nNOS was present in nucleated structures surrounding the endplate and nerve terminal. These were likely to be terminal Schwann cells (Fig.5.7).

Evaluation of hsp90 and nNOS colocalisation using IHC revealed that hsp90 and nNOS colocalisation in mSOD1 soleus muscle was far less pronounced than in mSOD1 TA. Treatment with Arimoclomol removed the majority of nNOS/hsp90 colocalisation at the sarcolemma (Fig.5.5f) and reduced the presence of sarcoplasmic nNOS/hsp90 colocalisation.

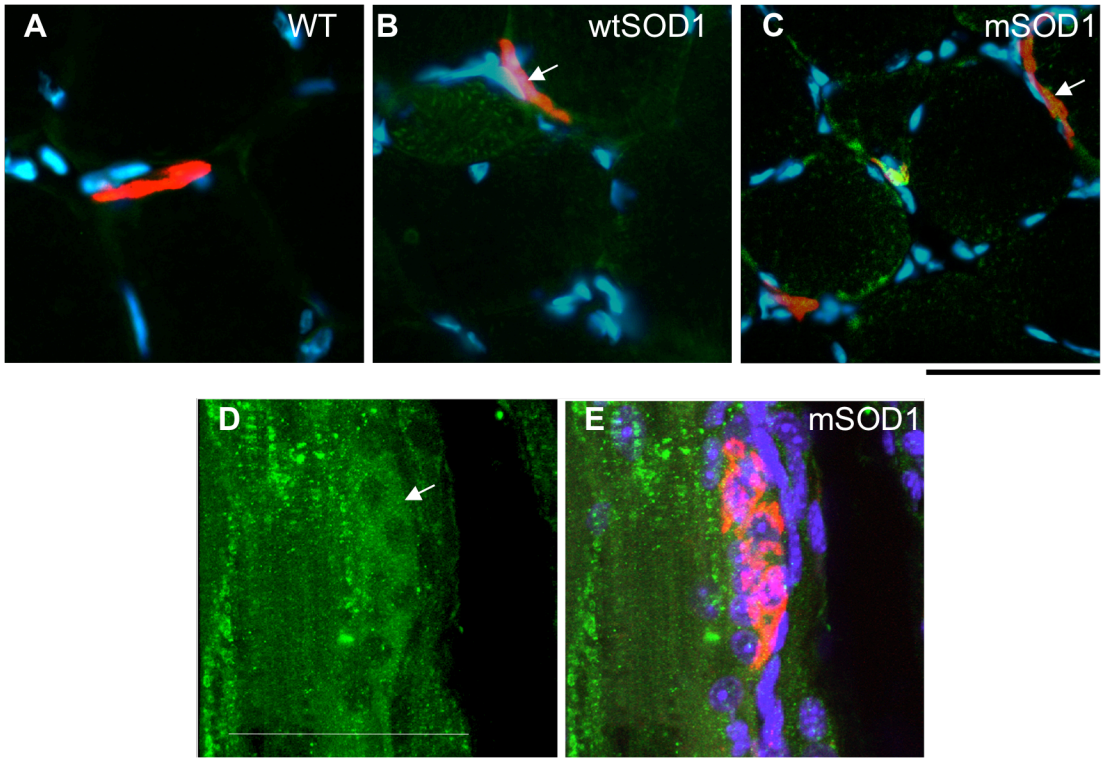

Figure 5.7: nNOS expression at the NMJ of soleus muscle from mSOD1 mice

Transverse sections of soleus muscle (A) WT, (B) wtSOD1 (C) 120-day-old mSOD1 mice were stained with nNOS (green), DAPI (blue) and α-bungarotoxin (red). Longitudinal sections from the soleus of mSOD1 mice (D&E) were also stained for nNOS, which was co-localised around AChRs in soleus muscles of 120-day-old mSOD1 mice. A merged image showing nNOS, AChR and nuclei is shown (E).

n=4; scale bar =50μm

5.3.3 iNOS expression in the TA muscle of mSOD1 mice

iNOS is an important enzyme that plays a role in the initiation of the inflammatory response in cells (Seago et al., 1995). Unlike nNOS, which is physiologically relevant to the normal function of muscle, iNOS is associated with pathological events in the muscle (Zhao and Qiu, 2004) and is found to be upregulated in a number of myopathies such as DMD and IBM (Yang et al., 1998, Louboutin et al., 2001).

Western blot analysis revealed that the level of iNOS in TA muscle of WT and wtSOD1 mice was very low (Fig.5.8). The level of iNOS in the TA muscle of wtSOD1 mice was 90.0% (±3.3 SEM; n=4) of WT (100%). iNOS levels remained low in the TA muscle of mSOD1 mice and in 45-day-old mSOD1 mice, levels were 98.9% (±4.3 SEM; n=4) of WT TA muscle, which was similar to wtSOD1 ($p=0.626$). But by 75 days, iNOS levels had more than doubled, so that levels were 244.0% (±10.5 SEM; n=4) of WT. This was significantly more than wtSOD1 ($p<0.001$). Levels remained elevated at 100 days of age, when they were 245.0% (±30.8 SEM; n=4) of WT, which was significantly more than wtSOD1 ($p<0.001$). By 120 days, iNOS had fallen to 167.0% (±3.6 SEM; n=4) of WT, which was significantly more than wtSOD1 ($p=0.003$).

Immunohistochemistry was used to examine the pattern of iNOS expression in wtSOD1 and mSOD1 TA muscle. As can be seen in Figure 5.8, iNOS immunoreactivity was low in wtSOD1 TA muscle as well as in the TA muscles of mSOD1 mice at all stages examined. Treatment with Arimoclomol increased iNOS levels in mSOD1 TA muscles so that they were 224.2% (±34.2 SEM; n=3) of WT levels. This was significantly more than untreated mSOD1 TA muscle ($p=0.002$). However, analysis of iNOS expression using IHC revealed that iNOS immunoreactivity was still low in Arimoclomol-treated mSOD1 TA muscle.

Figure 5.8: iNOS expression in mSOD1 TA muscle

(A) shows an example of a iNOS western blot of TA muscle from WT, wtSOD1 and mSOD1 mice at 45, 75, 100 and 120 days of age. (B) shows a representative iNOS blot of TA muscle from WT, untreated and Arimoclomol-treated mSOD1 mice at 120 days of age. The bar chart (C) summarises the optical line densities. (D) shows an example of iNOS (green) immunostaining in wtSOD1 TA muscle. iNOS expression in TA muscle from mSOD1 mice at 45 days (E), 75 days (F), 100 days (G) and 120 days (H) can also be seen, respectively. (I) shows iNOS expression in TA muscle from 120-day-old Arimoclomol-treated mSOD1 mice.

n=4; error bars= ± SEM; * = $p<0.05$; scale bar =50μm

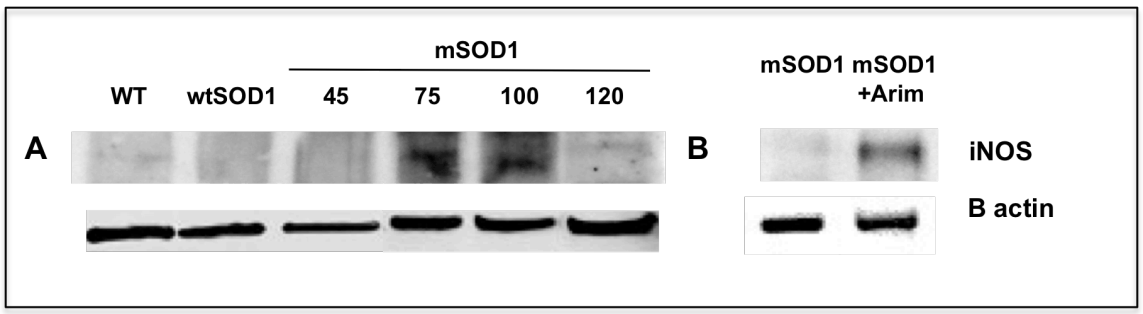
mSOD1
WT
wtSOD1
45
75
100
120
A
B
mSOD1
mSOD1
+Arim
iNOS
B actin

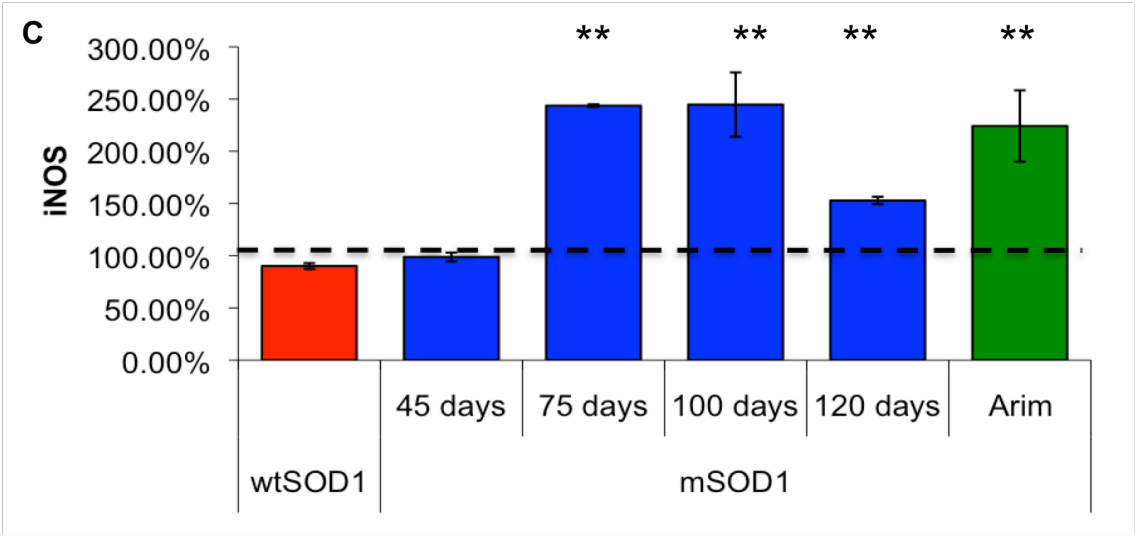
C
iNOS
300.00%
250.00%
200.00%
150.00%
100.00%
50.00%
0.00%
**
**
**
**
wtSOD1
45 days
75 days
100 days
120 days
Arim
wtSOD1
mSOD1

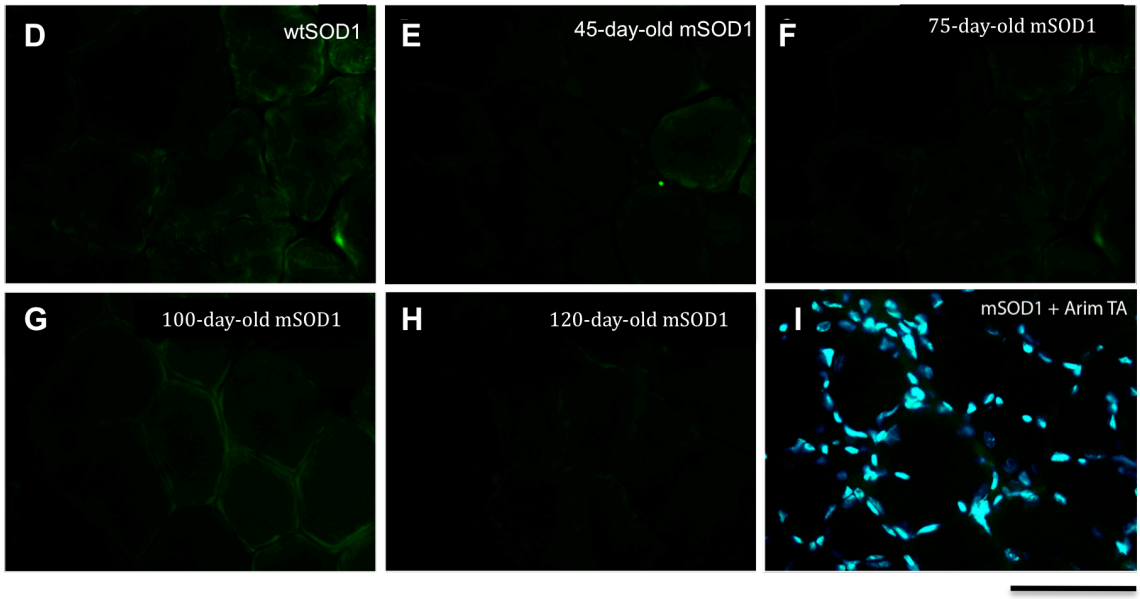
D
wtSOD1
E
45-day-old mSOD1
F
75-day-old mSOD1
G
100-day-old mSOD1
H
120-day-old mSOD1
I
mSOD1 + Arim TA

5.3.4 iNOS expression in mSOD1 soleus muscle

As can be seen in Figure 5.9, iNOS levels were similar in wtSOD1 soleus muscle to that in WT soleus: 133.5% (±9.6 SEM; n=4). However, iNOS levels in mSOD1 soleus changed significantly during disease progression. At 45 days of age, they were 146.9% (±26.3 SEM; n=4) of WT soleus muscle, which was not significantly more than wtSOD1 ($p=0.063$). By 75 days of age, this had increased to 174.9% (±32.6 SEM; n=4) of WT, which was significantly more than wtSOD1 soleus muscle ($p=0.032$). INOS levels continued to increase in mSOD1 soleus muscle, so that by 100 days of age iNOS levels were 232.3% (±21.7 SEM; n=4) of WT. This was significantly more than in wtSOD1 soleus muscle ($p=0.018$). Levels remained raised, so that at 120 days of age they were 180.8% (±7.2 SEM; n=4) of WT, and this was significantly more than wtSOD1 soleus muscle ($p=0.0313$).

Treatment with Arimoclomol decreased iNOS levels, so that at 120 days of age, they were 125.4% (±17.45 SEM; n=3) of WT. This was significantly less than in untreated mSOD1 soleus muscle ($p=0.05$). Immunohistochemistry revealed that there was very little iNOS in wtSOD1 soleus muscle (Fig.5.9), which was the case with mSOD1 soleus muscle. Treatment with Arimoclomol did not alter the pattern of staining in the mSOD1 soleus muscle.

Figure 5.9: iNOS expression in the soleus muscle of mSOD1 mice

(A) shows an example of a iNOS western blot of soleus muscle from WT, wtSOD1 as well as 45, 75, 100 and 120 mSOD1 mice. (B) shows an example of a iNOS western blot of soleus muscle from WT, untreated and Arimoclomol-treated mSOD1 mice at 120 days. The bar chart (C) summarises the line densities. (D) shows an example of iNOS (green) immunostaining in wtSOD1 soleus muscle. An example of iNOS expression in soleus muscle from mSOD1 mice at (E) 45 days (F) 75 days (G) 100 days and (H) 120 days can be seen. (G) shows an example of iNOS expression in the soleus muscle of Arimoclomol-treated mSOD1 mice, and the section is co-stained with DAPI (blue).

n=4; error bars= ± SEM; * = $p<0.05$; scale bar =50μm

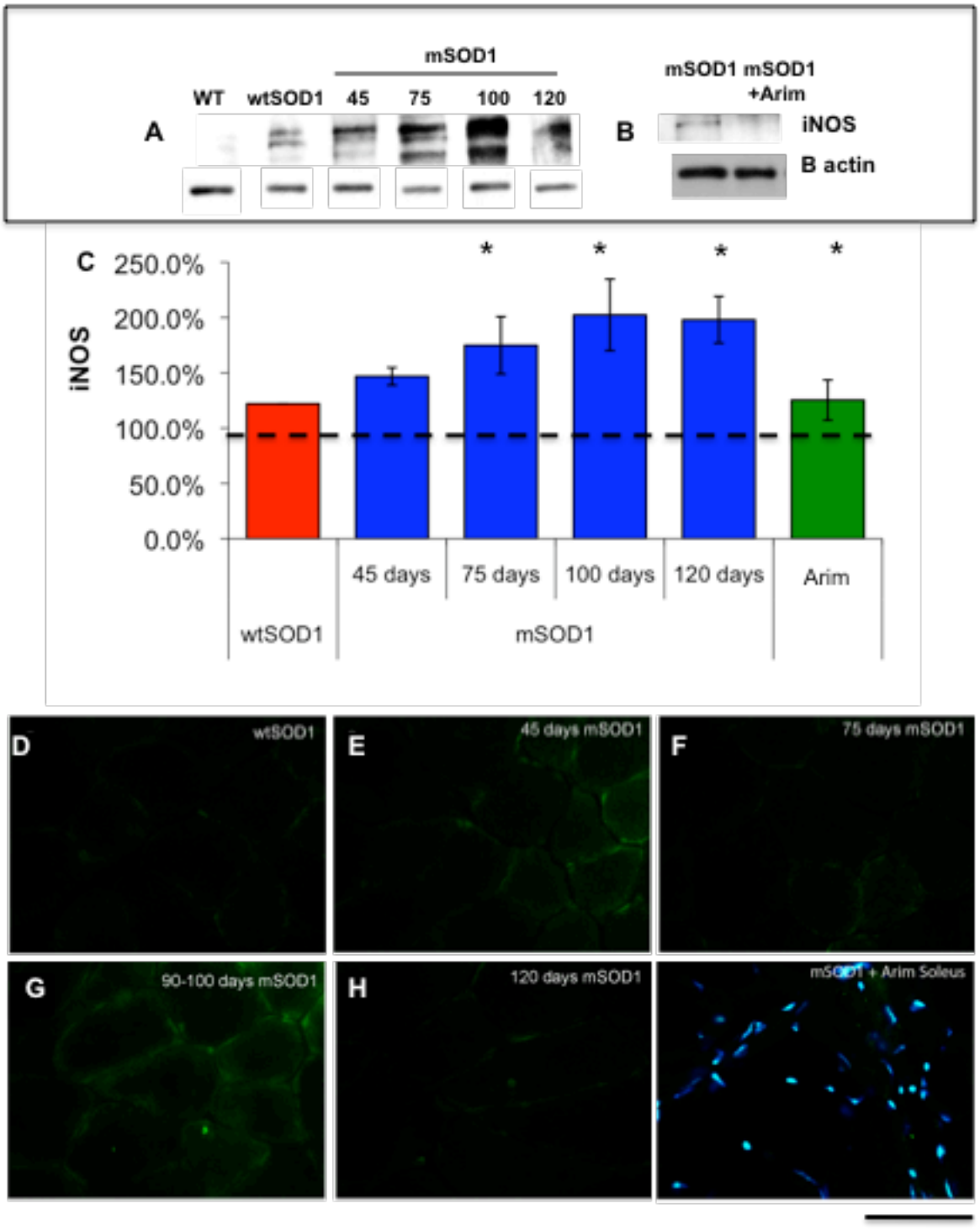
A
WT
wtSOD1
mSOD1
45
75
100
120
B
mSOD1
mSOD1 +Arim
iNOS
B actin
C
iNOS
250.0%
200.0%
150.0%
100.0%
50.0%
0.0%
*
*
*
*
wtSOD1
45 days
75 days
100 days
120 days
Arim
mSOD1
D
wtSOD1
E
45 days mSOD1
F
75 days mSOD1
G
90-100 days mSOD1
H
120 days mSOD1
mSOD1 + Arim Soleus

5.4 Discussion

This Chapter examined NOS expression in the fast-twitch TA and slow-twitch soleus muscle and the results revealed that nNOS and iNOS expression was significantly altered in muscles of mSOD1 mice. Furthermore, the results show that treatment with Arimoclomol, a co-inducer of the HSR, significantly alters mSOD1-mediated changes in nNOS and iNOS expression in muscle of mSOD1 mice.

5.4.1 Nitric Oxide synthase levels are altered in wtSOD1 TA muscle

The results presented in this Chapter show that nNOS expression is significantly raised in wtSOD1 TA muscle. While this has never been reported in mSOD1 muscle, it is of interest to note that nNOS overexpression has been shown to alter SOD1 expression in murine muscle (Baldelli et al., 2008), although the underlying mechanism is not fully understood. It is known that NO, produced by NOS, can react spontaneously with SOD1 and can generate protein tyrosine nitration (Ferrante et al., 1997). Furthermore, in motoneurons, after zinc depletion in mSOD1, superoxide anions lead to the generation of RNS; thus, it is possible that O2 levels influence nNOS expression. In addition, in cardiac muscle, superoxide and nNOS have been shown to work in opposing pathways in order to promote effective excitation-contraction coupling (ECC). Since a similar mechanism for ECC is present in skeletal muscle, it is possible that a similar nNOS/SOD1 relationship may also be present (Eu et al., 2000). This ECC pathway is illustrated in Fig.5.10.

5.4.2 Neuronal Nitric Oxide synthase expression is altered in mSOD1 muscle

To date, nNOS expression in muscles of ALS patients and mSOD1 mice has only been examined in a small number of studies and only at a late symptomatic stage when denervation is already extensive. In this study, nNOS was examined in the muscle of mSOD1 mice before symptomatic onset and was monitored over the course of the disease. This study demonstrated that in the TA muscle of mSOD1 mice there is a significant, but transient increase in nNOS expression at symptomatic onset, which is coupled with the translocation of nNOS to the sarcoplasm where it is likely to promote FOXO activation and muscle atrophy.

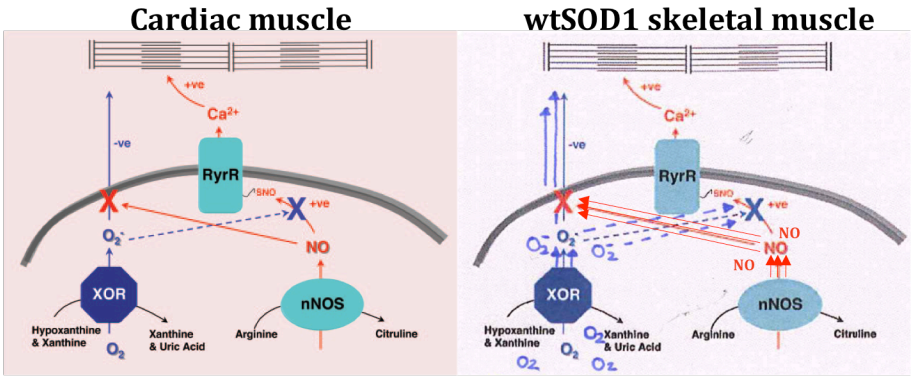

Figure 5.10: Possible mechanism for increased nNOS expression in wtSOD1 muscle

In cardiac muscle, the enzymes nNOS and xanthine oxidoreductase (XOR) are expressed in close proximity to the SR, promoting effective excitation-contraction coupling. These enzymes are similarly located in skeletal muscle. nNOS catalyses the production of NO, which can then S-nitrosylate a specific cysteine on the RyR1 SR calcium channel. This increases the probability of the channel opening and thus promotes calcium release during excitation–contraction coupling. XOR utilises O_2 (produced by SOD1) in order to produce superoxide, which can diffuse out of the SR and inhibit calcium responsiveness of contractile machinery, thus inhibiting contraction. In addition to activating calcium release through the RyR1, NO can increase contractility by impeding the release of superoxide from the SR by direct reaction (solid red arrow). This results in the spontaneous formation of peroxytnitrite. Additionally, superoxide may be able to inhibit contractility by inhibiting NO-mediated activation of the RyR1, via the spontaneous formation of peroxytnitrite (Cleveland and Rothstein, 2001) (dashed blue line). In wtSOD1 mice, excess SOD1 activity may result in increase H_2O_2 and O_2, which in turn may enable the production of O^-_2 by XOR. This results in an increase in O^-_2, which can then diffuse out of the SR and decrease the responsiveness of contractile machinery. Increased nNOS expression results in an increase in NO, which can counteract the effects of O^-_2. This results in normal muscle contraction (Image adapted from (Bonaventura and Gow, 2004).

After this stage, nNOS levels fall dramatically and by a late stage of disease, nNOS levels are significantly lower than wtSOD1 levels (Soraru et al., 2007; Suzuki et al.,2010). The translocation of nNOS from the sarcolemma to the sarcoplasm following denervation has been documented in ALS patients (Soraru et al., 2007) and mSOD1 mouse models (Suzuki et al., 2010). The results presented in this Chapter show that nNOS is initially upregulated at a time when sprouting becomes present, but then is quickly down-regulated as nNOS begins to translocate to the sarcoplasm. As the disease progresses in mSOD1 mice, increased levels of nNOS are found at the sarcoplasm and nNOS staining at the sarcolemma becomes discontinuous. This change is likely to result in muscle pathology via the FOXO pathway, as NO is known to activate the transcription factor FOXO (Suzuki et al., 2007). FOXO accumulates in the nucleus of muscle cells, and its actions consequently promote the degradation of muscle proteins via the proteosome (Senf et al., 2010).

5.4.3 Neuronal Nitric Oxide synthase is differentially expressed in fast and slow-twitch muscle in mSOD1 mice

Examination of nNOS expression in the fast-twitch TA and slow-twitch soleus muscle of mSOD1 mice also revealed a differential pattern of nNOS expression in the two muscle types. In the soleus muscle of mSOD1 mice, nNOS levels did not alter significantly over the course of the disease, while levels changed dramatically in the TA muscle of mSOD1 mice. NNOS was also found more readily at the sarcolemma in the TA muscle. Notably, the soleus muscle does not undergo significant muscle atrophy until a late stage of disease, while atrophy in the TA occurs at a far earlier stage (Kalmar et al. 2009). Furthermore, the fact that nNOS-/- mice display decreased muscle atrophy suggests that the differential expression of nNOS may underlie, at least in part, the preferential vulnerability of the TA muscle.

The results presented in this Chapter show that hsp90 colocalises strongly with nNOS in skeletal muscle from mSOD1 mice, but to a lesser extent in wtSOD1

mice. Furthermore, that hsp90/nNOS colocalisation is greatest in the sarcoplasm of the TA muscle of mSOD1 mice. Evidence indicates that hsp90's binding to nNOS inhibits the binding of hsp72, thus preventing its degradation via the proteosome (Peng et al., 2009). If so, higher levels of NO may be produced in more vulnerable fast-twitch muscles such as the TA muscle, and NO produced by the displaced nNOS may facilitate muscle atrophy via the FOXO pathway (Suzuki et al., 2007).

5.4.4 Neuronal Nitric Oxide synthase expression is altered at the endplate of muscle from mSOD1 mice

NNOS expression is essential for terminal Schwann cell activation, which promotes sprouting and reinnervation. Indeed, nNOS-deficient mice display no tSCh reactivity following denervation, and subsequently very little sprouting or reinnervation (Marques et al., 2006). Following denervation in nerve injury models, considerable sprouting ensures normal muscle function. This can result in up to a 8-fold increase in motor unit size (Vrbova and Gordon, 1994). This does not occur in mSOD1 mice, and instead sprouting (as shown in Chapter 3) persists for a short duration and then declines. NNOS' paramount role has been consistently demonstrated in reinnervation and has been implicated in Wallerian degeneration, sprouting and the general neuromuscular plasticity (Vrbova and Gordon, 1994). Thus, it is possible that the low level of sprouting in mSOD1 mice is due to, at least in part, an altered nNOS response.

This Chapter examined nNOS expression at the NMJ in the fast-twitch TA muscle and the slow-twitch soleus muscle of mSOD1 mice and demonstrated that nNOS was only found at a few NMJs in the TA and soleus muscles of 100-day-old mSOD1 mice, when denervation is significant in the TA muscle (as shown in Chapter three). Indeed, nNOS immunoreactivity was low in areas where AChRs expression was sparse, indicative of denervated emptied endplates. Furthermore, there is a body of evidence to suggest that some NMJs are intrinsically more vulnerable to denervation. These endplates are often innervated by fast-fatigable motor units (Santos et al., 2003). It is possible that these NMJs are the earliest to

become denervated, and are subsequently unable to up-regulate nNOS expression in tSCh. In turn, this makes them less likely to be reinnervated by a sprout, and thereby leaves those muscles fibres even more vulnerable to denervation, induced muscle atrophy and other mSOD1 pathology.

5.4.5 Inducible Nitric Oxide Synthase expression is altered in the muscle of mSOD1 mice

INOS expression in the muscle of mSOD1 mice was different from nNOS expression. This study revealed increasing, progressive iNOS levels in both the TA and the soleus muscle, indicative of a slow but mounting inflammatory response. These changes were greatest at points of vascularisation and colocalised with CD11b expression, a marker of macrophages, (appendix two, Fig. 9.1b,d). Together these data suggest that the iNOS present was not released by muscle, but rather by macrophages present in the blood stream; furthermore, macrophages that were elicited by a significant systemic inflammation response, in contrast to a muscle-mediated inflammatory response. Indeed, the strong immunostaining of the, more resilient but more vascular, soleus muscle for CD11b indicates the possibility of autoimmune response present in the mSOD1 mice during the later stages of disease.

It is interesting to note, that it has been established that ALS shares a number of pathological characteristics, such as oxidative stress and mitochondrial dysfunction with autoimmune neuropathies like multiple sclerosis (Staines, 2008) as well as autoimmune myopathies like IBM (see Table 1.2). Furthermore, it has been shown that Riluzole, an anti-glutamatergic drug and the only drug available for the treatment of ALS, can suppress autoimmune encephalitis (Gilgun-Sherki et al, 2003). In addition, muscle from ALS patients has been found to possess calcium channel binding kinetics similar to that seen in autoimmune motoneuron diseases (Smith RG et al., 1995). Thus, it is possible that the CD11b (indicative of macrophages) present at point of vascularisation, in both fast and slow muscles

may be a marker for an additional inflammatory pathology, which may be independent of the glial cell-mediated neuroinflammation present within the CNS.

5.4.6 Treatment with Arimoclomol alters nNOS & iNOS expression in mSOD1 muscle

The results in this Chapter showed that the systematic treatment of mSOD1 mice with Arimoclomol upregulated nNOS expression differentially in fast and slow-twitch muscle of in mSOD1 mice. Immunostaining revealed that this upregulation was largely limited to the NMJ, which demonstrated a strong increase in nNOS reactivity. Arimoclomol also resulted in the reduction of hsp90/nNOS colocalisation at the sarcoplasm. This effect was greatest in the fast-twitch TA muscle. These findings suggest that treatment with Arimoclomol is sufficient to reduce sarcoplasmic nNOS, while increasing nNOS at the NMJ. It is of interest to note that reduced sarcoplasmic nNOS would result in a reduction in muscle atrophy via the down-regulation of the FOXO pathway. Meanwhile, increased nNOS at the NMJ could be indicative of nNOS expression in tSChs, which could promote sprouting. These effects may increase reinnervation of denervation endplates, maintaining muscle function for longer within mSOD1 muscle and may be responsible, at least in part, for the beneficial effects of Arimoclomol presented in Chapter 3. Treatment with Arimoclomol increased iNOS expression in the more vulnerable TA muscle; however, this increase was not reflected in an increase in iNOS immunoreactivity. Paradoxically, treatment with Arimoclomol decreased in iNOS expression within the more resilient soleus muscle.

5.4.7 Conclusion

In conclusion, although Arimoclomol increases nNOS expression in fast-twitch muscles of mSOD1 mice, it has little effect on nNOS levels in slow-twitch muscles like the soleus. In the fast-twitch TA muscle, this upregulation is restricted to the sarcolemma and around the endplate region, suggesting that Arimoclomol may influence both muscle atrophy (via the FOXO/Akt pathway) and sprouting via nNOS.

Chapter 6 : The effect of mSOD1 expression in muscle cultures following cell stress

6.1 Introduction

ALS is known to be a non cell autonomous disease with non-neuronal cells in the CNS and spinal cord significantly contributing to motoneuron pathology (Ilieva et al., 2009). However, to date, the role of the primary target affected—muscle—remains unclear.

6.1.1 Muscle pathology in ALS

Some studies suggest that muscle pathology is not a primary target in ALS, and that neuromuscular events are secondary to events occurring in the CNS and that muscle pathology does not therefore contribute to disease pathogenesis (Miller et al., 2006). For example, Miller et al. (2006) demonstrated that the viral delivery of transcription-mediated silencing RNA to mSOD1 mice, which suppressed mSOD1 accumulation in muscle, was insufficient to alter disease onset or survival.

However, the extent of mSOD1 silencing is difficult to determine. Furthermore, a number of additional studies indicate a role for muscle in mSOD1 pathology and ALS (Dobrowolny et al., 2008). For example, Dobrowolny et al. (2008) showed, using transgenic mice that expressed mSOD1 selectively in skeletal muscle, that expression was sufficient to cause progressive muscle atrophy, significant muscle weakness, and increased ROS as well as contractile and mitochondrial dysfunction. Likewise, Wong and Martin (2010) showed that the selective transgenic expression of mSOD1 in skeletal muscle could cause significant motoneuron pathology in the spinal cord accompanied by distal axonopathy, inclusion formation and motoneuron degeneration via an apoptotic-like capsase-3 pathway (Dobrowolny et al., 2008, Wong and Martin, 2010).

A growing body of evidence demonstrates significant underlying pathology within the muscle of ALS patients (Dupuis et al., 2003, Pradat et al., 2007, Halter et al.,

2010). For example, prior to symptomatic onset and motoneuron death, there is significant denervation at the NMJ (Fischer et al., 2004) and mitochondrial pathology within muscle, resulting in increased mitochondrial uncoupling protein and the subsequent dismantling of the NMJ (Dupuis and Loeffler, 2009).

Nevertheless, evidence shows a clear differential vulnerability between fast and slow-twitch muscle fibres to ALS pathology (Frey et al., 2000). Indeed, it has been shown that NMJs on fast-twitch muscles from mSOD1 mice undergo earlier denervation than slow-twitch muscles (Frey et al., 2000). Furthermore, there is evidence demonstrating an intrinsic vulnerability of fast-twitch fibres to injury and general cell insult (Lowrie and Vrbova, 1984).

In previous Chapters, the results demonstrate a differential vulnerability of fast and slow-twitch muscles to mSOD1-mediated pathology. I have also highlighted pathways that are likely to contribute to this differential vulnerability. In agreement with other findings (Frey et al., 2000), the results in Chapter 3 revealed that mSOD1 fast-twitch muscle is more vulnerable to mSOD1 pathology than slow-twitch muscle. Furthermore, that denervation occurred before symptomatic onset, much earlier than in the slow-twitch soleus and proved more extensive than in the slow-twitch soleus over the course of disease. Furthermore, the results in Chapter 4 showed that fast-twitch muscle, such as the TA muscle, was less capable of mounting and maintaining a HSR over the course of the disease. In Chapter 5, the data showed a greater susceptibility for the dislocation of nNOS to the sarcoplasm, which is an event likely to promote denervation-induced muscle atrophy.

In addition, a number of myopathies, like IBM and DMD, which also display preferential vulnerability in fast-twitch muscle. Thus, it is possible that fast-twitch muscle is intrinsically more vulnerable to disease and cell insult than slow-twitch muscles like the soleus muscle. If so, it is likely that fast-twitch muscle is less

capable of dealing with non-pathological cell stress, such as glucose deprivation or a contractile/oxidative stress. It is also possible that the expression of mSOD1 renders muscle cells even more vulnerable to these stresses.

6.1.2 Cell stress in muscle cells

6.1.2.1 Muscle contraction

One vital component of muscle contraction is excitation contraction coupling (ECC). It is process by which a chemical or electrical signal at the sarcolemma is coupled to the release of calcium from the sarcoplasmic reticulum (SR) and muscle contraction (Dulhunty et al., 2002). The process begins with the activation of the AChR's at the endplate of the NMJ and is followed by the depolarisation of the sarcolemma, which propagates through the sarcolemma down to transverse tubules (T-tubules) activating the 'voltage sensor' dihydropyridine receptors (DHPR). The DHPRs are associated with the voltage-gated L-type Ca^{2+} receptors found in the T-tubules and lie next to the ryanodine receptors (RyR). Activation of this channel results in the opening of the RyR channel, resulting in a Ca^{2+} transient in the sarcoplasm. This initial Ca^{2+} transient is further amplified by Ca^{2+} induced Ca^{2+} release from the SR, resulting in an increase in cytoplasmic calcium, which binds to Troponin-C and allows the formation of cross-bridges. This enables the actin filaments to slide along the fibre towards the Z line, causing muscle contraction (Dulhunty et al., 2002).

Principally, there are two intracellular channels that are responsible for the release of Ca^{2+} from internal stores: the RyR and the inositol 1,4 5-triphosphate receptors (IP3Rs) (Berridge, 1997). **T**he RyR channel mediates the fast release of Ca^{2+} and is associated with muscle contraction, while the other type of receptor, the IP3Rs, mediate Ca^{2+} release that regulate the transcription of muscle activity-dependent genes (Powell et al., 2001).

It has been well documented that caffeine is a strong modulator of RyR_1 receptor, which helps mediate muscle contraction. The $RyRy_1$ receptor, approximately 565kDa in weight, is responsible for the release of Ca^{2+} from the SR. It is activated in a dose-dependent manner by low caffeine concentrations (0.5-5mM). Mutations in RyR receptors are thought to play a role in other neurodegenerative diseases, like Alzheimer's disease (Stutzmann, 2005).

6.1.2.2 Glucose deprivation in muscle

Energy deprivation in skeletal muscle can arise from prolonged exercise or fasting and poses a considerable stress in muscle (de Lange et al., 2007). However, muscle has a number of adaptive mechanisms in order to minimise damage and ensure normal muscle function. In general, glucose serves as the primary fuel for skeletal muscle (Rose and Richter, 2005). In times of glucose deprivation, the metabolism of fatty acids ensures normal function (Zenimaru et al., 2008). This requires the rapid activation of a number of tightly regulated transcription, translation, and phosphorylation pathways. One such pathway is the AMPK/IGF-1 pathway (Murphy, 2000). The activation of AMP-activated protein kinase (AMPK) results in the recruitment of factors such as peroxisome proliferator-activated receptor gamma, coactivator-1alpha, peroxisome proliferator-activated receptor delta, and their target genes (de Lange et al., 2007). These factors are involved in the formation of oxidative muscle fibres, mitochondrial biogenesis, oxidative phosphorylation, and fatty acid oxidation (de Lange et al., 2007). A muscle's ability to metabolise glucose may alter several aspects of muscle function, from its oxidative profile to mitochondrial biogenesis, and therefore may have lasting implications for energy metabolism.

6.1.3 Metabolic dysfunction in ALS muscle

There is a growing body of evidence indicating a role for metabolic dysfunction in muscle pathology in mSOD1 mice and ALS patients, who are sometimes

hypermetabolic (Funalot et al., 2009). Anomalies in energy metabolism have been found in ALS mice, which have been shown to benefit from high-energy diets (Dupuis et al., 2004). The mSOD1 mice, also display depleted ATP levels as well as increased glycogen content, a phenomenon also seen in diabetes (Derave et al., 2003) and impaired lipid peroxidation (Dupuis et al., 2008). Additionally, mitochondrial pathology in muscle is well-established and associated with the destruction of the NMJ in mSOD1 mice (Dupuis and Loeffler, 2009). As muscle has a high-energy demand, it is possible that changes within this pathway have serious consequences for muscle, NMJ and motoneuron health.

Not all muscles have the same energy demands (Shin'ichi, 1991), nor are all muscles equipped with the same metabolic apparatus for glucose and lipid uptake (Rose and Richter, 2005), or glucose and lipid metabolism (Villa Moruzzi et al., 1981, Samec et al., 2002). As a result, metabolic dysfunction may affect various muscles to different degrees. Indeed, it is well-known that fast and slow-twitch muscles have different metabolic demands (Villa Moruzzi et al., 1981) and so it is possible that intrinsic differences in their ability to cope with metabolic stress may effect mSOD1 muscles.

6.1.4 Exercise and mSOD1 muscle

The role of effect of exercise in ALS and models of the disease is controversial. Bohannon first noted the beneficial effect of exercise in ALS patients in 1983 (Bohannon, 1983). The study revealed that the application of resistance exercise to the upper extremities of an ALS patient resulted in improved static strength in a number of muscle groups. More recently, it has been suggested that moderate exercise delays the onset of symptoms by over a week, while high levels of exercise facilitate the onset of symptomatic onset (Carreras et al., 2009).

Furthermore, Carreras et al. (2009) showed that moderate exercise results in higher motor neuron density in the ventral horn of the lumbar spinal cord in mSOD1 mice. Equally, Deforges et al. (2009) showed that exercise promoting the relative maintenance of the fast phenotype in fast-twitch muscles in mSOD1 mice, as well as preserving large motoneuron, astrocyte and oligodendrocyte populations within the CNS and increasing life span by 25 days (Deforges et al., 2009).

Examination of the effect of exercise in human has also been carried out. While human studies did not yield as impressive results, moderate exercise was still sufficient to result in a moderate effect in patients with early-stage ALS (Lui & Byl, 2009).

6.1.5 Aim

One contributing factor to the controversy surrounding muscles role in ALS is the difficulty in separating effect of changes originating from motoneuron and those originating from the muscle. However, one possible method is to examine muscle pathology in aneural, muscle cultures. Thus, in this Chapter I aim to:

- Whether aneural muscle cultures derived from presymptomatic mSOD1 neonates display any intrinsic vulnerabilities to various stresses.
- Whether there is a fundamental difference in the vulnerability of aneural fast-twitch and slow-twitch muscles to various stresses.
- If so, whether mSOD1-mediated pathology is sufficient to exacerbate any existing differential vulnerabilities.
- Whether mSOD1 muscle may release factors detrimental to the neuron.

6.2 Methods

6.2.1 Cell cultures

6.2.1.1 Mixed hindlimb muscle cultures and Fast and slow-twitch muscle cultures

Mixed hindlimb muscle cultures from a modified protocol from Bryla et al. (2004) were prepared as described in Chapter 2, Section 2.1.3. A minimum of four animals were used for each culture. Cells were plated at 100,000/cm^2. Fast and slow-twitch muscle cultures were also prepared as described in Chapter 2, Section 2.3.4. A minimum of six animals were used for each culture and cells were plated at 100,000/cm^2. The myogenicity of the cultures and their pattern of differentiation was also monitored and graphs summarising this can be found in appendix 3.

6.2.2 SH-SY5Y cultures

SH-SY5Y cultures were also grown as detailed in Chapter 2, Section 2.3.9. The SH-SY5Y cell line was chosen, as they are a well characterised cell line, without any of the natural variation that would be present in primary motoneuron culture. Thus, making a sensible choice for a preliminary study.

6.2.3 The glucose deprivation (metabolic) stress

The glucose deprivation stress was carried out on mixed as well as fast and slow-twitch muscle cultures, as detailed in Chapter 2, Section 2.3.5.

6.2.4 The contractile stress (caffeine) stress

The contractile stress was carried out on mixed as well as fast and slow-twitch muscle cultures, as detailed in Chapter 2, Section 2.3.6 or a combination of the two, as detailed in Chapter 2, Section 2.3.7.

6.2.5 Muscle-conditioned medium preparation

The preparation of muscle-conditioned medium was carried out as detailed in Chapter 2, Section 2.3.8.

6.2.6 Cytotoxicity assay

The assay to measure LDH release (an indicator of cell viability) was carried out as detailed in Chapter 2, Section 2.3.10.

To obtain the minimum value for LDH release, I assayed 6 wells containing only media, which should contain no cells and therefore produce the lowest LDH release. This was taken as 0%, and the maximum LDH value for each culture was obtained by exposing cells from another six wells to 2% Triton X-100. This resulted in total cell lysis and thus the LDH release, while this value was taken as 100%. All LDH values reported were expressed as a percentage of the maximal LDH response obtained.

6.2.7 Statistical analysis

Statistical significance between the mean values was assessed using a student's t-test. Significance was set at $p \leq 0.05$.

6.3 Results

This Chapter examines the effect of mSOD1 expression on the on the myogenicity of muscle cultures. It subsequently examines the vulnerability of mSOD1 muscle cultures to cell stress. In addition, the viability of fast and slow-twitch muscle fibres following cell stress is examined in WT, wtSOD1 and mSOD1 muscle. In order to examine the intrinsic vulnerability of muscle cells, neonatal mouse muscle cells were exposed to cellular stresses that mimic some of the characteristic physiological stresses that may act on muscle *in vivo*. To examine the effect of inducing a stress mimicking contractile stress and the subsequent oxidative stress, muscle cells were treated with caffeine (a ryanodine receptor agonist). Measuring LDH release from the cultures assessed the effect of these cell stressors, in both mixed hindlimb muscle and fast and slow-twitch muscle cultures. In addition cell viability was examined in neuronal cells exposed to muscle-conditioned media from WT, wtSOD1 and mSOD1 mice.

Initially, the level of spontaneous differentiation was assessed and then a measure of the prevalence of myosin heavy chain I (MyHCI) and myosin heavy chain II (MyHCII) in the various muscle cultures was examined (Appendix 3) in the various genotypes examined. For each genotype a minimum of 3 wells for each 'n' number was counted and recorded as a percentage of the entire population. This revealed that there is a small increase in percentage of myotubes in the mSOD1 population, however, this did not reach significance. Likewise, examination of the MyHCI and MyHCII expression in WT, wtSOD1 and mSOD1 mice revealed a general increase in fibres that expressed MYHCII (Appendix 3, Fig. 10.2). While analysis of MyHCI and MyHCII expression in fast and slow WT and mSOD1 muscle cultures revealed that there was a general increase in the percentage of myogenic cells that expressed MyHCII in cultures originating from the fast muscle compared to cultures from the slow muscle (Appendix 3, Fig. 10.3).

6.3.1 The effect of mSOD1 expression on the vulnerability of muscle cultures to cell stress

By measuring LDH release, the effect of mSOD1 expression on muscle cell viability under basal and stress conditions was examined in primary muscle cultures. For each condition, LDH release (absorbance) was normalised against protein levels and then expressed as a percentage of the maximum LDH release, which was established by incubation with 2% Triton X-100. In all experiments, wtSOD1 values are compared to WT in order to establish whether SOD1 overexpression altered cell viability. mSOD1 data was compared to wtSOD1 data in order to examine the effect of mSOD1 expression.

6.3.2 Cell viability in WT, wtSOD1 and mSOD1 muscle cultures under basal conditions

As can be seen in Fig.6.1, in WT cultures LDH release was 2.7% (±0.2 SEM; n=6) of the maximal response. Compared to WT, LDH release in wtSOD1 muscle cultures was 2.8% (±0.2 SEM; n=6; p=0.67) of the maximal response. In mSOD1 cultures, LDH release was 3.4% (±0.5 SEM; n=6; p=0.284) compared to wtSOD1 mice. Thus, there is no significant difference in cell viability in mixed muscle cultures of any genotype under basal conditions.

6.3.3 Cell viability in WT, wtSOD1 and mSOD1 muscle cultures under conditions of metabolic stress

Next, the effect of a metabolic stress induced by glucose deprivation on cell survival in mixed muscle cultures from WT, wtSOD1 and mSOD1 mice was examined (see Fig.6.2). Glucose deprivation in WT cultures resulted in LDH levels that were 2.6% (±0.3 SEM; n=6) of the maximal response. Glucose deprivation resulted in higher LDH levels in wtSOD1 mixed muscle cultures, so that they were 4.3% (±0.4 SEM; n=6) of the maximal response. However, this was not significantly different from treated WT (p=0.062). In mSOD1 muscle cultures, glucose deprivation resulted in LDH levels that 5.6% (±0.3 SEM; n=6) of the maximal

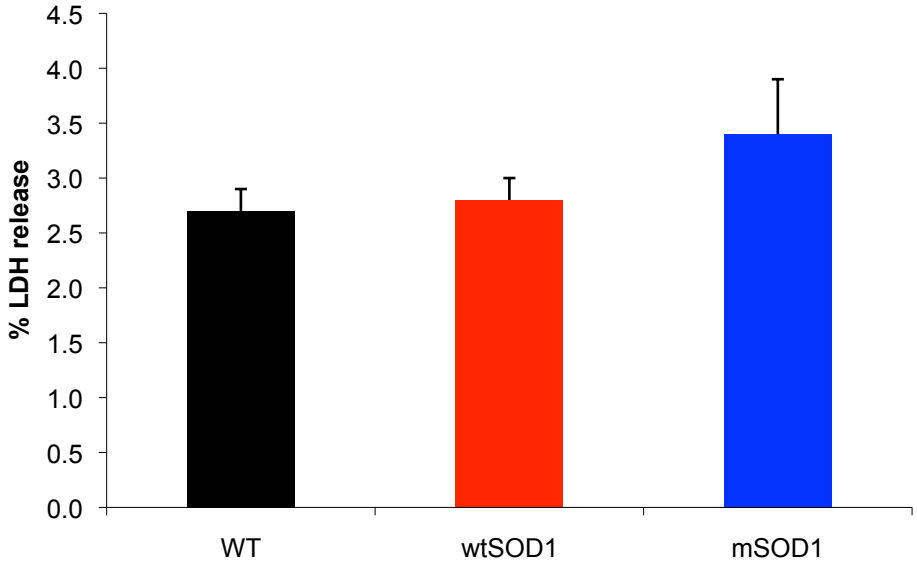

Figure 6.1: Cell viability in mixed hindlimb muscle cultures, under basal conditions, from wtSOD1 and mSOD1 neonate mice

WT, wtSOD1 and mSOD1 muscle cultures were incubated in muscle media for 24 hours. The media was then collected and the level of LDH in the media was determined and recorded as a percentage of the maximal LDH release calibrated using positive and negative controls. The results were then represented as a percentage of the maximal LDH release, which was taken as 100%.

*=$p<0.05$; n=6; error bars = ± standard error of the mean

response, which was significantly higher than in glucose-deprived in wtSOD1 cultures (p=0.046).

6.3.4 Cell viability in WT, wtSOD1 and mSOD1 muscle cultures under conditions of contractile stress

Cell survival following exposure to caffeine 1mM and 5mM, over 24hrs, was examined in WT mixed hindlimb muscle cultures in order to establish the most stressful concentration of caffeine. The results shown in Fig.6.3 revealed a dose-dependent significant increase in LDH release in WT muscle cultures that had been treated with caffeine. At 1mM, LDH release was 3.3% (±0.2 SEM; n=6) of the maximal response. At 5mM, LDH levels were significantly higher at 4.7% (±0.1 SEM; n=6) of the maximal response. This was significantly more than seen at 1mM (p=0.001).

As shown in Fig.6.3b, exposing wtSOD1 cultures to 1mM of caffeine for 24 hours resulted in LDH levels that were 3.6% (±0.1 SEM; n=6) of the maximal response. Incubation with 5mM of caffeine resulted in LDH levels that were 3.2% (±0.2 SEM; n=6) of the maximal response. As this was not significantly different compared to WT (p=0.221). Thus, there was no dose-dependent increase in LDH release in wtSOD1 muscle cultures treated with 1mM to 5mM caffeine.

In mSOD1 cultures, incubation with 1mM of caffeine resulted in elevated levels of LDH release so that they were 4.8% (±1.1 SEM; n=6) of WT controls. However, this was not significantly higher than wtSOD1 (p=0.302). Incubation with 5mM of caffeine increased LDH release further, so that levels were 7.2% (±1.1 SEM; n=6) of WT. This was significantly more than wtSOD1 (p=0.005).

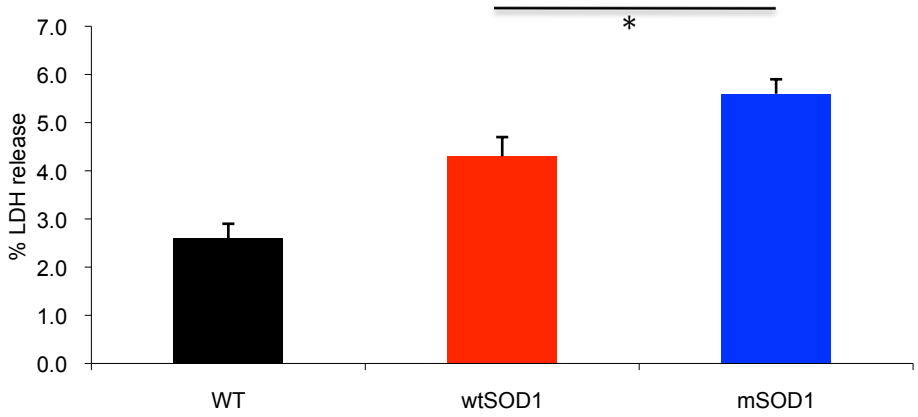

Figure 6.2: Cell viability in WT, wtSOD1 and mSOD1 mixed hindlimb muscle cultures following glucose deprivation

The effect of glucose deprivation on cell viability was examined in WT, wtSOD1 and mSOD1 mixed hindlimb muscle cultures. The results from all groups were represented as a percentage of the maximal LDH response, which was taken as 100%.

*=p≤0.05; n=6; error bars= ± standard error of the mean

Figure 6.3: Cell death in WT hindlimb muscle culture following incubation with Caffeine

The bar chart (A) shows LDH release following incubation with 1mM and 5mM in WT mixed muscle cultures. The bar chart (B) shows LDH release in wtSOD1 and mSOD1 mixed cultures following incubation with 1mM and 5mM caffeine, for 24 hours. All data was expressed as a percentage of the maximal LDH response, which was given the value 100%.

*=$p \leq 0.05$; n=6; error bars= ± standard error of the mean

A

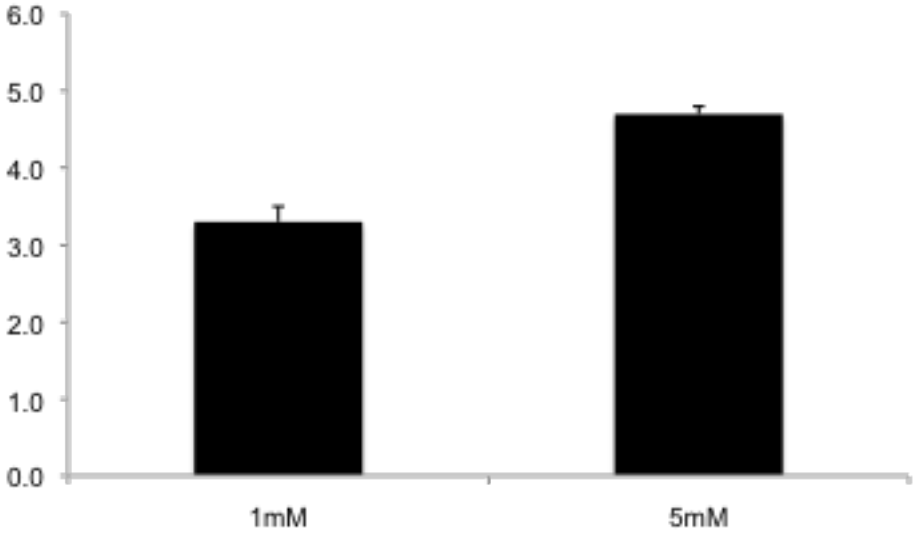
6.0
5.0
4.0
3.0
2.0
1.0
0.0
1mM
5mM

B

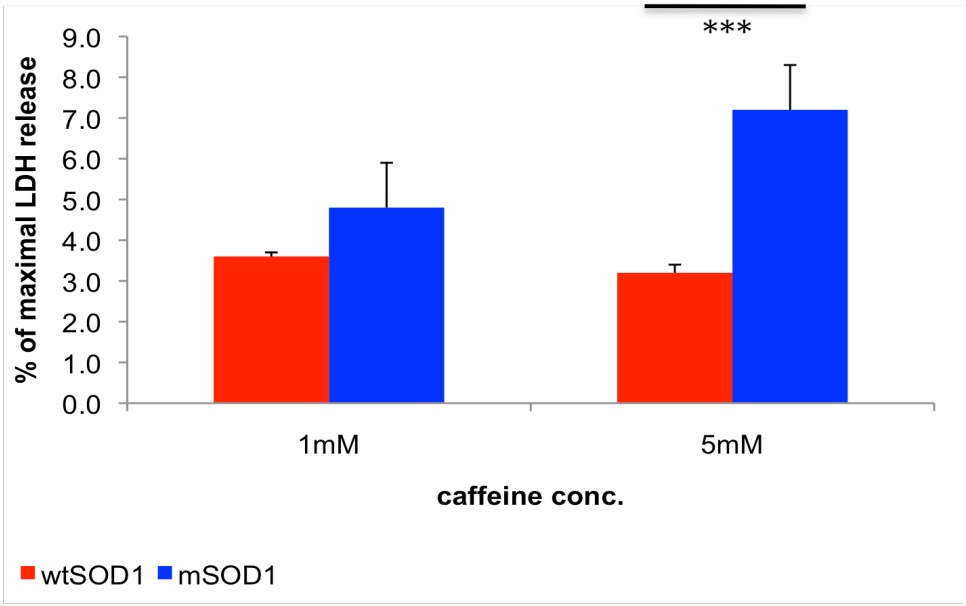
***
% of maximal LDH release
9.0
8.0
7.0
6.0
5.0
4.0
3.0
2.0
1.0
0.0
1mM
5mM
caffeine conc.
wtSOD1
mSOD1

6.3.5 Muscle cell survival following a metabolic and contractile stress.

The effect of exposure to glucose deprivation coupled with caffeine was examined next. The results are summarised in Fig.6.4. In WT muscle cultures, LDH release was measured following exposure to 1mM and 5mM caffeine in the absence of glucose. This resulted in LDH levels that were 5.4% (±0.2 SEM; n=6), 4.4% (±1.8 SEM; n=6) of the maximal response, respectively (see Fig.6.4).

Cell viability following exposure to a combined stress was next examined in wtSOD1 and mSOD1 muscle cultures. In wtSOD1 cultures, following glucose deprivation and treatment with 1mM of caffeine, the extent of cell death was not significantly different from that observed in WT muscles, so that LDH levels were 3.9% (±2.1 SEM; n=6; p=0.616) of the maximal response. At 5mM of caffeine, wtSOD1 muscle cultures produced 2.1% (±0.25 SEM; n=6) of the maximal response, which was not significantly different from the LDH values from WT cultures (p=0.234).

Comparing mSOD1 cultures to wtSOD1 after glucose deprivation and exposure to 1mM caffeine, LDH levels were 5.5% (±0.2 SEM; n=4; p=0.477) of the maximal response. However, there was a significant increase in cell death following glucose deprivation and incubation with 5mM caffeine over 24 hours, so that mixed mSOD1 muscle cultures released five times as much LDH compared to wtSOD1, or 10.5% (±2.2 SEM; n=4; p=0.009) of the maximal response. These results show that mixed hindlimb mSOD1 muscle cultures were more vulnerable to glucose deprivation and a combined oxidative/metabolic stress than WT or wtSOD1 muscle cultures.

Figure 6.4: Cell death following a caffeine exposure and glucose deprivation in mixed muscle cultures

The bar chart (A) shows LDH release following incubation with 1mM and 5mM combined with glucose deprivation for 24 hours, in WT mixed hindlimb muscle cultures from neonate mice. The bar chart (B) shows LDH release in wtSOD1 and mSOD1 mixed hindlimb muscle cultures from neonate mice following exposure to 1mM and 5mM caffeine, in the absence of glucose over 24 hours. WT, wtSOD1 and mSOD1 values were recorded as a percentage of the maximal LDH release, which was taken as 100%.

***= $p \leq 0.001$; n=4; error bars = ± standard error of the mean

A

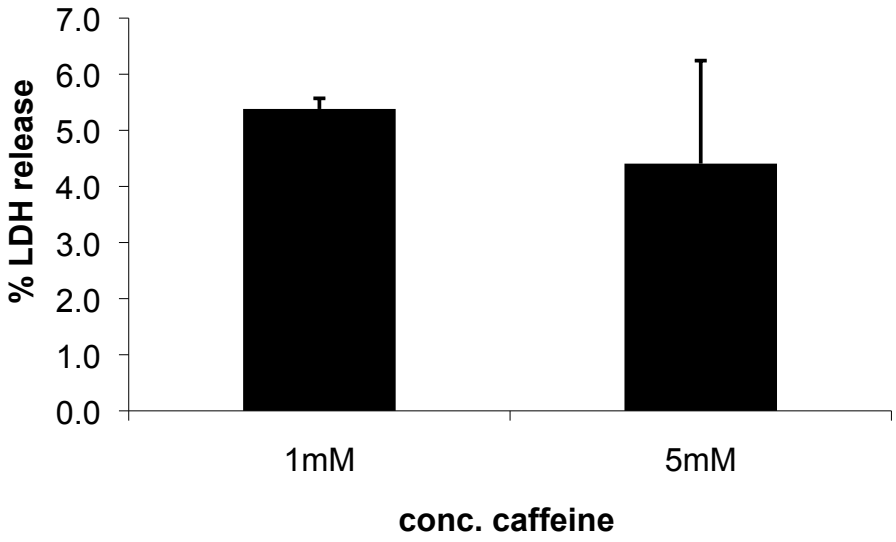
7.0
6.0
5.0
4.0
3.0
2.0
1.0
0.0
% LDH release
1mM
5mM
conc. caffeine

B

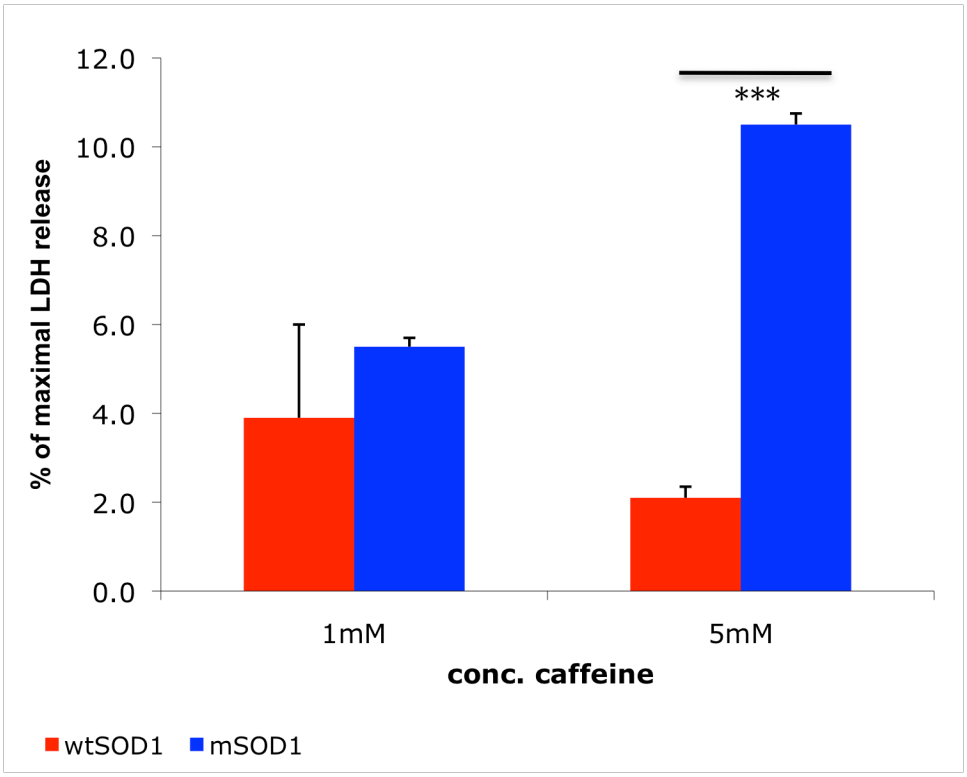
12.0
10.0
8.0
6.0
4.0
2.0
0.0
% of maximal LDH release
***
1mM
5mM
conc. caffeine
wtSOD1
mSOD1

6.3.6 Cell viability of fast and slow-twitch muscle cultures

These next set of experiments investigated whether muscle cultures originating from fast and slow-twitch muscles displayed differential vulnerability to these stresses. Therefore, these experiments compared the LDH release from fast and slow-twitch WT, wtSOD1 and mSOD1 muscle cultures under basal conditions, as well as under conditions of cellular stress induced by glucose deprivation.

6.3.6.1 Cell viability of fast and slow-twitch muscle cultures under basal conditions

Initially, the experiments established whether there was an innate difference in cell viability between muscle cells derived from fast and slow-twitch muscles under basal conditions. As can be seen Fig.6.5, in WT cultures from slow-twitch muscle, LDH levels were 4.01% (±0.2 SEM; n=4) of the maximal response. LDH levels in fast-twitch muscle cultures were 8.4% (±2.3 SEM; n=4) of the maximal LDH response. However, this was not significantly more than slow-twitch WT muscle cultures (p=0.118). wtSOD1 slow-twitch muscle cultures under basal conditions were examined next. wtSOD1 slow-twitch muscle cultures released LDH levels that were 14.3% (±10.3 SEM; n=4) of the maximal response, while mSOD1 slow-twitch muscle cultures released LDH levels that were 10.0% (±3.1 SEM; n=4) of the maximal response.

This was similar to wtSOD1 slow-twitch muscle cultures (p=0.703). However, cell viability in fast-twitch muscle cultures differed considerably. In fast-twitch wtSOD1 muscle cultures, LDH levels were 9.2% (±2.8 SEM; n=4) of the maximal response, while in fast-twitch mSOD1 muscle cultures LDH levels were triple that of wtSOD1. That is, LDH levels in fast-twitch mSOD1 muscle cultures were 34.2% (±9.2 SEM; n=4; p=0.041) of the maximal response, compared to fast-twitch wtSOD1 muscle cultures. This was also 3 times the LDH release of mSOD1 slow-twitch muscle cultures and significantly more than mSOD1 slow-twitch muscle cultures.

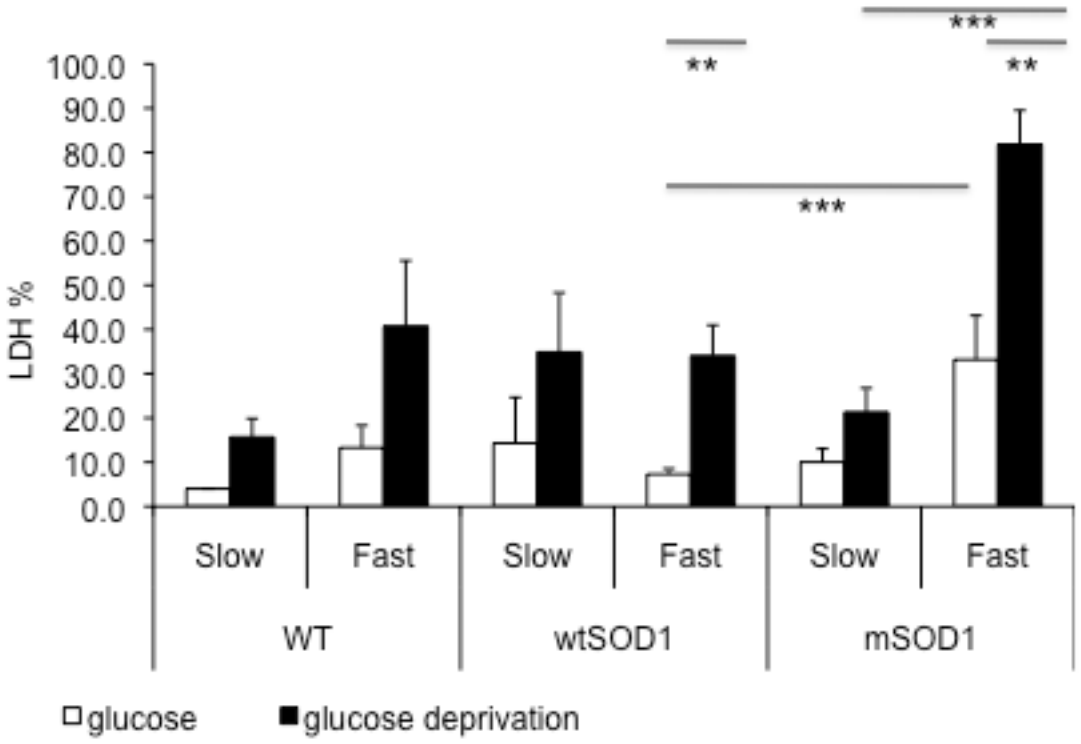

Figure 6.5: Cell viability in WT, wtSOD1 and mSOD1 fast and slow-twitch muscle cultures under basal conditions and following cell stress induced by glucose deprivation

The bar chart shows LDH release from slow and fast-twitch primary WT, wtSOD1 and mSOD1 neonate mice muscles cultures under basal and glucose deprived conditions. LDH readings were taken after 24 hours incubation in glucose depleted media. The maximal and minimal LDH release from the muscle cultures was determined and taken as 100% and 0% respectively. The maximal LDH reading was achieved by applying muscle media that contained 2% Triton X-100 solution.

**=p≤0.01; ***= p≤0.001; n=4; error bars = ± standard error of the mean

6.3.6.2 Cell viability in fast and slow-twitch muscle cultures following glucose deprivation

The results presented in this Chapter, show that there is a modest increase in cell death following glucose deprivation in mSOD1 muscle cultures. It was subsequently investigated whether mSOD1 expression in slow and fast-twitch muscle cultures differentially effected survival following cell stress. wtSOD1 and mSOD1 slow and fast-twitch muscle cultures were exposed to glucose deprivation for 24 hours and then assessed for LDH release. In slow-twitch muscle cultures from WT mice, glucose deprivation marginally increased cell death so that LDH levels were 15.7% (±4.2 SEM; n=4; p=0.062) of the maximal LDH response, compared to untreated slow-twitch WT cultures. Glucose-deprived WT fast-twitch muscle cultures released LDH levels that were 40.1% (±14.8 SEM; n=4; p=0.079) of the maximal LDH response, compared to untreated fast-twitch WT cultures. Thus, glucose-deprived fast-twitch cultures produced more than double the LDH seen in glucose deprived WT slow-twitch cultures (p=0.162).

As shown in Fig.6.5, wtSOD1 slow-twitch muscle cultures that had been treated with glucose-free media released 34.8% (±13.4 SEM; n=4) of the maximal LDH response. This was not significantly more than in untreated wtSOD1 slow-twitch cultures (p=0.27). While in mSOD1 slow-twitch muscle cultures, glucose deprivation resulted in 21.2% (±5.4 SEM; n=4) of the maximal LDH response, which was not significantly more than untreated mSOD1 slow-twitch cultures (p=0.122) or treated slow-twitch wtSOD1 muscle cultures (p=0.383). A different trend was seen when examining wtSOD1 and mSOD1 fast-twitch muscle cultures (Fig.6.5). Glucose-deprived wtSOD1 fast-twitch muscle cultures released 33.9% (±5.9 SEM; n=4) of the maximal response. This was significantly more than untreated wtSOD1 fast-twitch muscle cultures (p=0.009), but not treated wtSOD1 slow-twitch muscle cultures (p=0.899). Glucose-deprived mSOD1 fast-twitch muscle cultures released 81.8% LDH (±7.1 SEM; n=4) of the maximal response, which was significantly more than treated, wtSOD1 fast-twitch muscle cultures (p=0.003), as well as treated mSOD1 slow-twitch muscle cultures (p<0.001).

6.3.7 The effect of mSOD1 muscle-conditioned media on neuronal survival

In order to examine whether mSOD1 muscle is able to support motoneuron health, the effect of muscle-conditioned media (MCM) from WT, wtSOD1 and mSOD1 muscle cultures on the survival of neuronal cells was examined using SH-SY5Y cells. Prior to incubation with SH-SY5Y cells, LDH levels in the supernatant from WT, wtSOD1 and mSOD1 muscle cultures were examined. This indicated there was no significant difference in LDH release in the media from WT, wtSOD1 and mSOD1 muscle cultures under basal conditions (see Fig.6.1). LDH levels from SH-SY5Y cultures that were exposed to WT, wtSOD1 and mSOD1 MCM were normalised against protein levels and then represented as a percentage of the maximum LDH release achievable, which was given the value 100% (Fig.6.6). Incubating SH-5YSY cells with MCM taken from WT muscle cultures resulted in the release of LDH levels that were 44.1% (±0.2 SEM; n=4) of maximal levels. SH-5YSY cells incubated with MCM from wtSOD1 muscle cultures released slightly more LDH into the media ($p<0.01$), so that LDH levels were 51.46% LDH (±0.2 SEM; n=4) of the maximal LDH response, compared to WT. SH-5YSY cells incubated with media from mSOD1 muscle cultures released even more LDH, and levels reached 88.9% LDH (±0.4 SEM; n=3; $p<0.001$) of the maximal response, compared to cultures exposed to wtSOD1 (see Fig.6.6).

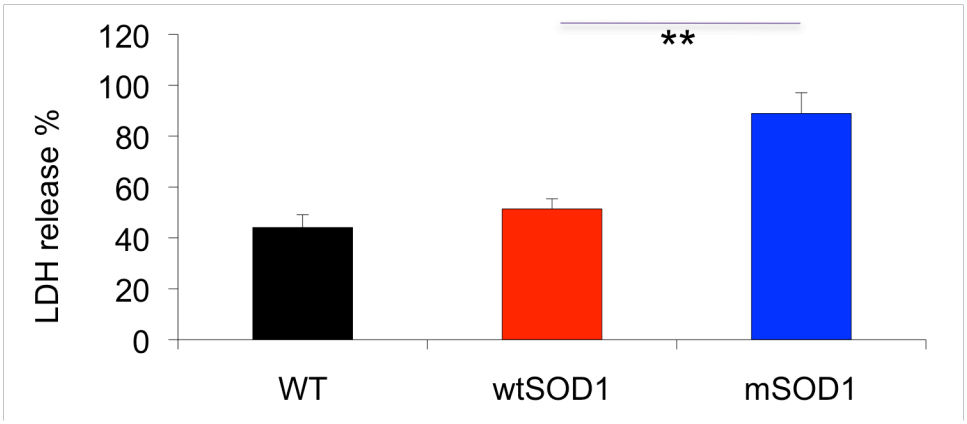

Figure 6.6: SH-SY5Y cell viability in muscle-conditioned media

The bar chart shows the percentage of LDH release from SH-SY5Y following incubation over 72 hours with muscle-conditioned media from WT, wtSOD1 and mSOD1 mixed hindlimb muscle cultures. All values were normalised against minimal values and then represented as a percentage of the maximal LDH reading, which was given the value 100%.

**=p≤0.01; n=4; error bars= ± standard error of the mean

6.4 Discussion

In this Chapter, I examined the effect of various cellular stresses on muscle cell survival in WT, wtSOD1 and mSOD1 primary muscle cultures. This study revealed that mSOD1 muscle cultures were more vulnerable to glucose deprivation than WT and wtSOD1 muscle cultures. Interestingly, exposure to 5mM but not 1mM caffeine increased cell death in mSOD1 cultures. Likewise, exposure to 5mM but not 1mM caffeine in a combined stress model was sufficient to significantly increase cell death. Examination of cytotoxicity in specific fast and slow-twitch primary muscle cultures revealed that fast-twitch muscle cultures were more vulnerable to cell stress than slow-twitch muscle, even in cultures derived from WT mice. Additionally, mSOD1 expression rendered fast-twitch muscle cultures even more vulnerable to glucose deprivation and caffeine stress. Finally, treatment of neuronal cells with MCM from muscle cultures showed that factors released by myotubes that express mSOD1 are detrimental to neuronal survival, indicating the possible presence of a toxic factor in mSOD1 MCM.

6.4.1 mSOD1 mixed muscle cultures are more vulnerable to cell death

This Chapter investigated the effects of three physiologically relevant stresses had on cell survival in the primary muscle cultures. Glucose deprivation resulted in a modest level of cell death in WT and wtSOD1 muscle cultures, but mSOD1 cultures were significantly more sensitive to glucose deprivation. WT, wtSOD1 and mSOD1 muscle cultures were highly resistant to low levels of caffeine stress, resulting in negligible levels of cell death. However, at higher caffeine concentrations, mSOD1 mixed muscle cultures showed significant level of cell death.

A similar pattern of vulnerability was seen in cultures exposed to a combined stress, which caused even greater levels of cell death. mSOD1 muscle cultures exposed to the combined caffeine and glucose deprivation stress demonstrated a

modest increase in cell death (10%) compared to a caffeine stress (7%), and, this did not reach significance (p=0.228).

Previous, studies aimed at examining the role of muscle in ALS have not extensively examined the effect of physiologically relevant stress. Moreover, those few studies that have investigated the role of physiological stress in ALS pathogenesis in muscle have examined innervated muscle *in vivo* where it is difficult to isolate the origin of dysfunction. Exercise, such as regular treadmill running, has been shown to be beneficial to survival in mSOD1 mice (Kirkinezos et al., 2003). However, the results presented here show that high levels of caffeine, indicative of greater contractile and oxidative stress, are selectively detrimental to mSOD1 muscle, although lower concentrations are not. This suggests that there is a trigger point at which contractile stress, and the associated oxidative stress, overwhelms the muscle and become deleterious.

Furthermore, Dupuis et al. (2009) have shown that increased ROS, a marker for oxidative stress, can trigger the dismantling of the NMJ. It is therefore possible that low levels of contractile stress may be beneficial for muscle function, while high levels of contractile stress, which generate high levels of ROS, facilitates the compromise of the NMJ in mSOD1 muscle.

The results presented in Chapter 3 and 4 have shown that fast and slow-twitch muscle such as the TA and the soleus muscles are differentially affected by mSOD1 pathology, with fast-twitch muscles displaying greater denervation, hsp expression and greater nNOS dysfunction. The results presented in Chapter have shown that mSOD1 muscle is intrinsically more vulnerable to glucose deprivation than WT muscle. Glucose homeostasis has been examined previously in ALS patients before (Pradat et al., 2009). The results showed that blood glucose in ALS patients was significantly higher than controls. Furthermore, the patients with

impaired glucose tolerance were more likely to have elevated free fatty acids, a marker of metabolic dysfunction. However, an examination of glucose metabolism in muscles of ALS patients or mSOD1 mice has not been previously undertaken. Thus, dysfunction in glucose homeostasis in muscle may possibly contribute to the general glucose homeostasis dysfunction that was demonstrated in ALS patients by Pradat et al. (2009).

The results of this Chapter also show that mSOD1 fast-twitch muscle cultures are preferentially vulnerable to glucose deprivation compared to wtSOD1 fast-twitch muscle cultures. This finding directly supports Dupuis et al. (2004b), which demonstrated that skeletal muscle hypermetabolism is present in mSOD1 mice and that a highly energetic diet extended survival by 20% in these mice (Dupuis et al., 2004). This suggests that metabolic dysfunction may well be a strong contributing factor to neuromuscular dysfunction in mSOD1 mice. Furthermore, as fast-twitch muscle cultures were preferentially vulnerable to glucose deprivation in all genotypes, it is possible that fast-twitch muscle is fundamentally more vulnerable to metabolic dysfunction. In light of research from Dupuis et al. (2004) this vulnerability is likely to contribute to the preferential denervation of fast-twitch muscles in ALS.

6.4.2 mSOD1 muscle-conditioned media induces cell death in neuronal cells

In order to examine whether muscle may play a directly deleterious role in motoneuron function in ALS, in this Chapter I examined the effect of treatment of neuronal cells with media collected from primary muscle cultures established from wtSOD1 and mSOD1 mice. Previous findings using a similar approach have clearly demonstrated that incubation of motoneurons with media from primary mSOD1 astrocytes has toxic effects on motoneurons (Nagai et al., 2007). Using SH-SY5Y neuronal cells in this Chapter I also found that factors released from mixed mSOD1 muscle cultures were sufficient to induce significantly higher levels of cell death in

SH-5YSY cells compared to wtSOD1 and WT cultures. This is clear evidence of the deleterious effect that mSOD1 expression in muscle cells has on neuron survival, supporting the findings Dobrowolny et al. (2008) and Wong and Martin (2010) who demonstrated that the expression of mSOD1 in muscle was sufficient to reduce neuron survival and thus confer cell-to-cell toxicity.

Although the muscle conditioned media did not undergo proteomic analysis, it is of interest to note that it has been shown that the release of mSOD1 from neuron like cells *in vitro* via exosomes, results in increase significant pathology, including cytoplasmic inclusions and protein insolubility that correlated with toxicity (Gomes et al., 2007). Similarly, in the CNS mSOD1 release from microglia has been found to induce the morphological and functional activation of microglia, via toll-like receptors (TLR) 2 and TLR4; thus, increasing their release of pro-inflammatory cytokines and free radicals (Henkel et al., 2009; Zhao et al., 2010). While mSOD1 release from muscles and a similar inflammatory response has yet to be examined, it is possible that a similar pathway exists mediating this cell-to-cell toxicity.

6.4.3 Conclusion

ALS is understood to be a non-cell autonomous disease, with microglia and astroglia playing a pivotal role in the onset and progression of disease. However, whether muscle also contributes to mSOD1 pathology and ALS has been disputed. While Dobrowolny et al. (2008) and Wong and Martin (2010) suggest that muscle is a primary target of ALS. Miller et al. (2006) have suggested that muscle pathology is merely a consequence of motoneuron pathology. Results from this Chapter support the hypothesis, put forward by Dobrowolny et al. (2008) and Wong and Martin (2010), that muscle does play a role in mSOD1 pathology and ALS, with factors secreted by muscle cells in cultures causing cell death in neurons.

In addition, this Chapter showed that mSOD1 muscle cultures are intrinsically different to WT and wtSOD1 muscle cultures equally, that muscle cultures from fast muscles are also intrinsically different from muscle cultures from slow muscle cultures. Furthermore, these muscle specific differences in muscle cultures are independent of genotype. Thus, aneural fast-twitch muscle cultures, like innervated fast-twitch muscles, are intrinsically more vulnerable to stress than aneural slow-twitch muscle cultures.

Furthermore, mSOD1 expression, even at a presymptomatic stage, is sufficient to exacerbate this intrinsic vulnerability, with fast-twitch muscle more vulnerable to glucose deprivation and caffeine stress. In addition, this study showed that only high concentrations of caffeine (5mM), a contractile and oxidative stress, result in increased cell death in muscle.

Chapter 7 : General discussion

7.1 Introduction

The overall aim of this Thesis has been to study muscle pathology in a mouse model of ALS by characterising the appearance and progression of ALS pathology in hindlimb muscles of the SOD1G93A mouse model of ALS. This characterisation was undertaken in muscles with either a predominantly fast or slow-twitch phenotype, since previous results have suggested that these different muscle types have a differential vulnerability to disease (Frey et al., 2000). Furthermore, I also tested whether the apparent greater vulnerability of fast-twitch muscles to stress observed in ALS was an intrinsic feature of this muscle fibre type that was not acquired as a result of aging or in disease and that if fast-twitch muscles have an intrinsically poor stress response to disease. In addition, I examined whether the pharmacological manipulation of the HSR, reduced muscle and NMJ pathology in mSOD1 mice. In doing so, I aimed to establish if the previously reported cytoprotective actions of Arimoclomol are limited to the CNS, or whether it may also act in skeletal muscles.

7.2 Fast-twitch muscle in mSOD1 mice is preferentially vulnerable to changes in neuromuscular transmission and denervation.

In Chapter 3, I established that in mSOD1 mice there is significant NMJ pathology, with evidence of denervation, sprouting and PNI in skeletal muscles, even during early stages of disease. Both denervation and sprouting occur prior to symptom onset in the more vulnerable EDL muscle and to a greater degree than in slow-twitch soleus muscles. Indeed, denervation and sprouting only reached significance at a late stage of disease (120 days) in the slow-twitch soleus muscle.

Compensatory nerve terminal sprouting in the fast-twitch EDL muscle peaked 75 days but quickly declined thereafter. Likewise, the level of PNI, which was significant at 45 days and 75 days in EDL muscles of mSOD1 mice, declined rapidly as disease progressed.

In the EDL muscle, denervation was accompanied by a significant decrease in endplate size, which took place before disease onset, but did not decrease with denervation. This was not the case in the soleus muscle. The mean endplate size in the soleus muscle from WT mice was similar to that seen in EDL muscle from WT mice. However, endplate size in the soleus of mSOD1 mice remained similar to wildtype throughout the course of disease, regardless of the level of denervation. This finding indicates that unlike in nerve injury models, endplate size in ALS is dependant on more factors than just denervation.

ChAT activity is known to decrease with age (Tucek and Gutmann, 1973) and following denervation (Tucek, 1973). Examination of the activity of enzymes associated with neurotransmission revealed that in mSOD1 mice, ChAT activity falls by almost one third over the course of the disease, in all muscles examined. In contrast, AChE activity is differentially affected in fast and slow-twitch muscles in mSOD1 mice. In the fast-twitch TA and EDL muscles AChE levels fell by 20-30% over the course of the disease compared to WT, while in the slow-twitch soleus muscle, AChE levels fell by approximately 50% over the course of disease, compared to WT. This differential decline in AChE activity would result in a different ChAT: AChE activity ratio in fast and slow-twitch muscles, with a greater ChAT: AChE ratio in the slow-twitch soleus and thus a relative increase in ChAT production in the soleus muscle. While the direct implication of these changes is unknown, it is of interest to note that a similar phenomenon is seen in the neuromuscular disease myasthenia gravis, and is considered to be a compensatory mechanism that ensures sufficient neuromuscular transmission (Molenaar et al., 1981). Thus, it is possible that this relative increase in ChAT activity in the soleus is also compensatory action to strengthen the synapse and promote muscle function, which may in the long-term, contribute to its relative resistance to disease in ALS.

7.3 A Peak in muscle hsp expression coincides with disease onset in mSOD1 mice.

The results presented in Chapter 4 revealed that in mSOD1 mice, levels of hsp90, hsp72 and hsp25 peak at symptom onset in fast-twitch muscles. This is the stage when muscle atrophy, denervation and nerve-terminal sprouting are significant. From this stage onwards, hsp levels in fast-twitch muscles decline rapidly to basal levels.

As hsp25 and hsp90 expression has been shown to promote neurite development *in vitro*, it is possible that increased hsp90 and hsp25 expression in the muscle during the period in which muscle fibres begin to loose their innervation may promote compensatory mechanism such as sprouting in mSOD1 fast-twitch muscle. Furthermore, hsp72 expression, which has been shown to increase synaptic efficacy, may increased help to maximise synaptic function in the particularly vulnerable fast-twitch muscles in mSOD1 mice at the time when synaptic connection become weak and vulnerable.

7.4 Fast-twitch muscles in mSOD1 mice have a reduced HSR, which is upregulated by treatment with Arimoclomol.

Although both fast and slow-twitch muscles mount a HSR in mSOD1 mice at symptom onset, the HSR in the TA muscle was relatively short-lived. In contrast, in slow-twitch muscles such as soleus, the increase in hsp expression was maintained throughout disease progression in mSOD1 mice. This finding suggests that fast-twitch muscles are intrinsically less able to respond to cellular stress by upregulation of cytoprotective proteins, such as hsps. This poor stress response may contribute to their greater vulnerability in ALS.

7.5 Fast-twitch muscles in mSOD1 mice display greater nNOS dysfunction than slow-twitch muscle.

Examination of the NOS response in hindlimb muscles of mSOD1 mice at various stages of disease progression revealed that despite clear evidence of neuroinflammation in the CNS (Conti et al., 2007), iNOS levels were low in skeletal muscles of mSOD1 mice. Thus, it is unlikely that iNOS plays an important role in muscle pathology in mSOD1 mice.

However, in mSOD1 mice, nNOS, a hsp90-mediated signalling protein (Peng et al., 2009), was found to translocate from the sarcolemma to the sarcoplasm, a phenomenon associated with muscle atrophy (Suzuki et al., 2010). Within the sarcoplasm, nNOS expression was colocalised with hsp90, but only in fast-twitch muscle of mSOD1 mice. Recently, Peng et al. (2009) demonstrated a clear relationship between hsp90 and nNOS. nNOS requires calmodulin in order to catalyse the production of NO and this is enhanced by the presence of hsp90, which inhibits the CHIP-dependent ubiquitination of nNOS (Peng et al., 2009). As nNOS undergoes toxic damage, hsp90 is thought to be unable to bind, enabling hsp70 mediated nNOS degradation. In mSOD1 TA muscle, the increased hsp90/nNOS colocalisation in the sarcoplasm indicates that the quality control machinery may be dysfunctional. This would result in increased nNOS activity in the sarcoplasm, and greater muscle atrophy.

7.6 Fast-twitch muscles in mSOD1 mice are intrinsically more vulnerable to cell stress than slow-twitch muscles.

In Chapter 6, the effect of various cellular stressors on the response of mSOD1 muscle cells in culture was examined. The results showed that mSOD1 muscle cultures were more vulnerable to 5mM caffeine than glucose deprivation. These results indicated that the contractile and oxidative stress were more cytotoxic to the mSOD1 muscle than 24hrs without media.

The effect of glucose deprivation was then examined in fast-twitch muscle cultures, which were shown to be more vulnerable to glucose deprivation than slow-twitch muscles. Indeed, slow-twitch muscle cultures were surprisingly resistant to glucose deprivation. However, as analysis of muscle from cultures has revealed an intrinsic difference in the level of differentiation in mSOD1 cultures it is possible that such factors may also be apparent in cultures from fast and slow muscle cultures (Appendix 3, Fig. 10.3). These results also suggest that there maybe an intrinsic differential energy metabolism in fast and slow-twitch muscles, which may influence the vulnerability of these muscles to disease in ALS.

Fast and slow-twitch muscles have different metabolic demands. In general, slow-twitch muscle tends to have a dense vascular network enabling the rapid delivery of nutrients and high glycogen levels. In comparison, fast-twitch muscles tend to have less dense vascularisation and a greater dependency on anaerobic respiration, metabolising fatty acids in preference to glycogen. Thus, it is therefore possible that mSOD1 fast-twitch muscle, which has a greater dependence on glycolytic pathways, is less able to respond and cope under conditions of metabolic stress than slow-twitch muscle. Interestingly, Dupuis et al. (2008) have found that ALS patients exhibit abnormal glucose tolerance, and that muscle from ALS patients demonstrates hypermetabolism (Gonzalez de Aguilar et al., 2005).

Furthermore, these authors reported a causal link between a muscle-restricted metabolic defect and the ensuing oxidative stress and denervation (Dupuis et al., 2009, Jang et al., 2010). Supporting these findings, the results presented in Chapter 4 suggest that this impaired energy metabolism may be selective to fast-twitch muscles. It has been suggested that this metabolic dysfunction was sufficient to induce motoneuron death (Dupuis, 2009). In support of this possibility, the results penetrated in Chapter 6 shows that incubation in mSOD1 muscle-conditioned medium can induce degeneration of neuronal cells, suggesting the presence of a toxic factor in muscle-conditioned media obtained from mSOD1 muscles in culture this toxic factor may be the result of altered micro RNA (miRNA)

activity as it has been shown that, a skeletal muscle-specific miRNA (miRNA-206), is up-regulated on the onset of neurological symptoms in mSOD1 mice. Furthermore, it has been suggested that miR-206 is needed to form new NMJs ones after denervation. Equally, as exosomes may mediate muscle- motoneuron toxicity via mSOD1 secretion. It is also possible that other toxic factors are released via the exosome.

The finding that incubation in mSOD1 muscle conditioned medium is sufficient to induce the death of neuronal cells adds further support to the hypothesis that mSOD1 pathology and ALS is a non-cell autonomous disease (Bruijn et al., 2004). Indeed, it is now widely accepted that glial cells in the CNS are not only involved in the normal maintenance and function of motoneurons (Clement et al., 2003), but under disease conditions glial cells play an important role in determining disease progression. Microglia have been shown to heavily influence disease onset (Bruijn et al., 2004) and astroglial reactivity influences disease duration (Bruijn et al., 2004). Equally, it is possible that muscle cells release exosomes that have deleterious effects on motoneurons. However, whether muscle, which interacts with motoneurons in the periphery, also plays a role in ALS and mSOD1 pathology is remains controversial.

Miller et al., (2006) found little evidence of a causal role for muscle using viral delivery of transcription-mediated siRNA to suppress mSOD1 expression in muscle. They found that the reduction of mSOD1 in muscle was not sufficient to alter a decline in grip strength, disease onset or duration. However, Dobrowolny et al. (2008) and Wong & Martin (2010) found that muscle-restricted transgenic expression of mSOD1 resulted in significant pathology in the muscle as well as motoneuron pathology and death. While these findings may appear contradictory it is possible that siRNA-mediated suppression of mSOD1 expression was not complete in the Miller et al. (2006) study.

Thus, one can conclude that the findings presented in this Thesis suggest that, as observed in the CNS, non-neuronal cells do play an important role in influencing disease progression in ALS, and that expression of mSOD1 in skeletal muscles in the periphery influences motoneuron function, which in turn is likely to influence motoneuron survival.

7.6.1 Effects of treatment with Arimoclomol on muscle pathology in mSOD1 mice.

Treatment of mSOD1 mice with Arimoclomol results in a significant delay in denervation. This improvement in the level of innervation was observed from the time of symptom onset and the level of innervation was maintained throughout disease progression. Arimoclomol also increased the level of sprouting in the fast-twitch EDL muscle, contributing to the maintenance of innervation observed in these muscles; this beneficial effect reached significance at a late stage as sprouting began to fall in untreated mSOD1 mice.

Treatment with Arimoclomol also increased sprouting in the slow-twitch soleus muscle, however, this increase was modest and did not reach significance. The levels of cellular stress and the necessity for compensatory sprouting are likely to be very low, may explain the relatively modest level of sprouting observed in soleus muscle, even following treatment with Arimoclomol. Arimoclomol had a limited effect on PNI in mSOD1 muscle, although the level of PNI did increase in the muscles of Arimoclomol treated mSOD1 mice, this only reached significance at a late stage of disease (120 days of age), when approximately 15% of endplates are innervated by more than one nerve terminal.

This study revealed that Arimoclomol exerted a modest effect on ChAT and AChE activity in both fast and slow-twitch muscles. In the TA and EDL muscles from

treated mice, ChAT and AChE activity was significantly increased before and at symptom onset (75 days).

Treatment with Arimoclomol resulted in a significant increase in hsp90, hsp72 and hsp25 expression in hindlimb muscles of mSOD1 mice. This was most apparent in the fast, comparatively vulnerable TA muscle, which otherwise mounted a limited HSR in untreated mSOD1 mice. Treatment with Arimoclomol was sufficient to reduce sarcoplasmic levels of nNOS in mSOD1 mice, with less hsp90/nNOS colocalisation in the sarcoplasm. This was most apparent in the more vulnerable fast-twitch TA muscle. As nNOS usually oscillates between hsp90 and hsp70 associations (Peng et al., 2009), it is possible that this decline in hsp90/nNOS colocalisation is the result of increased hsp70-mediated ubiquitination and degradation of sarcoplasmic nNOS (Peng et al., 2009). This could potentially downregulate the FOXO/atrogin-1 pathway, thus subsequently reducing denervation induced muscle atrophy (Suzuki et al., 2007b, Suzuki et al., 2010). While atrogin-1 expression was not examined in this Thesis it would be interesting to examine atrogin-1 expression in future work.

Although Arimoclomol decreased sarcoplasmic nNOS, it increased overall nNOS levels, notably at the NMJ. It had been previously reported, nNOS is essential for terminal Schwann Cell (tSCh) reactivity, which are required for various types of sprouting (Ribera et al., 1998, Pereira et al., 2001). Therefore, nNOS expression at the NMJ may be beneficial for compensatory sprouting and thus, the reinnervation of denervated endplates.

It is of interest to note that Kieran et al (2004) reported that treatment with Arimoclomol reduced muscle atrophy, and in Chapter 3, I found that treatment with Arimoclomol increases sprouting in mSOD1 muscle. Together, these findings suggest that nNOS is likely to contribute to muscle pathology in mSOD1 mice.

Furthermore, as treatment with Arimoclomol is sufficient to alter nNOS expression it may contribute to Arimoclomol's beneficial effects at the NMJ in mSOD1 mice.

7.7 Conclusion

The results presented in the Thesis demonstrate that skeletal muscles are affected early in disease in mSOD1 mice, before symptom onset and motoneuron death occurs. Furthermore, my results indicate that fast-twitch muscles are affected earlier and to a greater extent than slow-twitch muscles in mSOD1 mice and that this is due, at least in part, to an intrinsic difference in their ability to mount a stress response. Thus, fast-twitch muscles, which are intrinsically more vulnerable to cellular stress and are particularly affected in ALS, have a reduced ability to mount a significant HSR as well as a greater susceptibility to nNOS signalling dysfunction and metabolic dysfunction than slow-twitch muscles. These factors are likely to result in increased oxidative stress in fast-twitch muscles, decreased oxidative tolerance and destabilisation of the NMJ (Dupuis, 2009).

Together these results indicate that at least some of the previously reported beneficial effects of Arimoclomol (Kieran et al., 2004) are due, to Arimoclomol's actions in the periphery. Furthermore, these findings suggest that targeting pathology in the muscle and CNS is likely to be a successful therapeutic approach.

In conclusion, the data presented in this Thesis demonstrates that fast-twitch muscles are intrinsically more vulnerable to cell stress and this contributes to its increased vulnerability to cell stress such as denervation and oxidative stress in mSOD1 mice. Moreover, increasing the ability of muscles to respond to cellular stress by treatment of mSOD1 mice with Arimoclomol, results in a reduction in muscle pathology. Therefore, in mSOD1 mice, Arimoclomol clearly targets pathology both in the periphery in skeletal muscles, as well as centrally within glia and motoneurons, as previously shown (Kieran et al, 2004; Kalmar et al, 2009). Together with the data presented in this Thesis, these results support the proposal

that the targeting of pathological changes in skeletal muscles may be a successful approach to take, in combination with strategies that target pathology within the CNS, in ALS.

Chapter 8 : Bibliography

ABE, K., FUJIMURA, H., KOBAYASHI, Y., FUJITA, N. & YANAGIHARA, T. (1997a) Degeneration of the pyramidal tracts in patients with amyotrophic lateral sclerosis. A premortem and postmortem magnetic resonance imaging study. *J Neuroimaging,* 7**,** 208-12.

ABE, K., PAN, L. H., WATANABE, M., KONNO, H., KATO, T. & ITOYAMA, Y. (1997b) Upregulation of protein-tyrosine nitration in the anterior horn cells of amyotrophic lateral sclerosis. *Neurol Res,* 19**,** 124-8.

ABRUZZO, P. M., DI TULLIO, S., MARCHIONNI, C., BELIA, S., FANO, G., ZAMPIERI, S., CARRARO, U., KERN, H., SGARBI, G., LENAZ, G. & MARINI, M. (2010) Oxidative stress in the denervated muscle. *Free Radic Res,* 44**,** 563-76.

ADACHI, H., KATSUNO, M., MINAMIYAMA, M., SANG, C., PAGOULATOS, G., ANGELIDIS, C., KUSAKABE, M., YOSHIKI, A., KOBAYASHI, Y., DOYU, M. & SOBUE, G. (2003) Heat shock protein 70 chaperone overexpression ameliorates phenotypes of the spinal and bulbar muscular atrophy transgenic mouse model by reducing nuclear-localized mutant androgen receptor protein. *J Neurosci,* 23**,** 2203-11.

ADACHI, H., WAZA, M., TOKUI, K., KATSUNO, M., MINAMIYAMA, M., TANAKA, F., DOYU, M. & SOBUE, G. (2007) CHIP overexpression reduces mutant androgen receptor protein and ameliorates phenotypes of the spinal and bulbar muscular atrophy transgenic mouse model. *J Neurosci,* 27**,** 5115-26.

ADAMS, M. E., TESCH, Y., PERCIVAL, J. M., ALBRECHT, D. E., CONHAIM, J. I., ANDERSON, K. & FROEHNER, S. C. (2008) Differential targeting of nNOS and AQP4 to dystrophin-deficient sarcolemma by membrane-directed alpha-dystrobrevin. *J Cell Sci,* 121**,** 48-54.

ADHIKARI, A. S., SRIDHAR RAO, K., RANGARAJ, N., PARNAIK, V. K. & MOHAN RAO, C. (2004) Heat stress-induced localization of small heat shock proteins in mouse myoblasts: intranuclear lamin A/C speckles as target for alphaB-crystallin and Hsp25. *Exp Cell Res,* 299**,** 393-403.

AGUSTI, A., MORLA, M., SAULEDA, J., SAUS, C. & BUSQUETS, X. (2004) NF-kappaB activation and iNOS upregulation in skeletal muscle of patients with COPD and low body weight. *Thorax,* 59**,** 483-7.

AITMAN, T. J., HUDLICKA, O. & TYLER, K. R. (1979) Long-term effects of tetanic stimulation on blood flow, metabolism and performance of fast skeletal muscle [proceedings]. *J Physiol,* 295**,** 36P-37P.

ALBUQUERQUE, E. X. & MCISAAC, R. J. (1970) Fast and slow mammalian muscles after denervation. *Experimental Neurology,* 26**,** 183-202.

ALI, A., BHARADWAJ, S., O'CARROLL, R. & OVSENEK, N. (1998) HSP90 interacts with and regulates the activity of heat shock factor 1 in Xenopus oocytes. *Mol Cell Biol,* 18**,** 4949-60.

ALLISON, A. C., CACABELOS, R., LOMBARDI, V. R., ALVAREZ, X. A. & VIGO, C. (2001) Celastrol, a potent antioxidant and anti-inflammatory drug, as a possible treatment for Alzheimer's disease. *Prog Neuropsychopharmacol Biol Psychiatry,* 25**,** 1341-57.

AMATO, A. A. & BAROHN, R. J. (2009) Inclusion body myositis: old and new concepts. *J Neurol Neurosurg Psychiatry,* 80**,** 1186-93.

AMPHLETT, G. W., PERRY, S. V., SYSKA, H., BROWN, M. D. & VRBOVA, G. (1975) Cross innervation and the regulatory protein system of rabbit soleus muscle. *Nature,* 257**,** 602-4.

ANDERSON, M. J., COHEN, M. W. & ZORYCHTA, E. (1977) Effects of innervation on the distribution of acetylcholine receptors on cultured muscle cells. *J Physiol,* 268**,** 731-56.

ARRASATE, M., MITRA, S., SCHWEITZER, E. S., SEGAL, M. R. & FINKBEINER, S. (2004) Inclusion body formation reduces levels of mutant huntingtin and the risk of neuronal death. *Nature,* 431**,** 805-10.

ASEA, A. (2007) Hsp72 release: mechanisms and methodologies. *Methods,* 43**,** 194-8.

ASKANAS, V., ENGEL, W. K. & NOGALSKA, A. (2009) Inclusion body myositis: a degenerative muscle disease associated with intra-muscle fiber multi-protein aggregates, proteasome inhibition, endoplasmic reticulum stress and decreased lysosomal degradation. *Brain Pathol,* 19**,** 493-506.

ASTROW, S. H., QIANG, H. & KO, C. P. (1998) Perisynaptic Schwann cells at neuromuscular junctions revealed by a novel monoclonal antibody. *J Neurocytol,* 27**,** 667-81.

ATES, K., YANG, S. Y., ORRELL, R. W., SINANAN, A. C., SIMONS, P., SOLOMON, A., BEECH, S., GOLDSPINK, G. & LEWIS, M. P. (2007) The IGF-I splice variant MGF increases progenitor cells in ALS, dystrophic, and normal muscle. *FEBS Lett,* 581**,** 2727-32.

ATKIN, J. D., SCOTT, R. L., WEST, J. M., LOPES, E., QUAH, A. K. & CHEEMA, S. S. (2005) Properties of slow- and fast-twitch muscle fibres in a mouse model of amyotrophic lateral sclerosis. *Neuromuscul Disord,* 15**,** 377-88.

AULD, D. S. & ROBITAILLE, R. (2003) Perisynaptic Schwann cells at the neuromuscular junction: nerve- and activity-dependent contributions to synaptic efficacy, plasticity, and reinnervation. *Neuroscientist,* 9**,** 144-57.

BAKER, M. S. & AUSTIN, L. (1989) The pathological damage in duchenne muscular dystrophy may be due to increased intracellular oxy-radical generation caused by the absence of dystrophin and subsequent alterations in Ca2+ metabolism. *Medical Hypotheses,* 29**,** 187-193.

BALDELLI, S., AQUILANO, K., ROTILIO, G. & CIRIOLO, M. R. (2008) Glutathione and copper, zinc superoxide dismutase are modulated by overexpression of neuronal nitric oxide synthase. *The International Journal of Biochemistry & Cell Biology,* 40**,** 2660-2670.

BARBER, S. C., MEAD, R. J. & SHAW, P. J. (2006) Oxidative stress in ALS: a mechanism of neurodegeneration and a therapeutic target. *Biochim Biophys Acta,* 1762**,** 1051-67.

BARON, P., GALIMBERTI, D., MEDA, L., PRAT, E., SCARPINI, E., CONTI, G., MOGGIO, M., PRELLE, A. & SCARLATO, G. (2000) Synergistic effect of beta-amyloid protein and interferon gamma on nitric oxide production by C2C12 muscle cells. *Brain,* 123 (Pt 2)**,** 374-9.

BENSIMON, G., LACOMBLEZ, L. & MEININGER, V. (1994) A controlled trial of riluzole in amyotrophic lateral sclerosis. ALS/Riluzole Study Group. *N Engl J Med,* 330**,** 585-91.

BENTO-ABREU, A., VAN DAMME, P., VAN DEN BOSCH, L. & ROBBERECHT, W. (2008) The neurobiology of amyotrophic lateral sclerosis. *Eur J Neurosci,* 31**,** 2247-65.

BERRIDGE, M. J. (1997) The 1996 Massry Prize. Inositol trisphosphate and calcium: two interacting second messengers. *Am J Nephrol,* 17**,** 1-11.
BLOTTNER, D. & LUCK, G. (2001) Just in time and place: NOS/NO system assembly in neuromuscular junction formation. *Microsc Res Tech,* 55**,** 171-80.
BODINE, S. C., STITT, T. N., GONZALEZ, M., KLINE, W. O., STOVER, G. L., BAUERLEIN, R., ZLOTCHENKO, E., SCRIMGEOUR, A., LAWRENCE, J. C., GLASS, D. J. & YANCOPOULOS, G. D. (2001) Akt/mTOR pathway is a crucial regulator of skeletal muscle hypertrophy and can prevent muscle atrophy in vivo. *Nat Cell Biol,* 3**,** 1014-9.
BOILLEE, S., VANDE VELDE, C. & CLEVELAND, D. W. (2006) ALS: a disease of motor neurons and their nonneuronal neighbors. *Neuron,* 52**,** 39-59.
BONAVENTURA, J. & GOW, A. (2004) NO and superoxide: opposite ends of the seesaw in cardiac contractility. *Proc Natl Acad Sci U S A,* 101**,** 16403-4.
BORCHELT, D. R., LEE, M. K., SLUNT, H. S., GUARNIERI, M., XU, Z. S., WONG, P. C., BROWN, R. H., JR., PRICE, D. L., SISODIA, S. S. & CLEVELAND, D. W. (1994) Superoxide dismutase 1 with mutations linked to familial amyotrophic lateral sclerosis possesses significant activity. *Proc Natl Acad Sci U S A,* 91**,** 8292-6.
BORNFELDT, K. E. (2000) Stressing Rac, Ras, and downstream heat shock protein 70. *Circ Res,* 86**,** 1101-3.
BORNMAN, L., POLLA, B. S., LOTZ, B. P. & GERICKE, G. S. (1995) Expression of heat-shock/stress proteins in Duchenne muscular dystrophy. *Muscle Nerve,* 18**,** 23-31.
BOUCHENTOUF, M., BENABDALLAH, B. F. & TREMBLAY, J. P. (2004) Myoblast Survival Enhancement and Transplantation Success Improvement By Heat-Shock Treatment in Mdx Mice. *Transplantation,* 77**,** 1349-1356.
BREDT, D. S. (1998) NO skeletal muscle derived relaxing factor in Duchenne muscular dystrophy. *Proc Natl Acad Sci U S A,* 95**,** 14592-3.
BROOME, C. S., KAYANI, A. C., PALOMERO, J., DILLMANN, W. H., MESTRIL, R., JACKSON, M. J. & MCARDLE, A. (2006) Effect of lifelong overexpression of HSP70 in skeletal muscle on age-related oxidative stress and adaptation after nondamaging contractile activity. *FASEB J,* 20**,** 1549-51.
BROWN, D. D., CHRISTINE, K. S., SHOWELL, C. & CONLON, F. L. (2007) Small heat shock protein Hsp27 is required for proper heart tube formation. *Genesis,* 45**,** 667-78.
BROWN, I. R. (2007) Heat shock proteins and protection of the nervous system. *Ann N Y Acad Sci,* 1113**,** 147-58.
BROWN, M. C., HOLLAND, R. L. & HOPKINS, W. G. (1981) Motor nerve sprouting. *Annu Rev Neurosci,* 4**,** 17-42.
BROWN, M. C., HOLLAND, R. L. & IRONTON, R. (1980) Nodal and terminal sprouting from motor nerves in fast and slow muscles of the mouse. *J Physiol,* 306**,** 493-510.
BROWNE, S. E., BOWLING, A. C., BAIK, M. J., GURNEY, M., BROWN, R. H., JR. & BEAL, M. F. (1998) Metabolic dysfunction in familial, but not sporadic, amyotrophic lateral sclerosis. *J Neurochem,* 71**,** 281-7.

BRUIJN, L. I. & CLEVELAND, D. W. (1996) Mechanisms of selective motor neuron death in ALS: insights from transgenic mouse models of motor neuron disease. *Neuropathol Appl Neurobiol,* 22**,** 373-87.

BRUIJN, L. I. & CUDKOWICZ, M. (2006) Therapeutic targets for amyotrophic lateral sclerosis: current treatments and prospects for more effective therapies. *Expert Rev Neurother,* 6**,** 417-28.

BRUIJN, L. I., MILLER, T. M. & CLEVELAND, D. W. (2004) Unraveling the mechanisms involved in motor neuron degeneration in ALS. *Annu Rev Neurosci,* 27**,** 723-49.

BRYANTSEV, A. L., LOKTIONOVA, S. A., ILYINSKAYA, O. P., TARARAK, E. M., KAMPINGA, H. H. & KABAKOV, A. E. (2002) Distribution, phosphorylation, and activities of Hsp25 in heat-stressed H9c2 myoblasts: a functional link to cytoprotection. *Cell Stress Chaperones,* 7**,** 146-55.

BRYLA, K. & KARASINSKI, J. (2001) Diversity of myosin heavy chain expression in satellite cells from mouse soleus and EDL muscles. *Folia Histochem Cytobiol,* 39**,** 295-300.

BUCHANAN, J., SUN, Y. A. & POO, M. M. (1989) Studies of nerve-muscle interactions in Xenopus cell culture: fine structure of early functional contacts. *J Neurosci,* 9**,** 1540-54.

BUFFELLI, M., BURGESS, R. W., FENG, G., LOBE, C. G., LICHTMAN, J. W. & SANES, J. R. (2003) Genetic evidence that relative synaptic efficacy biases the outcome of synaptic competition. *Nature,* 424**,** 430-4.

CARNWATH, J. W. & SHOTTON, D. M. (1987) Muscular dystrophy in the mdx mouse: Histopathology of the soleus and extensor digitorum longus muscles. *Journal of the neurological sciences,* 80**,** 39-54.

CARRIER, H., FLOCARD, F., TAGLIATI, V., ARRIGO, A. P. & GODINOT, C. (2000) Immunolabelling of mitochondrial superoxide dismutase and of Hsp60 in muscles harbouring a respiratory chain deficiency. *Neuromuscul Disord,* 10**,** 144-9.

CHANG, D. M. (2001) Curcumin: a heat shock response inducer and potential cytoprotector. *Crit Care Med,* 29**,** 2231-2.

CHAO, D. S., GOROSPE, J. R., BRENMAN, J. E., RAFAEL, J. A., PETERS, M. F., FROEHNER, S. C., HOFFMAN, E. P., CHAMBERLAIN, J. S. & BREDT, D. S. (1996) Selective loss of sarcolemmal nitric oxide synthase in Becker muscular dystrophy. *J Exp Med,* 184**,** 609-18.

CHEN, K., NORTHINGTON, F. J. & MARTIN, L. J. (2009) Inducible nitric oxide synthase is present in motor neuron mitochondria and Schwann cells and contributes to disease mechanisms in ALS mice. *Brain Struct Funct*.

CHERONI, C., PEVIANI, M., CASCIO, P., DEBIASI, S., MONTI, C. & BENDOTTI, C. (2005) Accumulation of human SOD1 and ubiquitinated deposits in the spinal cord of SOD1G93A mice during motor neuron disease progression correlates with a decrease of proteasome. *Neurobiol Dis,* 18**,** 509-22.

CHU-WANG, I. W. & OPPENHEIM, R. W. (1978) Cell death of motoneurons in the chick embryo spinal cord. I. A light and electron microscopic study of naturally occurring and induced cell loss during development. *J Comp Neurol,* 177**,** 33-57.

CLEMENT, A. M., NGUYEN, M. D., ROBERTS, E. A., GARCIA, M. L., BOILLEE, S., RULE, M., MCMAHON, A. P., DOUCETTE, W., SIWEK, D., FERRANTE, R. J., BROWN, R. H., JR., JULIEN, J. P., GOLDSTEIN, L. S. &

CLEVELAND, D. W. (2003) Wild-type nonneuronal cells extend survival of SOD1 mutant motor neurons in ALS mice. *Science,* 302**,** 113-7.
CLEREN, C., CALINGASAN, N. Y., CHEN, J. & BEAL, M. F. (2005) Celastrol protects against MPTP- and 3-nitropropionic acid-induced neurotoxicity. *J Neurochem,* 94**,** 995-1004.
CLEVELAND, D. W., BRUIJN, L. I., WONG, P. C., MARSZALEK, J. R., VECHIO, J. D., LEE, M. K., XU, X. S., BORCHELT, D. R., SISODIA, S. S. & PRICE, D. L. (1996) Mechanisms of selective motor neuron death in transgenic mouse models of motor neuron disease. *Neurology,* 47**,** S54-61; discussion S61-2.
CLEVELAND, D. W. & ROTHSTEIN, J. D. (2001) From Charcot to Lou Gehrig: deciphering selective motor neuron death in ALS. *Nat Rev Neurosci,* 2**,** 806-19.
CONTI, A., MISCUSI, M., CARDALI, S., GERMANO, A., SUZUKI, H., CUZZOCREA, S. & TOMASELLO, F. (2007) Nitric oxide in the injured spinal cord: synthases cross-talk, oxidative stress and inflammation. *Brain Res Rev,* 54**,** 205-18.
DAI, Z. & PENG, H. B. (1995) Presynaptic differentiation induced in cultured neurons by local application of basic fibroblast growth factor. *J Neurosci,* 15**,** 5466-75.
DAL CANTO, M. C. & GURNEY, M. E. (1994) Development of central nervous system pathology in a murine transgenic model of human amyotrophic lateral sclerosis. *Am J Pathol,* 145**,** 1271-9.
DANGAIN, J. & VRBOVA, G. (1983) Elimination of polyneuronal innervation in a fast muscle of normal and dystrophic mice. *J Physiol,* 342**,** 267-75.
DASTUR, D. K. & RAZZAK, Z. A. (1973) Possible neurogenic factor in muscular dystrophy: its similarity to denervation atrophy. *Journal of Neurology, Neurosurgery & Psychiatry,* 36**,** 399-410.
DAVID, G., NGUYEN, K. & BARRETT, E. F. (2007) Early vulnerability to ischemia/reperfusion injury in motor terminals innervating fast muscles of SOD1-G93A mice. *Exp Neurol,* 204**,** 411-20.
DE LANGE, P., MORENO, M., SILVESTRI, E., LOMBARDI, A., GOGLIA, F. & LANNI, A. (2007) Fuel economy in food-deprived skeletal muscle: signaling pathways and regulatory mechanisms. *FASEB J,* 21**,** 3431-41.
DE PAEPE, B., CREUS, K. K., MARTIN, J. J., WEIS, J. & DE BLEECKER, J. L. (2009) A dual role for HSP90 and HSP70 in the inflammatory myopathies: from muscle fiber protection to active invasion by macrophages. *Ann N Y Acad Sci,* 1173**,** 463-9.
DESCHENES, M. R., WILSON, M. H. & KRAEMER, W. J. (2005) Neuromuscular adaptations to spaceflight are specific to postural muscles. *Muscle Nerve,* 31**,** 468-74.
DIAMOND, I., FRANKLIN, G. M. & MILFAY, D. (1974) The relationship of choline acetyltransferase activity at the neuromuscular junction to changes in muscle mass and function. *J Physiol,* 236**,** 247-57.
DING, L. & CANDIDO, E. P. (2000) HSP25, a small heat shock protein associated with dense bodies and M-lines of body wall muscle in Caenorhabditis elegans. *J Biol Chem,* 275**,** 9510-7.
DOBROWOLNY, G., AUCELLO, M., RIZZUTO, E., BECCAFICO, S., MAMMUCARI, C., BONCOMPAGNI, S., BELIA, S., WANNENES, F.,

NICOLETTI, C., DEL PRETE, Z., ROSENTHAL, N., MOLINARO, M., PROTASI, F., FANO, G., SANDRI, M. & MUSARO, A. (2008) Skeletal muscle is a primary target of SOD1G93A-mediated toxicity. *Cell Metab,* 8**,** 425-36.

DOBROWOLNY, G., GIACINTI, C., PELOSI, L., NICOLETTI, C., WINN, N., BARBERI, L., MOLINARO, M., ROSENTHAL, N. & MUSARO, A. (2005) Muscle expression of a local Igf-1 isoform protects motor neurons in an ALS mouse model. *J Cell Biol,* 168**,** 193-9.

DULHUNTY, A. F., HAARMANN, C. S., GREEN, D., LAVER, D. R., BOARD, P. G. & CASAROTTO, M. G. (2002) Interactions between dihydropyridine receptors and ryanodine receptors in striated muscle. *Prog Biophys Mol Biol,* 79**,** 45-75.

DUPREY, P. & LESENS, C. (1994) Control of skeletal muscle-specific transcription: involvement of paired homeodomain and MADS domain transcription factors. *Int J Dev Biol,* 38**,** 591-604.

DUPUIS, L., CORCIA, P., FERGANI, A., GONZALEZ DE AGUILAR, J. L., BONNEFONT-ROUSSELOT, D., BITTAR, R., SEILHEAN, D., HAUW, J. J., LACOMBLEZ, L., LOEFFLER, J. P. & MEININGER, V. (2008) Dyslipidemia is a protective factor in amyotrophic lateral sclerosis. *Neurology,* 70**,** 1004-9.

DUPUIS, L., DI SCALA, F., RENE, F., DE TAPIA, M., OUDART, H., PRADAT, P. F., MEININGER, V. & LOEFFLER, J. P. (2003) Up-regulation of mitochondrial uncoupling protein 3 reveals an early muscular metabolic defect in amyotrophic lateral sclerosis. *FASEB J,* 17**,** 2091-3.

DUPUIS, L., GONZALEZ DE AGUILAR, J. L., ECHANIZ-LAGUNA, A., ESCHBACH, J., RENE, F., OUDART, H., HALTER, B., HUZE, C., SCHAEFFER, L., BOUILLAUD, F. & LOEFFLER, J. P. (2009) Muscle mitochondrial uncoupling dismantles neuromuscular junction and triggers distal degeneration of motor neurons. *PLoS One,* 4**,** e5390.

DUPUIS, L., GONZALEZ DE AGUILAR, J. L., OUDART, H., DE TAPIA, M., BARBEITO, L. & LOEFFLER, J. P. (2004a) Mitochondria in amyotrophic lateral sclerosis: a trigger and a target. *Neurodegener Dis,* 1**,** 245-54.

DUPUIS, L. & LOEFFLER, J. P. (2009) Neuromuscular junction destruction during amyotrophic lateral sclerosis: insights from transgenic models. *Curr Opin Pharmacol,* 9**,** 341-6.

DUPUIS, L., OUDART, H., RENE, F., GONZALEZ DE AGUILAR, J. L. & LOEFFLER, J. P. (2004b) Evidence for defective energy homeostasis in amyotrophic lateral sclerosis: benefit of a high-energy diet in a transgenic mouse model. *Proc Natl Acad Sci U S A,* 101**,** 11159-64.

ELLMAN, G. L., COURTNEY, K. D., ANDRES, V., JR. & FEATHER-STONE, R. M. (1961) A new and rapid colorimetric determination of acetylcholinesterase activity. *Biochem Pharmacol,* 7**,** 88-95.

ENDO, S., HIRAMATSU, N., HAYAKAWA, K., OKAMURA, M., KASAI, A., TAGAWA, Y., SAWADA, N., YAO, J. & KITAMURA, M. (2007) Geranylgeranylacetone, an inducer of the 70-kDa heat shock protein (HSP70), elicits unfolded protein response and coordinates cellular fate independently of HSP70. *Mol Pharmacol,* 72**,** 1337-48.

EU, J. P., SUN, J., XU, L., STAMLER, J. S. & MEISSNER, G. (2000) The Skeletal Muscle Calcium Release Channel: Coupled O2 Sensor and NO Signaling Functions. *Cell,* 102**,** 499-509.

FACCHINETTI, F., SASAKI, M., CUTTING, F. B., ZHAI, P., MACDONALD, J. E., REIF, D., BEAL, M. F., HUANG, P. L., DAWSON, T. M., GURNEY, M. E. & DAWSON, V. L. (1999) Lack of involvement of neuronal nitric oxide synthase in the pathogenesis of a transgenic mouse model of familial amyotrophic lateral sclerosis. *Neuroscience,* 90**,** 1483-92.

FERGANI, A., OUDART, H., GONZALEZ DE AGUILAR, J. L., FRICKER, B., RENE, F., HOCQUETTE, J. F., MEININGER, V., DUPUIS, L. & LOEFFLER, J. P. (2007) Increased peripheral lipid clearance in an animal model of amyotrophic lateral sclerosis. *J Lipid Res,* 48**,** 1571-80.

FERNANDEZ, H. L., STILES, J. R. & DONOSO, J. A. (1986) Skeletal muscle acetylcholinesterase molecular forms in amyotrophic lateral sclerosis. *Muscle Nerve,* 9**,** 399-406.

FERRANTE, R. J., BROWNE, S. E., SHINOBU, L. A., BOWLING, A. C., BAIK, M. J., MACGARVEY, U., KOWALL, N. W., BROWN, R. H., JR. & BEAL, M. F. (1997) Evidence of increased oxidative damage in both sporadic and familial amyotrophic lateral sclerosis. *J Neurochem,* 69**,** 2064-74.

FERRARI, R., KAPOGIANNIS, D., HUEY, E. D. & MOMENI, P. (2011) FTD and ALS: A Tale of Two Diseases. *Curr Alzheimer Res*.

FERREIRA, L. F. & REID, M. B. (2008) Muscle-derived ROS and thiol regulation in muscle fatigue. *J Appl Physiol,* 104**,** 853-60.

FISCHER, L. R., CULVER, D. G., TENNANT, P., DAVIS, A. A., WANG, M., CASTELLANO-SANCHEZ, A., KHAN, J., POLAK, M. A. & GLASS, J. D. (2004) Amyotrophic lateral sclerosis is a distal axonopathy: evidence in mice and man. *Exp Neurol,* 185**,** 232-40.

FISHER, T. J., VRBOVA, G. & WIJETUNGE, A. (1989) Partial denervation of the rat soleus muscle at two different developmental stages. *Neuroscience,* 28**,** 755-63.

FRATTA, P., ENGEL, W. K., MCFERRIN, J., DAVIES, K. J. A., LIN, S. W. & ASKANAS, V. (2005) Proteasome Inhibition and Aggresome Formation in Sporadic Inclusion-Body Myositis and in Amyloid-{beta} Precursor Protein-Overexpressing Cultured Human Muscle Fibers. *Am J Pathol,* 167**,** 517-526.

FREY, D., SCHNEIDER, C., XU, L., BORG, J., SPOOREN, W. & CARONI, P. (2000) Early and selective loss of neuromuscular synapse subtypes with low sprouting competence in motoneuron diseases. *J Neurosci,* 20**,** 2534-42.

FUNALOT, B., DESPORT, J. C., STURTZ, F., CAMU, W. & COURATIER, P. (2009) High metabolic level in patients with familial amyotrophic lateral sclerosis. *Amyotroph Lateral Scler,* 10**,** 113-7.

GABAI, V. L., MABUCHI, K., MOSSER, D. D. & SHERMAN, M. Y. (2002) Hsp72 and stress kinase c-jun N-terminal kinase regulate the bid-dependent pathway in tumor necrosis factor-induced apoptosis. *Mol Cell Biol,* 22**,** 3415-24.

GAROFALO, O., KENNEDY, P. G., SWASH, M., MARTIN, J. E., LUTHERT, P., ANDERTON, B. H. & LEIGH, P. N. (1991) Ubiquitin and heat shock protein expression in amyotrophic lateral sclerosis. *Neuropathol Appl Neurobiol,* 17**,** 39-45.

GAUTAM, M., NOAKES, P. G., MUDD, J., NICHOL, M., CHU, G. C., SANES, J. R. & MERLIE, J. P. (1995) Failure of postsynaptic specialization to develop at neuromuscular junctions of rapsyn-deficient mice. *Nature,* 377**,** 232-6.

GERNOLD, M., KNAUF, U., GAESTEL, M., STAHL, J. & KLOETZEL, P. M. (1993) Development and tissue-specific distribution of mouse small heat shock protein hsp25. *Developmental Genetics,* 14**,** 103-111.

GIFONDORWA, D. J., ROBINSON, M. B., HAYES, C. D., TAYLOR, A. R., PREVETTE, D. M., OPPENHEIM, R. W., CARESS, J. & MILLIGAN, C. E. (2007) Exogenous delivery of heat shock protein 70 increases lifespan in a mouse model of amyotrophic lateral sclerosis. *J Neurosci,* 27**,** 13173-80.

GISSEL, H. (2005) The role of Ca2+ in muscle cell damage. *Ann N Y Acad Sci,* 1066**,** 166-80.

GOMES, C., PALMA, A., ALMEIDA, R., REGALLA, M., MCCLUSKEY, L., TROJANOWSKI, J. & COSTA, J. (2008) Establishment of a cell model of ALS disease: Golgi apparatus disruption occurs independently from apoptosis. *Biotechnology Letters,* 30**,** 603-610.

GONG, Y. H., PARSADANIAN, A. S., ANDREEVA, A., SNIDER, W. D. & ELLIOTT, J. L. (2000) Restricted expression of G86R Cu/Zn superoxide dismutase in astrocytes results in astrocytosis but does not cause motoneuron degeneration. *J Neurosci,* 20**,** 660-5.

GONZALEZ DE AGUILAR, J. L., DUPUIS, L., OUDART, H. & LOEFFLER, J. P. (2005) The metabolic hypothesis in amyotrophic lateral sclerosis: insights from mutant Cu/Zn-superoxide dismutase mice. *Biomed Pharmacother,* 59**,** 190-6.

GROZDANOVIC, Z. & BAUMGARTEN, H. G. (1999) Nitric oxide synthase in skeletal muscle fibers: a signaling component of the dystrophin-glycoprotein complex. *Histol Histopathol,* 14**,** 243-56.

GUPTE, A. A., BOMHOFF, G. L., SWERDLOW, R. H. & GEIGER, P. C. (2009) Heat treatment improves glucose tolerance and prevents skeletal muscle insulin resistance in rats fed a high-fat diet. *Diabetes,* 58**,** 567-78.

GURNEY, M. E. (1994) Transgenic-mouse model of amyotrophic lateral sclerosis. *N Engl J Med,* 331**,** 1721-2.

GURNEY, M. E., PU, H., CHIU, A. Y., DAL CANTO, M. C., POLCHOW, C. Y., ALEXANDER, D. D., CALIENDO, J., HENTATI, A., KWON, Y. W., DENG, H. X. & ET AL. (1994) Motor neuron degeneration in mice that express a human Cu,Zn superoxide dismutase mutation. *Science,* 264**,** 1772-5.

HALTER, B., GONZALEZ DE AGUILAR, J. L., RENE, F., PETRI, S., FRICKER, B., ECHANIZ-LAGUNA, A., DUPUIS, L., LARMET, Y. & LOEFFLER, J. P. (2010) Oxidative stress in skeletal muscle stimulates early expression of Rad in a mouse model of amyotrophic lateral sclerosis. *Free Radic Biol Med,* 48**,** 915-23.

HANSEN, J. J., DURR, A., COURNU-REBEIX, I., GEORGOPOULOS, C., ANG, D., NIELSEN, M. N., DAVOINE, C. S., BRICE, A., FONTAINE, B., GREGERSEN, N. & BROSS, P. (2002) Hereditary spastic paraplegia SPG13 is associated with a mutation in the gene encoding the mitochondrial chaperonin Hsp60. *Am J Hum Genet,* 70**,** 1328-32.

HARDING, D. I., GREENSMITH, L., CONNOLD, A. L. & VRBOVA, G. (1996) Stabilizing neuromuscular contacts increases motoneuron survival after neonatal nerve injury in rats. *Neuroscience,* 70**,** 799-805.

HARE, J. M. & STAMLER, J. S. (1999) NOS: modulator, not mediator of cardiac performance. *Nat Med,* 5**,** 273-4.

HEATH, P. R. & SHAW, P. J. (2002) Update on the glutamatergic neurotransmitter system and the role of excitotoxicity in amyotrophic lateral sclerosis. *Muscle Nerve,* 26**,** 438-58.

HEGEDUS, J., PUTMAN, C. T. & GORDON, T. (2007) Time course of preferential motor unit loss in the SOD1 G93A mouse model of amyotrophic lateral sclerosis. *Neurobiol Dis,* 28**,** 154-64.

HENDERSON, B., NAIR, S. P. & COATES, A. R. (1996) Molecular chaperones and disease. *Inflamm Res,* 45**,** 155-8.

HENRIQUES, A., PITZER, C. & SCHNEIDER, A. Characterization of a Novel SOD-1(G93A) Transgenic Mouse Line with Very Decelerated Disease Development. *PLoS One,* 5**,** e15445.

HENSLEY, K., ABDEL-MOATY, H., HUNTER, J., MHATRE, M., MOU, S., NGUYEN, K., POTAPOVA, T., PYE, Q. N., QI, M., RICE, H., STEWART, C., STROUKOFF, K. & WEST, M. (2006) Primary glia expressing the G93A-SOD1 mutation present a neuroinflammatory phenotype and provide a cellular system for studies of glial inflammation. *J Neuroinflammation,* 3**,** 2.

HERRERA, A. A. & WERLE, M. J. (1990) Mechanisms of elimination, remodeling, and competition at frog neuromuscular junctions. *J Neurobiol,* 21**,** 73-98.

HIGGINS, C. M., JUNG, C. & XU, Z. (2003) ALS-associated mutant SOD1G93A causes mitochondrial vacuolation by expansion of the intermembrane space and by involvement of SOD1 aggregation and peroxisomes. *BMC Neurosci,* 4**,** 16.

HO, H. K., JIA, Y., COE, K. J., GAO, Q., DONEANU, C. E., HU, Z., BAMMLER, T. K., BEYER, R. P., FAUSTO, N., BRUSCHI, S. A. & NELSON, S. D. (2006) Cytosolic heat shock proteins and heme oxygenase-1 are preferentially induced in response to specific and localized intramitochondrial damage by tetrafluoroethylcysteine. *Biochem Pharmacol,* 72**,** 80-90.

HOWARTH, J. L., KELLY, S., KEASEY, M. P., GLOVER, C. P., LEE, Y. B., MITROPHANOUS, K., CHAPPLE, J. P., GALLO, J. M., CHEETHAM, M. E. & UNEY, J. B. (2007) Hsp40 molecules that target to the ubiquitin-proteasome system decrease inclusion formation in models of polyglutamine disease. *Mol Ther,* 15**,** 1100-5.

HUEY, K. A., MCCALL, G. E., ZHONG, H. & ROY, R. R. (2007) Modulation of HSP25 and TNF-alpha during the early stages of functional overload of a rat slow and fast muscle. *J Appl Physiol,* 102**,** 2307-14.

HUEY, K. A., THRESHER, J. S., BROPHY, C. M. & ROY, R. R. (2004) Inactivity-induced modulation of Hsp20 and Hsp25 content in rat hindlimb muscles. *Muscle Nerve,* 30**,** 95-101.

HUGHES, P., BEILHARZ, E., GLUCKMAN, P. & DRAGUNOW, M. (1993) Brain-derived neurotrophic factor is induced as an immediate early gene following N-methyl-D-aspartate receptor activation. *Neuroscience,* 57**,** 319-28.

IKEDA, K., IWASAKI, Y., SHIOJIMA, T. & KINOSHITA, M. (1996) Neuroprotective effect of various cytokines on developing spinal motoneurons following axotomy. *J Neurol Sci,* 135**,** 109-13.

ILIEVA, H., POLYMENIDOU, M. & CLEVELAND, D. W. (2009) Non-cell autonomous toxicity in neurodegenerative disorders: ALS and beyond. *J Cell Biol,* 187**,** 761-72.

IMAI, J., YASHIRODA, H., MARUYA, M., YAHARA, I. & TANAKA, K. (2003) Proteasomes and molecular chaperones: cellular machinery responsible for folding and destruction of unfolded proteins. *Cell Cycle,* 2**,** 585-90.

IP, M. C., LUFF, A. R. & PROSKE, U. (1988) Innervation of muscle receptors in the cross-reinnervated soleus muscle of the cat. *Anat Rec,* 220**,** 212-8.

ISHIMOTO, T., KAMEI, A., KOYANAGI, S., NISHIDE, N., UYEDA, A., KASAI, M. & TAGUCHI, T. (1998) HSP90 Has Neurite-Promoting Activity in Vitro for Telencephalic and Spinal Neurons of Chick Embryos. *Biochemical and Biophysical Research Communications,* 253**,** 283-287.

JAARSMA, D., HAASDIJK, E. D., GRASHORN, J. A., HAWKINS, R., VAN DUIJN, W., VERSPAGET, H. W., LONDON, J. & HOLSTEGE, J. C. (2000) Human Cu/Zn superoxide dismutase (SOD1) overexpression in mice causes mitochondrial vacuolization, axonal degeneration, and premature motoneuron death and accelerates motoneuron disease in mice expressing a familial amyotrophic lateral sclerosis mutant SOD1. *Neurobiol Dis,* 7**,** 623-43.

JAFFREY, S. R., ERDJUMENT-BROMAGE, H., FERRIS, C. D., TEMPST, P. & SNYDER, S. H. (2001) Protein S-nitrosylation: a physiological signal for neuronal nitric oxide. *Nat Cell Biol,* 3**,** 193-7.

JANG, Y. C., LUSTGARTEN, M. S., LIU, Y., MULLER, F. L., BHATTACHARYA, A., LIANG, H., SALMON, A. B., BROOKS, S. V., LARKIN, L., HAYWORTH, C. R., RICHARDSON, A. & VAN REMMEN, H. (2010) Increased superoxide in vivo accelerates age-associated muscle atrophy through mitochondrial dysfunction and neuromuscular junction degeneration. *FASEB J,* 24**,** 1376-90.

JEPPESEN, T. D., SCHWARTZ, M., OLSEN, D. B. & VISSING, J. (2003) Oxidative capacity correlates with muscle mutation load in mitochondrial myopathy. *Ann Neurol,* 54**,** 86-92.

JO, S. A., ZHU, X., MARCHIONNI, M. A. & BURDEN, S. J. (1995) Neuregulins are concentrated at nerve-muscle synapses and activate ACh-receptor gene expression. *Nature,* 373**,** 158-61.

JOHNSTON, J. A., DALTON, M. J., GURNEY, M. E. & KOPITO, R. R. (2000) Formation of high molecular weight complexes of mutant Cu, Zn-superoxide dismutase in a mouse model for familial amyotrophic lateral sclerosis. *Proc Natl Acad Sci U S A,* 97**,** 12571-6.

JONSSON, P. A., ERNHILL, K., ANDERSEN, P. M., BERGEMALM, D., BRANNSTROM, T., GREDAL, O., NILSSON, P. & MARKLUND, S. L. (2004) Minute quantities of misfolded mutant superoxide dismutase-1 cause amyotrophic lateral sclerosis. *Brain,* 127**,** 73-88.

JURIVICH, D. A., SISTONEN, L., KROES, R. A. & MORIMOTO, R. I. (1992) Effect of sodium salicylate on the human heat shock response. *Science,* 255**,** 1243-5.

KALMAR, B., BURNSTOCK, G., VRBOVA, G., URBANICS, R., CSERMELY, P. & GREENSMITH, L. (2002) Upregulation of heat shock proteins rescues motoneurones from axotomy-induced cell death in neonatal rats. *Exp Neurol,* 176**,** 87-97.

KALMAR, B. & GREENSMITH, L. (2009a) Activation of the heat shock response in a primary cellular model of motoneuron neurodegeneration-evidence for neuroprotective and neurotoxic effects. *Cell Mol Biol Lett,* 14**,** 319-35.

KALMAR, B. & GREENSMITH, L. (2009b) Induction of heat shock proteins for protection against oxidative stress. *Adv Drug Deliv Rev,* 61**,** 310-8.
KALMAR, B., GREENSMITH, L., MALCANGIO, M., MCMAHON, S. B., CSERMELY, P. & BURNSTOCK, G. (2003) The effect of treatment with BRX-220, a co-inducer of heat shock proteins, on sensory fibers of the rat following peripheral nerve injury. *Exp Neurol,* 184**,** 636-47.
KALMAR, B., NOVOSELOV, S., GRAY, A., CHEETHAM, M. E., MARGULIS, B. & GREENSMITH, L. (2008) Late stage treatment with arimoclomol delays disease progression and prevents protein aggregation in the SOD1 mouse model of ALS. *J Neurochem,* 107**,** 339-50.
KAMPINGA, H. H., KANON, B., SALOMONS, F. A., KABAKOV, A. E. & PATTERSON, C. (2003) Overexpression of the cochaperone CHIP enhances Hsp70-dependent folding activity in mammalian cells. *Mol Cell Biol,* 23**,** 4948-58.
KANAZAWA, I. (2001) How do neurons die in neurodegenerative diseases? *Trends Mol Med,* 7**,** 339-44.
KARUNANITHI, S., BARCLAY, J. W., BROWN, I. R., ROBERTSON, R. M. & ATWOOD, H. L. (2002) Enhancement of presynaptic performance in transgenic <I>Drosophila</I> overexpressing heat shock protein Hsp70. *Synapse,* 44**,** 8-14.
KASPAR, B. K., LLADO, J., SHERKAT, N., ROTHSTEIN, J. D. & GAGE, F. H. (2003a) Retrograde viral delivery of IGF-1 prolongs survival in a mouse ALS model. *Science,* 301**,** 839-42.
KASPAR, B. K., LLADO, J., SHERKAT, N., ROTHSTEIN, J. D. & GAGE, F. H. (2003b) Retrograde Viral Delivery of IGF-1 Prolongs Survival in a Mouse ALS Model. *Science,* 301**,** 839-842.
KASTHURI, N. & LICHTMAN, J. W. (2003) The role of neuronal identity in synaptic competition. *Nature,* 424**,** 426-30.
KAWASHIMA, D., ASAI, M., KATAGIRI, K., TAKEUCHI, R. & OHTSUKA, K. (2009) Reinvestigation of the effect of carbenoxolone on the induction of heat shock proteins. *Cell Stress Chaperones,* 14**,** 535-43.
KAYANI, A. C., CLOSE, G. L., BROOME, C. S., JACKSON, M. J. & MCARDLE, A. (2008a) Enhanced recovery from contraction-induced damage in skeletal muscles of old mice following treatment with the heat shock protein inducer 17-(allylamino)-17-demethoxygeldanamycin. *Rejuvenation Res,* 11**,** 1021-30.
KAYANI, A. C., MORTON, J. P. & MCARDLE, A. (2008b) The exercise-induced stress response in skeletal muscle: failure during aging. *Appl Physiol Nutr Metab,* 33**,** 1033-41.
KEILHOFF, G., FANSA, H. & WOLF, G. (2002) Differences in peripheral nerve degeneration/regeneration between wild-type and neuronal nitric oxide synthase knockout mice. *J Neurosci Res,* 68**,** 432-41.
KERNELL, D. (1998) Muscle regionalization. *Can J Appl Physiol,* 23**,** 1-22.
KIAEI, M., KIPIANI, K., PETRI, S., CHEN, J., CALINGASAN, N. Y. & BEAL, M. F. (2005) Celastrol blocks neuronal cell death and extends life in transgenic mouse model of amyotrophic lateral sclerosis. *Neurodegener Dis,* 2**,** 246-54.
KIERAN, D. & GREENSMITH, L. (2004) Inhibition of calpains, by treatment with leupeptin, improves motoneuron survival and muscle function in models of motoneuron degeneration. *Neuroscience,* 125**,** 427-39.

KIERAN, D., KALMAR, B., DICK, J. R., RIDDOCH-CONTRERAS, J., BURNSTOCK, G. & GREENSMITH, L. (2004) Treatment with arimoclomol, a coinducer of heat shock proteins, delays disease progression in ALS mice. *Nat Med,* 10**,** 402-5.

KIRKINEZOS, I. G., HERNANDEZ, D., BRADLEY, W. G. & MORAES, C. T. (2003) Regular exercise is beneficial to a mouse model of amyotrophic lateral sclerosis. *Annals of Neurology,* 53**,** 804-807.

KO, C. P. (1985) Formation of the active zone at developing neuromuscular junctions in larval and adult bullfrogs. *J Neurocytol,* 14**,** 487-512.

KOBAYASHI, T., YASUDA, K. & ARAKI, M. Coordinated regulation of dorsal bone morphogenetic protein 4 and ventral Sonic hedgehog signaling specifies the dorso-ventral polarity in the optic vesicle and governs ocular morphogenesis through fibroblast growth factor 8 upregulation. *Dev Growth Differ*.

KOH, T. J. (2002) Do Small Heat Shock Proteins Protect Skeletal Muscle from Injury? *Exercise and Sport Sciences Reviews,* 30**,** 117-121.

KOIRALA, S., QIANG, H. & KO, C. P. (2000) Reciprocal interactions between perisynaptic Schwann cells and regenerating nerve terminals at the frog neuromuscular junction. *J Neurobiol,* 44**,** 343-60.

KORNELIUSSEN, H. & JANSEN, J. K. S. (1976) Morphological aspects of the elimination of polyneuronal innervation of skeletal muscle fibres in newborn rats. *Journal of Neurocytology,* 5**,** 591-604.

KRISHNAN, J., LEMMENS, R., ROBBERECHT, W. & VAN DEN BOSCH, L. (2006) Role of heat shock response and Hsp27 in mutant SOD1-dependent cell death. *Exp Neurol,* 200**,** 301-10.

KRISHNAN, J., VANNUVEL, K., ANDRIES, M., WAELKENS, E., ROBBERECHT, W. & VAN DEN BOSCH, L. (2008) Over-expression of Hsp27 does not influence disease in the mutant SOD1(G93A) mouse model of amyotrophic lateral sclerosis. *J Neurochem,* 106**,** 2170-83.

KRIZ, J., GOWING, G. & JULIEN, J. P. (2003) Efficient three-drug cocktail for disease induced by mutant superoxide dismutase. *Ann Neurol,* 53**,** 429-36.

KURTHY, M., MOGYOROSI, T., NAGY, K., KUKORELLI, T., JEDNAKOVITS, A., TALOSI, L. & BIRO, K. (2002) Effect of BRX-220 against peripheral neuropathy and insulin resistance in diabetic rat models. *Ann N Y Acad Sci,* 967**,** 482-9.

KUZUHARA, S. (2008) [Recent progress in ALS research: ALS and TDP-43]. *Rinsho Shinkeigaku,* 48**,** 625-33.

LAGIER-TOURENNE, C. & CLEVELAND, D. W. (2009) Rethinking ALS: the FUS about TDP-43. *Cell,* 136**,** 1001-4.

LEE, J., RYU, H. & KOWALL, N. W. (2009a) Differential regulation of neuronal and inducible nitric oxide synthase (NOS) in the spinal cord of mutant SOD1 (G93A) ALS mice. *Biochemical and Biophysical Research Communications,* 387**,** 202-206.

LEE, J., RYU, H. & KOWALL, N. W. (2009b) Differential regulation of neuronal and inducible nitric oxide synthase (NOS) in the spinal cord of mutant SOD1 (G93A) ALS mice. *Biochem Biophys Res Commun,* 387**,** 202-6.

LEE, M. W., MURAMATSU, T., UEKUSA, T., LEE, J. H. & SHIMONO, M. (2008) Heat stress induces alkaline phosphatase activity and heat shock protein 25 expression in cultured pulp cells. *Int Endod J,* 41**,** 158-62.

LEIGH, P. N., WHITWELL, H., GAROFALO, O., BULLER, J., SWASH, M., MARTIN, J. E., GALLO, J. M., WELLER, R. O. & ANDERTON, B. H. (1991) Ubiquitin-immunoreactive intraneuronal inclusions in amyotrophic lateral sclerosis. Morphology, distribution, and specificity. *Brain,* 114 (Pt 2)**,** 775-88.

LEWIS, C. & OHLENDIECK, K. (2010) Proteomic profiling of naturally protected extraocular muscles from the dystrophin-deficient mdx mouse. *Biochem Biophys Res Commun,* 396**,** 1024-9.

LEXELL, J. (1995) Human aging, muscle mass, and fiber type composition. *J Gerontol A Biol Sci Med Sci,* 50 Spec No**,** 11-6.

LI, L., OPPENHEIM, R. W., LEI, M. & HOUENOU, L. J. (1994) Neurotrophic agents prevent motoneuron death following sciatic nerve section in the neonatal mouse. *J Neurobiol,* 25**,** 759-66.

LI, W., BRAKEFIELD, D., PAN, Y., HUNTER, D., MYCKATYN, T. M. & PARSADANIAN, A. (2007) Muscle-derived but not centrally derived transgene GDNF is neuroprotective in G93A-SOD1 mouse model of ALS. *Exp Neurol,* 203**,** 457-71.

LIN, K. M., LIN, B., LIAN, I. Y., MESTRIL, R., SCHEFFLER, I. E. & DILLMANN, W. H. (2001) Combined and Individual Mitochondrial HSP60 and HSP10 Expression in Cardiac Myocytes Protects Mitochondrial Function and Prevents Apoptotic Cell Deaths Induced by Simulated Ischemia-Reoxygenation. *Circulation,* 103**,** 1787-1792.

LIU, J., SHINOBU, L. A., WARD, C. M., YOUNG, D. & CLEVELAND, D. W. (2005) Elevation of the Hsp70 chaperone does not effect toxicity in mouse models of familial amyotrophic lateral sclerosis. *J Neurochem,* 93**,** 875-82.

LIU, Y. & STEINACKER, J. M. (2001) Changes in skeletal muscle heat shock proteins: pathological significance. *Front Biosci,* 6**,** D12-25.

LOCKE, J. E., BRADBURY, C. M., WEI, S. J., SHAH, S., RENE, L. M., CLEMENS, R. A., ROTI ROTI, J., HORIKOSHI, N. & GIUS, D. (2002) Indomethacin lowers the threshold thermal exposure for hyperthermic radiosensitization and heat-shock inhibition of ionizing radiation-induced activation of NF-kappaB. *Int J Radiat Biol,* 78**,** 493-502.

LOCKE, M. (1997) The cellular stress response to exercise: role of stress proteins. *Exerc Sport Sci Rev,* 25**,** 105-36.

LOCKE, M., NOBLE, E. G. & ATKINSON, B. G. (1991) Inducible isoform of HSP70 is constitutively expressed in a muscle fiber type specific pattern. *Am J Physiol,* 261**,** C774-9.

LOTT, J. A. & LANDESMAN, P. W. (1984) The enzymology of skeletal muscle disorders. *Crit Rev Clin Lab Sci,* 20**,** 153-90.

LOUBOUTIN, J. P., ROUGER, K., TINSLEY, J. M., HALLDORSON, J. & WILSON, J. M. (2001) iNOS expression in dystrophinopathies can be reduced by somatic gene transfer of dystrophin or utrophin. *Mol Med,* 7**,** 355-64.

LOWRIE, M. B., KRISHNAN, S. & VRBOVA, G. (1987) Permanent changes in muscle and motoneurones induced by nerve injury during a critical period of development of the rat. *Brain Res,* 428**,** 91-101.

LOWRIE, M. B. & VRBOVA, G. (1984) Different pattern of recovery of fast and slow muscles following nerve injury in the rat. *J Physiol,* 349**,** 397-410.

LUDOLPH, A. C., BENDOTTI, C., BLAUGRUND, E., CHIO, A., GREENSMITH, L., LOEFFLER, J. P., MEAD, R., NIESSEN, H. G., PETRI, S., PRADAT, P. F.,

ROBBERECHT, W., RUEGG, M., SCHWALENSTOCKER, B., STILLER, D., VAN DEN BERG, L., VIEIRA, F. & VON HORSTEN, S. (2010) Guidelines for preclinical animal research in ALS/MND: A consensus meeting. *Amyotroph Lateral Scler,* 11**,** 38-45.

LUO, S., ZHANG, B., DONG, X.-P., TAO, Y., TING, A., ZHOU, Z., MEIXIONG, J., LUO, J., CHIU, F. C. A., XIONG, W. C. & MEI, L. (2008) HSP90[beta] Regulates Rapsyn Turnover and Subsequent AChR Cluster Formation and Maintenance. *Neuron,* 60**,** 97-110.

MAGEN, D., GEORGOPOULOS, C., BROSS, P., ANG, D., SEGEV, Y., GOLDSHER, D., NEMIROVSKI, A., SHAHAR, E., RAVID, S., LUDER, A., HENO, B., GERSHONI-BARUCH, R., SKORECKI, K. & MANDEL, H. (2008) Mitochondrial hsp60 chaperonopathy causes an autosomal-recessive neurodegenerative disorder linked to brain hypomyelination and leukodystrophy. *Am J Hum Genet,* 83**,** 30-42.

MARQUES, M. J., PEREIRA, E. C. L., MINATEL, E. & NETO, H. S. (2006) Nerve-terminal and Schwann-cell response after nerve injury in the absence of nitric oxide. *Muscle & Nerve,* 34**,** 225-231.

MARTINOU, J. C., MARTINOU, I. & KATO, A. C. (1992) Cholinergic differentiation factor (CDF/LIF) promotes survival of isolated rat embryonic motoneurons in vitro. *Neuron,* 8**,** 737-44.

MARUYAMA, H., MORINO, H., ITO, H., IZUMI, Y., KATO, H., WATANABE, Y., KINOSHITA, Y., KAMADA, M., NODERA, H., SUZUKI, H., KOMURE, O., MATSUURA, S., KOBATAKE, K., MORIMOTO, N., ABE, K., SUZUKI, N., AOKI, M., KAWATA, A., HIRAI, T., KATO, T., OGASAWARA, K., HIRANO, A., TAKUMI, T., KUSAKA, H., HAGIWARA, K., KAJI, R. & KAWAKAMI, H. (2010) Mutations of optineurin in amyotrophic lateral sclerosis. *Nature,* 465**,** 223-226.

MCARDLE, A., PATTWELL, D., VASILAKI, A., GRIFFITHS, R. D. & JACKSON, M. J. (2001) Contractile activity-induced oxidative stress: cellular origin and adaptive responses. *Am J Physiol Cell Physiol,* 280**,** C621-7.

MICHAEL, C. S., MASASHI, K., MICHAEL, B., VINCENT, J. C., HENRY, W. Q. & FRANK, M. L. (2006) Pathogenic accumulation of APP in fast twitch muscle of IBM patients and a transgenic model. *Neurobiology of aging,* 27**,** 423-432.

MILLER, R. (2003) Riluzole for ALS: what is the evidence? *Amyotroph Lateral Scler Other Motor Neuron Disord,* 4**,** 135.

MILLER, T. M., KIM, S. H., YAMANAKA, K., HESTER, M., UMAPATHI, P., ARNSON, H., RIZO, L., MENDELL, J. R., GAGE, F. H., CLEVELAND, D. W. & KASPAR, B. K. (2006) Gene transfer demonstrates that muscle is not a primary target for non-cell-autonomous toxicity in familial amyotrophic lateral sclerosis. *Proc Natl Acad Sci U S A,* 103**,** 19546-51.

MOHAJERI, M. H., FIGLEWICZ, D. A. & BOHN, M. C. (1999) Intramuscular grafts of myoblasts genetically modified to secrete glial cell line-derived neurotrophic factor prevent motoneuron loss and disease progression in a mouse model of familial amyotrophic lateral sclerosis. *Hum Gene Ther,* 10**,** 1853-66.

MOLENAAR, P. C., NEWSOM-DAVIS, J., POLAK, R. L. & VINCENT, A. (1981) Choline acetyltransferase in skeletal muscle from patients with myasthenia gravis. *J Neurochem,* 37**,** 1081-8.

MORUZZI, E. V. & BERGAMINI, E. (1983) Effect of denervation on glycogen metabolism in fast and slow muscle of rat. *Muscle Nerve,* 6**,** 356-66.
MULVEY, C., HARNO, E., KEENAN, A. & OHLENDIECK, K. (2005) Expression of the skeletal muscle dystrophin-dystroglycan complex and syntrophin-nitric oxide synthase complex is severely affected in the type 2 diabetic Goto-Kakizaki rat. *Eur J Cell Biol,* 84**,** 867-83.
MURPHY, L. J. (2000) Overexpression of insulin-like growth factor binding protein-1 in transgenic mice. *Pediatr Nephrol,* 14**,** 567-71.
MUTHNY, T., KOVARIK, M., SISPERA, L., TILSER, I. & HOLECEK, M. (2008) Protein metabolism in slow- and fast-twitch skeletal muscle during turpentine-induced inflammation. *Int J Exp Pathol,* 89**,** 64-71.
NAMBA, T., NAKAMURA, T. & GROB, D. (1967) Staining for nerve fiber and cholinesterase activity in fresh frozen sections. *Am J Clin Pathol,* 47**,** 74-7.
NGUYEN, K. T., GARCIA-CHACON, L. E., BARRETT, J. N., BARRETT, E. F. & DAVID, G. (2009) The Psi(m) depolarization that accompanies mitochondrial Ca2+ uptake is greater in mutant SOD1 than in wild-type mouse motor terminals. *Proc Natl Acad Sci U S A,* 106**,** 2007-11.
NIEBROJ-DOBOSZ, I. & JANIK, P. (1999) Amino acids acting as transmitters in amyotrophic lateral sclerosis (ALS). *Acta Neurologica Scandinavica,* 100**,** 6-11.
NOGALSKA, A., WOJCIK, S., ENGEL, W. K., MCFERRIN, J. & ASKANAS, V. (2007) Endoplasmic reticulum stress induces myostatin precursor protein and NF-kappaB in cultured human muscle fibers: relevance to inclusion body myositis. *Exp Neurol,* 204**,** 610-8.
O'BRIEN, R. A., OSTBERG, A. J. & VRBOVA, G. (1982) The reorganization of neuromuscular junctions during development in rats. *Prog Clin Biol Res,* 91**,** 247-57.
ODA, Y., IMAI, S., NAKANISHI, I., ICHIKAWA, T. & DEGUCHI, T. (1995) Immunohistochemical study on choline acetyltransferase in the spinal cord of patients with amyotrophic lateral sclerosis. *Pathol Int,* 45**,** 933-9.
OISHI, Y., OGATA, T., OHIRA, Y., TANIGUCHI, K. & ROY, R. R. (2005) Calcineurin and heat shock protein 72 in functionally overloaded rat plantaris muscle. *Biochem Biophys Res Commun,* 330**,** 706-13.
OISHI, Y., TANIGUCHI, K., MATSUMOTO, H., ISHIHARA, A., OHIRA, Y. & ROY, R. R. (2002) Muscle type-specific response of HSP60, HSP72, and HSC73 during recovery after elevation of muscle temperature. *J Appl Physiol,* 92**,** 1097-103.
OKADO-MATSUMOTO, A. & FRIDOVICH, I. (2002) Amyotrophic lateral sclerosis: a proposed mechanism. *Proc Natl Acad Sci U S A,* 99**,** 9010-4.
OPPENHEIM, R. W. (1987) Muscle activity and motor neuron death in the spinal cord of the chick embryo. *Ciba Found Symp,* 126**,** 96-112.
OPPENHEIM, R. W. & HAVERKAMP, L. J. (1988) Neurotrophic interactions in the development of spinal cord motoneurons. *Ciba Found Symp,* 138**,** 152-71.
OPPENHEIM, R. W., PREVETTE, D., YIN, Q. W., COLLINS, F. & MACDONALD, J. (1991) Control of embryonic motoneuron survival in vivo by ciliary neurotrophic factor. *Science,* 251**,** 1616-8.
PARKER, K. C., KONG, S. W., WALSH, R. J., SALAJEGHEH, M., MOGHADASZADEH, B., AMATO, A. A., NAZARENO, R., LIN, Y. Y., KRASTINS, B., SARRACINO, D. A., BEGGS, A. H., PINKUS, J. L. &

GREENBERG, S. A. (2009) Fast-twitch sarcomeric and glycolytic enzyme protein loss in inclusion body myositis. *Muscle Nerve,* 39**,** 739-53.
PAULSEN, G., VISSING, K., KALHOVDE, J. M., UGELSTAD, I., BAYER, M. L., KADI, F., SCHJERLING, P., HALLEN, J. & RAASTAD, T. (2007) Maximal eccentric exercise induces a rapid accumulation of small heat shock proteins on myofibrils and a delayed HSP70 response in humans. *Am J Physiol Regul Integr Comp Physiol,* 293**,** R844-53.
PENG, H. M., MORISHIMA, Y., CLAPP, K. M., LAU, M., PRATT, W. B. & OSAWA, Y. (2009) Dynamic cycling with Hsp90 stabilizes neuronal nitric oxide synthase through calmodulin-dependent inhibition of ubiquitination. *Biochemistry,* 48**,** 8483-90.
PERCIVAL, J. M., ANDERSON, K. N., GREGOREVIC, P., CHAMBERLAIN, J. S. & FROEHNER, S. C. (2008) Functional deficits in nNOSmu-deficient skeletal muscle: myopathy in nNOS knockout mice. *PLoS One,* 3**,** e3387.
PERCIVAL, J. M., ANDERSON, K. N., HUANG, P., ADAMS, M. E. & FROEHNER, S. C. (2010) Golgi and sarcolemmal neuronal NOS differentially regulate contraction-induced fatigue and vasoconstriction in exercising mouse skeletal muscle. *J Clin Invest,* 120**,** 816-26.
PEREIRA, E. C., NETO, H. S. & MARQUES, M. J. (2001) Immunolocalisation of neuronal nitric oxide synthase at the neuromuscular junction of MDX mice: a confocal microscopy study. *J Anat,* 198**,** 663-71.
PHUKAN, J. (2010) Arimoclomol, a coinducer of heat shock proteins for the potential treatment of amyotrophic lateral sclerosis. *IDrugs,* 13**,** 482-96.
PINELLI, P., PISANO, F., CERIANI, F. & MISCIO, G. (1991) EMG evaluation of motor neuron sprouting in amyotrophic lateral sclerosis. *Ital J Neurol Sci,* 12**,** 359-67.
PORTER, B. E., WEIS, J. & SANES, J. R. (1995) A motoneuron-selective stop signal in the synaptic protein S-laminin. *Neuron,* 14**,** 549-59.
PRADAT, P. F., BRUNETEAU, G., GONZALEZ DE AGUILAR, J. L., DUPUIS, L., JOKIC, N., SALACHAS, F., LE FORESTIER, N., ECHANIZ-LAGUNA, A., DUBOURG, O., HAUW, J. J., TRANCHANT, C., LOEFFLER, J. P. & MEININGER, V. (2007) Muscle Nogo-A expression is a prognostic marker in lower motor neuron syndromes. *Ann Neurol,* 62**,** 15-20.
PRADAT, P. F., BRUNETEAU, G., GORDON, P. H., DUPUIS, L., BONNEFONT-ROUSSELOT, D., SIMON, D., SALACHAS, F., CORCIA, P., FROCHOT, V., LACORTE, J. M., JARDEL, C., COUSSIEU, C., FORESTIER, N. L., LACOMBLEZ, L., LOEFFLER, J. P. & MEININGER, V. (2009) Impaired glucose tolerance in patients with amyotrophic lateral sclerosis. *Amyotroph Lateral Scler***,** 1-6.
PRAMATAROVA, A., LAGANIERE, J., ROUSSEL, J., BRISEBOIS, K. & ROULEAU, G. A. (2001) Neuron-specific expression of mutant superoxide dismutase 1 in transgenic mice does not lead to motor impairment. *J Neurosci,* 21**,** 3369-74.
PREVILLE, X., SCHULTZ, H., KNAUF, U., GAESTEL, M. & ARRIGO, A. P. (1998) Analysis of the role of Hsp25 phosphorylation reveals the importance of the oligomerization state of this small heat shock protein in its protective function against TNFalpha- and hydrogen peroxide-induced cell death. *J Cell Biochem,* 69**,** 436-52.

PUN, S., SANTOS, A. F., SAXENA, S., XU, L. & CARONI, P. (2006) Selective vulnerability and pruning of phasic motoneuron axons in motoneuron disease alleviated by CNTF. *Nat Neurosci,* 9**,** 408-19.

RAFFAELLO, A., LAVEDER, P., ROMUALDI, C., BEAN, C., TONIOLO, L., GERMINARIO, E., MEGIGHIAN, A., DANIELI-BETTO, D., REGGIANI, C. & LANFRANCHI, G. (2006) Denervation in murine fast-twitch muscle: short-term physiological changes and temporal expression profiling. *Physiol. Genomics,* 25**,** 60-74.

RAKONCZAY, Z., JR., IVANYI, B., VARGA, I., BOROS, I., JEDNAKOVITS, A., NEMETH, I., LONOVICS, J. & TAKACS, T. (2002) Nontoxic heat shock protein coinducer BRX-220 protects against acute pancreatitis in rats. *Free Radic Biol Med,* 32**,** 1283-92.

READ, D. E. & GORMAN, A. M. (2009) Heat shock protein 27 in neuronal survival and neurite outgrowth. *Biochem Biophys Res Commun,* 382**,** 6-8.

REAUME, A. G., ELLIOTT, J. L., HOFFMAN, E. K., KOWALL, N. W., FERRANTE, R. J., SIWEK, D. F., WILCOX, H. M., FLOOD, D. G., BEAL, M. F., BROWN, R. H., JR., SCOTT, R. W. & SNIDER, W. D. (1996) Motor neurons in Cu/Zn superoxide dismutase-deficient mice develop normally but exhibit enhanced cell death after axonal injury. *Nat Genet,* 13**,** 43-7.

REICHMANN, H. & NIX, W. A. (1985) Changes of energy metabolism, myosin light chain composition, lactate dehydrogenase isozyme pattern and fibre type distribution of denervated fast-twitch muscle from rabbit after low frequency stimulation. *Pflugers Arch,* 405**,** 244-9.

REID, M. B. (1998) Role of nitric oxide in skeletal muscle: synthesis, distribution and functional importance. *Acta Physiol Scand,* 162**,** 401-9.

REYNOLDS, A. (2007) The theory of the cell state and the question of cell autonomy in nineteenth and early twentieth-century biology. *Sci Context,* 20**,** 71-95.

RIBERA, J., MARSAL, J., CASANOVAS, A., HUKKANEN, M., TARABAL, O. & ESQUERDA, J. E. (1998) Nitric oxide synthase in rat neuromuscular junctions and in nerve terminals of Torpedo electric organ: its role as regulator of acetylcholine release. *J Neurosci Res,* 51**,** 90-102.

RICHTER, K. & BUCHNER, J. (2001) Hsp90: Chaperoning signal transduction. *Journal of Cellular Physiology,* 188**,** 281-290.

RIDDOCH-CONTRERAS, J., YANG, S. Y., DICK, J. R., GOLDSPINK, G., ORRELL, R. W. & GREENSMITH, L. (2009) Mechano-growth factor, an IGF-I splice variant, rescues motoneurons and improves muscle function in SOD1(G93A) mice. *Exp Neurol,* 215**,** 281-9.

RIPPS, M. E., HUNTLEY, G. W., HOF, P. R., MORRISON, J. H. & GORDON, J. W. (1995) Transgenic mice expressing an altered murine superoxide dismutase gene provide an animal model of amyotrophic lateral sclerosis. *Proc Natl Acad Sci U S A,* 92**,** 689-93.

ROMMEL, C., BODINE, S. C., CLARKE, B. A., ROSSMAN, R., NUNEZ, L., STITT, T. N., YANCOPOULOS, G. D. & GLASS, D. J. (2001) Mediation of IGF-1-induced skeletal myotube hypertrophy by PI(3)K/Akt/mTOR and PI(3)K/Akt/GSK3 pathways. *Nat Cell Biol,* 3**,** 1009-13.

ROSE, A. J. & RICHTER, E. A. (2005) Skeletal Muscle Glucose Uptake During Exercise: How is it Regulated? *Physiology,* 20**,** 260-270.

ROSEN, D. R., SIDDIQUE, T., PATTERSON, D., FIGLEWICZ, D. A., SAPP, P., HENTATI, A., DONALDSON, D., GOTO, J., O'REGAN, J. P., DENG, H. X. & ET AL. (1993) Mutations in Cu/Zn superoxide dismutase gene are associated with familial amyotrophic lateral sclerosis. *Nature,* 362**,** 59-62.

ROSENHEIMER, J. L. (1990) Ultraterminal sprouting in innervated and partially denervated adult and aged rat muscle. *Neuroscience,* 38**,** 763-770.

ROTUNDO, R. L. (2003) Expression and localization of acetylcholinesterase at the neuromuscular junction. *J Neurocytol,* 32**,** 743-66.

SANTOS, A. F. & CARONI, P. (2003) Assembly, plasticity and selective vulnerability to disease of mouse neuromuscular junctions. *J Neurocytol,* 32**,** 849-62.

SASAKI, S. & IWATA, M. (1998) Characterizations of heterotopic neurons in the spinal cord of amyotrophic lateral sclerosis patients. *Acta Neuropathol,* 95**,** 367-72.

SASS, J. B., MARTIN, C. C. & KRONE, P. H. (1999) Restricted expression of the zebrafish hsp90alpha gene in slow and fast muscle fiber lineages. *Int J Dev Biol,* 43**,** 835-8.

SEAGO, N. D., CLARK, D. A. & MILLER, M. J. (1995) Role of inducible nitric oxide synthase (iNOS) and peroxynitrite in gut inflammation. *Inflamm Res,* 44 Suppl 2**,** S153-4.

SENF, S. M., DODD, S. L. & JUDGE, A. R. (2010) FOXO signaling is required for disuse muscle atrophy and is directly regulated by Hsp70. *Am J Physiol Cell Physiol,* 298**,** C38-45.

SHAN, Y. X., YANG, T. L., MESTRIL, R. & WANG, P. H. (2003) Hsp10 and Hsp60 suppress ubiquitination of insulin-like growth factor-1 receptor and augment insulin-like growth factor-1 receptor signaling in cardiac muscle: implications on decreased myocardial protection in diabetic cardiomyopathy. *J Biol Chem,* 278**,** 45492-8.

SHARP, P., KRISHNAN, M., PULLAR, O., NAVARRETE, R., WELLS, D. & DE BELLEROCHE, J. (2006) Heat shock protein 27 rescues motor neurons following nerve injury and preserves muscle function. *Exp Neurol,* 198**,** 511-8.

SHARP, P. S., DICK, J. R. & GREENSMITH, L. (2005) The effect of peripheral nerve injury on disease progression in the SOD1(G93A) mouse model of amyotrophic lateral sclerosis. *Neuroscience,* 130**,** 897-910.

SHAW, C. E., AL-CHALABI, A. & LEIGH, N. (2001) Progress in the pathogenesis of amyotrophic lateral sclerosis. *Curr Neurol Neurosci Rep,* 1**,** 69-76.

SHIAO, T., FOND, A., DENG, B., WEHLING-HENRICKS, M., ADAMS, M. E., FROEHNER, S. C. & TIDBALL, J. G. (2004) Defects in neuromuscular junction structure in dystrophic muscle are corrected by expression of a NOS transgene in dystrophin-deficient muscles, but not in muscles lacking alpha- and beta1-syntrophins. *Hum Mol Genet,* 13**,** 1873-84.

SHIN'ICHI, S. (1991) Regulation of glucose uptake in fast and slow skeletal muscles with fasting and refeeding. *Comparative Biochemistry and Physiology Part A: Physiology,* 98**,** 107-110.

SICILIANO, G., D'AVINO, C., DEL CORONA, A., BARSACCHI, R., KUSMIC, C., ROCCHI, A., PASTORINI, E. & MURRI, L. (2002) Impaired oxidative metabolism and lipid peroxidation in exercising muscle from ALS patients. *Amyotroph Lateral Scler Other Motor Neuron Disord,* 3**,** 57-62.

SLAWINSKA, U., TYC, F., KASICKI, S. & VRBOVA, G. (1996) Functional reorganization of the partially denervated hindlimb extensor and flexor muscle in rat. *Acta Neurobiol Exp (Wars),* 56**,** 441-7.

SOMASEKHAR, T., NORDLANDER, R. H. & REISER, P. J. (1996) Alterations in neuromuscular junction morphology during fast-to-slow transformation of rabbit skeletal muscles. *J Neurocytol,* 25**,** 315-31.

SORARU, G., VERGANI, L., FEDRIZZI, L., D'ASCENZO, C., POLO, A., BERNAZZI, B. & ANGELINI, C. (2007) Activities of mitochondrial complexes correlate with nNOS amount in muscle from ALS patients. *Neuropathol Appl Neurobiol,* 33**,** 204-11.

SOTI, C. & CSERMELY, P. (2006) Pharmacological modulation of the heat shock response. *Handb Exp Pharmacol***,** 417-36.

SREEDHAR, A. S., KALMAR, E., CSERMELY, P. & SHEN, Y. F. (2004) Hsp90 isoforms: functions, expression and clinical importance. *FEBS Lett,* 562**,** 11-5.

STAMLER, J. S. & MEISSNER, G. (2001) Physiology of nitric oxide in skeletal muscle. *Physiol Rev,* 81**,** 209-237.

STEELE, A. D. & YI, C. H. (2006) Neuromuscular Denervation: Bax up against the Wall in Amyotrophic Lateral Sclerosis. *J. Neurosci.,* 26**,** 12849-12851.

STITT, T. N., DRUJAN, D., CLARKE, B. A., PANARO, F., TIMOFEYVA, Y., KLINE, W. O., GONZALEZ, M., YANCOPOULOS, G. D. & GLASS, D. J. (2004) The IGF-1/PI3K/Akt pathway prevents expression of muscle atrophy-induced ubiquitin ligases by inhibiting FOXO transcription factors. *Mol Cell,* 14**,** 395-403.

STUTZMANN, G. E. (2005) Calcium dysregulation, IP3 signaling, and Alzheimer's disease. *Neuroscientist,* 11**,** 110-5.

SUZUKI, M., MCHUGH, J., TORK, C., SHELLEY, B., KLEIN, S. M., AEBISCHER, P. & SVENDSEN, C. N. (2007a) GDNF secreting human neural progenitor cells protect dying motor neurons, but not their projection to muscle, in a rat model of familial ALS. *PLoS One,* 2**,** e689.

SUZUKI, N., MIZUNO, H., WARITA, H., TAKEDA, S., ITOYAMA, Y. & AOKI, M. (2010) Neuronal NOS is dislocated during muscle atrophy in amyotrophic lateral sclerosis. *J Neurol Sci,* 294**,** 95-101.

SUZUKI, N., MOTOHASHI, N., UEZUMI, A., FUKADA, S., YOSHIMURA, T., ITOYAMA, Y., AOKI, M., MIYAGOE-SUZUKI, Y. & TAKEDA, S. (2007b) NO production results in suspension-induced muscle atrophy through dislocation of neuronal NOS. *J Clin Invest,* 117**,** 2468-76.

SUZUKI, T., MARUYAMA, A., SUGIURA, T., MACHIDA, S. & MIYATA, H. (2009) Age-related changes in two- and three-dimensional morphology of type-identified endplates in the rat diaphragm. *J Physiol Sci,* 59**,** 57-62.

SWEENEY, H. L. & BARTON, E. R. (2000) The dystrophin-associated glycoprotein complex: what parts can you do without? *Proc Natl Acad Sci U S A,* 97**,** 13464-6.

TAIYAB, A., SREEDHAR, A. S. & RAO CH, M. (2009) Hsp90 inhibitors, GA and 17AAG, lead to ER stress-induced apoptosis in rat histiocytoma. *Biochem Pharmacol,* 78**,** 142-52.

TAKUMA, H., KWAK, S., YOSHIZAWA, T. & KANAZAWA, I. (1999) Reduction of GluR2 RNA editing, a molecular change that increases calcium influx

through AMPA receptors, selective in the spinal ventral gray of patients with amyotrophic lateral sclerosis. *Ann Neurol,* 46**,** 806-15.
TAM, S. L., ARCHIBALD, V., TYREMAN, N. & GORDON, T. (2002) Tetrodotoxin prevents motor unit enlargement after partial denervation in rat hindlimb muscles. *J Physiol,* 543**,** 655-63.
TAM, S. L. & GORDON, T. (2003) Mechanisms controlling axonal sprouting at the neuromuscular junction. *J Neurocytol,* 32**,** 961-74.
THOMAS, M., HARRELL, J. M., MORISHIMA, Y., PENG, H.-M., PRATT, W. B. & LIEBERMAN, A. P. (2006) Pharmacologic and genetic inhibition of hsp90-dependent trafficking reduces aggregation and promotes degradation of the expanded glutamine androgen receptor without stress protein induction. *Hum. Mol. Genet.,* 15**,** 1876-1883.
TOKUI, K., ADACHI, H., WAZA, M., KATSUNO, M., MINAMIYAMA, M., DOI, H., TANAKA, K., HAMAZAKI, J., MURATA, S., TANAKA, F. & SOBUE, G. (2009) 17-DMAG ameliorates polyglutamine-mediated motor neuron degeneration through well-preserved proteasome function in an SBMA model mouse. *Hum Mol Genet,* 18**,** 898-910.
TONKISS, J. & CALDERWOOD, S. K. (2005) Regulation of heat shock gene transcription in neuronal cells. *Int J Hyperthermia,* 21**,** 433-44.
TRAYNOR, B. J., BRUIJN, L., CONWIT, R., BEAL, F., O'NEILL, G., FAGAN, S. C. & CUDKOWICZ, M. E. (2006) Neuroprotective agents for clinical trials in ALS: a systematic assessment. *Neurology,* 67**,** 20-7.
TUCEK, S. (1973) Choline acetyltransferase activity in skeletal muscles after denervation. *Experimental Neurology,* 40**,** 23-35.
TUCEK, S. & GUTMANN, E. (1973) Choline acetyltransferase activity in muscles of old rats. *Experimental Neurology,* 38**,** 349-360.
TUPLING, A. R., BOMBARDIER, E., VIGNA, C., QUADRILATERO, J. & FU, M. (2008) Interaction between Hsp70 and the SR Ca2+ pump: a potential mechanism for cytoprotection in heart and skeletal muscle. *Appl Physiol Nutr Metab,* 33**,** 1023-32.
TURNER, B. J. & TALBOT, K. (2008) Transgenics, toxicity and therapeutics in rodent models of mutant SOD1-mediated familial ALS. *Prog Neurobiol,* 85**,** 94-134.
TYC, F. & VRBOVA, G. (1995) The effect of partial denervation of developing rats fast muscles on their motor unit properties. *J Physiol,* 482 (Pt 3)**,** 651-60.
UEDA, K., UEYAMA, T., OKA, M., ITO, T., TSURUO, Y. & ICHINOSE, M. (2009) Polaprezinc (Zinc L-carnosine) is a potent inducer of anti-oxidative stress enzyme, heme oxygenase (HO)-1 - a new mechanism of gastric mucosal protection. *J Pharmacol Sci,* 110**,** 285-94.
VAN DEN BOSCH, L. & ROBBERECHT, W. (2008) Crosstalk between astrocytes and motor neurons: What is the message? *Experimental Neurology,* 211**,** 1-6.
VASILAKI, A., MCARDLE, F., IWANEJKO, L. M. & MCARDLE, A. (2006) Adaptive responses of mouse skeletal muscle to contractile activity: The effect of age. *Mechanisms of Ageing and Development,* 127**,** 830-839.
VILLA MORUZZI, E., BERGAMINI, E. & GORI BERGAMINI, Z. (1981) Glycogen metabolism and the function of fast and slow muscles of the rat. *Pflügers Archiv European Journal of Physiology,* 391**,** 338-342.

VOELLMY, R. & BOELLMANN, F. (2007) Chaperone regulation of the heat shock protein response. *Adv Exp Med Biol,* 594**,** 89-99.
VOSS, M. R., STALLONE, J. N., LI, M., CORNELUSSEN, R. N., KNUEFERMANN, P. & KNOWLTON, A. A. (2003) Gender differences in the expression of heat shock proteins: the effect of estrogen. *Am J Physiol Heart Circ Physiol,* 285**,** H687-92.
VRBOVA, G. & FISHER, T. J. (1989) The Effect of Inhibiting the Calcium Activated Neutral Protease, on Motor Unit Size after Partial Denervation of the Rat Soleus Muscle. *Eur J Neurosci,* 1**,** 616-625.
VRBOVA, G. & GORDON, T. (1994) *Nerve-Muscle Interaction*, Chapman and Hall.
WANG, J., GINES, S., MACDONALD, M. E. & GUSELLA, J. F. (2005) Reversal of a full-length mutant huntingtin neuronal cell phenotype by chemical inhibitors of polyglutamine-mediated aggregation. *BMC Neurosci,* 6**,** 1.
WATANABE, M., DYKES-HOBERG, M., CULOTTA, V. C., PRICE, D. L., WONG, P. C. & ROTHSTEIN, J. D. (2001) Histological evidence of protein aggregation in mutant SOD1 transgenic mice and in amyotrophic lateral sclerosis neural tissues. *Neurobiol Dis,* 8**,** 933-41.
WEBSTER, C., SILBERSTEIN, L., HAYS, A. P. & BLAU, H. M. (1988) Fast muscle fibers are preferentially affected in Duchenne muscular dystrophy. 52**,** 503-513.
WHITEHEAD, N. P., YEUNG, E. W. & ALLEN, D. G. (2006) Muscle damage in mdx (dystrophic) mice: role of calcium and reactive oxygen species. *Clin Exp Pharmacol Physiol,* 33**,** 657-62.
WILLIS, M. S., SCHISLER, J. C., PORTBURY, A. L. & PATTERSON, C. (2009) Build it up-Tear it down: protein quality control in the cardiac sarcomere. *Cardiovasc Res,* 81**,** 439-48.
WILSON, M. H. & DESCHENES, M. R. (2005) The neuromuscular junction: anatomical features and adaptations to various forms of increased, or decreased neuromuscular activity. *Int J Neurosci,* 115**,** 803-28.
WINEINGER, M. A., GORIN, F., TAIT, R., FROMAN, B. & CARLSEN, R. C. (1991) Reduced glycolytic metabolism in regenerated fast-twitch skeletal muscle. *Am J Physiol,* 261**,** C169-76.
WINKLHOFER, K. F., REINTJES, A., HOENER, M. C., VOELLMY, R. & TATZELT, J. (2001) Geldanamycin restores a defective heat shock response in vivo. *J Biol Chem,* 276**,** 45160-7.
WITZEMANN, V. (2006) Development of the neuromuscular junction. *Cell Tissue Res,* 326**,** 263-71.
WONG, M. & MARTIN, L. J. (2010) Skeletal Muscle-Restricted Expression of Human SOD1 Causes Motor Neuron Degeneration in Transgenic Mice. *Hum Mol Genet*.
WONG, P. C., PARDO, C. A., BORCHELT, D. R., LEE, M. K., COPELAND, N. G., JENKINS, N. A., SISODIA, S. S., CLEVELAND, D. W. & PRICE, D. L. (1995) An adverse property of a familial ALS-linked SOD1 mutation causes motor neuron disease characterized by vacuolar degeneration of mitochondria. *Neuron,* 14**,** 1105-16.
WOOD, J. D., BEAUJEUX, T. P. & SHAW, P. J. (2003) Protein aggregation in motor neurone disorders. *Neuropathol Appl Neurobiol,* 29**,** 529-45.

WOOTEN, G. F. & CHENG, C. H. (1980) Transport and turnover of acetylcholinesterase and choline acetyltransferase in rat sciatic nerve and skeletal muscle. *J Neurochem,* 34**,** 359-66.

YAMAMOTO, M., KOBAYASHI, Y., LI, M., NIWA, H., MITSUMA, N., ITO, Y., MURAMATSU, T. & SOBUE, G. (2001) In vivo gene electroporation of glial cell line-derived neurotrophic factor (GDNF) into skeletal muscle of SOD1 mutant mice. *Neurochem Res,* 26**,** 1201-7.

YAMASHITA, N., HOSHIDA, S., NISHIDA, M., IGARASHI, J., AOKI, K., HORI, M., KUZUYA, T. & TADA, M. (1997) Time course of tolerance to ischemia-reperfusion injury and induction of heat shock protein 72 by heat stress in the rat heart. *J Mol Cell Cardiol,* 29**,** 1815-21.

YAN, D., SAITO, K., OHMI, Y., FUJIE, N. & OHTSUKA, K. (2004) Paeoniflorin, a novel heat shock protein-inducing compound. *Cell Stress Chaperones,* 9**,** 378-89.

YANAGISAWA, N. & SHINDO, M. (1996) [Neuroprotective therapy for amyotrophic lateral sclerosis (ALS)]. *Rinsho Shinkeigaku,* 36**,** 1329-30.

YANG, C. C., ALVAREZ, R. B., ENGEL, W. K., HELLER, S. L. & ASKANAS, V. (1998) Nitric oxide-induced oxidative stress in autosomal recessive and dominant inclusion-body myopathies. *Brain,* 121 (Pt 6)**,** 1089-97.

YOH, T., NAKASHIMA, T., SUMIDA, Y., KAKISAKA, Y., NAKAJIMA, Y., ISHIKAWA, H., SAKAMOTO, Y., OKANOUE, T. & MITSUYOSHI, H. (2002) Effects of glycyrrhizin on glucocorticoid signaling pathway in hepatocytes. *Dig Dis Sci,* 47**,** 1775-81.

YOSHIHARA, T., ISHII, T., IWATA, M. & NOMOTO, M. (1998) Ultrastructural and histochemical study of the motor end plates of the intrinsic laryngeal muscles in amyotrophic lateral sclerosis. *Ultrastruct Pathol,* 22**,** 121-6.

ZEKE, T., MORRICE, N., VAZQUEZ-MARTIN, C. & COHEN, P. T. (2005) Human protein phosphatase 5 dissociates from heat-shock proteins and is proteolytically activated in response to arachidonic acid and the microtubule-depolymerizing drug nocodazole. *Biochem J,* 385**,** 45-56.

ZENIMARU, Y., TAKAHASHI, S., TAKAHASHI, M., YAMADA, K., IWASAKI, T., HATTORI, H., IMAGAWA, M., UENO, M., SUZUKI, J. & MIYAMORI, I. (2008) Glucose deprivation accelerates VLDL receptor-mediated TG-rich lipoprotein uptake by AMPK activation in skeletal muscle cells. *Biochemical and Biophysical Research Communications,* 368**,** 716-722.

ZHAO, Y. & QIU, G. X. (2004) [Expression of neuronal nitric oxide synthase and inducible nitric oxide synthase in the erector spinal muscles in idiopathic scoliosis]. *Zhongguo Yi Xue Ke Xue Yuan Xue Bao,* 26**,** 451-4.

Word count: 56362

Appendix one

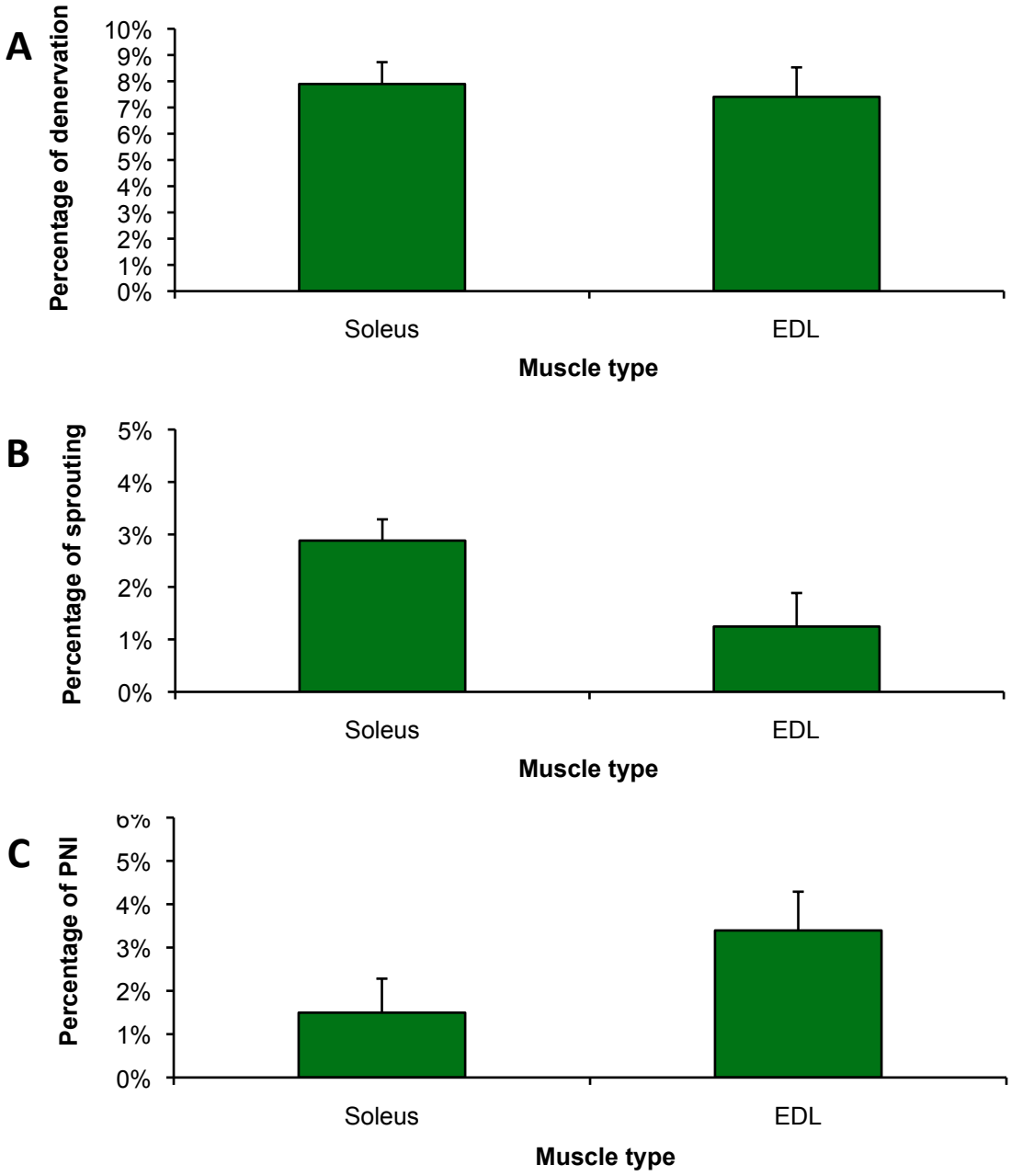

Figure 8.1 Innervation characteristics in the muscle of EDL and soleus muscle from wtSOD1 mice

The extent of denervation (A) sprouting (B) and PNI (C) was examined in the EDL and soleus muscles of wtSOD1 mice by silver cholinesterase staining.

n=4; error bars = SEM

Appendix two

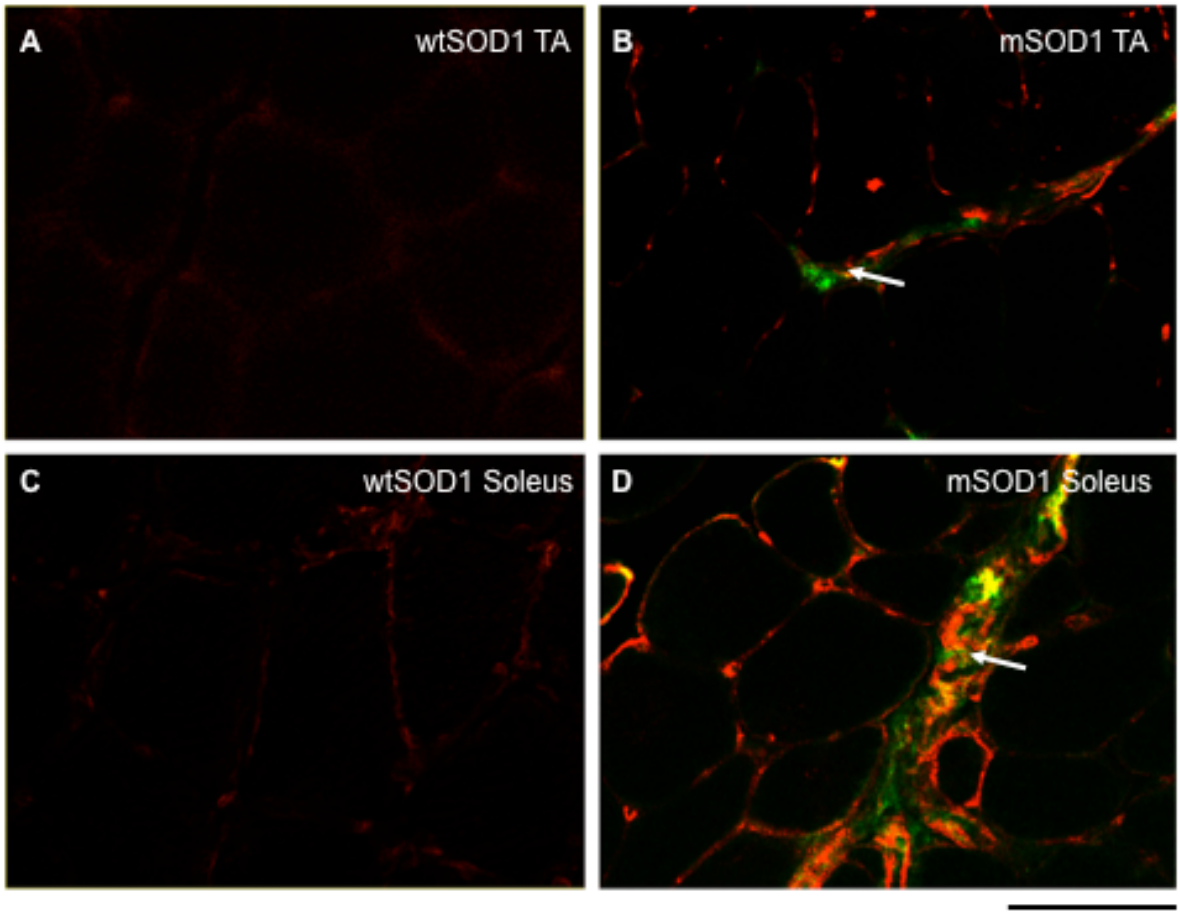

Figure 9.1 Inducible Nitric oxide synthase and CD11b expression in the TA and soleus muscle of wtSOD1 and mSOD1 mice at 120 days of age.

Immunohistochemical staining was carried out using an iNOS antibody (Invitrogen) and CD11b (Abcam, Hertfordshire) on transverse sections of muscle. (A) shows an example of iNOS (red) and CD11b (green) immoreactivity in wtSOD1 TA muscle. (B) shows an example of iNOS and CD11b staining in mSOD1 TA muscle where colocalisation of iNOS and CD11b expression is present at a point of vascularisation (arrow). (C) shows an example of wtSOD1 soleus muscle stained for iNOS and CD11b. (D) shows an example of iNOS and CD11b expression in 120-day-old soleus muscle from mSOD1 mice. iNOS and CD11b colocalisation is strong at points of vascularisation (arrow).

Scale bar = 50μm; n=5

Appendix three

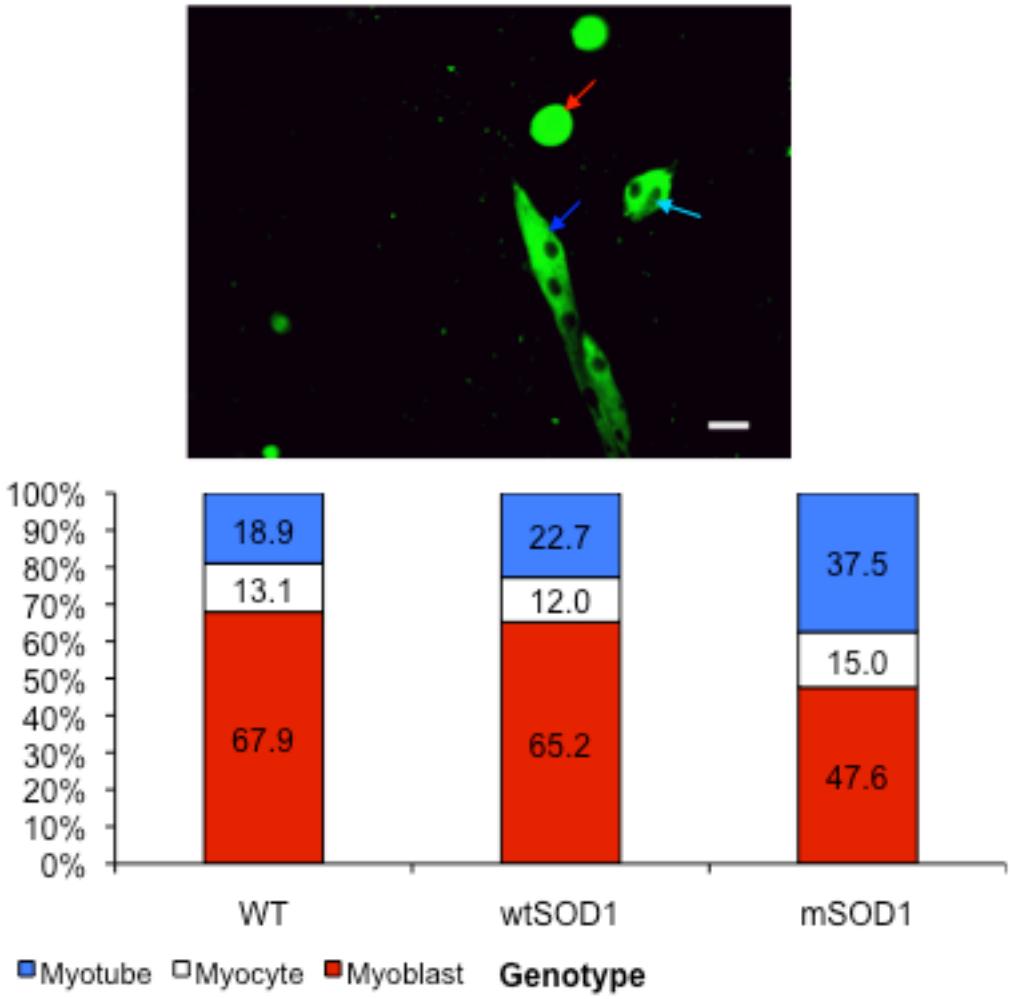

Figure 10.1 Myogenic differentiation in muscle cultures from the hindlimb of WT, wtSOD1 and mSOD1 neonate **mice.**

The ratio of myoblasts, myocytes and myotubes in a 7-day-old culture were examined in WT, wtSOD1 and mSOD1 cultures. The cultures were immunostained for myosin and then the three structures counted. Myoblasts were taken to be spherical structures (red arrow), spindle-like myocytes (light blue arrow) and the elongated multi-nucleated structures myotubes (dark blue arrow). The Graph shows the percentage of myoblasts, myocytes and myotubes in WT, wtSOD1 and mSOD1 cultures.

*=$p<0.05$; n=6; error bars = ± standard error of the mean

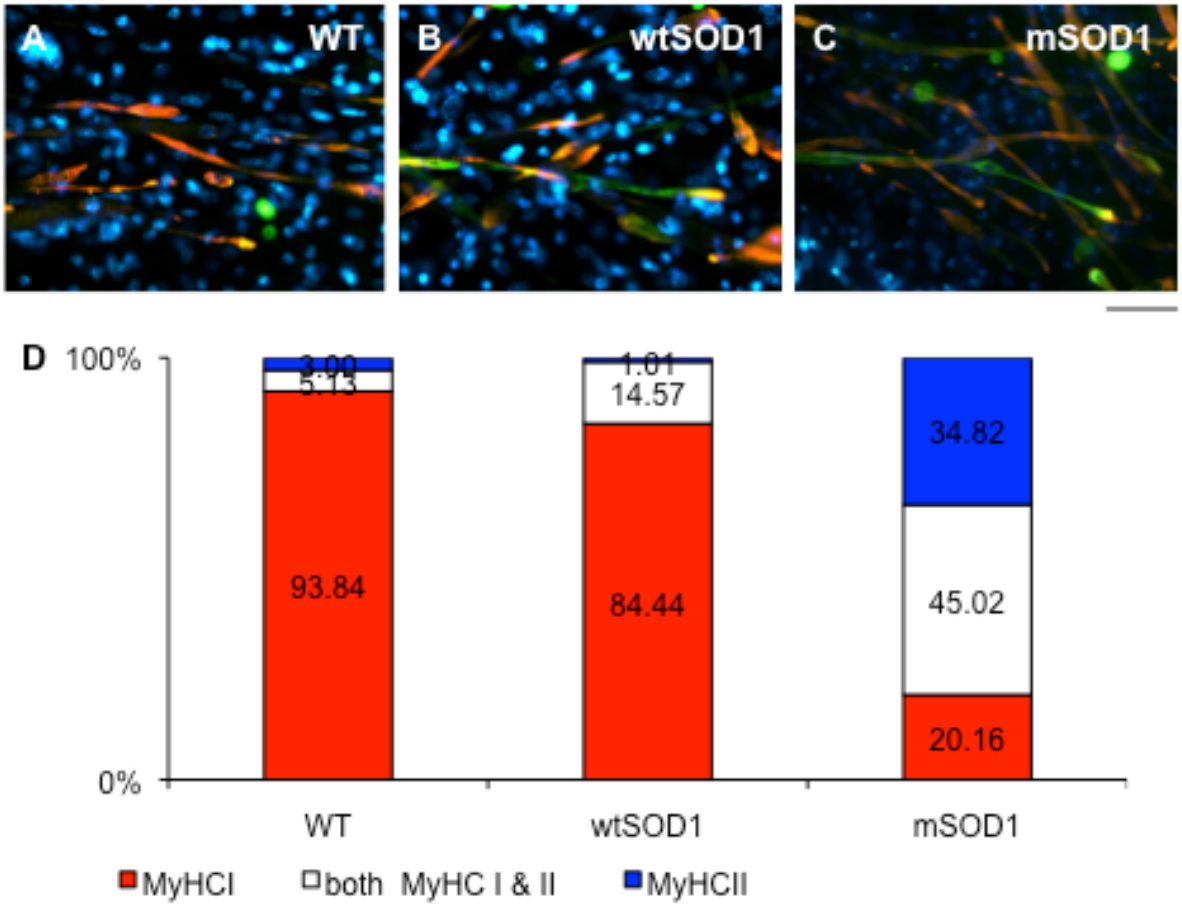

Figure 10.2 Myosin heavy chain slow and fast (MyHCII) expression in mixed muscle cultures from the hindlimb of WT, wtSOD1 and mSOD1 neonate mice.

(A-C) WT, wtSOD1 and mSOD1 cultures were immunostained for MyHCI (red - Novocastra) following 7DIV, respectively. They were subsequently costained for MyHC II (green- Novocastra) and DAPI (blue), and then the number of myogenic structures with either or both were counted. This data is summarised in chart (D).

n=3; scale bar = 20μm

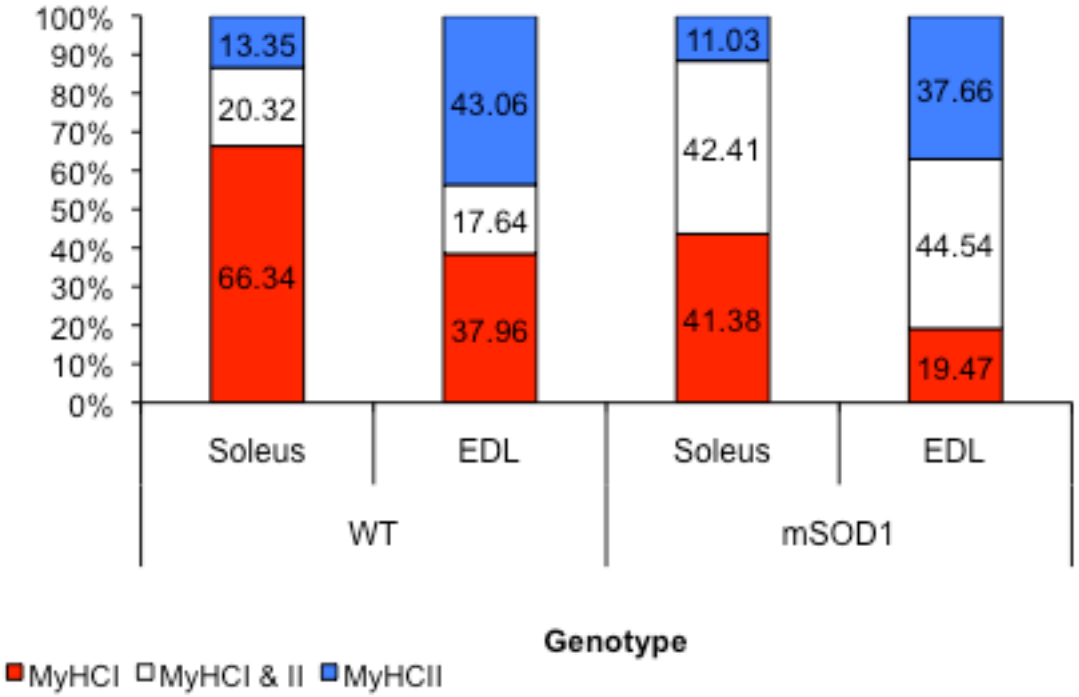

Figure 10.3 Myosin heavy chain slow and fast (MyHCII) expression in fast and slow muscle cultures from WT and mSOD1 neonate mice.

Cultures that were immunostained for MyHCI (Novocastra) following 7DIV. They were subsequently costained for MyHC II (Novocastra), and then the number of myogenic structures with either or both were counted.

n=4